KTH Electrical Engineering

Dielectric response and partial discharge measurements on stator insulation at varied low frequency

NATHANIEL TAYLOR

Doctoral Thesis
Stockholm, Sweden 2010

TRITA-EE 2010:037
ISSN 1653-5146
ISRN KTH/EE--10/037--SE
ISBN 978-91-7415-713-0

Elektroteknisk teori och konstruktion
Teknikringen 33
SE-100 44 Stockholm
SWEDEN

Akademisk avhandling som med tillstånd av Kungl Tekniska högskolan framlägges till offentlig granskning för avläggande av teknologie doktorsexamen fredag den 24 september 2010, klockan 10:00 i sal F3, Lindstedtsvägen 26, Kungl Tekniska högskolan, Stockholm.

Tryck: Universitetsservice, US-AB

Abstract

This is a study of potential improvements of diagnostic methods used on high-voltage generators and motors. It considers offline electrical measurements on the main insulation of stator windings, where a sinusoidal voltage is applied between the winding and the stator-core, and the total current through the insulation (dielectric spectroscopy, DS) and the rapid current-pulses arising from discharges (partial discharge, PD) are measured.

The proposed methods differ from existing practice in industrial DS and PD measurements in that the applied voltage is varied in amplitude and in frequency, harmonics of the voltage and current are measured, and the DS and PD measurements are made simultaneously, with comparison of results. Based on literature, models and measurements, the problems and advantages of these methods are assessed in this work.

Harmonics provide a way of separating linear and nonlinear sources of current, and reveal the waveform of the current. Measurement of total PD charge by DS methods provides complementary information to the conventional PD measurement; the difference in results between these types of measurement is shown by literature and experimental results to be large. Simultaneous measurement allows direct comparison of the relation between the DS and PD results, and saves time compared to separate measurements. The varied frequency, down to the millihertz range, provides additional information about the insulation. Much of the potential for DS methods on machine insulation is spoiled by the end-winding stress grading. Models and measurements of the currents in this grading are presented, with discussion of how much effect the disturbance has and how well it can be predicted by modelling.

Chapters

Contents

List of Tables

List of Figures

Acknowledgements

I am very thankful for the opportunity I have had to study in this broad and deep area of high-voltage insulation. This work has been carried out within Elektra project 36019, financed jointly by the Swedish Energy Agency, Elforsk, ABB and Banverket.

Hans Edin has been the most directly involved supervisor in this work, from the formulation of the proposal through to this, the culmination, giving encouragement and help throughout and coping admirably with my frequent application of 'just-in-time management'. This work in some parts continues his PhD [Edi01], considering its possible application to stator insulation.

Roland Eriksson introduced me to this subject during my exchange year in 2001, and later offered me the PhD position. To hear again such physicsy words as 'electron', after having been away for nearly two years working in the area of power-systems, was most refreshing. The smooth running of the division during this time, including the easy availability of whatever resources have been needed in the laboratory and computer rooms, has been much appreciated.

Rajeev Thottappillil moved here from Uppsala as the new professor on Roland's retirement, and therefore ended up adopting the project at about the time when the original plans would have suggested it to be finishing (the discrepancy being due to earlier parental leave). I've appreciated our chats about electromagnetics, and the instructive course in EMC that he gave long before we knew that we would later be in the same department.

Sven Jansson has faithfully represented Elektra at all of the half-yearly 'reference group' meetings for the project, keeping us in touch with related projects and industrial interest.

Eva Mårtensson of ABB Motors helped with advice at the project meetings, and with providing specimens for the tests of real stator bars and materials. Hans-Åke Eriksson was Eva's predecessor, and provided other stator coils and help in my first years here.

Tommy Karlsson of Vattenfall Power Consultant gave useful advice at our meetings, also organising some field-measurements about half-way through this project and providing extra data to help me get a better idea of typical generator-parameters and results from conventional diagnostic measurements. Within the same company, Kristoffer Backström helped by providing data from measurements on whole stators.

Ingvar Hagman, while at STRI, very helpfully and efficiently organised access to some generators for field-measurements. I deeply regret that I have not (yet) been able to take advantage of these, owing to the long delays in having all the parts of the measurement system in working order and then the more pressing need of finishing the laboratory work.

Cecilia Forssén was the first 'room sharer', patiently enduring my practice in spoken Swedish. Our later discussions of PDs, measurement methods and experimental design helped my knowledge and enthusiasm. Valentinas Dubickas started at the same time as I did, and we shared a room in his last year here. His

help with my few forays into high-frequency work, and general discussions at starting-work time, were well appreciated. Nadja Jäverberg then moved in, and we have had shared interest in dielectric measurements, battles against certain instruments, and welcome tea-breaks from all of this. Mohamad Ghaffarian and Xiaolei Wang, who recently joined the research group, have already awakened my interest in their projects. Lars Jonsson of the electromagnetic theory group within our department has brought stimulation to some afternoons by visits to discuss ways of doing all manner of things with computers, and has done much to encourage communication between the diverse research-groups in our seminar series.

Valerijs Knazkins was in the power systems department, upstairs, even before my arrival at KTH. A wealth of shared interests, and my liking for slightly keeping up on the work of other divisions, have made for many enjoyable lunches, fikas, and small-hours email exchanges. Katherine Elkington started working upstairs a few years ago, and has similarly brightened the scene of lunches, tea-breaks and extra-departmental technical discussions. Dmitry Svechkarenko, from the machines department along the corridor, has been a regular lunch-taker and a contact with yet another department's work, and his company and table-tennis playing are eagerly requested by my children if we pass by 'the work place' at the weekend.

Peter Lönn, the computer administrator for our building, has been most helpful in obtaining many parts and programs and organising purchases for all my activities with lab computers, file servers and computation servers.

Many people around the world have done the work of writing and polishing the computer programs that have made some parts of this work a pleasure, rather than the agony of most of the alternative offerings. The GNU utilities, TEX, Perl, Octave, KDE, Linux, the Gentoo build-system and FreeBSD, along with countless other programs, were of immense value on our computers in the lab, on the desktop, in the server room and on the move. Thank you Stallman, Knuth, Torvalds, Lamport, Eaton, Wall, and countless others.

My family — Malin, Nicholas, Philip and William — have suffered sporadic periods of over-activity around particular equipment-troubles or deadlines, and have been particularly helpful in these last months. I hope the benefits of this flexibly timetabled job have not been too heavily outweighed by these downsides!

Chapter 1

Introduction

1.1 Background

Stator insulation is a critical part of the high-voltage rotating machines that are used as generators to produce practically all electrical power, and as large motors to consume some of this power in driving industrial processes.

The high capital-costs of high-voltage machines themselves, and the usually high costs arising from a machine being unavailable for service, result the use of 'diagnostic' measurements. These are typically applied at regular maintenance intervals, with the intention of predicting failures and thereby avoiding them by suitable maintenance.

Many types of diagnostic measurement are in widespread use on stator insulation, yet the complexity of the insulation and of the aging and failure processes make each method just a further indication of insulation condition: there is nothing that reliably gives warning if and only if there is a real problem, and certainly nothing that gives accurate predictions of how long the insulation will tolerate given stresses without failure.

The diagnostic methods can be improved by any combination of increasing the likelihood of identifying an important problem, reducing the likelihood of missing an important problem, or reducing the time taken for measurements, or reducing the capital cost of equipment used for these measurements.

The methods investigated here are an extension and combination of two of the many types of measurement used to assess the condition of stator insulation for the purpose of guiding decisions about operation and maintenance. Dielectric spectroscopy (DS) measures all the current that flows between electrodes of an insulation system in response to a voltage stimulus. Partial discharge (PD) pulse measurement measures sharply pulsed components in the current due to breakdown of small volumes of gas that are exposed to a strong electric field within an insulation system.

1.2 Aim

The aim of the project is to investigate a combined system for frequency-domain DS and phase-resolved PD measurements, and its application to diagnostic measurements on stator insulation. The DS and PD methods are extended in ways beyond the current practice: the harmonic components in the DS current are studied to help distinguish different sources and see the shape of the current waveform; the simultaneous use of the DS and PD measurements permits two complementary measurements of the charge due to PD, which increases the available information; a variable frequency is used, down to values much lower than in operation, permitting distinctions to be made between different types of defect that could give similar results at the single frequency that is current practice. Several ideas have been pursued for these extensions of established methods could be applied in diagnostic measurements on stator insulation. Investigations have been made based on literature, laboratory studies, field data and simulation.

1.3 Main contributions

The following are the main new results in this thesis.

Measurement of PD charge waveforms has been compared between the two types of measurement, DS and PD, for several types of test object, showing similar measurement of PD charge in simple objects, and strong differences in larger objects. The differences mean that the two types of measurement give complementary results for stator windings.

Tests of instruments and measurements have been made, to assess the practicality of measuring PD currents with the DS instrument, to establish how to make the instruments work together, and to show that the results of swept diagnostic measurements can depend strongly on details of sequence and timing.

A review of stator insulation and diagnostic methods is given in the early chapters, focused on points relevant to the proposed methods. It is based on books, old and recent research papers, laboratory measurements and results of industrial diagnostic measurements. Its usefulness is in providing details that are needed for evaluating the usefulness of the proposed methods, for example the relative sizes of signals and disturbances, and the relative influence of different defects on lifetime.

The current in end-winding stress-grading have been measured on simple objects and on real stator bars, and numerical models have been made. The detailed appearance of this current, showing capacitance, loss and harmonics as functions of voltage amplitude and frequency, has not been found elsewhere, yet it is important for understanding the influence on DS measurements and possibly reducing this influence by modelling.

Characterisation of stress-grading materials was necessary for the modelling. Several simple materials models have been used in previous work, with little justification or detail about the range of applicability. Results are presented from measurements over wide ranges of electric field and low frequency, with comparison of the fit of mathematical models from the literature.

1.4 Reading guide

The table of contents is the probably the best starting place for a reader with very limited time, followed by chapter 11 if wanting to get an overview.

Chapters 2 to 8 give background information about stator insulation, faults in stator insulation, general diagnostic methods, and the phenomena and measurements associated with the DS and PD methods studied here. The starting level may seem rather basic, but there are many points of relevance to whether the proposed types of measurement might have a benefit. Each of these background chapters covers a subject that could easily fill a book, so they are necessarily biased towards the matters relevant to stator insulation.

Chapters 9 and 10 describe the instruments, and chapters 12 and 13 describe some tests that were made on them: these are all quite detailed, and may be of interest to the reader who wishes to understand the potentials and limitations of the measurements, or who uses these instruments.

Chapter 11 brings together the project description with details from the previous chapters, to give a description of which of the many possible uses of the proposed measurements seem most promising.

Chapters 14 and subsequent chapters, up to the conclusion in chapter 21, investigate the questions raised in chapter 11, for example the phase-resolved measurement of total PD charge, the display of DS and PD data measured at many points, and disturbances due to currents in the end-windings.

The Appendix is an anomaly, detouring into such subjects as working-practices, computers, and attitudes to experiment and scientific inference.

* * *

I hope the quite long, dense structure of this thesis is not too off-putting to potential readers. It is partly due to the unusually broad scope of the project, studying two broad types of measurement, each extended to an extra controlled variable, and with their relation also being considered. Part of the work is assessment of the possibilities, so there is not just a single tightly-defined thread to follow. Diagnostic methods, particularly in stator insulation, involve many possible types of defect, differing in their criticality and in the extent of overlap or difference that they show in results of measurements.

I know only too well how most people who read a thesis will be interested only in extracting a few results, quickly. I, too, have seldom felt able to justify the time needed to read a whole thesis in detail, even when of only some fifty lightly filled pages. For some reason, I wanted to make a thorough compilation of the main ingredients of the project. Quite how long this would take was not remotely realised at the start of writing: had more time been available, there would have been much more careful shortening, checking and honing, pulling together of the different threads of the work, and more thorough cross-referencing and indexing. Nevertheless, I hope the current structure, along with the contents and index, makes it fairly easy for readers to skip to the particular details in which they are interested, in spite of the large range of subjects included.

1.5 Summary of work conducted

Literature studies have been made on several key subjects: stator insulation systems, aging of stator insulation, accelerated-aging testing, diagnostic methods, dielectric response of materials and stator insulation systems, PD in stator insulation, methods and limitations of PD detection, and PD signal transmission in stator windings. Some of the main results are included in the early chapters.

Stress-grading material made for stator end-windings has been characterised for use in the models of end-winding currents. Measurements in the lab have studied conductivity and permittivity and their dependence on the amplitude and frequency of the applied electric field. The literature has been searched for models and measurements on these types of materials, to get an idea of how variable the parameters are likely to be in different machines.

Currents in end-windings flowing in stress-grading systems have been studied by laboratory models, several levels of numerical models, and measurements on real stator bars. The frequency-domain representation of this current, including low-order harmonics, has been studied as a function of the applied voltage's amplitude and frequency.

Measurement systems for DS and PD measurements have been acquired as two commercially available instruments, and programs have been written to control them in ways more versatile than their provided programs, partly to facilitate the later combined measurements; a lot of work was taken in determining how to control the instruments and make them work together. Together with an external amplifier the DS instrument can apply voltages at amplitudes up to 20 kV and frequencies from 100 µHz to above 100 Hz.

Simultaneous measurement with both of the measurement systems required some modifications compared to separate measurements, due to the signal-earthing arrangements and to the problem of electrical noise from the HV source affecting the PD measurement.

PD charge-measurements have been compared between PD-pulse measurements and measurement of the whole current by DS methods. Reasons for the differences between DS and PD measurements of PD charge have been investigated, by a study of literature on PD detection and calibration, some analysis, and some laboratory work.

Presentation of measurement-results is particularly important given the large number of controlled and measured variables compared with conventional diagnostic methods. Suitable ways of presenting results have been considered, and programs have been written to implement them. Suggestions have been made of apparently useful indices of insulation condition.

Dependence on voltage and frequency of the currents in various features and defects of stator insulation have been considered, based on literature, simple models and measurements.

Thermal aging in the laboratory has been made possible by building an oven large enough for several bars to fit in, and able to be heated to 200 °C.

Stator coils received in new condition have been used for measurements of material properties and of currents in the end-windings, before and after slow heating to finish curing the insulation.

1.6 Scope and limitations of this work

The measurements considered here require a sinusoidal voltage of controlled amplitude and frequency to be applied to the terminals of entire isolated sections of stator-winding. The neutral-point of the winding must be able to be isolated from earth, and preferably split to separate the phases. This makes these methods inherently 'offline', requiring some work in preparing for the measurement, but still more convenient than methods that require direct access to parts deep inside the machine. The main insulation is stressed between the equipotentials of the conductor and the earthed core of the machine; the insulation between turns in a multiturn coil is therefore not directly tested. The mica-based form-wound type of insulation that is assumed here is used at rated voltages of about 1 kV and above. The end-winding stress grading that has been studied in this work is used above about 5 kV: this range is the main focus here, but some of the work is also relevant to rather lower rated voltages.

This work is deliberately limited to the diagnostic purpose of relating results of measurements to the probable state of the insulation that has given these results. Even this, in view of the many possible types of defect in stator insulation and the uncertainties involved in distinguishing them, is a quite vague and difficult subject. The further important steps, of deciding the future operation and maintenance in order to optimise the use of the machine, are largely ignored for the sake of limiting the scope. There is however some distinction made between defects known to give very fast or very slow failure, when discussing the potential of the new types of measurement.

1.7 Comparison with initial aims

The initial project-proposal suggested several paths that have been followed and several that have not. The measured dielectric response current due to PD was to be investigated: this has indeed been a large part of the work. The role of end-winding stress grading systems in obscuring the results of DS measurements has taken a prominent place in the work; the initial interest in this grading was as a possible source of PD when at low frequencies, but this turned out to be unimportant. Simultaneous measurement of DS and PD was mentioned, just with respect to 'on-site' (field) measurements: simultaneous measurement has been an important part of the work, but has not yet been applied to whole stator windings on-site. Variable-frequency phase-resolved PD analysis (VF-PRPDA) was to be used: it has been, but there has not been time for a systematic experimental investigation of PD frequency-dependence of various common types of stator PD-source. Other proposals were more towards doing analyses on naturally aged insulation from old machines by the electrical methods, comparing results with dissection and chemical analysis: there has instead been work with laboratory objects and artificial aging. Investigation of the economic benefits of these methods for maintenance was to be studied: this has been avoided for the reasons explained in section 1.6. On the other hand, extensive consideration mainly based on literature has been given to the importance of identifying particular types of defect.

1.8 Conferences, publications and other external contact

Papers have been presented at some conferences, giving the opportunity of meeting people with an academic and industrial interest in this work. These conferences and papers were CEIDP 2004 [Tay04], ISH 2005 [Tay05], NordIS 2007 [Tay07] and NordIS 2009 [Tay09]. Similar events that were attended without presenting work were NordIS 2005 in Trondheim, the International Symposium on Electrical Insulation ISEI 2006 in Toronto, and the European Electrical Insulation Manufacturers' seminar EEIM 2005 in Berlin.

A paper about stress-grading models has been accepted for a rotating-machines special issue of the IEEE Transactions on Dielectrics and Electrical Insulation, due later this year. Papers on several other subjects started in this thesis are hoped to be submitted to reviewed journals in the near future.

A licentiate thesis [Tay06] was published at the half-way point of this project in November 2006. The main parts are either covered in more detail here or are referred to when needed.

Several industrial contacts have resulted in useful exchanges of information, and opportunities for studying or fabricating real stator insulation. Contacts with these companies have been maintained through the half-yearly meetings about this project, and by some intermediate visits to discuss results. In collaboration with Vattenfall Power Consultant, measurements have been made on a hydro-generator before and after some maintenance work; DS measurements were performed as well as the standard set of measurements, as has already been described in [Tay06]. Vattenfall has also provided some results from routine measurements on various sizes of hydro-generator, which have been used to get an idea of the range of typical values. ABB Motors has provided two batches of new epoxy-mica stator coils: the first batch was studied in [Tay06], and the second batch has been partially studied here, including a specially fabricated coil with many material-samples. ABB Corporate Research gave use of its ovens for the earlier thermal aging, before a large enough oven was constructed in the laboratory at KTH. Contact with STRI has made some generators available for measurements, but the opportunity has not yet arisen to carry out this work.

1.9 Notation and style

Emphasis is shown by *italic* type, and technical terms being defined are indicated by *slanted* type. Names and abbreviations are explained in the most relevant chapter, not necessarily where they first appear; the index on page 247 should allow the definitions to be found. Symbols are defined close to their first use.

Having been expected to write in English, I have followed my preference of having notational conventions match the language conventions. Examples are the use of the letter V to denote voltage, a dot as the decimal separator, and the 'cross' symbol for multiplication; these are usual in English and are used in many countries outside Europe, but not in most other European languages, including Swedish. The modern sense of 'data' as a singular word describing 'stuff' is used without the slightest compunction when it seems natural; so, too, is the plural sense....

Quantities that are functions of time are generally lower-case, for example $i(t)$, and their frequency-domain transforms are upper-case, $I(\omega)$. Phasor quantities, represented as complex numbers, are so common that no special bar or boldness is used to emphasise their vectorial nature. Subscripts denoting names are roman, i_{in}, and subscripts denoting variables are italic, i_n. Some special mathematical symbols are indicated by roman type: i is the imaginary unit, e the base of natural logarithms, and d the differential operator.

The widely varying magnitudes of physical quantities can be expressed using SI prefixes, for example 530 pC, or by using standard-index notation with non-prefixed units, for example 5.30×10^{-10} C. The prefix method has been chosen here. For quantities in the limited exponent-range needed for most of this work it is rather shorter, and it permits many discussions to stick to a simple range of ones to thousands of some unit such as picocoulombs; its disadvantage is that one cannot see whether, for example, the zero in '530 pC' is a significant digit.

The units of quantities presented in plots and tables are shown in brackets, for example Q [pC], which is concise and unambiguous for all the needs in this work. The method recommended by standards organisations, of writing the quantity together with its conversion into a 'pure number', for example Q/pC, is indeed more versatile for some complex cases, but is arguably less concise when divisions are desired within quantities such as i/v or units such as V/mm, which prompts an ugly proliferation of grouping-parentheses or a recourse to exponents such as $\mathrm{V}\cdot(\mathrm{mm})^{-1}$. Prefixes are used consistently, and are chosen to fit the subject: for example, kV/mm and mm/µs seem more appropriate than the base quantities or other prefixes when dealing with PD in cavities.

Equations are referred to by just their number in parentheses. Some 'empirical' equations are included, using a convenient function to describe a relation to an acceptable accuracy within some range; examples are (7.1) and (20.1). In contrast to derived equations, the empirical equations may be dimensionally inconsistent; explicit division of each variable by its unit has not been used, so the variables should be treated as being already pure numbers. This convention is common in the engineering subjects in which such equations are used.

Cross-references mostly use a compact notation of sections or pages in brackets: this sentence is in [s.1.9] on [p.7]. Citations of papers and books use the author-year format, taking the first three letters of the first author's surname then the last two digits of the year, and appending a letter if disambiguation is needed: this thesis could be [Tay10]. Citations of standards-documents use a single letter to denote the organisation, followed by the standard-number. Compared to the simple numbering that seems the commonest method in engineering, this takes rather more space and can be a little ugly, but it is much clearer and more memorable: a reader familiar with the field would be able to guess many of the sources at a glance. The bibliography is right at the end to make it easy to flick over to it for looking up citations whenever this does become necessary. If a freely available electronic version of a document is known of, a link to it is included in the bibliography entry. References to particular parts of long works include a page, section or chapter number within the citation, such as [Tay10, p.7]. Only one citation or cross-reference is ever used within a pair

of brackets.

Chapter 2

Stator insulation

This chapter describes the components of a stator, variations between machines of different power and speed ratings, commonly used insulation systems, and some common types of defect and fault. Diagnostic methods used on stator insulation are described later, in chapter 4. The focus here is mainly on details that are needed in the later chapters. For a broader and deeper treatment of rotating-machine insulation in the stator, rotor and core, over a wide range of ages and power ratings, [Sto04] is highly recommended. Some papers giving good descriptions of stator insulation materials are [Bou04] and [McD93].

2.1 Construction and materials

The stator of an ac *rotating machine* (motor or generator) is a stationary construction consisting of a *core* of laminated steel that carries the magnetic fields, surrounding structures that support this core, and *windings* of insulated conductors that carry currents to produce the stator's magnetic field. A simple diagram of a stator core is shown in figure 2.1, as a cross-section that indicates the shape of each thin ($< 1\,\mathrm{mm}$) steel *lamination*, and as a three-dimensional view showing the length.

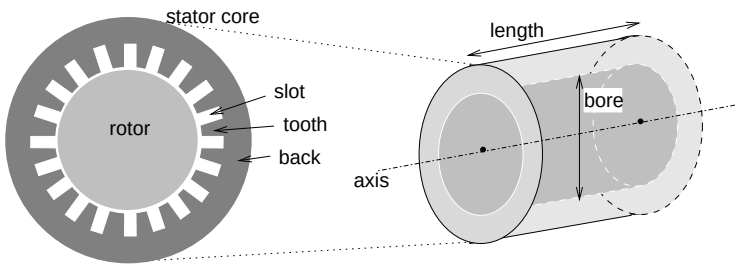

FIGURE 2.1: Basic construction of the stator core. To the left is a cross-section, indicating how a single lamination would look. There would typically be many more slots and teeth. Details of the rotor are not shown.

The steel of the core is an *electrical steel*, suitable for carrying alternating magnetic flux without high power losses. Such steel is often referred to as the *iron* of the machine. It is an alloy of iron with some percent of silicon, a little aluminium, and possibly some copper; several other elements, in particular carbon, have to be excluded as much as possible in order to get good magnetic properties. The laminations have thin insulation on their surfaces to prevent the large circulating currents that would otherwise be induced by the magnetic flux passing through the core.

Each lamination has pieces punched out to form the central *bore* in which the *rotor* is placed. Around the bore, *slots* are punched out, with *teeth* left

between the slots to carry the magnetic flux that links with the rotor. Radially beyond the teeth and slots is the *back*, which links the teeth together to carry the magnetic flux between the groups of slots forming different magnetic *poles*. There are radial gaps forming *cooling ducts* at regular intervals along the axial length of the core to allow cooling air or other gas to circulate.

The winding occupies the slots, and extends beyond the core in the *end-winding* (or *overhang*) region, where each insulated conductor emerges from its slot and travels tangentially some way around the end of the core before passing into another slot or connecting to a terminal.

Figure 2.2 shows end-views of a large motor whose rotor has been removed to expose the inside of the stator core. The bore is about 1 m in diameter.

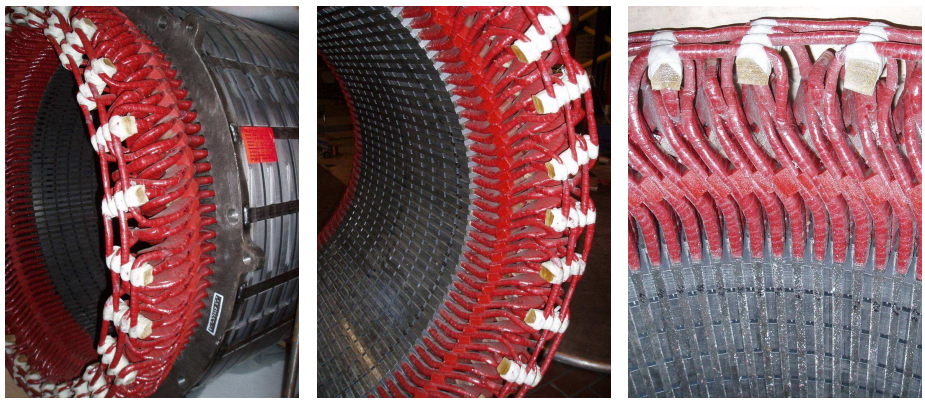

FIGURE 2.2: The stator core and winding of a several-megawatt motor, with the rotor removed.

In the left picture some of the supporting structure outside the core can be seen. In the centre picture and the close-up on the right, the stator slots can be seen running axially, the cooling ducts that carry radial air-flows can be seen running tangentially, along the *face* of the stator iron on the inside surface of the bore. The winding can only be seen at the end-winding parts, as the slot parts are covered by the wedges that hold the winding in place. In the right picture the supports within the end-winding can be seen.

Although these images give a useful impression of the main features of the construction of high-voltage stator windings, it should be borne in mind that there is much variation in the size and appearance between different machines.

The electrical connection of windings is very varied between machines. It can be expected that there will be three phases, usually with one side of each phase-winding connected to a star-point (neutral). In a small machine each phase-winding may simply consist of a single piece of copper, a *conductor*, passing back and forth through the slots between the neutral and high-voltage terminals. In a large machine a phase-winding may consist of several such conductors at different positions around the stator, connected in parallel to thick *ring-buses* that run around the end-windings; each of these conductors may in turn consist of several parallel *strands* (also known as *subconductors*) running adjacent, to cope with the high currents.

2.1.1 Multiturn coils and Roebels bars

Low-voltage generators and motors, with rms line-voltage† not more than about 1 kV, have *random-wound* stators in which a thinly insulated wire is inserted in the slots without particular attention to the relative placement of the many adjacent wires; the insulation is mainly determined by mechanical requirements. This type of machine is not considered at all in this work.

Stator windings of higher voltage-ratings have a *form-wound* construction, in which units with carefully configured conductors and insulation are prefabricated to fit neatly into the width of a slot. Conductors of rounded-rectangular cross-section are thinly insulated then are assembled into a conductor bundle with well-defined relative positions; the bundle is then wrapped in a thicker layer of outer insulation to separate the conductors from the earthed core of the stator. There are two broad types of these form-wound prefabricated units, the multiturn *coil* and the Roebel *bar*; these are contrasted in figure 2.3.

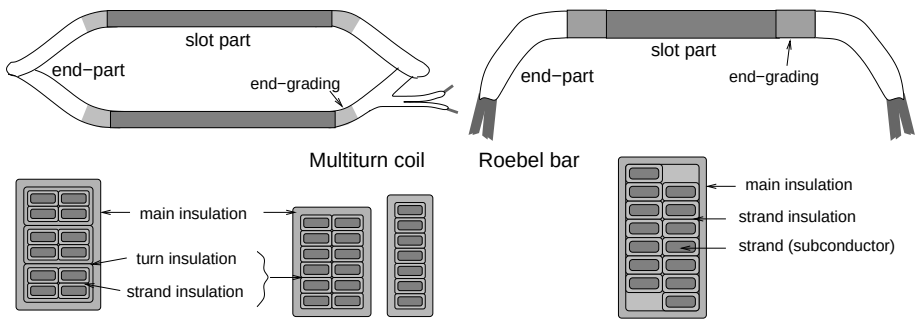

FIGURE 2.3: Form-wound units: multiturn coil and Roebel bar. Examples of cross-sections are shown below the coil and bar. The 'slot part' will run along the full length of the core (figure 2.1), and the 'end parts' will protrude.

Medium-rated machines, generally up to tens of megawatts, have coil-type windings. This covers most motors and the lower range of generators. A *conductor* is covered with a layer of insulation that will tolerate the voltages in the order of hundreds of volts that are built up within a few turns through the stator; the conductor is wrapped into several turns to form a coil that has two long straight sections that will fit along two slots at different positions around the stator core. Both ends of the conductor emerge at one end of the coil, to be connected in the end-winding to other coils or the terminals. When the conductors need to have a large cross-section several *strands* (subconductors) may be used in parallel to improve flexibility and reduce eddy-current losses, with light insulation against the few volts that may occur between the parallel strands. In modern coils it is common for just one type of insulation to be used on each piece of copper, to provide both the *strand insulation* between parallel strands and

† The conventional way of quoting the rated voltage of power equipment is followed here: it is the rms *line-voltage*, the voltage between phases. The rms *phase-voltage* applied between each the conductor and the earthed metal in normal operation is therefore $1/\sqrt{3}$ of this rated voltage. However, in all laboratory work reported in this thesis the voltage is a *peak* value (amplitude) from HV to earth.

the *turn insulation* between series-connected turns of the conductor. Insulation for the low voltages that strand and turn insulation experience in operation is determined more by mechanical than electrical breakdown properties, though the turn insulation is exposed to much higher voltages when transients enter the winding.

Around the bundle of lightly insulated conductors the *main-insulation* (or 'groundwall' insulation) is applied, to withstand the full voltage between the conductors and the earthed metal of the stator core.

For the coil shown in figure 2.3, three cross-section examples are given: the first has four strands in each of three turns, with separate turn and strand insulation; the others are a double then a single stack with either a combined turn and strand insulation or with non-stranded conductors. In a typical construction the main insulation would be some millimetres thick and the strand or turn insulation less than a millimetre.

Failures of insulation between strands can cause overheating, leading to slow deterioration. Failure of insulation between *turns* causes large currents, immediate melting of the conductor, and probable destruction of the main insulation. Failure of the main insulation is the main type of failure that is caused by continuous aging rather than by mechanical damage or severe transients. The methods considered in this work excite the whole of a phase-winding at a single potential with respect to the core, so that only the main insulation is highly stressed. Problems in the turn or strand insulation are therefore not directly tested.

Larger ratings of machine use bar-type windings, in which the prefabricated unit is a bar that runs along a single slot. All the subconductors in the bar are strands that will eventually be connected in parallel. They are continuously *transposed* (swapped in position) within the bar so as to minimise the difference in induced voltage between them and thereby reduce circulating currents. Each bar adds only a half-turn of voltage to the winding, and needs to be connected to another bar at each end of the stator core. The avoidance of multiple turns means that only the main insulation is critical: breakdown of strand insulation is undesirable, but its effect on the main insulation is slow.

To avoid having to keep referring to 'coil-side or bar' in this thesis, the term 'bar' will sometimes be used as the general case of the unit of insulated conductors that passes through a slot, regardless of whether this in fact is a side of a multiturn coil or a true Roebel bar. Apart from concerns about turn-insulation faults, the difference is usually unimportant.

2.1.2 Insulation materials

To make a compact rotating electrical machine, the facing surfaces of the stator and rotor need to maximise the amount of copper for carrying axial currents and the amount of iron for carrying radial magnetic flux [Lai66]. Space wasted due to the volume occupied by insulation between the iron and copper results in a larger, heavier and more expensive stator construction. Thermal sensitivity of the insulation reduces the permissible currents in the copper, with the same effect. The chosen insulation should therefore be highly tolerant of heat, electric

stress and the discharges that may occur in any small gaps that may arise within the insulation.

The natural mineral *mica* is strongly resistant to damage by thermal, chemical and electrical mechanisms, and for this reason has provided the electrical strength in main-insulation of high-voltage machines for about a century. An organic *impregnant* is used to fill the spaces between the pieces of mica, and to give greater mechanical strength and heat transfer. This composite insulation is unique to the special demands of rotating machines, contrasting with the waxed and oiled papers common in transformers, bushings[†] and power cables, or the synthetic polymers of more modern power cables.

Mica is a laminar structure of highly chemically-inert flakes. There are several forms, differing a little in chemical structure and physical properties. The *muscovite* form is used in machine insulation. It can operate up to about 550 °C [Sto04, p.83], well beyond the capability of any impregnant that is used.

Up until the 1940s the mica for main insulation was in the form of *splittings*, layers split from sheets of natural mica. These were mounted on a backing of a natural-polymeric substance such as Kraft paper, and bonded with the natural resin shellac, forming *micafolium* sheets. The development of *mica-paper* in the 1940s was first driven by scarcity of large pieces of mica for making micafolium. Small pieces of mica are broken into very small pieces, then a paper-making process is used to produce a thin layer on a backing material such as fibres of glass or synthetic polymer. It was soon found that although there is more free-space in the mica paper compared to micafolium, a thorough pressing and removal of surplus impregnant can increase the density of mica, and combined with the much more consistent thickness of mica paper the final product is actually better. In the decades following the introduction of mica paper, some stators were insulated with micafolium, some with mica paper, and some with a combination of the two [Eva81]. An approximate cross-section of insulation built from mica paper is shown in figure 5.1 [p.48]. Modern production processes use machines to wind the tape with more consistent position and tightness than is achieved by hand; later parts, in particular around connections in the end-winding, are taped by hand. In spite of being applied by machine, tapes applied in normal production facilities are found sometimes to have defects of gaps and wrinkles [Vog06] in a newly manufactured winding.

Mica in the forms described above would provide very little mechanical strength and would contain voids all over where discharges could happen. The spaces are filled with an impregnant compound that holds the flakes together, filling whatever gaps remain. Again, the period from 1940 to the early 1950s was a time of large change. The impregnant used up to this time was an *asphalt*, sometimes called an *asphaltic-resin* or *bitumen*. This is a thermoplastic material, meaning that it softens at increased temperature. The asphalt can migrate out of some parts of the insulation when at high temperature. The high chance of spaces being left in the insulation due to migration of asphalt limited the service stress to about 2 kV/mm. The asphalt and the varnishes

[†]Bushing: an insulating structure around a high-voltage conductor, to allow it to pass through a surface at another potential, typically earth.

applied between layers of micafolium sometimes had *drying-oils* included, to give less softening of the insulation with temperature; operating temperatures would generally be above the glass-transition temperature, so the insulation was still soft even if not readily flowing. The effect of oxidation by long exposure at high temperature in air also helps to harden the asphalt, but this will not happen in hydrogen-cooled machines. Asphaltic insulation expands considerably with temperature, making a much tighter fit of bars in slots when at operating temperature rather than cold. The asphalt-micafolium type of insulation has a high dielectric loss compared to later insulation, and has a non-negligible conductivity. It also absorbs water, causing an increased dielectric loss and capacitance. Asphalt-micafolium insulation is usually of temperature class[†] 130, which implies a normal operating temperature some tens of celsius lower than this number. In the early 1940s *polyester-resin* started to be used as a replacement for asphalts. This is a thermoset material that is *cured* after impregnation, to become a stable solid. It has the advantages of not melting even at high temperature, having higher mechanical strength, and being much less absorbant of water. In the late 1940s *epoxy-resin* started to be used. Epoxides have all the functional advantages of polyesters, along with even better mechanical strength and thermal stability; they also shrink far less on curing. The main troubles were the cost and the high viscosity of impregnant, which required incorporation in the mica tapes since it would not easily flow into the insulation from outside. The viscosity was soon improved, and the cost is apparently considered worthwhile in modern stator insulation, which in high-voltage machines almost always uses epoxy-resin. The resultant composite of mica, glass-fibre and epoxy resin is mechanically strong, with a tensile strength rather greater than that of copper [Tav08, p.14]. Electrical stresses are typically 3 kV/mm, and can be as much as 5 kV/mm [Sto04, p.75]. The thinner insulation permitted by the thermoset materials leads to greater thermal conductance out of the windings, and more space available for copper. The thermosets also permit higher operating-temperatures, epoxy-mica being usually of class F, 155 °C. All of these factors increase the potential rating or compactness of a machine. The transition from asphalts to epoxy-resin did not of course happen as a sharp step: asphaltic systems continued to be used for some decades after the introduction of the synthetic resins. A standard [E43, p.17] for testing 'insulation resistance' [s.6.4.2] assumes that post-1970 insulation will be synthetic.

There are three main ways of getting the impregnant into the assembled mica-based insulation. Vacuum-pressure impregnation, *VPI*, was used even on early asphaltic systems and is still in wide use. The insulation is dried and put in a chamber where it is exposed to a very low pressure, to get air and dampness out. The chamber is then flooded with impregnant, and the pressure is driven up to several atmospheres to force the impregnant into the insulation. Excess impregnant is cleaned off, and the modern systems are then heated to cure

[†] The insulation temperature-classes are either a number or (deprecated) a letter. The number is the temperature, in degrees Celsius, expected to give a 20 000 hour lifetime by some definition of thermal degradation [Sto04, p.57]. Common in stator insulation are classes 155 (F) and 130 (B). The actual operation is usually well below this value.

them, a typical treatment being 160 °C for two hours. VPI can be categorised as having two variations, global and individual. In *global VPI* the coils or bars are inserted in their slots in the core, with connections made and end-winding supports assembled, then this entire stator assembly is put into the VPI process. This has the advantage of not requiring already-hardened coils to have to be forced into their slots; it also creates a firm bond and good heat-transfer between the coils and the slots. It is the method commonly used for machines rated in the tens of megawatts, which includes most large motors. In *individual VPI* of coils or bars, these components are put through the VPI and curing processes and then are inserted in the stator. Although global VPI has been used on increasingly large machines, up to some 200 MW on some recent turbo-generators [Sto04, p.143], the larger sizes all use individually processed bars or coils, with the further advantage that each one can be inspected and electrically tested before being accepted for insertion in the stator. The non-VPI method is *resin-rich* insulation, where the impregnant is combined in the mica tapes, and the bars or coils are then cured by hot-pressing to force the layers together at the curing temperature. This was originally used when epoxy-resin compounds were too viscose to impregnate the windings from outside, but it is still the preferred method by some manufacturers.

The turn and strand insulation will not be covered in detail here, as only the main insulation is stressed in the types of measurement used in this work. Traditional turn-insulation is like thin main-insulation, and modern combined strand/turn insulation sometimes uses specially durable synthetic polymers together with thin mica paper.

2.1.3 PD prevention at the surface

Small gaps are inevitable between a bar and the stator core, or between adjacent bars connected to different phases. In stators of some 5 kV rating and higher, these gaps could have high enough electric field to cause PD if they were not shielded. A mildly conductive coating called the *slot semiconductor* or *slot corona-protection* is applied around the outside of the main insulation, in the form of varnishes painted onto the bars or tapes wrapped outside the taped insulation. The material must conduct enough to prevent PD, but not so much as to cause considerable loss by currents driven by the induced voltage along the length of the slot. Carbon-black is a filler commonly used to provide the conductivity. The surface resistivity[†] to achieve this ranges from about 100 Ω up to 2 kΩ [Eme96] or 10 kΩ [Sto04, p.24]. It is quite variable, depending on batch variations, the layer's applied thickness, and manufacturing treatments such as impregnation; it is also affected by aging, which can reduce the resistivity by several times [Eme96] over the insulation's lifetime.

[†] Surface-resistivity: the resistance between opposite sides of any square slab of the surface: this depends on material (bulk) resistivity and surface thickness, and is independent of the size of the square. It is a useful description for situations where the current runs along a layer whose thickness as well as material are fixed. The unit is Ω as opposed to Ωm for bulk conductivity, and is sometimes written 'Ω/sq' to emphasise that it is a general property of any square of the surface, not the resistance of a particular object.

As the windings emerge into the end-winding region, another type of semiconductive coating may be applied, extending some ten centimetres along the bars to limit the surface electric field around the end of the slot-semiconductor. This is explained in more detail in chapter 19. It is referred to in this work as the end-winding *stress-grading*; among its other names are *end corona protection* and *end semiconductor*. It is common in windings rated above about 5 kV, and is increasingly adopted at voltages down to about 3.3 kV [Sto04, p.158] on machines that are to be used with IFDs [s.7.3.1]. The material has strongly nonlinear conductivity [s.20.3]: the surface resistivity of the coating is a few gigohms at quite high fields around 300 V/mm, and increases some orders of magnitude at low fields. The end-winding region beyond this region has no surrounding conductor or semiconductor, so capacitive coupling exists between the end-windings.

Within a Roebel bar a soft semiconducting layer may also be put around the whole group of strands, providing an equipotential layer between the lightly insulated strands and the main insulation, to prevent PD in voids between the rounded strands and the wound main-insulation tape.

It is common for the entire end-winding part of a coil to be covered with a top layer of insulating material, even covering the stress-grading. This provides some protection against chemical and mechanical damage, but makes assessment and repair of the stress-grading more difficult.

For very high-voltage stators a mildly conductive layer may be applied on the surfaces of the end-windings; this is thought to help in passing a 'hipot' test. The surface resisitivity of hundreds of kilohms quoted in [Sto04, p.26] makes this closer to slot semiconductor than to the end-winding grading; presumably it results in a surface at a high and substantially uniform potential, separated from the slot semiconductor by the usual stress-grading.

2.1.4 Assembly in the slots

The bars or coils are inserted in the slots, usually with two bars or coil-halves stacked radially in each slot. In figure 2.4 cross-sections are shown of coil-sides and bars in their slots. Note that some of the strands in the bar-type winding have ducts for direct water-cooling, as described in section 2.1.6.

A *slot wedge* of insulating material runs in grooves along the open end of each slot to hold the bars in place. It is very important to hold the bars tight in the slot, even after the changes in the insulation that occur from curing, aging and exposure to electromagnetic forces. Vibration can mechanically abrade the outer surfaces of the bars. In machines of some 20 MW and above it is common to have a two-part wedge with some degree of elasticity, to maintain some force even if the bars slightly shrink [Sto04, p.27]. The need of elasticity in the wedging is greater in thermoset insulation [McD93]; the insulation has not the thermoplastic materials' tendency to fill extra space, and the hard edges of the bars are readily abraded at their relatively few contact-points with the surrounding core. Filler strips of elastic material may be used as *packing*; the *top*, *midstick* and *bottom* packings lie along short sides of bars by the core, between bars and by the wedge; there may also be *side*-packing between the bars and the teeth. A springy rippled sheet known as a *ripple-spring* is

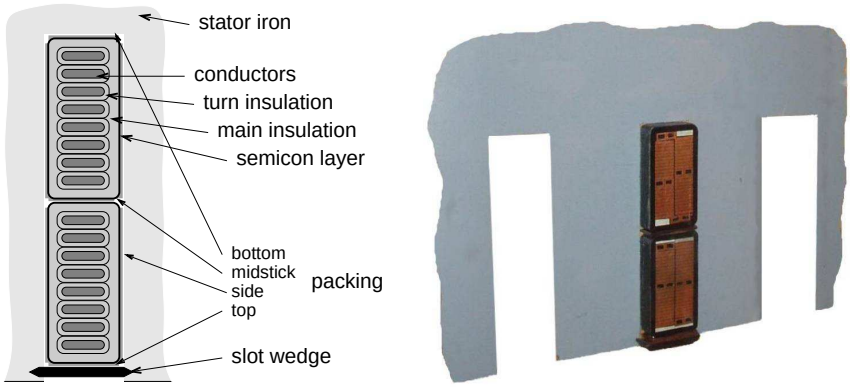

FIGURE 2.4: Cross-sections of stator windings in their slots. Left: diagram of sides of two multiturn coils occupying a slot. Right: a pictorial cross-section of two large water-cooled Roebels bars in a slot, with empty slots shown on either side.

sometimes used instead of soft packing, particularly under the wedge and at the side; ripple-springs are common in turbo-generators [McD93]. In machines of above about 5 kV, packing and ripple-springs will be made semiconductive so as to connect the outsides of the bars to the stator core, preventing breakdown of the gas in any gaps.

2.1.5 Rotational speed

There are two main families of generators defined by speed of rotation and the consequent shape. Motors that are large enough to have high-voltage stators usually have a design closer to the higher-speed generators. The large differences in shape are significant for the measurements being investigated here: they affect the ratio of winding-lengths in the slot and end-winding regions, and the distances from the terminals to the furthest parts of the winding.

Turbines driven by steam or other gas operate best at high rotational speeds, even as high as the electrical network frequency of 50 Hz or 60 Hz. The *turbo-generators* used with these turbines have just one or two pairs of poles per phase, rotating therefore at the whole or half of the frequency of the ac network. The high speed and the consequent low number of magnetic poles lead to a relatively small diameter and long length of the core; even large generators of 660 MW have bores in the order of 1 m.

Turbines driven by water operate at low rotational speeds, generally some tens of times less than the network frequency. The *hydro-generators* used with these turbines therefore need tens of pairs of poles to in order to satisfy the combined requirements of mechanical and electrical frequencies. The diameters are large, as is required by the large number of poles and permitted by the low rotational speed. Large hydro-generators, from tens to hundreds of megawatts, differ from some smaller ones and turbo-generators in having a vertical axis. The axial length of the stator core is much less than in a turbo-generator, but the diameter can be many times more, in the order of 10 m, and has connections running all around it linking the many groups of windings. There

is therefore generally a greater ratio of end-winding length to slot length in a hydro-generator than in a turbo-generator.

In the end-winding there is *blocking* by wooden blocks that maintain separations, and *lashing* by fibrous bands that bind the windings together, even when high currents exert forces between the conductors; these are seen in figure 2.2. There may be *bracing rings* to give a strong mechanical support all the way around the circumference of the end-winding.

2.1.6 Cooling

Heat is generated by losses in the copper conductors, the iron core and the insulation itself. To permit high loadings with modest physical size and cost of the machine, the temperature rise caused by this heat must be kept low. There are several methods of cooling used in different sizes of machine, and all have an influence on aging and diagnostic measurements.

Removal of heat from the windings only after it has passed out through the insulation is called *indirect cooling*; this is normal in small machines, and is used in some as large as a few hundred megawatts. Removal of heat by a fluid passing within the windings is *direct cooling*. The fluid may be water or hydrogen. In some cases a few of the conductor strands are hollow to carry the fluid; in others stainless-steel pipes may be included. The connections in the end-windings are made with insulating pipes. Hydro-generators use only water for direct cooling, and only on large machines of 500 MW and more [Sto04, p.7]. Turbo-generators use water or hydrogen, in sizes from some 200 MW and up; in old machines direct-cooling may be used in even lower ratings. Direct water cooling results in a 100 °C limit to the conductor temperature, reducing the thermal stress on the insulation as long as cooling channels are not blocked; it also gives the risk of leaks that slowly moisten the insulation, although high pressure is used in the surrounding gas to try to prevent water from escaping.

The gas that circulates within the machine, passing through the cooling ducts in the core, over the iron and the outside of the coils or bars, is either air or hydrogen. The *air-cooled* machines are usually at atmospheric pressure. They have the variation of being either *open-ventilated* using air from outside, possibly through a filter, or *recirculated-air* with the air sealed in and passing its heat to external air or water in a heat-exchanger. The *hydrogen-cooled* machines are usually at a high pressure such as 3 atmospheres (300 kPa). Hydrogen cooling is used in recent machines only above a few hundred megawatts, but has been used down to 50 MW [Sto04, p.6]. An open-ventilated machine has its components exposed to the external humidity and to fresh oxygen that can react with hot insulation. On the other hand, recirculated air forces harmful products of discharges, such as ozone, to remain until they have reacted within the machine. The absence of oxygen in hydrogen-cooled machines prevents much of the oxidative aging that is the major cause of the organic part of the insulation becoming weak and brittle. The high pressure usual with hydrogen cooling increases the breakdown strength of the gas, reducing the tendency to discharges; even when discharges do occur, they cannot produce ozone without oxygen, so the wear on the insulation is reduced.

2.2 Failures in stator insulation

A failure in stator insulation is a low-impedance path between conductors that are supposed to be insulated from each other, such as those of different turns, bars, or phases, or from phase to core. This section indicates the potential usefulness of diagnostic measurements [s.4.1] on stator insulation, and lists some common ways in which failure occurs. More details are given in later chapters about the gradual processes of aging [s.3.2] and about partial discharges in stator insulation [s.7.5].

2.2.1 Failures of rotating machines

Two ways of classifying failures of high-voltage rotating machines are by the component in which the final failure was seen, or by the suspected root cause. To a designer the root cause may be of more interest, but for diagnostic purposes the important matter is whether the development of a failure would be predictable from the studied component. The distribution of failures over components and causes varies between different types of machine, but a rough indication is given by the following references.

According to [Tav08, ch.2], which considers all types of rotating machines including low voltage ones, about half of the failures occur in stator insulation. The root cause is usually *not* direct electrical wear, but a weakness introduced by damage from other mechanisms or by problems in design or construction; the final breakdown of the weakened insulation is then electrical.

In hydro-generators, experience within a large operator is that most failures are electrical [Hud05], or in other words stator or rotor insulation; it is again noted that the root causes may be non-electrical. In [Sto04, p.131] a large IEEE[†] study is cited as finding about 40% of failures of hydro-generators to occur in stator insulation; it is also mentioned as an opinion that large *turbo*-generators generally have a higher proportion of rotor faults. A CIGRE[‡] study of hydro-generators examined 69 failure incidents in detail, and is summarised in [Bru08b] as finding 56% of the cases to involve insulation damage, with root causes determined as 31% aging, 25% contamination, 22% internal PD, 10% loosening in slot or end, 7% thermal cycling or overload, 3% defective corona-protection, and 2% overvoltage. Large studies of failed components and causes in turbo-generators have not been found for comparison.

A study by EPRI[§], cited found failures in motors to have root causes located 41% in bearings, 37% in the stator, 10% in the rotor, and 12% in accessories. In [Gup96] an IEEE study is cited as finding about a third of 'forced outages' of large motors to be failures of stator insulation.

In summary of the above, it seems that about a third to a half of failures of high-voltage rotating machines occur in the stator insulation. Even if the root cause is not the electrical stress, detection of the stator insulation's deterioration by diagnostic measurements is a useful way to predict and avoid failure, for those failure-types that occur over timescales long enough for warning to be given.

[†]IEEE — Institute of Electrical and Electronics Engineers (N. America).
[‡]CIGRE — International Council on Large Electric Systems.
[§]EPRI — Electric Power Research Institute (N. America).

2.2.2 Some stator insulation failure-modes

The stresses leading to failures of stator insulation may usefully be divided into two groups: aging [s.3.2] has a gradual effect over a long time, and its causes such as temperature or working voltage are generally well known and controlled; transient stresses occur seldom and generally unpredictably, such as voltage impulses from the network, out-of-phase synchronisations of a machine to the network, or loose metallic parts flung from the rotor.

These differences in stresses are relevant to the predictability of failures. Immediate failures due to extreme transient stresses clearly cannot be predicted by diagnostic measurements on the stator insulation, even if some might be prevented by checks and measurements on other parts of the machine. In insulation that has been deteriorated by aging, the final failure is likely to stimulated by a mild transient stress that would not have been a trouble in new insulation [Sto04, p.131]. A succession of mild transient stresses may also cause progressive deterioration, or may cause changes that enable aging mechanisms to have a faster effect.

The remainder of this section brings together short decriptions of some root causes and final manifestations of stator insulation failure, including approximate timescales of failure. It does not try to be thorough, as the details are only used here to give a grasp of the extremes of very mild and more worrying problems; more detail can be found in [Sto04], [Tav08], [E56] and other books and standards. The diagrams in figures 5.2 [p.50] and 7.3 [p.90] may be helpful in considering the mentions of leakage paths and partial-discharge sites.

Failures of turn insulation in multiturn coils also mean immediate failures of the machine, often including damage to the main insulation [s.2.1.1] so that they may appear as main-insulation failures. The turn insulation can be stressed in service when driven from an IFD [s.7.3.1], with repetitive fast-rise-time pulses causing large voltages and between the first turns of the winding, with the possibility of PD. Common offline diagnostic measurements do not stress the turn insulation, so they cannot find weaknesses between turns [Gup96]; tests of impulse-voltage withstand [E792] provide some degree of confidence of turn-insulation quality.

Extreme currents during bad synchronisations, or fault conditions on the electricity network, cause quadratically increased magnetic force between bars; in the end-winding this can cause loosening of the lashing or even cracking of the insulation. Thermoset insulation, being harder than thermoplastic, is often more vulnerable [McD93] to looseness of windings and short-circuit forces. Long-term vibration in end-windings with poor lashing and blocking can cause damage to the insulation directly [s.3.2.5], or indirectly by causing problems such as water leaks and broken conductors. In thermoplastic insulation systems, where generally the tapes are weaker as well as the asphalt being softer, a *girth-crack* can occur, where the main insulation is 'necked' (thinned) by gradual movements of the tape layers under thermal cycling [Kle04, p.368], commonly few centimetres outside the core. This is sometimes called tape-separation, although that term can be used more generally for loose tapes anywhere. In

rare cases cracks may reach the conductor, permitting contaminants to form a mildly conductive path.

Mechanical *slot discharge*, often just called slot discharge, develops from looseness of bars in the slot, due for example to shrinking of insulation or loosening of ripple-springs. The bars can then vibrate in the slot, and have large areas without good contact with the slot [Jac82]. This leads to mechanical abrasion, and to significant contact-sparking that transfer current from the slot semiconductor to the earthed laminations of the core; the problem is particularly strong with the harder thermosetting insulation [McD93], which more easily makes contact with just a few points of the core. The discharges occur as the bar vibrates, so the problem is often impossible to see in offline measurements, and strongly load-dependent† in online measurements. The discharges can be very large compared to any other PD source within the slot-part of a bar. The removal of the slot semiconductor then leads to simple PD in the air-gap between the solid insulation and the core; this 'stage 2 slot discharge' can increase the wear rate beyond the effect of the mechanical abrasion. By machine standards this is a fast mechanism, taking perhaps two years to failure [Sto04, p.149].

Electrical slot-discharge differs in that there is no need of looseness, the root cause being a poor semiconductor layer of insufficient conductivity or with voids between it and the insulation [Sto04, p.152]. Displacement currents in the insulation must flow out into the core, requiring passage along parts of the slot semiconductor at cooling ducts and on the faces of the bar that are not in direct contact with the core. Insufficient conductivity leads to excessive heating and consequent wear, with surface discharges across particularly weak regions. The discharges are not specially large, but are generally many. The wear is much slower than for mechanical slot discharge, more like twenty years to failure.

Regions where layers are not in good contact are *delaminations*, which can occur due to poor winding of the mica-paper tape [s.3.2.3], poor impregnation, or stresses in service such as thermal cycling [s.3.2.2]. The spaces thus formed are relatively short in the radial direction along which the electric field is aligned, but longer in the other directions. Delaminations between layers within the main insulation do not tend to develop in modern Roebel bars, but are more common in multiturn coils [Hud05]. Delaminations at the conductors can occur in either type of construction, but are much more dangerous for multiturn coils where wear of the thin and possibly non-micaceous turn insulation by PD can lead to failure more quickly than could happen if the whole main insulation had to be worn through [Sto04, p.146]. The risk associated with delaminations is given by [C3427, s.E.1.2] as 'high', placing it above all considered sources other than slot discharge.

The overlap where the end-winding stress-grading connects to the slot semiconductor can develop poor contact, particularly when the stress-grading is painted rather than taped [Sto04, p.155]. There was PD at this point in about half of the hydro-generators studied in [Hud05]. The discharge is across the surface between the two coatings, and does not cause rapid wear of the actual

†Load-dependent: dependent on the current in the conductors.

insulation; failure is not very likely even in twenty years. Discharges may also appear at the open end of a grading that is too short for its purpose.

Further out in the end-windings, surface contamination with water or dust can lead to *electrical tracking*, where the nonuniform conductivity leads to discharges in particular regions, which then become carbonised and more conducting, moving the stress out to other regions. A surface resistivity below some tens of megohms allows this to occur [Sto04, p.161]. Tracking may be across bar surfaces, or along the surfaces of blocking and lashing between bars. The track of relatively high conductivity grows across the surface, and discharges can work slowly into the insulation. Failure times can be ten years or more.

Also in the end-windings, insufficient clearances can lead to PD in the air-gaps between the long sides[†] of bars from different slots, or between the short sides of bars that share the same slot, or from bars to the earthed metal *pressure fingers* that sometimes are located between slots [Hud05]. This is much more common in air-cooled than in hydrogen-cooled machines, and can be increased by poorly cured epoxy with abnormally high permittivity. Times to failure by penetration of the main insulation are five years or more [Sto04, p.168].

[†]long/short side: consider the cross-sections in figure 2.3 [p.11].

Chapter 3

Aging of Insulation, Natural and Accelerated

The irreversible changes that gradually occur in an insulation system due to stresses from operation and the surroundings are known as *aging*. Aging generally makes the insulation less able to withstand the stresses to which it is exposed. This chapter starts by describing common stresses and aging-mechanisms, particularly in stator insulation; it then describes how studies of insulation systems attempt to accelerate aging-rates to permit evaluation of materials and test-methods within acceptably short times.

3.1 Insulation aging: mechanisms and synergies

A popular way of dividing the stresses involved in aging of insulation is the acronym *TEAM*, for thermal, electrical, 'ambient' and mechanical stress. The ambient category is the least self-explanatory: it includes for example the effects of chemicals and radiation.

One type of stress may cause another directly, such as when electrical stresses cause PD which generates heat, ionising radiation and reactive chemicals, or when differential thermal expansion causes mechanical forces. The aging effects of one type of stress may change the effects of another, such as when thermal aging reduces mechanical strength or when thermal or mechanical aging produces gaps in which PD can occur. Strong nonlinearity in the effect of each stress is also to be expected.

These synergies makes investigation particularly difficult: however carefully one might have gathered results for the effect of, for example, high temperature or electric field acting alone on an insulation system, the effect of both together is only a moderately educated guess.

3.2 Aging of stator insulation

Stator insulation is a complicated construction, both in the radial direction from conductor to stator core, and in the axial direction from the slot-part through to the end-winding. There are several interfaces, between metals, semiconducting tape, insulation material and stress-grading, as well as within the composite mica-based insulation material itself; the interfaces are critical points in many aging mechanisms [Kau02]. The following are the main effects of the TEAM stresses in stator insulation.

3.2.1 Thermal aging

The thermal decomposition of organic insulation materials is a well-established feature of service aging of stator insulation. In air-cooled machines there can be

oxidation and scission of polymer chains [Sto04, p.138], and cross-linking [Tav08, ch.2]. Asphaltic insulation becomes harder, which to some extent may be an advantage in preventing weak puffy regions of mica caused by migration of soft asphalt. Epoxy, however, is only worsened by these reactions, becoming weaker and more brittle. In machines with a hydrogen atmosphere, the generally lower insulation-temperatures and the lack of oxygen make thermal aging relatively unimportant.

A severe case of poorly bonded epoxy-mica insulation after thermal aging is shown in [Bru08b], with many small cavities where PD could occur. The brittle insulation is more easily delaminated by mechanical stresses, and the cavities allow the electrical stresses to cause PD, which in turn produces heat, radiation and reactive chemicals.

The rate of thermal decomposition of organic insulation, even at several tens of celsius above the rated temperature, is often considered as an *Arrhenius rate reaction*, where an activation energy is needed by the reactants. This results in an exponential temperature-dependence: a doubling of reaction rate for an increase of 10 °C is widely assumed for stator insulation [Sto04, p.45]. The temperature has to be quite high for this reaction to happen to any considerable extent: thermal stress of epoxy in aging tests is relevant above about 140 °C [Bru08a].

3.2.2 Thermal cycling

This form of stress, although originating in changes of temperature, results in a mechanical stress on the insulation. Copper has a greater coefficient of thermal expansion than the modern types of insulation [Sto04, p.45]; the coefficients can vary as much as ten times between the copper, insulation and core [Kau02]. Changes in temperature therefore cause different degrees of expansion in these tightly bonded materials. The difference in expansion is increased when load-changes happen so suddenly that the temperature in the copper, where most of the heat is generated, changes significantly without the temperature in the insulation and core having had time to change.

The differential expansion causes shear stresses at all the interfaces that lie between the copper conductors and the core: conductor to insulation, tape-layers in the insulation, and bar to core. The mechanically stressed interfaces are susceptible to delaminations [s.2.2.2]. The stresses are greater for longer slot-lengths, such as those of large turbo-generators, and they are enhanced when the bars have no external freedom to elongate: thermoplastic insulation tends to expand radially into cooling ducts, locking the outer parts of the bars in place; global VPI on thermsetting insulation also results in bars being locked into the slot.

3.2.3 Electrical aging

The main electrical degradation process in micaceous stator insulation is treeing [Vog03a], and final breakdown is usually through a tree-channel [Bru08b]. Electrical treeing usually starts from an edge of the conductor-bundle [Bru08a] [Kim92], where there is high electrical stress and sharp bending of the taped layers of insulation [Vog03b]. Even on coils newly manufactured by automatic

taping, there can be considerable imperfections in the layers [Vog06], and effects of other aging stresses can create further such weaknesses. Dominant mechanisms enabling trees to form are thermal degradation of the polymer, mechanical stress from vibration and transient currents, and mechanical stresses from thermal expansion [Bru08b].

In pure polymeric insulation, such as plain epoxy or polyethylene, failures through PD in cavities are almost always by treeing [Lau92]. Cavity PD affects the polymer surface by heating, chemical effects such as ozone and nitric acid, and ionising radiation [Kre64], and strong local fields from charges in the surface can break down the insulation over distances of a micrometre or so, eventually starting a tree into the solid from the cavity's surface. A tree can be initiated even without an initial cavity, if local field-concentrations, perhaps caused by metallic particles, give stresses of some 100 kV/mm, resulting in electrochemical changes that can form a small cavity [Bau91]. The subsequent speed of tree-growth is much greater than the speed of initiation, so the total thickness of insulation is less important than the stress [Kre64]. Under the very high stresses sometimes used in laboratory treeing, the initiation may instead be very quick, for example one power-frequency cycle [Vog05].

Stator insulation is special among high-voltage apparatus, in that it consists mainly of mica and is therefore highly resilient to internal PD. Mica can degrade under the combined action of organic acid and ionisation [Jia06], but it gives a far higher strength against treeing than the other components of stator insulation. The effect of a thin mica barrier on treeing in epoxy is shown in [Vog05, fig.8], where the tree is forced to detour a long way around the surface of the mica. It has been observed that treeing in stator main-insulation is never direct, but goes a long way around the mica layers, getting through particularly easily at points of imperfections such as delaminations, cracks and cavities [Bru08b].

The power-law relation of electrical aging to applied voltage is often used, although the exponent itself may vary: "The relationship between failure time and voltage follows the inverse power law" [E434]. An exponent of 7 to 9 is given in [Kre64] for general PD and treeing. In [Sto04, p.46] an exponent of 9 to 12 is given for the effects PD in stator insulation, and the effect of electrical aging is considered to be zero below some threshold voltage.

The mechanism of breakdown by electric stress changes with the level of stress. For stator insulation [E434] the moderate stresses and long lifetimes found in service can lead to breakdown through erosion from PD and 'electrochemical attack', as discussed in the above description of treeing; at the higher stresses and consequently shorter times that might be found in extreme laboratory tests, a thermal mechanism due to losses may be dominant; higher still, discharges with high charge-concentration break down insulation around their tip, in 'streamer breakdown failure'.

An increased frequency of the applied voltage has sometimes been used, such as hundreds of hertz up to some kilohertz, to study electrical aging at an increased rate [Sto04, p.62], on the assumption that a certain amount of PD or treeing occurs in each cycle. A review [Joh79] suggests there often *is* a strong proportionality of these types of aging to frequency, but not reliably enough to

warrant standardisation.

3.2.4 Ambient

One class of ambient stresses comes from the atmosphere in the machine, which may contain water vapour, oxygen and possibly ozone and other reactive gases from PD activity. The presence of dust or salt in the air around an open-ventilated machine may cause blocking of cooling ducts and contamination of the winding surfaces [E56]. Oil from mechanical parts in the machine or from outside can slowly degrade the organic insulation. Water penetrates quickly into asphaltic insulation, causing swelling and weakness, more slowly in polyester, causing depolymerisation, and over timescales of months or years even into epoxy insulation [Sto04, p.166].

3.2.5 Mechanical stress

The currents flowing in the windings cause oscillating forces between bars, at twice the power frequency. Looseness of bars in slots or of the lashings in the end-windings permits relative movement, which can lead to cracking, delamination and abrasion [Tav08, ch.2]. Particularly strong forces occur during fault conditions in the external network: these may cause immediate damage. The relation of lifetime to the stress of mechanical aging by vibration is sometimes treated as inverse power law [Wei05].

3.3 Accelerated aging

When a new material or new construction of insulation system is proposed, or when an existing insulation system is to be subjected to a previously little-tested combination of stresses, tests are needed that will provide some idea of lifetime, at least by qualitative comparison with well-known insulation and stresses. The insulation of stator-windings has a typical design-lifetime of more than twenty years, so any 'natural' aging should result in few failures even after decades. A quicker type of test is clearly necessary, to permit development and application of new insulation systems within a reasonable time and to avoid the high cost of keeping tests running for long periods.

One method is to study relatively easily-measured material properties such as breakdown voltage or abrasion-resistance, and to infer from these the suitability of a material for its intended use [Sto04, p.68]. In view of the complexity of typical insulation constructions and failure mechanisms, there is only weak justification for the assumed relations between the properties of constituent materials and the performance of the whole system under multiple stresses. Other types of tests are obviously desirable for better confirmation. An *accelerated aging* test is performed on objects that are more or less similar to the real insulation system, for example real stator bars in model slots, but makes at least one stress be higher than in service, to shorten the aging time. The discussion of aging in stator insulation [s.3.1] gives indications of how sharply the levels of stresses may affect the aging rate.

Accelerated aging may also be useful for the evaluation of new diagnostic methods, and for establishing criteria for interpreting the results. In these situations the use of real insulation systems under natural service conditions has

several problems. One is the slowness of the changes due to aging, although this is not so critical as in design, since measurements can be made on a wide range of ages of existing machines. Another is the availability of sufficient numbers of machines on which down-time can be accepted for making measurements. Another greater problem is that the relation between measurements and subsequent failures of the insulation is not easily obtained: in particular, it is unlikely that apparently bad insulation will be left in service just to check whether the verdict of badness was correct. Even if accelerated aging cannot be considered to be very realistic, its advantage of permitting multiple objects to have measurements made regularly, up to failure, and within practicable timescales, may make it worth using as one way of testing new diagnostic methods and criteria.

The simplistic description of accelerated aging is that a fairly similar effect to the natural aging is made to occur in a shorter time. Bearing in mind the synergies involved between different stresses in service, and the likely variation in the stresses caused by operation of similar machines in different environments and applications, little confidence can really be had about similarity of the insulation's state after 'service' or accelerated aging. The realism of the acceleration depends at least on the acceleration-factor being not so high as to modify the dominant aging-mechanism; for example, this would happen if an accelerated voltage-stress causes abnormally high temperature, or causes discharges where there never would be any in normal operation.

Several forms of accelerated testing are widespread enough to be the subject of standards, such as *functional evaluation* of mica-based main-insulation for high-voltage stators [E434] by thermal, electrical, cyclic and mixed stresses, as well as even more specific standards for thermal-cycle testing [E1310] and voltage-endurance [E1043].

The standards avoid claims of direct similarity to effects of service, setting out only to provide a method by which different groups of test objects, such as an established and an experimental insulation system, can be compared. It is implicit that the accelerated methods of the standards will give results that are correlated to those that would be seen in service.

There are several ways of assessing which group performed better: a test imposing a fixed stress for a fixed time may be made at intervals between periods of accelerated aging, until the specimen fails; alternatively, a guaranteed destructive test such as a breakdown-voltage measurement may be performed after a single fixed time of aging; nondestructive methods compare results of measurements such as PD and DS, appearance, mechanical properties, chemical or physical composition, or emission of particular chemicals.

The 'equivalence' of aging mechanisms in test and service should be verified [E943], particularly for higher degrees of acceleration. Examples of verifications are a qualitatively similar pattern of PD pulses, or the same location and type of failure in destructive tests, at different levels of stress. Other factors that might influence the aging should be kept close to the values expected in service: examples are any surrounding gas or other medium, or whether heating occurs from inside or outside a stator-bar.

The standardised methods of accelerated testing generally use only one

accelerated stress, other stresses being either absent or at the levels found in normal service, although one group of test-objects may have multiple high stresses to give an idea of the combined effect [E434].

> Complications arise when simultaneous applications are made of more than one factor, even if only one of the factors is intensified.
> [E943]

It is not even obvious that all types of stress will have a monotonic effect when in combination: for example, the increased flexibility of epoxy-mica insulation at higher temperature can give several times higher endurance of mechanical stresses at 90 °C rather than at room temperature [Wei05], with the combination of mechanical and thermal aging effects minimised at about 135 °C for modern epoxy-mica [Bru08a]. The means of acceleration may be more imaginative than just a direct increase of a stimulus: for example, extra-long bars can be made to increase the degree of mechanical stress during thermal cycling [E434].

The amount of variance between results on supposedly similar specimens, whether aged by service or in an accelerated way, clearly makes it necessary to use several specimens in each group. The prescription of [E434] is to use at least five, and preferably ten, and to use at least three levels of stress.

The *Weibull distribution* is commonly used in reliability studies. It is well-suited to fitting the 'weakest-link' properties typical of lifetime data. Different mechanisms of failure can sometimes be distinguished by the Weibull parameters needed to fit the results [Tav08, ch.3]. Some examples of Weibull plots for varied stress and varied insulation can be seen in [Bru08b]. When the lifetime as a function of stress requires different Weibull parameters over different ranges of stress, this suggests changes in the dominant mechanism of failure, which would make assumed acceleration factors invalid.

Chapter 4

Diagnostics and Prognostics

High-voltage insulation systems in power apparatus are given many tests and measurements during design and manufacture, before delivery, on installation, and throughout their lifetime. The results are used to verify suitability of a new design, verify quality of a batch, optimise planning of operation and maintenance of the apparatus, or locate a suspected defect.

The manufacturer-oriented measurements have been sufficiently covered in section 3.3. This chapter considers measurements made by end-users during the service life of an insulation system; this category includes the types of measurement studied in this work. The focus is not technical details of the measurements but a discussion of the aims of collecting and analysing data, and some important categories of measurement. Stator insulation is used for examples throughout the chapter, and current practice for measurements and interpretation of stator insulation is summarised at the end.

Some words are used in this chapter in senses more specific than their everyday use. A *test* gives a simple result of pass or fail; in the high-voltage context this probably involves subjecting insulation to a level of electric stress giving a much increased risk of failure. An *inspection* gives a result through the human senses, such as checking colours, sounds, smells or looseness; it involves no electric stresses. A *measurement* gives a more complicated result than a test, needing interpretation, and uses stresses expected not to make the failure-risk much greater than in normal operation; in this chapter the definition is taken to include inspections. A *method* is used as a rather vague term for a particular measurement and its interpretation, or a group of measurements.

4.1 Diagnostic and prognostic aims

The terms *diagnostic measurement* and *condition assessment* are widely used to describe measurements made on insulation systems: both terms suggest the determination of a current physical state rather than the assessment of future behaviour. If an apparatus has already failed and cannot be used, a purely diagnostic measurement and interpretation may help to identify the problem's type or location, as a step to correcting it. Otherwise, the diagnostic step is not directly useful in itself: some sort of *prognostic* step is needed from which decisions can be made about operation and maintenance. The term *prognostic measurement* would seem more appropriate to many of the measurements made on stator insulation by end-users, but 'diagnostic' is firmly rooted in use. The distinction will be preserved only in this chapter: in the rest of this work, just the diagnostic step from measurements to an estimate of current state is attempted.

The impossibility of precise prediction of failures, which often depend on localised 'weakest link' breakdowns in response to unexpected disturbances

such as transients, may make a suggestion of prognosis or lifetime estimation seem foolish. But regardless of the term used to describe the conversion of measurement data to decisions about operation and maintenance, there surely *is* a prognostic element involved, however implicit it is in the procedure.

> "Prediction is very difficult, especially about the future."
> Niels Bohr

The prognostic aims are quite different from the pure sense of a diagnostic process as the determination of present state. A diagnostic result makes a more or less specific claim about some feature of state: for example, 'there is a mildly conducting path between the conductors and earth', or 'the epoxy is strongly depolymerised, with poor binding and many small cavities', or 'there is at least one delamination next to the conductor stack'. A prognostic result makes a more or less explicit claim about future behaviour: for example, 'this level and type PD of is usually followed by failure within a year', or 'this insulation seems good as new', or 'company policy for a winding giving results in this range is that it should be returned to service and have a further measurement after two years'.

4.2 Obtaining and interpreting data

An attempt is given in figure 4.1 at a description of the process of collecting relevant data about an apparatus and making decisions from it; this is supposed to be general enough to represent data and rules ranging anywhere from vague notions in one person's head through to carefully recorded details and rules used in a large organisation or a computer program.

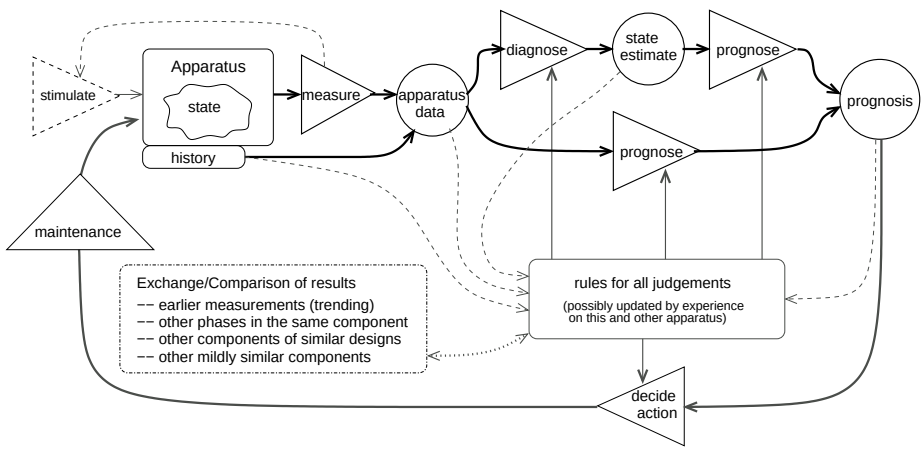

FIGURE 4.1: The generalised diagnostic/prognostic process. Triangular blocks are actions, such as judgements based on input data and rules. Circular blocks represent measured or inferred knowledge. The heavy lines in the top right are the main prognostic process; the lighter lines provide data for assessment and revision of the rules.

An apparatus whose exact physical composition, or *state*, was guaranteed never to change would have the same chance of failing at all times, given the

same stresses: no useful purpose would be served by making routine measurements on it. The state of a real insulation system *does* vary, and affects the chance of failure: the variation includes reversible short-term effects, some examples of which are given in chapter 16, and irreversible effects of the long-term aging-processes discussed in chapter 3.

The diagnostic or prognostic result is based on apparatus data and on rules stating how to convert the data to results. The apparatus data makes the necessary link between the state and the diagnostic or prognostic process. Part of the apparatus data may be 'history', based on operational conditions expected to have had some influence *on* the current state. Examples include loading, ambient temperatures and humidities, winding-temperatures, PD during service, cleaning, and 'traumas' such as transient voltages and out-of-phase switching. The other part of the apparatus data may be 'measurement' of quantities that are determined *by* the current state. Examples include polarisation and conduction currents, partial discharge, and results from visual inspections. Measured data may be able to be obtained without added stimulus, as for online PD measurement or offline inspection of insulation-surfaces, or it may require control of the stimulus as for an offline PD measurement at varied voltage. There is not a rigid division of phenomena into those that purely affect and those that are purely affected by the state: the above example of PD can be in both categories.

Having gathered apparatus data, rules are used to make diagnostic or prognostic inferences. The diagnosis estimates an aspect of the state, such as the presence of some minimum size of PD cavity, a conductive path between surfaces of end-windings, or a degree of degradation of a material. In view of the many types of problems that can occur in a complex apparatus, a sensible diagnosis may well return a range of possible states that would fit with the apparatus data. One automated 'expert' system [Sto04, p.231], which can be seen as explicitly going through many of the steps that a human expert would take, presents not just the one or several proposed diagnoses but also a description of why these were chosen, a list of other possibilities that came close, and suggestions for what further measurements would most effectively resolve the diagnostic question. Although the above examples of diagnoses sound like *model-based* inferences that would be based on considering physical models of the apparatus and the 'inverse problem' back from measurements made on its state, the alternative *data-based* approach could be used instead, based in some way on correlations observed from previous apparatus data and subsequent revelations of the state from further inspection. For the diagnostic step the data-based approach seems an unlikely choice; some of the 'measurement' data of inspections would presumably be the ultimate source of testing the correctness of inferences made on the remaining data.

Having reached the diagnostic estimate of state, the work is finished if the sole aim was to decide the most likely type of fault in an apparatus that already has been decided to need repair. In most cases it is actually the prognostic results that are desired. The prognosis is shown as following two possible routes. The lower route is direct from apparatus data to the prognostic result; this

implies a data-based approach, probably working from statistics of historical data. The upper route may also be a data-based prognosis, but with its input from the estimated state of the diagnostic step rather than from the raw data; otherwise it may be a model-based prognosis, using physics-based considerations to predict future changes in the apparatus.

4.3 Maintenance decisions

From the prognostic result, decisions must be made about what action to take: what maintenance, if any, should be performed; should there be any change in the operation of the apparatus; when should the next assessment be made? The optimal decision depends both on the apparatus and on what application it is used in, as well as on the reliability of the prognostic process.

The relation between apparatus data and the correct prognosis is determined by the construction of the apparatus and the loading that will be put on it by its application. The relation between a correct prognosis and the correct decision is determined by the costs of all the alternative actions and the probabilities assigned to them based on the prognosis. Costs may be due to the repair of a failed apparatus, unplanned downtime or damage to the apparatus' application due to a failure, or costs of planned downtime and work if maintenance is performed. The prognosis may be wrong, giving a clean bill of health to an apparatus that has a severe weakness, or recommending downtime and maintenance of an apparatus that could have survived for years. This is relevant whether the prognostic result is a probability distribution or a run/stop value. The decision-making should take into account the probabilities of these errors and their costs for the particular apparatus and application.

The many types and applications of motors and generators result in wide variations in the balance of costs of faults occurring versus costs of measurements and maintenance. Extremes are small, cheap, easily-replaced machines in noncritical applications, and machines that could take weeks to repair after failure and would cost vast sums per hour of lost operation, such as a large generator in a nuclear power-station. The amount of attention given to making and interpreting measurements and to performing maintenance is therefore also very varied. In the relatively high-power machines for which this work is relevant, the machine itself is expensive and not easily replaced, and its unavailability is likely to have a high cost. It is unlikely that pure 'corrective maintenance', of waiting for failures to happen, will be used; some degree of prognosis will be made to allow 'predictive maintenance' even in the less-critical cases. Some suggestions for policies of measurements and maintenance in different applications of machines are given in [Sto04, p.351].

4.4 Establishing and updating rules

Rules are used at each stage: they can be seen as determining even *what* data should be gathered, as well as how the subsequent stages of inference should be made on the data. Rules for a data-based method may be anything from a rule-of-thumb of long-forgotten origin and without any verification, through a regression analysis of historical measurement results and failure data, up to a

Bayesian model [Lin08] with continual fine-tuning of rules in the light of new information [s.A.2.5]. Rules for a model-based method may be based on anything from microscopic phenomena to equations based on sample-measurements representing some component of the apparatus.

Regardless of how they are chosen, the rules will be severely imperfect. The diagnostic, prognostic and decision problems are difficult ones to study: the actual service conditions vary, failures cannot be reliably predicted from models of deterioration processes, accelerated tests are only an approximation of effects in service, and good life-data for real aging up to a natural failure is hard to obtain. Some large databases covering routine diagnostic measurements on thousands of generators and motors have been built up by large owners and consultancies. Even in these there will be long delays, of the order of decades, between starting to use a model of apparatus and getting a useful amount of data about its failures. It is unlikely that checks will be made of whether a prediction of imminent failure would actually have turned out to be true, so it is hard to get strong supporting evidence for later predictions; less realistic checks such as quick overvoltage-testing and dissection after removal from operation are probably the best methods available in practice. Part of this problem of 'censored' data where failures have not yet occurred or apparatus was retired before failure occurred, is discussed in [Lin08].

A good system for diagnostic or prognostic results will not just choose some rules and leave them, but will take advantage of experiences gained during its use, to consider adjusting its rules. The dashed arrows into the 'rules' box in the diagram carry information about data, diagnoses, prognoses and decisions. This information can be linked to external information that confirms or contradicts the goodness of the inferences, for example an inspection performed after a diagnosis or a failure after a prognosis. The arrow to 'other apparatus' should be an important part of the setting of rules: it is likely that much of the initial rule-set for an apparatus will be based on experience with other more or less similar apparatuses, and the changes to the rules should likewise be based on all the relevant data that is available.

4.5 Measurements offline and online

An *offline measurement* requires the apparatus to be out of service. This is true for the methods studied in this work: they require the applied voltage to have widely varied amplitude and frequency, and the winding to be isolated from earth and preferably split at the neutral point to allow separate treatment of the phases. An *online measurement* is made when the apparatus is in operation, giving an immediate advantage of avoiding downtime. An extreme case of online measurement is *online monitoring*, where a measurement-system is permanently connected during operation of the apparatus.

Inspections involving some disassembly, such as visual inspection of slot-wedges and end-winding insulation surfaces, will require the apparatus to be offline. Electrically-based offline measurements may need a separate power-source, which for large apparatus at high voltage and power frequency can be expensive and large. An advantage gained is the ability to control the voltage to

obtain extra information: the PD inception and extinction voltages, PDIV and PDEV, are commonly measured in offline PD measurements, requiring variation of a sinusoidal excitation. By selecting different combinations of high-voltage and earth potentials in a multi-electrode system, specific parts can be stressed: offline measurements on stator windings usually excite one winding at a time then all together, helping to distinguish defects between phase and earth from defects between phases. Offline measurements also tend to have the advantage of lower noise, permitting better measurements of PD and measurement of the small current in the insulation.

Online methods allow measurement of phenomena that actually occur during operational levels of parameters such as gas-pressure, temperature, forces on conductors due to load-currents, external vibration and voltage-stress. They also allow variation of certain parameters, such as conductor temperature, or vibration from load-current, that cannot easily be controlled when not in operation. Studying a parameter such as PD over a range of load-currents or temperatures may help to detect defects or distinguish between possible locations of a defect: for example, mechanically induced slot-PD is heavily increased by high current-loading.

The realism of the stresses during online measurements does not make online methods unconditionally superior. The important aim is to make a good diagnostic or prognostic inference. If a particular measurable phenomenon, such as vibration-dependent slot-PD, occurs under online conditions but may be missed in offline measurements, *and* if this phenomenon is strongly related to dangerous deterioration as either a symptom or a cause, then the online measurement has an advantage. But the same is partly true the other way round: a phenomenon that can be detected by offline but not by online methods, such as a crack that is only noticed by measuring small currents through the insulation at high voltage and low frequency, will put the offline method at an advantage, as long as this phenomenon is a symptom of dangerous deterioration; the difference from the previous example is thus that a phenomenon which occurs only in offline measurements and is a cause but not a symptom of deterioration, is *not* a useful indicator of a problem but merely a good reason to stop the offline measurement.

The above comparisons suggest that the offline and online methods are complementary rather than directly competing; it is common to use both. For example, when online stator PD measurements suggest the start of a problem, offline measurements are recommended [E1434, p.30] to gather further information before deciding what further action to take.

Online monitoring typically has automation of data collection, with different levels of alarms to alert operators to probable urgent problems and alert only maintenance staff to problems predicted to be too distant to worry about immediately. The frequently-logged data permits extremely fine trending: instead of having to compare results with a few previous measurements at one-year or perhaps five-year intervals and at probably rather different temperatures and humidities, the entire past behaviour of the apparatus is available for assessment.

4.6 Cross-comparison, trending, and relative measures

A recurring theme in standards and recommendations about interpreting measurement data, particularly for prognostic purposes in machines, is that trends, and comparisons with similar objects are generally better guides than trying to set limits for a whole class of apparatus. In some cases, such as PD measurements on polymeric high-voltage cables, any detectable PD is worrying, so there is some sense in responding to a single measurement without making comparisons; even here a rapidly growing level seen in online monitoring would be more worrying than a steady level. In stator insulation, PD at tens of times the detection-level for a cable would be mild, and is to be expected throughout a long and happy service life: a lot more detail than the existence of a moderate size of PD is needed for a good prognosis.

In the absence of other knowledge about limits, comparison with the most similar apparatus that has not yet failed is a reasonable way to make a simple decision of fitness for service. An example of the importance of similarity is the dependence of signal attenuation on winding-construction; similar PD sources in machines with different winding-layouts may show very different results in measurements. A comparison with an identically constructed apparatus avoids some such problems, but does not help with some other causes of differences in results, such as different ambient conditions between the two apparatuses. For stator insulation, the presence of two other phases usually of very similar constructions and in very similar ambient conditions, permits useful comparative measurements.

Even comparing between phases in the same stator, there is the problem that similar deterioration may appear differently in measurements depending on its position within the test-object and reference-object. For example, similar PD sources in different parts of a winding may give very different results. At the expense of the guarantee of similar ambient conditions, a comparison can be made between previous measurement occasions on the same object, allowing for example a source of unusually large PD pulses to be treated as less worrying if it has been constant or slowly increasing over several occasions than if it has recently appeared.

A focus on changes and their *relative* values is a common way to reduce the effects of slowly-changing disturbances and differences in instrument calibration. External factors such as atmospheric conditions and apparatus temperature can influence measurements, making direct comparisons between occasions difficult. Significant differences in calibration may exist between instruments, and instruments may themselves be temperature-dependent; small differences in large measured quantities may be obscured by the calibration difference between measurement occasions.

Temperature and humidity have a strong influence on measurement of insulation resistance (IR) [s.6.4.2]. Use of the ratio (PI) between IR values at two or more time-points in a single measurement solves much of the problem of temperature-dependence, as well as dividing out the effect of test-object size.

Calibration differences as well as temperature effects would affect the small voltage-dependent changes due to PD, in the large values of capacitance and loss

in stator insulation. The 'tip-up' measurements [s.6.4.1] of capacitance and loss record variations with voltage, between results obtained with one instrument at immediately consecutive times; they can therefore be compared between different measurement occasions with much less sensitivity to calibration.

Measurement of PD on stators cannot be calibrated into apparent charge at the PD source, and differences in instruments and test-circuits may make even the relative sizes of different PD sources within a measurement vary between measurement occasions. This is not so simple a problem as an error of scale-factor, but on the other hand the stochastic nature of PD reduces the degree of precision that is ever expected in a PD measurement. PD is normally recorded as absolute values; that is, relative only to a calibrator, not for example to the maximum charge. A phase-resolved PD pattern is, however, often interpreted *as* a pattern, where the general shape is more important than the registered charge; in this respect a PD measurement can also be seen as using relative values of results to avoid some of the differences caused by instrumentation.

A final consequence of the dependence of so many measured phenomena on external factors is the importance of recording the factors most likely to be important, along with measurement data. The atmospheric temperature and relative humidity are significant in all high-voltage measurements on machines; pressure is important too when external PD is involved. Other details such as internal temperatures, the degree of disassembly or the layout of test-connections, may be useful when later using the data; photography can help to capture a lot of this information in a short time.

4.7 Current practice for stator insulation

Elaborate *protection systems* are used on large machines, for rapid disconnection after detection of a fault in the machine or a form of operation that will harm the machine. They protect the network from a faulted machine and prevent further damage to the machine. These systems include 'relays' that detect over-current and earth-faults, under-frequency and over-frequency, voltage-imbalance between phases, and more [Tav08].

In contrast, the 'diagnostic' (although ultimately for prognostic purposes) and 'monitoring' methods are intended to allow faults to be predicted in enough time to reduce unplanned downtime and damage to the machine. The main types of data gathered about stator insulation are listed below; more detail about these and methods for other parts of rotating machines can be found in [Sto04] and [Tav08]. Using several types of measurement allows a better assessment of the insulation's condition.

The removal of a generator's or motor's covers and rotor, followed by inspection of insulation surfaces, end-winding blocking and lashing, insulation firmness, and tightness of wedges and bars in slots, is held as one of the most useful sources of information about the insulation's state [Sto04, p.229]. This has of course the disadvantage of being an offline method and of requiring further time for the disassembly.

As a rather detailed investigation of insulation condition, bars can be removed from a few points around a winding, replaced with spare bars, and the

removed samples can then be subjected to destructive tests such as voltage-endurance and dissection.

Partial discharges are very commonly measured in stator insulation, online and offline; this is covered in chapter 8. The currents in the insulation, including in some cases PD currents, are commonly measured offline by methods known as insulation resistance and tip-up, covered in section 6.4.

Temperature measurements online are very common and have been used for decades. The sensors may be placed at points in many of the slots, typically between bars for a good measure of the insulation temperature. Results from end-winding sensors depend also on the surrounding gas temperature; thermography by heat-sensitive cameras can instead be used to check end-winding hot-spots. Temperature may reveal problems with electrical cause, such as a worn semiconductor layer, or other sources of overheating that may affect the insulation.

Chemical measurements are made online to detect the chemicals and smoke particles from overheating of organic insulation (generator condition monitor, GCM, or core-monitor); this is relevant to insulation between core-laminations as well as to stator insulation. Tracer-paints can be put on parts of windings, to release distinguishable chemicals from different parts of the winding at different temperatures. The complicated matters of rates of generation and loss of chemicals, and gas volume and detection thresholds, limit the sorts of overheating than can be detected in this way [Tav08, ch.3]. Ozone from partial discharges is commonly measured online, as an occasional measurement or a monitoring system.

Vibration monitoring may be performed on various parts; in many cases the vibrations are concerned with rotor and mechanical problems, but excessive vibration of end-windings may have consequences for stator insulation.

A commonly used test, in the sense defined at the start of this chapter, is the *hipot* (high-potential) or 'pressure' test, where a voltage considerably higher than the normal service level is applied for a time in the order of one minute. The chosen voltage is not widely standardised but is generally well over twice the service level [Sto04, p.243]. The result is then a simple pass/fail depending on whether a breakdown occurred; this makes clear that it is not worth doing such a test on a machine whose in-service failure has little cost beyond the machine: a hipot failure may happen even on a winding that would have survived long in service. A dc hipot test permits a small supply, but the field-distribution in the insulation may be very different from the field in service. The current may be measured too, to get a more detailed result than the simple test. Hipot tests with ac may use normal power frequency, or may use low frequencies such as 0.1 Hz to reduce power-supply demands but keep an approximately ac field-distribution [E433]. A summary of relative advantages and disadvantages of ac and dc hipot is given in [E95]. Another form of overvoltage test, designed to test the turn insulation, is the *surge test* [Sto04, p.265], injecting a high-frequency pulse into the winding; this stressing of the turn insulation is in contrast to the other offline electrical methods.

Chapter 5

Dielectric Response

Conduction and displacement currents within an insulation system are measured in several common diagnostic methods. This chapter describes the origins of these currents, moving from simple homogeneous and isotropic materials to the complicated structures of high-voltage insulation systems. Stator insulation is then considered, from the dielectric properties of constituent materials and the composite insulation system that they form, to the effects of different forms of deterioration upon the measured current. Common ways of measuring the currents for material studies and for diagnostic purposes on insulation systems are described in chapter 6.

There are many books available about dielectric response: a good exposition of models and mechanisms is given in [Jon83] along with data from a wide range of solids; an overview of mechanisms and measurement methods is also given in [Hel00], which has the advantages of easy availability and a focus on pristine epoxy-based stator insulation.

5.1 Basic electrical properties of materials

Every material contains positive and negative charges on which an applied electric field exerts forces in opposite directions. Most charges are not free to move more than fractions of an atomic size within a material under an applied electric field. Except in a plasma, charges are mainly bound to opposite charges to form neutral atoms and molecules, with bonds stronger than macroscopic electric fields found in normal service of high-voltage equipment.

An electric field applied to non-free charges causes *polarisation*, a limited displacement between the positive and negative charge-centres. When the applied electric field changes, there is a new steady-state value for the polarisation: the change in polarisation towards this steady state is the dielectric *relaxation*. Different mechanisms of polarisation give rise to a vast range of relaxation times. Pure *dielectric response*, DR, is the dynamic behaviour of the polarisation in response to an applied field. Measurements referred to as DR often include other phenomena such as free-space capacitance and conduction, sometimes as desired extra information and sometimes as an undesired disturbance.

A conductive material contains many charges that are free to move throughout the material, such as conduction electrons in metals, or ions in solutions. These are generally a distinct minority of the *total* charges in the material, but even a single free charge per several atoms results in strong conductivity. Copper, for example, has a conductivity $\sigma = 6{\times}10^7\,\mathrm{S/m}$, relating current-density of the moving charges to an applied electric field E; expressing this as $6\,(\mathrm{kA/cm^2})/(\mathrm{V/m})$ makes clear what a large current-density this entails even for a tiny electric field.

The conduction and polarisation processes are generally distinct and largely independent [Jon83, p.47]. Polarisation of the bound charges in a good conductor is not usually of interest, as the achievable fields in the material are so weak and the conduction currents are so much stronger than any measurable effect of polarisation. Polarisation is therefore a phenomenon associated with poor conductors — semiconductors and insulators.[†]

High-voltage insulation uses only good insulators such that the typical service stresses of easily 3 kV/mm cause conduction currents in the order of nanoamps down to femtoamps, in spite of the large conductor-surface of a cable or winding. For example, the XLPE (cross-linked polyethylene) widely used in power cables has a resistivity at room-temperature in the order of $10^{16}\,\Omega$m, corresponding to some $100\,(\mathrm{pA/m^2})/(\mathrm{kV/mm})$.

True conduction through a material is a process in which the charge density throughout the material can stay constant but charges keep moving between the electrodes. A *conduction current* is thus sustainable for any period and stores no energy. In insulating solids, electrons are made available for conduction by the presence of impurities or by thermal energy. The conductivity can increase by orders of magnitude when temperatures change between ambient temperature and the typical working temperatures just some tens of celsius higher; this is in contrast to good conductors, whose conductivity *decreases*, much more gradually, with increased temperature. A strong field in an insulator may affect how many charges are available for conduction, but at weaker fields the available charges are largely independent of the field.

Polarisation within a material changes the electric displacement field. The rate of change of this field with time is the displacement current, so changes of polarisation result in a particular type of displacement current, *polarisation current*. In a good insulator the small conduction current and the strong electric field that can be built up permit the polarisation to be the dominant cause of current even at the moderate frequencies of power frequency and lower that are considered in this work. Polarisation changes the charge densities in the material, and cannot continue for ever; energy is stored by polarisation, and some of it can be returned.

DR measurements on materials are typically used to assess the composition and freedom of molecules. This is of interest in several disciplines, among them chemistry, polymer and solid-state physics, semiconductor and insulation engineering, and some biological applications. Between these disciplines there are many different names, equations and types of plot used to describe and present the same concepts; even within the 'insulation community' there are differences between countries and periods in the choice of terminology. A description of the relation between many industrially oriented terms for dielectric properties is given in [T150]. The following section includes names and notation for the main features of dielectric response that are discussed in this work.

[†]The distinction between a *dielectric* and an *insulator* is a matter of application or taste. Both words are used for materials that can keep conductors electrically separated, withstanding high fields with minimal conduction; if high polarisability is a *desired* feature, as in a capacitor, then the material will probably be referred to as a dielectric.

5.2 Mechanisms and descriptions of dielectric response

Measurements of dielectric response usually consider just a narrow band of the whole range of times or frequencies over which polarisation mechanisms operate. The mechanisms with significant dynamics in this band are the interesting dielectric response, and other mechanisms are treated as instantaneous if much faster or as nonexistent if much slower.

Even across a vacuum an electric displacement $D^{\dagger}$ occurs in response to an electric field E, related by the *free-space permittivity* ε_0 as $D = \varepsilon_0 E$. The significance of D to measurements is its relation to charge-density $\varrho = \nabla \cdot D$; its surface integral determines the charge on an electrode whose potential is held constant by an external circuit, and the time rate of change in this charge is the measured current in the circuit. Polarisation in a material increases D by the total volume-density of dipole moments, P_{t}, so that $D = \varepsilon_0 E + P_{\mathrm{t}}$.

In practical insulation materials exposed to service-levels of electric field the steady-state polarisation is very close to proportional to the electric field, and therefore gives the same effect as an increased ε_0. The total electric displacement can then be treated as a part due to free-space and a part due to all polarisation, or at the other extreme as a single effective *permittivity* ε with no explicit polarisation term. An intermediate form is relevant to cases where some polarisation takes long enough that it is not practically instantaneous compared to the changes in electric field being measured, and therefore cannot be included in a constant ε: the free-space permittivity together with the components of the polarisation that are practically instantaneous are the *prompt response*, treated as a single value of *high-frequency permittivity* ε_∞, and the remaining, slower polarisation P is kept separate. These three ways of distributing the polarisation between an explicit and implicit part are

$$\begin{aligned} D &= \varepsilon_0 E + P_{\mathrm{t}} \\ &= \varepsilon E \\ &= \varepsilon_\infty E + P. \end{aligned} \tag{5.1}$$

The fastest polarisation mechanisms are the *induced polarisation* displacements between electrons and nuclei or between ions in a lattice, happening in times short enough to correspond to optical or infra-red frequencies, and without strong temperature-dependence. Slower mechanisms that give dynamic dielectric response at the frequencies met in electric circuits are *dipolar*, *carrier-dominated* and *interfacial* polarisations. Interfacial polarisation is a consequence of inhomogeneity rather than a microscopic feature of a simple material, with charge conduction through the volume being blocked at barriers and building up to the equilibrium where its electrostatic field prevents further movement.

[†] The quantities E, D and P_{t} are all point-values of vector fields; spatial coordinates are omitted for brevity. Material properties, such as the permittivity ε used later, will for anisotropic materials be tensors rather than scalars. The stator insulation studied in this work is certainly anisotropic on account of the layers of different materials in its construction, as indicated in figure 5.1. However, most work with stator insulation concerns fields applied normal to the plane of the tapes, so the anisotropy is not important. In the present section isotropy is assumed.

This is mentioned in [s.5.4], and has a relevance to the composite material of stator insulation [s.5.5.4]. Carrier-dominated systems, of poor insulators where movement of electrons or ions has a significant effect, can give rise to continued polarisation without any reduction in rate towards an equilibrium being apparent even at frequencies well below the millihertz range [Jon96, p.206]; this is the least relevant form of dynamic polarisation to this work. Dipolar polarisation involves movements of groups of atoms that have dipole moments. The groups may be whole molecules or parts of flexible molecules, and the dipoles may be the permanent dipoles of polar groups of atoms, or temporary induced dipoles. The distribution of thermal energy gives dipoles an occasional chance to move beyond the energy barriers caused by their interactions with neighbouring atoms; an applied electric field biases these movements, making polarisation more energetically favourable, and resulting in an equilibrium state of polarisation that depends on the applied field. Dipolar polarisation is thus microscopically a 'flip' of particular dipoles rather than a gradual movement of all dipoles together [Jon96, p.10]. Even at electric fields of many times the normal service levels used in high-voltage equipment, the equilibrium state of polarisation due to the field's bias is a small proportion of the total of the dipole moments. Solid high-voltage insulation is usually polymeric: single-bonds in polymers permit rotation of groups of atoms in small sections of the chain, such as an H-C-H group in polyethylene or the naturally dipolar H-C-Cl in PVC; the energy barrier to the rotation is partly due to the outer atoms passing neighbouring groups [Ged95].

The equilibrium polarisation expected for dipolar and interfacial mechanisms after a long time is sometimes expressed as a *static permittivity*, ε_s. The difference $\varepsilon_\mathrm{s}{-}\varepsilon_\infty$ is then the amount of polarisation due to the mechanisms that are treated as dynamic.

For all uses of the concept of permittivity, such as the high-frequency value or the complex frequency-dependent value seen later, a *relative permittivity* $\varepsilon_\mathrm{r} = \varepsilon/\varepsilon_0$ is often preferred to the absolute permittivity ε, as it results in numbers close to unity, more easily interpreted. Sometimes the name 'permittivity' and the variable ε are used in this relative sense: there is seldom any doubt as to the meaning, as the ratio, ε_0, is a factor of $8.85{\times}10^{-12}$.

An example of the components of relative permittivity is seen from the case of epoxy. Due to free space alone, $\varepsilon_\mathrm{r} = 1$. The refractive index is about $\eta = 1.5$ signifying an optical-frequency value of $\varepsilon_\mathrm{r} \simeq \eta^2 \gtrsim 2$ and therefore an electronic polarisation already contributing more to the permittivity than free space. Models of the dielectric response in the kilohertz range and lower have used $\varepsilon_{\mathrm{r}_\infty} = 3$ [Hel00, ch.7], an increase of nearly 1 due to rapid but sub-optical mechanisms. At power frequency $\varepsilon_\mathrm{r} \simeq 4$, and at the very low frequencies as implied by ε_s it may be over 6.

The dynamic polarisation mechanisms measured as dielectric response are described by the *dielectric response function*, $f(t)$. This relates a dielectric's polarisation P at time t to the applied electric field E throughout history,

$$P(t) = \varepsilon_0 \int_0^\infty f(\tau) E(t-\tau) \mathrm{d}\tau. \tag{5.2}$$

For the sustained sinusoidal excitation used in this work, the Fourier transform $\mathscr{F}\{\cdot\}$ of $f(t)$ is a more convenient description,

$$\chi(\omega) = \chi'(\omega) - \mathrm{i}\chi''(\omega) = \mathscr{F}\left\{f(t)\right\}, \tag{5.3}$$

where $\chi(\omega)$ is known as the *susceptibility*, describing the relation of polarisation to applied field as functions of frequency,

$$P(\omega) = \varepsilon_0\, \chi(\omega)\, E(\omega), \tag{5.4}$$

from which the total displacement due to this dynamic polarisation and the prompt response is

$$D(\omega) = E(\omega)\left[\varepsilon_\infty + \varepsilon_0\chi'(\omega) - \mathrm{i}\varepsilon_0\chi''(\omega)\right]. \tag{5.5}$$

Several common notations for splitting up the total $\varepsilon(\omega)$ are

$$\begin{aligned}\varepsilon(\omega) &= \varepsilon_\infty + \varepsilon_0\chi'(\omega) - \mathrm{i}\varepsilon_0\chi''(\omega)\\ &= \varepsilon_\infty + \Delta\varepsilon'(\omega) - \mathrm{i}\varepsilon''(\omega)\\ &= \varepsilon'(\omega) - \mathrm{i}\varepsilon''(\omega)\\ &= \varepsilon_0\left[\varepsilon'_\mathrm{r}(\omega) - \mathrm{i}\varepsilon''_\mathrm{r}(\omega)\right],\end{aligned} \tag{5.6}$$

where $\Delta\varepsilon'(\omega)$ denotes just the dynamic component of the real permittivity, and the components of relative permittivity are the *dielectric constant* ε'_r and the *loss-index* ε''_r.

The imaginary part of $\chi(\omega)$ makes it possible to describe a delayed response; the delay implies some dissipation of energy, a *dielectric loss* due to polarisation mechanisms that take a significant time on the scale of the frequency being studied. In fact, a change of $\chi'(\omega)$ with ω (*dispersion*) is always accompanied by a nonzero value of $\chi''(\omega)$, given a linear and causal dielectric response function [Jon90]. This is a consequence of the Kramers-Kronig relations of real and imaginary parts of Fourier transforms; these relations are widely used in optics and in studies of dielectric materials. The real and imaginary parts of $\chi(\omega)$ describe respectively the peak stored energy in a cycle and the mean energy dissipation per radian [Jon83, p.249].

For high-voltage apparatus, and for DR measurements on material samples at the low frequencies of electric power applications, the field quantities are not directly measured but are converted to circuit quantities measured on an electrode system. A convenient concept is the *geometric capacitance* C_0, sometimes known as the *vacuum capacitance*. This is the capacitance that a pair of electrodes would have in free space: if they are instead surrounded by a homogeneous dielectric of permittivity $\varepsilon(\omega)$, the *complex capacitance* $C(\omega)$ is

$$C(\omega) = C'(\omega) - \mathrm{i}C''(\omega) = C_0\varepsilon(\omega). \tag{5.7}$$

In this thesis the real, non-lossy component $C'(\omega)$ is referred to as *capacitance* and the imaginary component $C''(\omega)$ as *loss*. Similarly to $\varepsilon(\omega)$ in (5.6), $C(\omega)$ can be split into prompt and polarisation parts, C_∞ and $\Delta C'(\omega)$.

A common description of the loss is the *loss tangent*

$$\tan\delta = \varepsilon''/\varepsilon' = C''/C', \tag{5.8}$$

in which δ is the *dielectric loss angle*. This quantity has the endearing feature of dividing out geometric terms and distinctions of absolute or relative permittivity; at least for an homogeneous material, $\tan\delta$ is a material property even when based only on measurements of current and voltage.

5.3 Dielectric responses of materials

The dielectric response function named after Curie and von Schweidler was proposed about a century ago, based on experimental data,

$$f(t) \propto t^{-n}, \quad 0 < n < 1. \tag{5.9}$$

This is sometimes called the 'fractional-power law' response; it is highly relevant in this work, being a good description of pristine stator insulation material [s.5.5.2] and of a distributed series resistance and shunt capacitance as found in contaminated end-windings or end-winding stress grading systems at low enough fields for linearity to be assumed [s.19.4].

A model of more theoretical origin is the Debye model, where the rate of polarisation is proportional to the amount of the static polarisation that has not yet occurred; this gives the same response as a series RC circuit,

$$f(t) \propto \mathrm{e}^{-t/\tau}, \tag{5.10}$$

and is considered reasonable where independence of the dipoles can be assumed, of which an example is sometimes given as gases or 'dilute solutions' of dipoles. In frequency, the Debye model is

$$\chi(\omega) \propto (1 + \mathrm{i}\omega\tau)^{-1}, \tag{5.11}$$

which is widely used in studies of solid materials [Ged95], generally needing some extra exponents to stretch it to fit the data acceptably. Its main relevance in this work is in the simplest models of end-winding stress-grading [s.19.4], or the response measured towards high frequencies when there is extra series resistance in the measurement circuit, such as significant lengths of slot-semiconductor.

The Fourier transform of the fractional-power law response (5.9) is also a fractional-power law,

$$\chi'(\omega) - \mathrm{i}\chi''(\omega) \;\propto\; (\mathrm{i}\omega)^{n-1} \;=\; [\sin(n\pi/2) - \mathrm{i}\cos(n\pi/2)]\,\omega^{n-1}, \tag{5.12}$$

where n has the same definition and restriction as in (5.9). The imaginary and real part are in a frequency-independent ratio depending only on n,

$$\chi''(\omega)/\chi'(\omega) = \cot(n\pi/2), \tag{5.13}$$

so the log-log plots of $\chi'(\omega)$ and $\chi''(\omega)$ against frequency, which are straight lines due to being power laws, are also parallel to each other. Values of $n > 0.5$,

which would give a rapidly falling response function in time, therefore result in a relatively small imaginary part of the susceptibility, and a shallow change of susceptibility with frequency; these are properties of good insulating materials with low loss. Values of $n < 0.5$ would give a shallow response function, and a susceptibility changing rapidly with frequency, with a relatively large imaginary part of the susceptibility.

Solid materials are often well described by (5.12), with different materials showing values of n over its full permitted range [Jon83, p.198] [Jon90], although at the upper end of the range for good insulators. This relation is followed over the range of frequency where the dynamic mechanisms are significant. At higher frequencies the dynamic polarisation mechanisms do not react quickly enough to have much effect, so their susceptibility becomes negligible compared to the effects of high-frequency permittivity. Towards lower frequencies there are two very different ways in which (5.12) may change [Jon90]: the dipolar mechanisms, which tend to an equilibrium, tend to a constant $\chi'(\omega)$ and a falling $\chi''(\omega)$ as the frequency decreases; carrier-dominated systems may instead transition to a fractional-power law with n closer to zero, giving a large $\chi''(\omega)$ and a strong change with frequency, which has been labelled low-frequency dispersion, *LFD* . As was indicated before, when describing carrier-dominated systems, the dipolar behaviour is more relevant to stator insulation, and in the practical frequency range for cured materials the loss-peak is not reached.

5.4 Dielectric response of whole insulation systems

The above descriptions of DR have a bias to *material* properties, working in terms of point-quantities and fields, or of properties of electrodes surrounded by a homogeneous material. Pure material properties are sometimes the focus of DR studies, but DR can also be of interest for an insulation *system*, usually measuring currents between the electrodes that the insulation is designed to keep separate. Insulation systems may consist of several dielectric materials arranged in complicated and possibly poorly known geometries.

Even for a simple, homogeneous material, a well-defined geometry of electrodes is needed for calculation of material properties such as χ, ε_∞ and σ, from measured current and voltage. Extraneous currents such as leakage around the material surface must also be avoided. Guarded test-cells provide a well-defined geometry of the measured sample of material, and reduce the effect of surface currents.

When DR is measured between terminals of high-voltage equipment such as cables, bushings, transformers and machine windings, there may be poor knowledge of the conductor geometry and the placement of materials. If it is known that the dielectric material is homogeneous between the electrodes then some meaningful material properties can still be deduced, where the geometry-dependent C_0 term cancels. Examples are the loss-tangent $\tan\delta$, and *relative* changes of a variable such as C' or C'' with frequency.

In a composite material, perhaps made of layers of different materials or of particles of one material dispersed within another, the measured DR may be very different from that of either material alone. Classic reasons are build-up

of surface charges at interfaces between materials with different ratios of σ/ε, or plain mixing of currents due to parallel-connected materials.

High-voltage insulation systems often involve highly heterogeneous dielectrics. An overview of some effects of insulation constructions on DR results is given in [Gäf04]. Transformers have a complex structure of paper and oil; stator-windings have a composite of mica, backing tape and a binder such as epoxy-resin; old cables have layers of paper with oil in and around them, and modern cables with polymeric insulation may be caused to be inhomogeneous by the spatial variation of conductivity caused by spatial variation of temperature.

The measured dielectric response in high-voltage equipment may therefore differ widely from the dielectric responses of the constituent materials, and may therefore have little value as a measure of material properties. The apparent 'dielectric response' resulting from various circuit-connections of capacitors and resistors is studied in [Jon83, ch.3]; when analysing results from systems, rather than from simple materials, the correct assumptions of the geometrical arrangement, and therefore of appropriate types of circuit-connection model and graph, can make the interpretation much easier. In some cases measurement of DR, for comparison with similar equipment or with past measurements on the same item, may be of use in condition assessment without needing to consider material properties. In others an inverse problem may be solved by means of suitable assumptions, to estimate a material property from a composite measurement; the DR of paper in transformers based on assumptions of oil properties and geometry is an example of this [Gub03].

5.5 Dielectric response of stator insulation

This section considers the features of stator insulation, in good and in bad condition, that make up the total apparent 'dielectric response' of the system measured between one or several phase conductors and earth. The focus is on the linear or smoothly nonlinear sources other than partial discharges. The effect of PD on measured dielectric response is covered in more detail in later chapters [s.8.2].

5.5.1 Mica, epoxy and asphalt

The main dielectric involved in stator main-insulation [s.2.1.2] is small pieces of mica, with the spaces filled with an impregnant and possibly by gas if the impregnant has failed to reach some parts or has migrated. The modern stator insulation most likely to be found in service will usually have an epoxy resin as the impregnant around tapes of mica-paper with a backing material of glass-fibre or a synthetic polymer tape or fibre. The following paragraphs summarise the dielectric behaviour of the main materials, based on several sources; bear in mind that none of these materials is a rigidly defined substance.

Mica occurs in many forms. The muscovite mica used as a dielectric varies in coloured tints and qualities [T351], a popular type being 'ruby' mica. Being laminar, mica will not necessarily exhibit similar properties for fields across or along the cleavage-planes. When used in the modern way in insulation, as a paper made of small mica flakes, mica is further altered from the properties of the natural sheets that were used in older insulation. Early users of mica

dielectrics quoted a wide range of properties, prompting detailed measurements [Dye24] that found muscovites to have typical relative permittivity of about 7 and loss tangent sometimes as low as 3×10^{-4}, at 800 Hz.

Dielectric-response measurements have been presented for fields along the cleavage planes of mica sheets [Cha85b] and through industrial mica-paper [Cha85a]. In the range of frequency and temperature of interest in this work, the dielectric response of these sheets was seen to follow a power-law (5.12) with $n \simeq 0.7$. The mica paper in this frequency range had a steep slope, even to the point of $n < 0.1$, and its properties depended strongly on relative humidity. The interfaces in the mica paper apparently had more effect than the bulk, but the presence of impregnant would presumably change the contacts and the relevance of humidity; the measurements on sheet mica may be more relevant to the composite of mica-paper and epoxy. From measurements in [Hel00, p.167] the dielectric properties of mica vary from relative permittivity about 7 or 8 and loss-tangent 3×10^{-4} at 100 Hz, to about 10 and 1×10^{-2} at 1 mHz.

Asphalt is not used in modern stator insulation, and detailed descriptions of dielectric properties of asphaltic stator-insulation impregnants before mixing with mica have not been found. Dielectric and mechanical studies of 'regular asphalts' are reported in [Sta99], which describes asphalts as a mixture of molecules ranging from molecular weights of only hundreds, up to thousands or hundreds of thousands. The dielectric data shown in [Sta99, p.725] spans the frequency-range of most interest in this work, and extends higher: current due to conduction dominates the measured loss below about 10 Hz, and a conductivity of 10^{-10} S/m can be inferred from the plotted low-frequency ε''; the relative permittivity is below 3 at the higher frequencies of hundreds of hertz, but rises to 10 by 10 mHz; the loss-tangent at frequencies above significant conduction is a few percent.

Epoxy-resin is characterised dielectrically in [Hel00, ch.7] based on measurements and literature. Models based on the power-law, and on the Debye-based descriptions favoured by chemists, are given for cured and uncured states. The experimentally determined parameters are found by fitting a composite-material model to measurement data, so the values should only be used as a rough guide to properties of pure epoxy. The prompt response in all cases is taken as $\varepsilon_\infty = 3$. In the cured state that is expected for in-service machine insulation, the conductivity σ is about 1×10^{-17} S/m from the measurement and 2.5×10^{-15} S/m from literature; the fully-relaxed relative permittivity is about 9 based on the measurement and 6.5 based on literature; the exponent n for (5.12) was 0.9 based on the measurement. In the uncured state the significant differences were a fully relaxed permittivity several times higher, and a conductivity some six or seven orders of magnitude higher, as much as 10^{-10} S/m. Easier movement of dipoles, and conduction by ions, are familiar phenomena in uncured epoxy [Sen86].

In this work, the fully cured state is of most relevance, but there are three reasons for an interest in partial curing: the insulation within newly manufactured test-objects will not quite be fully cured; poorly cured impregnant, particularly around end-winding connections, can be a cause of overheating

and failure in stator insulation; and the similarity in conductivity of asphalt and uncured epoxy makes it likely that some results from composite models of uncured insulation in [Hel00] will have a close connection to asphaltic insulation.

5.5.2 The epoxy-mica or asphalt-mica composite

Considering now the composite material formed from mica, impregnant and backing-material, there are two main levels of detail, shown in figure 5.1. Within

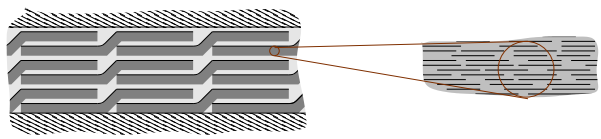

FIGURE 5.1: Illustrative cross-sections (without good attention to scale) of stator insulation construction around and in the tape. Left: half-lapped layers of mica tape, with the length of the tape running normal to the page; a film of backing-material is seen on the top-side of the tape, and an impregnant fills remaining spaces (exaggerated) between the electrodes. Right: small pieces of mica within a piece of tape, surrounded by impregnant.

the tape, pieces of mica form barriers to charge movement within the surrounding material. The tapes then form overlapping layers to make up the insulation, a typical width of the tape being 25 mm. Note that the mica in real insulation is the major part of the volume; this may not be obvious from the illustrative figure. Backing materials of solid films rather than weaves result in a further set of barriers within the material. The applied field is mainly normal to the surface of the tapes; descriptions of the composite material tend to quote electrical properties for fields and currents in this direction, although the other directions are important on a smaller scale for treeing and for current-flow around voids within the insulation.

Models of this composite contruction were tested in [Hel00, ch.7], using electrical networks with components representing mica, epoxy and backing-materials. Epoxy was used in cured and uncured states, with backing tapes of glass-fibre and polyester film. The uncured epoxy showed a strong difference between film and fibrous backing, the film acting as a barrier to conduction; an H-shaped network rather than a simple series connection of materials was needed for a good model in the presence of the film, implying that significant currents follow paths passing around even these broad obstacles. The type of backing made much less difference with fully cured epoxy, and a plain series-model worked almost as well as an H-model. From these results it seems that fully cured epoxy-based stator insulation does not show radical differences in dielectric response compared to its constituent materials, due to the composite construction.

In well-bonded thermoset insulation the conductivity is 'essentially zero' [E43, p.5]: as this claim was made in relation to dc measurements lasting at least 600 s, it should mean that conductivity contributes considerably less than polarisation and leakage current even at 1 mHz. In old asphalt-impregnated insulation the conductivity is significant and the effect of the interspersed barriers of mica, blocking conduction, can be expected to be more important, as seen

for the uncured epoxy in [Hel00]; in [E43] the hygroscopic cotton backing tapes used before about 1970 are claimed to contribute to the conductivity.

The relaxation approximates a power law over the frequency range of power-frequency to millihertz at room temperature. This can be seen in $\tan\delta$ for fully cured epoxy-mica insulation in [Hel00, ch.6]. The power law is widely assumed for the polarisation current in time-domain measurements on stator insulation [E43], implying power law of the polarisation in frequency too [s.5.3]. The response to a step-voltage V can be expressed as $i_{\mathrm{pol}}(t) = C_0 V K t^{-n}$, where K is called the absorption coefficient (*absorption* is often used, in time-domain work on machines, to mean general polarisation including dipolar and interfacial mechanisms). Estimated K and n values based on measurements from times of 60 s, 190 s and 600 s on several examples of the main types of stator insulation are shown in [McD00]. For asphalt-based insulation $n \sim 0.8$, and for the polyesters and epoxies $n \sim 1.0$, both of these with about $\pm 20\%$ variation between machines and different occasions, taking the exponent well beyond a fractional power for some values. Variation in K was as much as a factor of four between occasions, and values were generally more than ten times greater for asphalt than for polyester or epoxy.

Taking the above results together with some practically oriented claims from standards, modern stator insulation in good condition can be said to have a a simple dielectric response over the frequency-range of interest in this work, and a low conductivity such that the displacement currents are dominant even at the lower range of frequencies relevant to the diagnostic methods considered in this work. The power-frequency relative permittivity is about 4 and a typical loss-tangent is about 0.5% [Sto04, p.250], in contrast to about 3% to 5% for asphalt-mica [Sto04, p.257]. Measurements made on newly manufactured epoxy-mica stator bars in this work [s.18.3] gave quite similar values, with a power-law exponent $n \simeq 0.86$.

5.5.3 Currents in a healthy stator insulation system

The above discussion covers only the relatively simple matter of a composite material between a pair of parallel electrodes. There are plenty of other sources of the current that flows during measurements of the electrical properties of stator insulation. The main paths of current in the insulation are shown in figure 5.2 and described in the following paragraphs. The upper bar in the figure is a 'good' one, in which the normal sources of currents are shown. The lower bar is a remarkably bad one, and the diagram shows the main ways in which deterioration of insulation can change the currents flowing in the paths found in good insulation or can add further paths. These effects of deterioration are examined in the following subsections.

In a stator insulation system in good condition the current flowing between the conductor and earth is due mainly to the capacitance of the insulation within the slot. The symbolic capacitor representing this insulation in the diagram is the frequency-dependent complex-capacitance due to the prompt response and polarisation of the composite insulation material described above. A resistance has been added, parenthesised, as a component that might be significant in

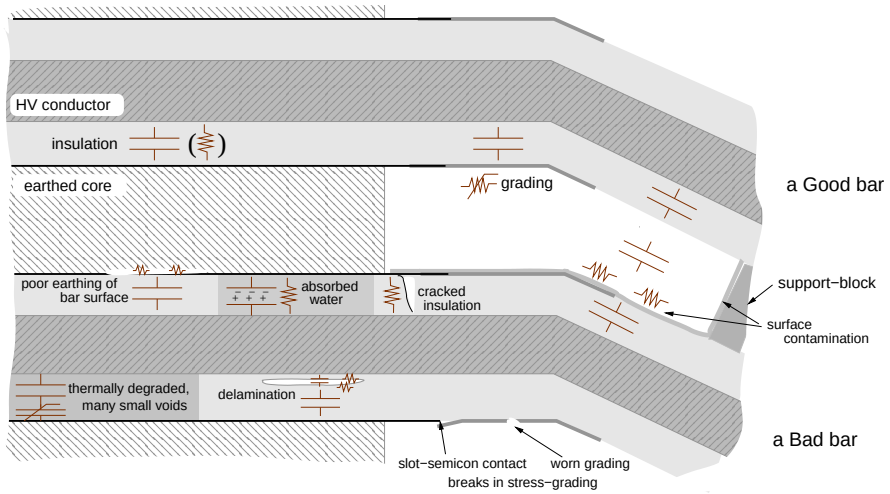

FIGURE 5.2: Sources of current in the overall DR behaviour of stator insulation. This illustrative example uses a cross-section of two adjacent bars from a little way into the slot and a little way outside; figure 2.2 puts this into context for a relatively small high-voltage motor.

asphaltic insulation but that should be negligible within epoxy-based insulation in good condition.

In the transition between the core and end-winding the nonlinear resistive stress-grading layer across the insulation surface forms a composite dielectric system whose current includes capacitance and loss components and harmonics, all dependent on the amplitude and frequency of the applied voltage; this is analysed in much more detail in chapter 19.

Out in the end-winding region there will be very little current between the conductor and earth if adjacent bars' conductors have the same potential; if adjacent bars are on different phases and a diagnostic measurement is made with one phase excited and others earthed, there will be capacitive coupling through the air and solid insulation.

5.5.4 Chemical changes in the insulation

The organic part of the insulation, mainly the epoxy, polyester or asphalt, changes chemically over time. Thermal aging [s.3.2.1] in an air-cooled machine results in oxidation of the polymeric insulation material, which tends to increase the number of polar groups, increasing the loss [Sto04, p.255]. The capacitance may fall in spite of more polar gorups, due to voids and insulation expansion that arise from the weakening of the insulation by thermal aging.

Some attempts have been made to obtain diagnostic information from inferences about these materials based on measurements on the whole winding. Stator insulation systems make this difficult, with their dielectric response having so many other effects than just those of the organic solid; on the other

hand the decomposition of this solid during the insulation's lifetime is considerably more than would be tolerable in pure dielectrics such as polymeric cable-insulation. In [Dac89] the space-charge accumulation at mica barriers due to ionic and electronic conduction mechanisms in epoxy has been considered as an explanation of some of the time-dependence of current in stator insulation and as a guide to the degree of thermal aging. Greater aging is assumed to increase the ionic mobility for conduction, due to 'de-structuring' of the polymer, and to decrease the electronic mobility for conduction, due to deeper traps. The time-constants of these mechanisms are different, and the degree of aging is inferred from the dominant time-constant in the current due to a dc voltage held for many minutes. Capacitance measured at stages of accelerated thermal aging has been seen to have an initial fall from post-polymerisation (completion of curing) then a rise with a peak after considerable aging [Gof98].

5.5.5 Voids and insulation-expansion

As a result of thermal aging the epoxy or asphalt may be weak or largely missing from some parts of the insulation. Severely aged insulation is quite soft, with many small voids (cavities) between poorly bound pieces of mica and around edges or wrinkles in the tapes. The substitution of gas for solid epoxy will increase the capacitance of the bulk of the insulation even if the total volume between the electrodes is fixed. Slight extra expansion at the cooling ducts allows the electrodes of the inner conductors and slot semiconductor layer to move further from each other, reducing the capacitance still further. About a 1% decrease in capacitance can be expected due to the voids that arise from 'considerable' thermal aging of epoxy-mica insulation [Sto04, p.250].

Discharges across the cavities at high voltage serve, as a first approximation, to short the cavities and thereby increase the capacitance as well as increasing the loss. Slightly conducting surfaces in the cavities allow currents that the cavities, giving increased capacitance and introducing a dielectric loss due to the energy lost in the resistance. In contrast to PD across the void, the conductivity could have effect even at low fields. PD activity is a likely cause of surfaces becoming more conductive (chapter 7). The effect of conduction on void surfaces is considered in [Gof78] as a way of explaining some of the variation of capacitance and loss with voltage amplitude and degree of aging, for which simple PD models alone are not sufficient.

Within the main insulation there may be substantial delaminations; wide, shallow voids between tape-layers or between tapes and electrodes. At moderate applied voltage these will block any conduction in the gap, and will reduce the insulation's capacitance by adding a series gas-capacitor; the situation is qualitatively similar to the smaller cavities already mentioned. The relatively large area of a delamination normal to the applied field, and the consequent large ratio of the displacement current across the delamination to the length of the delamination walls that might have some conductivity to bypass the delamination, result in some quantitative differences. PD can be of large magnitude and cannot so easily be avoided by slight conductivity of the dielectric surfaces. At low fields a given surface conductivity will not short-circuit the delamination so effectively as it would short-circuit a smaller void.

5.5.6 Electrostatic compression

A further effect on dielectric response from the voids and softening of thermally aged insulation is due to electric-field-induced compression of the insulation between the electrodes. A simple model would expect compressive forces in proportion to the square of the applied voltage, resulting in an increased capacitance at increased voltage even in the absence of PD. Odd-harmonic currents will be caused by the changes of capacitance within each half-cycle.

This has been studied in [Bur88], including measurements on thermally aged stator bars of both types of impregnant, asphalt and epoxy. At 7 kV in bars rated about 20 kV with insulation thickness of 6 mm, a displacement of 0.1 μm was seen in the epoxy type and 0.5 μm in the asphalt type; the field in the epoxy was taken high enough to get 0.5 μm there too at 18 kV. Displacement increased with lower frequencies. Variation of capacitance, ΔC, around the low-field value of about 480 pF was measured at voltages below PD inception, at 120 Hz, 12 Hz and 1 Hz. The variation was seen to be several picocoulombs, fitting better with a model based on solid insulation moving to fill a delamination than with a model predicting smaller changes of capacitance based on uniform compression of a solid with many small voids. Much larger ΔC, by some seven times, was seen at the lowest than at the highest frequency; as the measured displacements did not change this much, one might wonder whether for example surface conductivity is playing a part. A suggestion of [Bur88] was the use of this variation of capacitance as a measure of delamination, possibly measuring the response to a small ac voltage superimposed on a large dc voltage.

The study of voltage-dependence due to mechanical effects was taken further in [Pin91], with an analysis of effects of compression on capacitance, loss and harmonics, and several measurements on a complete stator winding. This winding was in a micafolium-insulated 6.6 kV motor with severe delaminations. It was measured at power-frequency at voltages below the (detected) PD inception of 3.3 kV; this old insulation system had fortunately no end-winding grading to disturb the results. The variation in capacitance was 60 pF within the total capacitance of 50 nF, with a quite good fit to $\Delta C \propto V^2$. The variation in $\tan\delta$ was some 2.4% of the initial value of about 0.06. The third-harmonic current was also measured, and was seen to increase by a factor of three between 1 kV and 3 kV; unfortunately the absolute value is not reported. The $\tan\delta$ and third-harmonic variations also fitted well to the square of the voltage.

5.5.7 Poor earthing of the bar surfaces

The outer surface of the main insulation is ideally held at earth potential by the presence of a semiconductor layer in good contact with the core. A worn semiconductor, or a poor contact with the core requiring currents from the insulation to flow far along the semiconductor, will introduce a further resistance in series with the insulation's capacitance, introducing a frequency-dependent loss. In extreme cases of practically no conductivity on part of the bar-surface, there will either be a straightforward reduction in measured capacitance, or at high enough voltages PD will perform the task of conducting the displacement

current away, permitting some of the insulation capacitance to be measured but introducing losses.

The change of the stator's dielectric response due to lack of earth potential around the bar can be estimated for some simple cases. The effect will be stronger at higher frequencies where the series capacitance of the insulation has a lower impedance. If the bar has lost contact with the core, and the slot semiconductor is missing over an area of larger size than the insulation thickness, the situation described earlier for a delamination is a good approximation, reducing the total capacitance by introducing the further series capacitance of the gas-gap. If a significant length of the bar must be travelled by the current in the slot-semiconductor before good contact with the core is made, then the 'linear distributed' model of end-winding grading discussed in section 19.4 is relevant. This could even be relevant for the length of bar within a cooling duct, if the semiconductor had an excessively low conductivity.

5.5.8 Water absorption

Water is highly polar, having by itself a relative permittivity of about 80 at the frequencies of interest here. It also introduces some ions that can form a conduction current. Water absorption will therefore increase the capacitance and loss of the insulation. Old thermoplastic insulation is hygroscopic [E43, p.9], so is rapidly affected. Modern insulation is very resistant to water absorption, but it is possible, particularly with direct water-cooled windings, for a slow, long-term presence of water to permeate through the whole thickness of insulation in a matter of years. The capacitance measured at power frequency may be increased by some 5% by 'significant' water absorption [Sto04, p.252]; the presence of water is described by [E43] as 'greatly affecting' the permittivity.

The phenomenon of *electroendosmosis* can result in polarity-dependence of the current in the insulation [E43]; the current measured after many seconds at a high dc voltage is then typically 'much higher' when the winding's conductors are negative with respect to the core than when they are positive. Even-order harmonics are therefore to be expected in the insulation system's current at low frequency in this case.

5.5.9 Surface contamination

If the end-winding surface is contaminated with a somewhat conductive layer, such as of dust and condensation, a distributed circuit is formed from the shunt insulation-capacitance and series surface-resistance, rather like the stress-grading. The conductivity may be very varied between different points, and rather nonlinear with electric field; dry-bands and discharges across them may form as is common on other contaminated insulator surfaces [LaF82]. Displacement currents through the end-winding insulation can be carried along the contaminated insulation surfaces: the main destinations are the earthed core or the surfaces of end-windings of other phases, reached through contamination on support blocking and lashing.

5.5.10 Fractures and pinholes

Cracks and holes in the insulation, ultimately permitting a mildly conductive path from the internal conductor onto the insulation surface, are most common in the end-winding region [s.2.2.2]. In this case there may be a significantly conductive path all the way between high-voltage and earthed conductors, other than just the bulk insulation's conductivity that is so low for modern insulation. Removing the presence of a pure series capacitance removes the limit to the charge that can move per cycle; a conductive path will show increasing charge, and therefore capacitance, with decreasing frequency. This situation's sustained conductive path is in contrast to all of the previously mentioned current-sources, apart from the possibility of surface-leakage at the winding terminals. Increased temperature may reduce the conduction in cracks [E95], presumably due to thermal expansion closing the crack or to less condensation; other conduction is increased.

5.5.11 Summary

Defects in the stress-grading, other than surface contamination, tend to reduce the current into the core. Worn grading or broken contact at the contact between slot semiconductor and end-grading are shown in the figure. Discharges, as with a delamination, may help to reduce the amount of 'lost' current due to such breaks.

The relevance of all these types of deterioration and their effect on the apparent DR of the insulation system is the desire to find indications of particular sorts of deterioration from the measurements. The above discussion of different forms of deterioration gives very little obvious help: some forms decreased the capacitance, and some increased it; some had a nonlinearity or frequency-dependence, but so do end-winding grading systems. Cracks permitting a full path between the high-voltage conductor and earth without series capacitance have probably the most distinctive result, but even this depends on a significant conductivity in the crack. The identification of a small change in permittivity in a small part of the insulation is hopelessly unrealistic; deterioration that affects most of the insulation or has a very severe local effect may be detected.

Chapter 6

Dielectric Response measurement

Currents flow in the electrodes of an insulation system due to the phenomena of conduction and polarisation described in the previous chapter. These currents are measured in material studies and in several common diagnostic methods. There are dynamic effects due to the pure material dielectric response and due to arrangements of different materials in complicated insulation systems: measurements made over a range of time or frequency permit some of the dynamics to be seen. Some common methods of dielectric response measurement are described in this chapter, with a focus on instrumentation and interpretation of the type of frequency-domain measurement used in this work. Common applications to diagnostic measurements on high-voltage insulation are described, considering stator insulation in particular.

6.1 Dielectric-response measurements in time and frequency

A measurement at the low frequencies of interest here involves circuit properties at electrodes. Most commonly, a specified voltage-signal $v(t)$ is applied, and the current $i(t)$ that this voltage causes in the dielectric is measured; from these the dielectric response is derived.

Calculation of some material properties requires further information about the arrangement of electrodes and dielectrics, which for simple homogeneous cases can be expressed as the geometric capacitance C_0. For measurements on complicated insulation systems it may be that the apparent dielectric response of the whole system is all that is needed, perhaps for comparison with other results, or it may be that a property of a constituent material is to be inferred. In the following sections it will be assumed that the circuit properties between electrodes are the 'dielectric response' to be measured.

The two common descriptions of material dielectric response [s.5.2] are the dielectric response function $f(t)$ and the susceptibility $\chi(\omega)$ [s.5.3]. The choice of suitable $v(t)$ to give easy calculation of one or the other of these functions defines the measurement as being *time-domain* or *frequency-domain*. The choice of $v(t)$ also affects the extent to which the prompt response ε_∞ and conductivity σ can be distinguished from the polarisation, other than by further assumptions and calculations [s.5.2].

Measurements that study dielectric response as a function of frequency are *dielectric spectroscopy*, DS. The obvious way of doing this is a frequency-domain measurement, FDDS, but sometimes a time-domain measurement is made and then transformed into a function of frequency, in TDDS.

6.1.1 Time-domain measurements

The most obvious time-domain method is the response to a step-voltage. If the voltage $v(t)$ consists of a step V_Δ, with constant values before and after this, then the current due to polarisation after the step is $i_{\mathrm{pol}}(t) = V_\Delta C_0 f(t)$. Added to this is the pulse of current carrying a charge $V_\Delta \varepsilon_\infty C_0/\varepsilon_0$ to the prompt capacitance at the time of the step, and the current due to steady conduction, $i_{\mathrm{con}}(t) = (v(t^-) + V_\Delta)\,\sigma C_0/\varepsilon_0$, where $v(t^-)$ is the voltage before the step.

A virtue of stepped voltage when interested in the dynamic polarisation is that the prompt response is absent from all but the short time around the step, leaving the polarisation dynamics more clearly seen. The lower limit of time-resolution is governed by how quickly the voltage on the test-object can be changed and how accurately the times of measurements can be related to this step. With power-electronic switching of measurements on material samples the times can be submicrosecond [Jon96, p.269], but for high-voltage measurements on insulation systems the charging may take in the order of seconds for a reasonable size of voltage-source. Noise-rejection of a single measurement is low compared to frequency-domain methods that can be tuned to an expected frequency, but a time-domain measurement obtains results corresponding to a range of frequencies from a single set of time-points, and the results can be averaged over several repetitions of the measurement to reduce noise.

A common type of step-response measurement is polarisation and depolarisation currents, *PDC*. The initial step is the connection of a dc voltage-source to a test-object that has previously been at zero voltage for a long time; after the initial transient the polarisation and conduction currents are measured until a time when the voltage source is replaced with a short circuit, and the depolarisation current, in other words the polarisation current for a negative step, is measured.

The results are only valid for measurements much shorter than the time for which the preceding voltage was held, as the direct relation of (de)polarisation current to dielectric response function requires the initial state to be fully relaxed to the pre-step voltage. A common suggestion for acceptable results is a polarisation-time ten times as long as the measurement of depolarisation current; a similar condition is assumed for the short-circuit time before the polarisation. Some effects of a non-relaxed pre-step state may also be analytically compensated, given knowledge of the earlier voltages.

An advantage of PDC over a single step is that the steps of opposite direction should result in the depolarisation currents being the negation of the polarisation currents; the conduction current can then be estimated from their sum. For DS measurements on high-voltage insulation this appears to be widely held as an acceptable method of separating conduction and polarisation currents; but according to [Jon96, p.8], concerned with the detailed study of materials over a wide range of times, the difference between the polarisation and depolarisation current magnitudes does not give the constant value of these simple models.

Another form of time-domain measurement uses a ramped voltage: the simple model of ε_∞, σ and $f(t)$ then gives a constant current from the prompt-response, a ramp from conductivity and a messy convolution from the dielectric

response function. This form of voltage is more easily justified for industrial insulation-testing [s.6.4.3] than for studies of dielectric response of materials: the ramp can reach voltages that stress the insulation considerably, but the gradual increase gives a chance of stopping if alarming trends in current are seen.

6.1.2 Frequency-domain measurements

The simplest frequency-domain measurement applies a sinusoidal voltage $V(\omega)$ as excitation, and measures the sinusoidal current $I(\omega)$ that flows. The concept of functions of frequency implies that these signals extend forever in time, or in a practical sense that an equilibrium response to sinusoidal excitation has been reached [s.16.3]. Given a linear object and an instrument without such problems as decaying terms in its feedback [s.6.2], a single cycle should suffice, although more may be needed to reduce the effect of noise; less ideal situations may require a few cycles of excitation before the current is measured.

The *measured* complex capacitance is then

$$C(\omega) = C'(\omega) - \mathrm{i}C''(\omega) = \frac{I(\omega)}{\mathrm{i}\omega V(\omega)}, \tag{6.1}$$

which in contrast to the pure complex capacitance of (5.7) includes the effects of conductivity in its imaginary part. For an arrangement of electrodes with geometric capacitance C_0, surrounded by a material of permittivity ε according to (5.6) and of constant conductivity σ, the complex capacitance relates to the polarisation, prompt response and conductivity as

$$\begin{aligned} C(\omega) = C'(\omega) - \mathrm{i}C''(\omega) &= C_0 \left[\frac{\varepsilon_\infty}{\varepsilon_0} + \chi'(\omega) - \mathrm{i}\chi''(\omega) - \mathrm{i}\frac{\sigma}{\omega\varepsilon_0} \right] \\ &= \frac{C_0}{\varepsilon_0} \left[\varepsilon_\infty + \Delta\varepsilon'(\omega) - \mathrm{i}\varepsilon''(\omega) - \mathrm{i}\sigma/\omega \right] \\ &= \left(C_\infty + \Delta C'(\omega) \right) - \mathrm{i} \left(C''_{\mathrm{pol}}(\omega) + G/\omega \right), \end{aligned} \tag{6.2}$$

where C''_{pol} is subscripted to distinguish it as the pure C'' due to polarisation (5.6) rather than the measured C'' (6.1). In the later practical uses it is the measured values that are used, with any conduction term G included in C''.

Other representations such as complex conductance may be useful in some applications. The behaviour of high-voltage insulation systems will however generally be closer to that of a capacitor, with the charge-per-cycle varying much less with frequency than the charge-per-second does. The complex capacitance therefore makes the material's frequency-dependence clearer.

The last form of (6.2) is the most useful for a measurement on a whole apparatus, where material properties are not the focus and where geometric details may not be known. It is clear that the currents due to the prompt response and conduction will be unavoidably mixed with the currents due to polarisation. Given that both of these extra currents are frequency-independent it is possible to use the Kramers-Kronig relations [s.5.2] to calculate the pure polarisation components from the changes in the complementary parts. This

is used more in materials studies than when analysing the mixture of current sources found in a stator insulation system.

Knowledge of the expected frequency of the current in FDDS permits tight filtering to reduce noise, but a separate measurement is needed for each frequency. This is time-consuming at low frequencies such as the millihertz range, and several cycles are needed at each frequency if a strong advantage is to be gained from the ability to filter the signal [s.6.4].

An overview of measurement methods used in the study of materials is given in [Jon96, ch.10], from about twenty years ago. The classic bridge methods were used down to about 10 Hz, or even to 0.1 Hz with clever use of xy traces on an oscilloscope. The availability of frequency-response analysers, *FRA* , in about 1980 enabled measurements down to 10^{-4} Hz or 10^{-5} Hz, using an analogue correlator to compare measurements of the voltage and current on the test-object, with an electrometer as the input stage for measuring the current. The DS instrument used in this work, described in chapter 9, can be seen as a digitally based FRA that includes the necessary electrometer and feedback.

6.2 Some practicalities of FDDS measurements

This section considers some general features of FDDS measurements using a feedback electrometer to convert the small current to a measurable voltage, then extracting the Fourier components of this current. More specific details of the instrument used in this work are found in chapter 9.

6.2.1 Input signals

A good insulator excited at a low frequency gives a very small current. A laboratory sample may be only some tens of picofarads, which for applied voltage of tens of volts and frequencies in the millihertz range corresponds to a current of picoamps. Industrial insulation systems will usually have higher capacitance, such as hundreds of nanofarads for a stator winding, and may also be tested at high voltages; the current can then come into the order of amps, but the power-supply of the instrument [s.9.1.2] may have a lower limit.

Measurement of the small currents requires an input stage between the very high-impedance test-object and the relatively low input-impedance of the FRA or analogue-digital converter that is used as the recording instrument; an *electrometer* provides a suitable interface. The instrument called an electrometer is a 'highly refined dc multimeter' [Kei04] specialised in measuring very low currents, down to a few femtoamps, and voltages from very high-impedance sources; at the core of the electrometer instrument is a pure electrometer, which can be regarded as an op-amp optimised for very small currents. The input stage for measuring current in FDDS uses such an electrometer in feedback mode [Jon96, ch.10] with feedback components selected so that the expected input current will produce an output voltage within a reasonable range for the recording instrument. The feedback components have to be variable over a wide range of impedances, to allow for the range of test-objects that may be used and the range of amplitudes and frequencies of the voltage applied to them; consider the above examples ranging from picoamps to amps.

The voltage applied to the test-object must also be measured, with the same demands on precision as for the current [s.6.2.5]. DS measurements at low voltage permit direct connection of the recording instrument to the voltage source. At the high voltage required for most of this work, some conversion is needed. The most obvious method is to use a voltage-divider with good phase-response; an alternative used in this work is described in [s.9.1.3], involving measurement of the current in a capacitor of accurately known value.

The result of the above input stages is that the voltage and current at the test-object are both represented by a voltage signal within a range easily measured by standard electronic circuits.

6.2.2 DFT components

The description of a measurement as 'frequency-domain' suggests that sinusoidal components in the measured quantities will be the desired final result. The following is an explanation of how these components are derived from the time-domain signals that come from the electrometer and the voltage measurement. It goes into what may seem excessive detail about the mundane matter of Fourier series; this is useful as a background for later discussion of disturbances and measurement of PD pulses, and is also a good opportunity to define some terminology.

Consider a time-signal $s(t)$ of an arbitrary waveform repeating with period $T = 1/f = 2\pi/\omega$. The periodicity permits the signal to be described as the sum of a Fourier series of sinusoids, with frequencies of integer multiples of f and with arbitrary amplitude and phase. The double-sided Fourier series popular in maths splits each harmonic magnitude into a half for positive frequencies and a half for negative frequencies: for a real-valued input such as a physical measurement in time, it is preferable to use just positive frequencies and to scale the transform so that the amplitudes of the harmonics describe directly the amplitudes of the sinusoidal signals that must be summed to reproduce the original time-signal. The sinusoid at the frequency nf is described by the nth *Fourier-series coefficient*, either in polar form as a complex coefficient S_n or in rectangular form as cosine and sine coefficients A_n and B_n. Coefficients satisfying the above condition for the amplitude can be calculated from an integer number N of periods of $s(t)$ as

$$S_n = A_n + \mathrm{i}B_n = \frac{2}{NT}\int_0^{NT} s(t)\exp(\mathrm{i}n\omega t)\mathrm{d}t. \tag{6.3}$$

These are the *harmonic components*, and n is the *harmonic order*. The component for $n = 1$ is the first harmonic, or *fundamental* component of the signal, the component of the signal at the same frequency as its periodicity. The higher harmonics $n = 2, 3, \ldots$ are the second, third, and higher *harmonics*. In the engineering use of these terms, 'harmonics' is often used to refer *only* to components above the fundamental: this convention is followed in the later chapters, as a short way of making a useful distinction. The other important component is the zeroth harmonic, the *dc component* or *dc term*, giving the mean of the signal: this is calculated from (6.3) with $n = 0$, but multiplying by $1/NT$ rather than $2/NT$.

In the ideal case, $s(t)$ is truly periodic with period T, and (6.3) is calculated perfectly: there is no difference between using one or more periods, and the orthogonality of sinusoids of different frequencies ensures that only the component of $s(t)$ at the frequency nf appears in S_n. In some calculations of S_n from measured data there may be a trouble of not knowing exactly the frequency of the periodicity, and therefore having an error in the ω in the exponential of (6.3); this is not a problem with DS as long as a single reference source can be used to generate the voltage applied to the test object and to provide the signal corresponding to the exponential. In practical DS measurements the signal $s(t)$ can be expected to consist of a part that is periodic at the expected frequency, due to the known applied voltage, but there will also be components that are aperiodic or that are periodic with a period other than T. The condition of periodicity made for $s(t)$ is then violated, and S_n can be affected even by a signal that would have no component at frequency nf if extended over all time. The extent of this effect can be seen by solving (6.3) for the particular disturbance.

There are several disturbance signals relevant to later discussions of DS. A constant ramp or decaying exponential may occur with particular combinations of electrometer feedback [s.6.2.6] and measured current [s.6.2.7]. Pulses of random noise may occur at some points in the signal, differing from PD charges only in that they are not expected to have periodicity; for infrequent PD over small numbers of cycles the distinction from noise is weak. High-frequency noise such as background radiated noise and thermal noise is filtered well from the measurement of S_n, since it integrates close to zero over any small part of T. Sinusoids at frequencies quite similar to the measured frequencies may be picked up from external sources: disturbances at the power frequency are particularly common [s.12.4]. A signal consisting only of a disturbance $M_\mathrm{d}\cos(2\pi f_\mathrm{d} t)$ results in an nth cosine-coefficient A_n of

$$A_n = M_\mathrm{d}\,\mathrm{sinc}\left(2\pi N\frac{nf-f_\mathrm{d}}{nf}\right), \tag{6.4}$$

where $\mathrm{sinc}(x) \equiv \sin(x)/x$ [Jon96, p.277]. A larger number of periods clearly gives better noise-rejection, but with local maxima and minima as the total time-window of NT passes multiples of the frequency difference $f-nf_\mathrm{d}$.

It can be seen from (6.3) that a measurement over N cycles gives the arithmetic mean values of the separate measurements over single cycles. Parts of the signal occurring only in some periods will appear as weaker signals occurring in all periods. Parts whose mean S_n over many periods tends to zero will be better removed by including large numbers of periods, as was seen for the sinusoid at nonharmonic frequency. The larger number of periods is no help with a ramp: this can be decomposed into the sum of a zero-centred ramp, similar in each period, and a dc term that gets larger in each period; the effect on a particular harmonic order other than the dc term is independent of the number of periods used. A decaying exponential has a progressively lower decay, in absolute terms, over subsequent periods, and only for this reason has a reduced effect when more periods are used.

The contributions of several functions of time on the fundamental component S_1 are shown in figure 6.1 for varied N. The sinusoid of frequency f and the

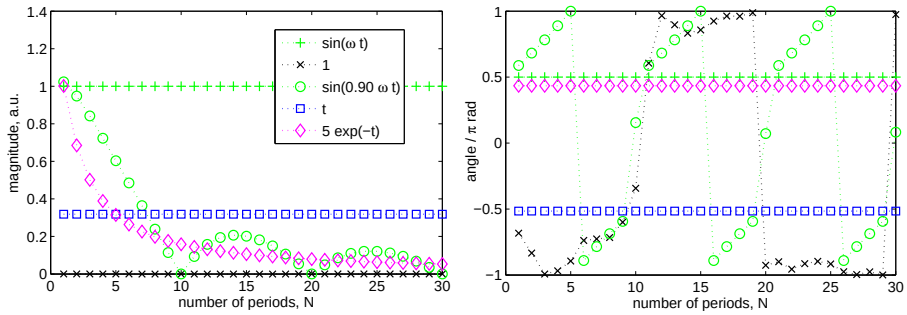

FIGURE 6.1: Contributions of various time-functions to the 1st harmonic (fundamental-frequency) component S_1 of equation (6.3) at $f = 1\,\mathrm{Hz}$, for varied numbers of periods N.

dc signal are already pure harmonic components, so they give the expected contributions of 1 and 0 to the fundamental component, along with some numerical noise in the phase caused by the dc signal. The sinusoid at a 10% difference in frequency behaves according to (6.4); note that figure 6.1 shows the magnitude of the complex coefficient, which changes only half as fast with N as the real part used in (6.4). The ramp and exponential give constant and decaying magnitudes.

The correlator of the analogue type of FRA works directly on the input voltages representing voltage and current at the test-object. The current is multiplied by sinusoids in phase and in quadrature with the voltage, which ideally is sinusoidal. These sinusoids are like the real and imaginary part of the exponential in (6.3), and the integrals over a whole number of cycles give the rectangular-form coefficients A_n and B_n. Compensation for phase-shifts in the circuit and feedback allows calculation of the complex capacitance by (6.1).

A more modern approach takes advantage of cheap commodity-hardware that can sample and process signals at for example rates of hundreds of kilohertz and resolutions of 16 bits. The input voltages representing voltage and current at the test object are directly sampled and digitised, and signal processing is all on the digital side. The calculation by (6.3) of the nth Fourier series coefficient is replaced with a discretised version, the *discrete Fourier transform* (DFT), operating on K samples $s[k]$ taken at regular intervals over N periods,

$$S_n = \frac{2}{K} \sum_{k=0}^{K-1} s[k] \exp\left(\mathrm{i}\frac{2\pi k n N}{K}\right), \tag{6.5}$$

where again the dc term $n = 0$ is a special case for which the result of (6.5) must be halved. The similarity of S_n between (6.3) and (6.5) is dependent on the sampling; the many samples per period of the instrument used in this work [s.9.1.6] make the approximation close.

The implementation of (6.5) requires for each sample $s[k]$ the generation of numbers corresponding to the real and imaginary parts† of the exponential term; the product of each with $s[k]$ is *accumulated* (summed with an existing value) into a variable for the real and for the imaginary part of S_n. The same is done for several values of n: the instrument used in this work includes the components from 0 to 8. The sampling must clearly be coordinated with the expected periodicity of the signal: a small error such that the K samples of supposedly N cycles actually occur over a slightly different number of cycles is the same as the error in ω already discussed for (6.1). The sampling must therefore be locked to the generation of the output voltage, so as to guarantee measurements based on exactly the right fundamental frequency. Just as for the analogue FRA, the results of S_n for the inputs representing voltage and current must be adjusted for effects of the electrometer circuits and external circuit, to give the desired frequency-domain results for the quantities at the test-object.

6.2.3 Distorted sources and nonlinear test-objects

The discussion of FDDS, up to this point, has described how the dc, fundamental-frequency and higher harmonic terms are measured for the voltage and current at the test-object, but has only considered the use of capacitance and loss, both of which relate only to the fundamental-frequency.

The voltage applied to the test-object surely has some level of *distortion*, a deviation from a pure sinusoid, meaning that not all the *voltage harmonics* $V_{2,3,\ldots}$ are nonzero. Even if the test-object is linear, the nth voltage harmonic V_n will result in a nonzero nth *current harmonic* I_n. The capacitive nature of a typical test-object will result in the amplitude of a current harmonic being proportional to its harmonic order as well as to the amplitude of the respective voltage harmonic, so that similar amplitudes of V_2 and V_8 would give $|I_8| = 4|I_2|$.

With the amplifier and DS instrument used in this work [s.9.1.2], driving a largely linear load at 10 kV, the harmonic voltages are in the order of 1 V when the amplifier is giving a large proportion of its rated current, and much lower for small currents. Although these may sound small, the effect of voltage harmonics often needs to be removed before using the current harmonics in calculations. For delicate measurements of the contribution of small nonlinear sources to the much larger total current in a capacitive object, even the currents due to these small voltages can be significant. For measurements on strongly nonlinear objects the strong current harmonics will cause extra voltage harmonics due to the supply impedance, leading to further current harmonics in the capacitance.

Unless there is very high dispersion it is a reasonable first-approximation to use the capacitance C' measured from the fundamental components of voltage and current to estimate the current harmonics $\mathrm{i}n\omega V_n(\omega)C'$ due to the measured voltage harmonics $V_n(\omega)$, and to *compensate* the original measured current $\hat{I}_n$ for the effect of the voltage harmonics by subtract this estimate,

$$I_n(\omega) = \hat{I}_n(\omega) - \mathrm{i}n\omega V_n(\omega)C', \quad n = 2, 3, \ldots. \tag{6.6}$$

† These are often called the DFT coefficients, but this name is avoided here as S_n is the (approximated) 'Fourier series coefficient', probably leading to some confusion.

The measurement of the harmonics is good enough that applying this compensation to the case of a very linear gas-capacitor reduces the current harmonics by several times. Other methods than (6.6) may be preferable in certain circumstances: complex capacitance can be used instead of pure capacitance, and the frequency-dependence of capacitance can be modelled or measured to give a better estimate of the value at the harmonic frequency.

Nonlinearity of the test-object results in current harmonics even for a purely sinusoidal voltage. Several sources of nonlinearity in stator insulation have already been mentioned in [s.5.5]. Most of the sources give a quite smooth nonlinearity, so that most of the information is in the first few harmonics. Even for the inherently pulse-like phenomenon of PD, the individual PD events in a whole stator are only a tiny part of the whole DS current, and aggregation of the many events that are needed to get a discernible measurement gives again a relatively smoothly distorted current where the harmonics beyond about the tenth are of very little importance.

The approximate time-signal $\bar{s}(t)$ formed from just the spectrum up to and including the Nth harmonic can be calculated from the DFT results S_n as

$$\begin{aligned}\bar{s}(t) &= \Re\left[\sum_{n=0}^{N} |S_n| \exp\left(\mathrm{i}\,(n\omega t - \angle S_n)\right)\right] \\ &= \sum_{n=0}^{N} \Big(A_n \cos(n\omega t) + B_n \sin(n\omega t)\Big) \\ &= \sum_{n=0}^{N} |S_n| \cos\left(n\omega t - \angle S_n\right), \end{aligned} \tag{6.7}$$

which is useful for physically based consideration of the shape of the current from its fundamental and harmonic components. One useful purpose of having the DFT components rather than just working with time data directly is that the tight filtering of harmonics allows even very small nonlinear currents to be studied against a background of a large fundamental component.

6.2.4 Calculation of input current

The circuit in figure 6.2 is an electrometer 'EM' with its feedback components R_{fb} and C_{fb} The direction of components and signal is right-to-left in order to be consistent with later diagrams of the whole measurement system, where the applied voltage goes left-to-right to the test object C_{x}, and the current is measured on its return to the instrument.

The input current $I(\omega)$ to the electrometer circuit needs to be calculated from the measured electrometer output voltage $V_o(\omega)$. This would be a simple op-amp problem if the electrometer were an ideal op-amp: in fact, its input resistance and capacitance are finite, and its gain $H(\omega)$ is finite, complex and frequency-dependent. The approximate values of the electrometer parameters in the instrument used in this work are given in section 9.1.5. For very accurate calibration the values of feedback components may also need to be modelled as functions of frequency.

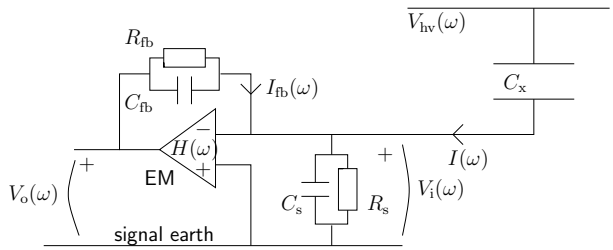

FIGURE 6.2: Circuit diagram of electrometer feedback, test-object, and parasitic components, for analysis of the relation between output voltage and input current.

The shunt components R_{s} and C_{s} in the figure can include the connections to the test object and the electrometer input. Note that if the electrometer's gain were perfect, always holding its inverting input to the signal earth potential, then the shunt components would be irrelevant. For measurements with long leads, high frequencies or large test-objects the series impedance of leads may need to be modelled too.

The resulting relation of current at the input to measured voltage at the output is

$$\frac{I(\omega)}{V_{\mathrm{o}}(\omega)} = -\left[\left(\frac{1}{R_{\mathrm{fb}}} + \mathrm{i}\omega C_{\mathrm{fb}}\right) + \frac{1}{H(\omega)}\left(\frac{1}{R_{\mathrm{fb}}} + \mathrm{i}\omega C_{\mathrm{fb}} + \frac{1}{R_{\mathrm{s}}} + \mathrm{i}\omega C_{\mathrm{s}}\right)\right] \quad (6.8)$$

The first term here, involving the feedback components, is the 'ideal' relation if the electrometer had a perfectly high gain so that its inverting input would be a true virtual earth. The further terms with the factor $1/H$ are the consequence of the inverting-input's node not being at true signal earth potential, causing the feedback voltage to change and some of the input current to be shunted away from the feedback components.

6.2.5 Error sensitivity

There are errors in the measurement of magnitude and phase of the voltage and current at the terminals of a test-object; these come from calibration errors in feedback components, circuit elements not perfectly modelled, temperature-dependence of calibration, and more. Relative errors in magnitude and absolute errors in phase contribute similarly to the errors of complex capacitance, as can be seen by considering (6.1) and de Moivre's theorem.

Dielectric measurements are generally concerned with the components of current in phase and in quadrature with the voltage, corresponding to loss and capacitance. In a low-loss dielectric such as most high-voltage insulation, the ratio of these components, $\tan\delta$, can be very low, in the order of 10^{-5} in some polymers. With this huge difference in relative sizes, even a 10 microradian phase error will be a 100% error in C''. The effect of magnitude errors is much less severe, resulting in a similar relative error in C' and in C''.

The calibration and modelling of components of the instrument and the external circuit must therefore be done very carefully. Modelling of, for example,

an extra filter would need to be very confident of limits of variation of component values with movement and temperature.

Stator insulation is actually not as critical as the above example, having typical power-frequency loss-tangents of significant fractions of a percent, for good modern insulation at moderate voltage, and several percent for old insulation. It is nevertheless desirable that phase-errors be small, particularly for laboratory work where detailed inferences may be desired from the data.

A further point about phase errors and feedback calibration is made in [Wer01a, p.47]. If a single feedback component is used, such as just a capacitor, it would need a phase error in itself in order to create a phase error in the result. When the feedback current is instead shared between a parallel capacitor and resistor, a relative error in magnitude in the value of one of the components will give a phase error in the total feedback impedance that is used in calculating the current. The effect is greatest when the components have similar impedance. This is just a further reason, beyond those in [s.6.2.7], for choosing one feedback component to be strongly dominant.

6.2.6 Choice of feedback

The electrometer output voltage, V_o in figure 6.2, is likely to have an optimal level in the few-volt range of electronic circuits; this voltage across the feedback components must provide a current that matches the measured current. DS measurements generally are made over at least several decades of frequency, and the capacitive test-object typical of high-voltage insulation will pass a current largely proportional to frequency. Measurements using resistive feedback therefore require switching between several different feedback resistances in order to keep the electrometer output voltage within its desired range; measurements using capacitive feedback can use a single capacitor over all the frequencies unless the test-object is highly dispersive.

A disadvantage of capacitive feedback is that the total charge that can be passed through the capacitor is limited by its capacitance and the range of electrometer output voltage. A test-object with significant conduction will pass large amounts of charge per half-cycle at very low frequencies, which may be too much for a reasonable size of feedback capacitor to supply. There may be a dc component required in the feedback current, which would make it impossible to continue with capacitive feedback beyond the time taken for this current to push the electrometer output voltage to its limit. This dc component is necessary if the test-object has polarity-dependent behaviour such as electroendosmosis [s.5.5.8] or an asymmetric external PD-source [s.7.2.1], or if interference is coupled in from extraneous currents sharing part of the measurement circuit, or if the electrometer itself has a significant input offset current [Sed91, p.100]. Resistive feedback permits a dc currents to be sustained for any time by a constant electrometer output voltage. It also simplifies the relation of output voltage to measured current, making them directly proportional. Even if a measurement is not run for long enough to drive the electrometer into overload, a dc current with capacitive feedback will result in a continual ramping of the electrometer output voltage: if the ramp changes significantly within a cycle, this ramping will affect the DFT results for the sinusoidal components as well

as the dc term [s.6.2.2]. Resistive feedback would permit the true dc current to be measured, *and* would not disturb the other DFT components.

A disadvantage of resistive feedback is seen when the measured current contains pulses of many times the mean amplitude of the signal; this is expected in the case of a test-object that contains PD or poor connections, particularly at low frequencies where the mean current is low. The feedback resistor will either be so low as to give a poor signal to noise ratio when measuring the signal between pulses, or will be so high that the electrometer voltage will hit its limit (electrometer overload) during the large current-pulses. This disadvantage comes from the same feature as was an advantage for dc currents: that is, the resistive feedback forms a proportional 'transresistance' amplifier, while capacitive feedback forms an integrator. A pulse of current into capacitive feedback simply requires a step change in output voltage rather than a very quick rise to high values.

The feedback should be kept mainly capacitive or mainly resistive, for reasons described in [s.6.2.5] and [s.6.2.7]. In this work the mainly resistive feedback has been preferred for several reasons: some test objects are expected to be polarity-dependent, measurements are made at low frequencies and with lossy objects such as those with external PD, and dc components are expected from some types of PD source. It has been seen that a small amount of capacitive feedback can be sufficient to buffer sharp pulses while allowing the other benefits of resistive feedback to be obtained; this is described further in chapter 14.

6.2.7 Feedback ratio

The description of some relative merits of resistive and capacitive feedback may make a quite even mixture seem a good idea: this could provide a resistive bypass for dc currents, and a capacitive buffer to hold pulsed charges until enough time has passed for them to leave through the feedback resistance.

In fact, a significantly mixed feedback has problems from output voltage waveform as well as from the effects of feedback calibration errors that were mentioned in section 6.2.5. Even with a linear test-object the previous, frequency-domain, analyses of the electrometer feedback circuit have problems. It is not true that a particular frequency has been present forever: the applied voltage is at some time turned on from zero or from an earlier value. Nor is it true that the output voltage is unlimited: even if the presence of a constant offset voltage on the output would not affect the measured fundamental-frequency value, it may drive the electrometer output into overload.

The circuit of figure 6.3 is used for analysis of the effects of feedback components on transient response. The test-object is represented, at a particular frequency, as a pure capacitance C_x and a parallel resistance R_x; the loss-angle $\delta = \tan^{-1}(1/\omega C_x R_x)$ then gives the phase-lag of the current $i(t)$ compared to the case where C_x is a pure capacitance. The electrometer is treated as ideal: the supply and test-object therefore form an independent current-source $i(t)$ into the virtual-earth node on the inverting input, and the feedback current

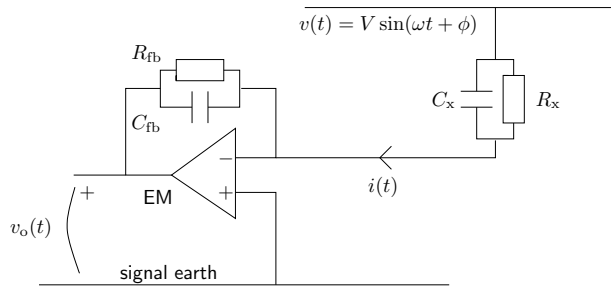

FIGURE 6.3: Circuit diagram of electrometer feedback and test-object for analysis of offset voltages at the electrometer output.

exactly cancels this current,

$$i(t) = \frac{v(t)}{R_{\rm x}} + C_{\rm x}\frac{{\rm d}v(t)}{{\rm d}t} = -\left[\frac{v_{\rm o}(t)}{R_{\rm fb}} + C_{\rm fb}\frac{{\rm d}v_{\rm o}(t)}{{\rm d}t}\right]. \tag{6.9}$$

The supply voltage $v(t)$ is known to be sinusoidal: for now it is assumed to start at arbitrary phase ϕ at time $t = 0$, being zero before this,

$$v(t) = 1(t) \times V\sin(\omega t + \phi), \tag{6.10}$$

where $1(\cdot)$ is the Heaviside step and V is the amplitude of the sinusoid. If ϕ is such that $v(0) \neq 0$, the step in voltage at $t = 0$ will cause a sharp current-pulse in $i(t)$ if there is any capacitance $C_{\rm x}$ in the test-object. Without significant capacitive feedback on the electrometer this situation cannot be handled, as the limited electrometer output voltage range and slew-rate cannot provide a quick pulse of charge through a resistor. With significant capacitive feedback the output voltage will also have a step, by $-V\sin(\phi)\,C_{\rm x}/C_{\rm fb}$.

It seems in fact that the instrument used in this work always starts the applied voltage from a negative-going zero, so that $\phi = \pi$; there is no step, so the input current $i(t)$ can only be a zero-centred sinusoid. It is convenient to use the polar form of the feedback impedance, whose angle is $\theta = \tan^{-1}(\omega C_{\rm fb}R_{\rm fb})$, describing the lag of $v_{\rm o}(t)$ with respect to the case of pure resistive feedback. Note that the definitions of δ and θ restrict them to $0 \leq (\delta, \theta) \leq \pi/2$. The solution of (6.10) can then be expressed as

$$v_{\rm o}(t) = V\sqrt{\frac{1/R_{\rm x}^2 + \omega^2 C_{\rm x}^2}{1/R_{\rm fb}^2 + \omega^2 C_{\rm fb}^2}}\left(\cos\left(\omega t - (\delta+\theta)\right) - \cos(\delta+\theta)\,{\rm e}^{-t\,\omega/\tan\theta}\right), \tag{6.11}$$

which shows the output voltage as having a sinusoidal and an exponential term.

Only the sinusoid is desired: this is what corresponds to the sinusoid in the steady-state input current rather than to turn-on transients in the electrometer circuit. The exponential term may give two problems. If it stays sufficiently high during a cycle that the peak of the electrometer voltage is significantly increased by the 'offset' voltage of the exponential, the electrometer output voltage may

be pushed beyond its limit. If it decays slowly enough that it has not vanished within a small part of the period of one of the measured DFT components, but quickly enough that there is a significant difference in its values between a positive half-cycle and a negative half-cycle, it will contribute to that DFT component, introducing an error in the measurement of the desired steady-state periodic current.

The best behaviour is for there to be no exponential term. This could be achieved by choosing θ so that $\delta+\theta=\pi/2$ to make the cosine term of the exponential become zero; this means making the test-object and feedback have the same ratio of capacitive and resistive currents, in other words the same time-constants, similar to a good voltage-divider design! It could also be achieved by $C_{\mathrm{fb}} = 0$, giving $\theta = 0$, as is obvious from considering that pure resistive feedback has no integrator-effect. A very quickly decaying exponential, much quicker than a cycle, will also avoid the problems: this is possible if $\theta \simeq 0$, which implies that the capacitive current in the feedback is only a small proportion of the total.

Alternatively, a very slow change in the exponential term will require consideration of maximum output voltage but will not disturb the DFT result significantly. The slow decay is only possible, under the conditions that have been put on the parameters of (6.11), with strongly capacitive feedback, where $\tan\theta$ is very large *and* where the test-object is not also strongly capacitive which would make $\cos(\delta+\theta)$ be small. The peak value of electrometer output voltage can be in the worst case twice as high as the peak of the sinusoidal component, but this requires dominantly capacitive feedback *and* a dominantly resistive test-object.

The capacitive feedback ratio, *CFBR*, is a definition used within the program for controlling the DS instrument used in this work: it is the proportion of the total feedback current that flows in the capacitive branch,

$$\text{“CFBR”} = \omega C_{\mathrm{fb}} / \sqrt{1/R_{\mathrm{fb}}^2 + \omega^2 C_{\mathrm{fb}}^2}. \tag{6.12}$$

Considering that most test-objects are mainly capacitive, the cases where feedback is mainly resistive or mainly capacitive will not cause significant errors in the result, and the offset voltage will in either case be small as long as the applied voltage starts at zero. The CFBR should therefore be kept close to one of its extreme values of 0 or 1 in order to keep mainly to resistive or capacitive feedback. A variation of up to a few percent from these values is permissible without severe effect on the results, particularly if letting some cycles of voltage be applied before using the measurement.

6.3 DS measurements for general HV diagnostics

Insulation based on wood-pulp and petroleum is used in several important types of high-voltage equipment: the insulation of transformers consists of paper and pressboard surrounded by oil, and the insulation of bushings and old power cables consists of paper impregnated with wax or oil. Water in the paper accelerates decomposition of the cellulose, and this decomposition results in water: the water content is therefore a useful quantity to measure for diagnostic

purposes, and water is fortunately easy to detect by dielectric measurements as it is so polar. A transformer is a complex construction involving liquid and solid insulation, so other effects such as oil conductivity are influential in the measured result. Nevertheless dielectric spectroscopy methods in time and in frequency have been widely applied to the insulation of transformers [Gub03], with water content a particular interest. Voltages of just a few volts can be used to good effect in frequency-domain measurements. Dielectric spectroscopy has also been used on paper-insulated cables [Nei04].

Cables with XLPE insulation have largely superseded the paper-insulated ones. Degradation by water-treeing was a large and wholly unanticipated problem of this type of insulation, leaving early generations of cables from the 1960s and 1970s particularly vulnerable. Water has a strong effect on the dielectric response of a low-loss dielectric such as XLPE, although the relatively low proportion of water trees in the total volume makes sensitive measurements important. Frequency-domain dielectric spectroscopy has been extensively investigated [Wer01b] [Wer01a, ch.4,5], including the use of varied high-voltage to stimulate the nonlinearity of water-treed insulation. The stress-grading sometimes used at cable terminations and joints has strong similarities to the end-winding stress-grading considered in chapter 19, so it is a further source of voltage-dependence. These accessories make up only a small part of the total length of cable, in contrast to the two winding-ends per metre or so of stator winding, so their contribution to the total response is relatively weak.

6.4 DS measurements on stator insulation

No diagnostic measurement in common use on stator insulation can be seen as having a main interest in the dynamic response of the insulation material's polarisation. Several commonly used measurements are strongly related to DS, and several approaches to purer DS measurements have been taken by researchers.

6.4.1 Capacitance and loss

Measurements of capacitance and loss-tangent are widely used. In contrast to true spectroscopy the measurements are at just one frequency, usually the power frequency for the sake of a simple voltage-source. Instruments for these measurements typically use bridge methods [Kuf00, s.7.2], permitting relative accuracies of the order of 10^{-4} [Sto04, p.255]. The result is a total value for the whole measured part of the winding, and the effects even of quite severe problems can be small changes of the order of a percent: these types of measurements will only be sensitive to problems affecting a significant proportion of the insulation.

If the solid insulation-material is the focus, the voltage will be kept low to reduce nonlinear contributions such as PD and surface-leakage. Used in this way the measurement is moderately effective at detecting the increased C-tan δ due to water absorption [s.5.5.8], and the decreased C' due to voids [s.5.5.5] and increased tan δ due to oxidised polymer [s.5.5.4]. Changes during manufacture, as impregnant fills the gaps in the insulation and then is cured, are also sometimes tracked with low-voltage C-tan δ measurements.

The capacitance and loss measurements are often made at high voltages, sometimes well beyond the service stress; in these case PD is arguably the *main* interest. To give more information than just a single measurement at, for example, the rated voltage, it is normal to use several voltages, below and above the expected inception level for PD; common values are 20% increments from 20% to 120% of the rated line-voltage, applied between a phase and earth. Advantage can then be taken of using relative values [s.4.6], by studying the variation of C' or $\tan\delta$ between different voltage levels; the increase in these quantities with voltage is called the *tip-up*. The common $\tan\delta$ tip-up test compares measurements at the several voltages, often plotting the change to give an idea of the extent of the PD activity and the voltage ranges in which it most increases. Capacitance tip-up is sometimes measured too, more in Europe than in North America; the relative change in value is less than for $\tan\delta$, since cavity PD tends to have quite similar absolute contributions to both of these quantities and the absolute capacitance of the insulation is much greater than the loss. The main feature of the insulation that is measured by the tip-up is the 'void content', on the assumption that a high enough voltage causes all voids to be 'shorted out' by nonlinear effects such as PD. A reduction of $\tan\delta$ with increasing voltage, beyond a high value where much PD is occurring, is widely reported [E286]; this has been studied in [Gof78], which considers the tip-up to have a more complex description than simply more cavities breaking down.

Some examples of C-$\tan\delta$ tip-up are given in figure 6.4. These are from industrial measurements made on 24 hydro-generators of rated power from 10 MVA to 250 MVA, rated voltage mainly around 10 kV but up to 20 kV for the largest powers. The machines are from several manufacturers and their insulation is mostly of epoxy-mica, the one exception being polyester-mica. Measurements have been made on phases separately then phases all together; the measurements on all together are shown by dashed rather than dotted lines between the measured points. The plots of relative C' and of $\tan\delta$ show a relative change of a few percent in C' and C'' with voltage.

6.4.2 Insulation 'resistance' and polarisation index, IR/PI

The measurement of *insulation resistance*, IR, is a primitive 'polarisation-current' measurement [s.6.1.1] using one or a few time-points. A dc voltage is applied between the conductor and earth, and the current that flows in the insulation system is measured at some later times. Instead of presenting the measured current directly, the ratio of the applied voltage to the current is taken, and is referred to as a resistance although it is changing in time due to the polarisation terms in the current.

Times are generally at least 60 s, and commonly up to 600 s. The voltages are not as high as the working level of ac, but are usually some kilovolts to give a chance of nonlinear conduction being seen. The results, as for C-$\tan\delta$ measurements, are totals for the whole measured part of the winding, which reduces the sensitivity to a problem in a small part of the winding. However, the low bulk conductivity of thermoset insulation and the low polarisation current after times of several minutes give a good chance of detecting the small conduction path provided by a single fracture [s.5.5.10] or by water absorption.

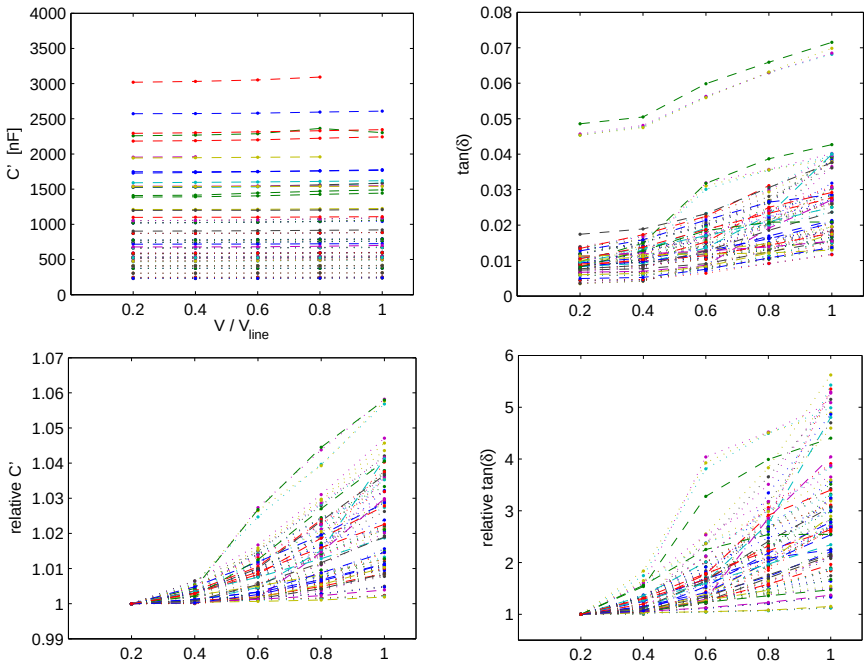

FIGURE 6.4: Measured tip-up of capacitance C' and loss-tangent $\tan\delta$ on 24 hydro-generators with thermoset insulation, applying $0.2, 0.4, 0.6, 0.8, 1.0$ of the rated *line*-voltage between phase and earth. Lines link points to clarify the trends: dashed lines show measurements made from all phases to earth, dotted lines single phases to earth.

A conduction path to the end-winding capacitance, due to surface contamination [s.5.5.9], can also be detected as unexpectedly high current even after many seconds. Common criteria for minimum IR(60 s) are $> 100\,\mathrm{M\Omega}$ for post-1970 insulation and $> (U_\mathrm{n}/1\,\mathrm{kV} + 1)\mathrm{M\Omega}$ for older insulation [E43]; good insulation may commonly have many times higher values.

Conductivity is highly temperature-dependent [s.5.1]. IR measurements are conventionally given as values 'corrected' to 40 °C, using an exponential dependence such that conductivity increases by a factor of 2 for an increase of 10 °C. According to [Sto04, p.239] the correction factors simply 'don't work', giving quite different corrected results from the same object at different temperatures. The conventional values are based on studies from the 1950s, but the change in temperature for a doubled conductivity has more recently been found to range from 2 °C to 20 °C [E43, p.10].

Condensation on winding surfaces has strong effect [E43] on the surface conductivity, and the winding should be above the dew-point if the results are to be meaningful. Direct water-cooled windings should have the cooling water removed, or at least checked for low conductivity, so as not to upset the results [E43, p.12]; this would clearly be very important in making FDDS measurements at low frequency, and is even mentioned in relation to power-frequency C-$\tan\delta$

measurements [E286, p.24].

To make IR results less dependent on temperature and on knowledge of the geometric capacitance, the ratio of IR values at two times can be used, to give the *polarisation index*, PI. Ratios of the 10 minute to 1 minute IR values are often used. For any mica-based insulation system likely to be found in service, a standard criterion is PI > 2.0 [E43]. A lower value suggests so little change between these two times that a significantly conductive element in the current is likely. PI, or any IR based method, "only finds contamination and serious defects"; it is "excellent" at finding cracks, contamination and water-soaking [Sto04, p.238].

6.4.3 Less-common industrial methods

The simple dc hipot test [s.4.7] is a pure test of endurance, without measurement. By making a current measurement during this test, further information can be obtained, making it like a form of high-voltage polarisation-current measurement. The applied voltage may be a single step, multiple steps or a ramp [Sto04, p.245]. The *ramp test*, including use at voltages of service rather than hipot levels, is popular among some hydro-generator operators, particularly in North America [Rux04]. There has been recent work to standardise methods and spread information about the appearance of different defects in the measured current [E95], and to analyse the components in the current in comparison with stepped-voltage excitation [Dav06].

Chapter 7

Partial Discharges

This chapter introduces gas discharge mechanisms, situations in which partial discharges arise, and the effect of the applied voltage's frequency. The nature and effect of partial discharge in stator insulation systems is described based on literature and industrial industrial measurements. Sources of partial discharge in stator insulation are described. Measurements of partial discharges are left until chapter 8.

7.1 Gas discharges

The mechanisms of gas discharges (electrical discharges in gases) were widely investigated during the late nineteenth and early twentieth century. They are the usual starting point in discussing such apparently disparate phenomena as partial discharge, lightning and other long discharges, and liquid and solid breakdown [Kuf00, ch.6]; of these, partial discharge and solid breakdown are of most interest in studies of stator insulation.

Just the details most relevant to later discussion of PD are now given; a lot more than this is needed in order to get a good grasp of the subject. Use of several sources is advisable in view of the range of approaches and emphases. Any text on high-voltage engineering is likely to devote at least one chapter to the subject. There is a good treatment in [Coo03, ch.3], which has been used for many of the numerical details in this section.

7.1.1 Discharge and breakdown

A *discharge*, in the context of electrical insulation, is a significant current flowing in a normally insulating medium. The current in a discharge is carried by charges arising from ionisation. A *breakdown* of an insulating medium is its transition to a state of significant ionisation and consequent conductivity, which is self-sustainable by the current that flows in it, needing no further external source of ionisation. In the study of electricity in gases, even a small current in non-self-sustained ionisation is described as a discharge. In the practical study of insulation, the mention of a discharge generally implies the self-sustaining state, even though the discharge may later extinguish itself by moving enough charge to reduce the electric field.

A discharge between electrodes of high-voltage equipment supplied from a low-impedance source is likely to result in ionisation and current causing each other to increase, until a hot and highly conducting channel is formed, practically short-circuiting the electrodes; in engineering terminology this is a *disruptive discharge* [C001], whose extinction requires disconnection of the supply. In self-restoring insulation such as air, prompt reconnection is possible after extinction of a disruptive discharge, as is common practice on overhead

lines after breakdown across insulators due to lightning or birds. In solid insulation, even the momentary presence of a disruptive discharge implies the presence of a break in the insulation, and probable extensive damage from the energy released; repair is therefore necessary before the voltage can be restored.

Detection of deterioration before this stage is reached is the aim of diagnostic measurements and monitoring. Partial discharges [s.7.2] are often a precursor to disruptive discharge, whether as a symptom or a cause of the deterioration, so their measurement is common within diagnostic methods for high-voltage insulation.

7.1.2 Paschen's law

An empirical description of the voltage needed to cause electrical breakdown of the gas in a gap between electrodes was given by Paschen in 1889. A notable feature is that gas-pressure p and the gap-distance d are similar in their effect, so the breakdown voltage V_B can be expressed as a function of the product pd. The exact form of this function is of course dependent on the type of gas. In air at NTP[†] and with gaps in the order of centimetres, the relation of V_B to pd is quite linear, as seen from (7.1). Towards lower pd products V_B reaches its *Paschen minimum* of about 330 V at $pd = 10^{-2}$ bar·mm [Coo03, p.94] and increases sharply when pd is further reduced. At first sight it is remarkable that, below the Paschen minimum, a smaller gap is harder to break down; the reason will be seen when considering electron avalanches. A common approximation of Paschen's law for air, at pd above the Paschen minimum, is

$$V_\mathrm{B} \simeq 2.13\sqrt{pd} + 2.44pd, \tag{7.1}$$

with pd in bar·mm and V_B in kilovolts [Kuf00, p.338].

Paschen's law is a good approximation to experimental data until pressures of several times the atmospheric level make the breakdown fields so high that field-emission at electrodes is important, or temperatures of thousands of kelvins cause significant thermal ionisation or chemical change [Coo03, p.96]. Other situations where Paschen's law does not work well are when the pressure is so low that the gas becomes less significant than the electrodes, and when particular mixtures of gases result in special interactions [Kuf00, p.339].

7.1.3 Electron avalanches

The mechanism central to electrical breakdown in a gas stressed with a high electric field is an electron *avalanche*. A free electron is accelerated in the field, sometimes colliding with *neutrals* (neutral atoms or molecules). If its kinetic energy reaches the neutrals' ionisation energy, which for common gases is around 10 eV to 15 eV [Coo03, p.50], its next collision may generate a positive ion and a further free electron that can cause further ionisation.

In suitable conditions the number of electrons can increase greatly as the avalanche moves through the field towards the anode.

[†] Normal Temperature and Pressure: in this context, room-temperature and atmospheric-pressure are a sufficient definition; for more precise use in measurements a *standard atmosphere* can be defined, such as the 20 °C, 101.3 kPa and 11 g/m^3 humidity in [C001].

The collisional ionisations caused by a free electron are *primary ionisation*. Townsend's first *ionisation coefficient*, α, describes the mean number of primary ionisations made by an electron moving a unit distance along the field; this coefficient depends on the electric field strength, the types of molecules in the gas, and such details of state as temperature and pressure. Electrons freed by these ionisations may recombine with positive ions, or be captured by attachment to the electronegative neutrals of an *attaching* gas to form negative ions; the *attachment coefficient*, η, is the corresponding reduction in number per unit distance. The effective ionisation coefficient,

$$\bar{\alpha} = \alpha - \eta, \tag{7.2}$$

then describes the overall number of electrons resulting from each electron that moves a unit distance along the path of an avalanche. Air is significantly attaching, due to its oxygen content [Coo03, p.58].

Having started with n_0 electrons, the number at a distance d further along an avalanche in a uniform field is then

$$n(d) = n_0 \mathrm{e}^{\bar{\alpha} d}, \tag{7.3}$$

which in a nonuniform field would require an explicit integral over the path that makes up d, on account of the field-dependence of $\bar{\alpha}$.

The Paschen minimum [s.7.1.1] and the increasing breakdown voltage for lower *pd* products can be qualitatively understood in terms of avalanches: at very low *pd* products it is likely that electrons will reach the cathode without having met any neutral to ionise; at high *pd* products electrons are likely to have collisions before they attain the energy needed to ionise neutrals.

7.1.4 Starting-electrons

For an avalanche to occur, a free electron must be present at a point within the *critical volume* where there is a sufficiently long distance to the anode, with sufficiently high field along that path, that the electron has a good chance of causing further ionisations. Earlier avalanches may provide a source of electrons for new avalanches [s.7.1.5], but the first avalanche needs a *starting-electron* provided by another source within the gas or at the cathode.

The natural background level of ionising radiation causes electron generation at a rate of about $3\,/\mathrm{cm}^3{\cdot}\mathrm{s}$ in air at NTP [Bog90c], due in fairly similar proportions to cosmic radiation and radioactive isotopes [Mor93, p.4]. External sources of ionisation, such as ultra-violet, X-rays or gamma-rays, are sometimes used to increase this rate for laboratory work and testing.

Electrons can be emitted from the cathode if the energy barrier of their attachment to the solid material can be overcome. This *work-function* is usually around 4 eV for metals. It can be overcome by some combination of energy from heat (thermionic emission), electric field (field emission), or bombardment by positive ions or radiation. Pure *thermionic emission* at significant levels requires high temperatures, generally above 1500 K [Kuf00, p.318], but thermal energy together with reduction of the energy barrier by a strong electric field can produce *Schottky emission* even at moderate temperatures. From smooth,

clean metallic electrodes, significant *field-emission* due to just the electric field requires some orders of magnitude higher field-strength than the mean values found in gas discharges [Kuf00, p.319], but sharp edges and surface roughness can provide local intensifications of the field, and surface impurities reduce the energy barrier [Coo03, p.65], so that field emission can be significant even in conditions around NTP.

7.1.5 Continued supply of electrons

The free electrons directly generated in an avalanche are along a path moving towards the anode. The Townsend mechanism of breakdown [s.7.1.6], active at moderate *pd* products, depends on avalanches freeing electrons that can start new avalanches, in a self-sustaining process. An avalanche must therefore be able to generate some free electrons behind its starting point, at or closer to the cathode. This is possible through several mechanisms of *secondary ionisation*, mainly involving *cathode emission*.

Positive ions produced in an avalanche move towards the cathode; they do not develop enough speed to cause significant ionisation within the gas, but they can free electrons when they bombard the cathode. Atoms excited by collisions in an avalanche can produce ultra-violet radiation, which can act on the cathode to free an electron or can cause ionisation within the gas.

Townsend's *secondary ionisation coefficient*, γ, represents the mean number of electrons generated by all the secondary mechanisms [Coo03, p.91], for each ionisation within an avalanche.

7.1.6 The Townsend breakdown mechanism

An avalanche by itself need not result in more than a small and very short-lived group of ionisations: if arising from ionisation within the gas, an avalanche may start close to the anode, having little space to develop; even if arising at or close to the cathode, the effective ionisation coefficient and gap distance may give little multiplication.

Studies of gas discharges were made by Townsend around 1910, using low-pressure gases between electrodes in tubes. Several stages of discharge can be seen in such constructions as the current is increased. The relation of current and voltage is nonmonotonic: for a given current, there may be several possible voltages, depending on the state of the gas.

Starting from a neutral gas at room temperature, an external source of ionisation or cathode-emission is needed in order to keep generating charges to carry a current. When the electric field is high enough to cause avalanches, the current increases, as seen from an increase of $\bar{\alpha}$ in (7.3), but the external source of electrons is still needed.

With further-increased field the secondary ionisation mechanisms permit avalanches to generate enough starting-electrons for new avalanches to make the discharge self-sustaining. This is the *Townsend criterion* for breakdown, expressed as

$$\frac{\alpha\gamma}{\bar{\alpha}}\left[\mathrm{e}^{\bar{\alpha}d}-1\right]=1\simeq\gamma\mathrm{e}^{\bar{\alpha}d}, \tag{7.4}$$

where the approximation on the right is based on the usual ranges of values of the parameters [Kuf00, p.325].

The *Townsend discharge* with current limited to values around this breakdown level is a *cold* discharge. The *electron temperature* describing the energy of electrons is in the order of 10^4 K [Bar95], but the neutrals are close to ambient temperature; the discharge is not in thermodynamic equilibrium. The discharge is sustained by cathode emission.

Further increase of current causes a transition to a *glow discharge*: ionisation increases, and in contrast to the earlier Townsend discharge there are regions of significant space-charge, making the electric field vary across the gap. Some regions are luminous, hence the name. There is still not thermodynamic equilibrium, and the electron temperature is still around 10^4 K or rather over. The discharge is sustained by cathode emission. The total gap-voltage is lower than at the critical breakdown point, in spite of the higher current; over a wide range of currents the gap-voltage stays quite constant, while the area of the discharge varies with the current.

If the current is then forced even higher, to some 1 A or more, the voltage rises again, until several processes of energy-transfer between ionic and neutral species and between vibrational and thermal states result in the transition of the gas to an *arc discharge*. This is a hot discharge in a constricted channel, with electrons and neutrals at similar temperatures, and with a high electron density of at least 10^{12} /mm^3 [Bar95]. Cathode emission is responsible for sustaining the arc. Once the arc state is reached the voltage is low even for very high currents. In many practical high-voltage insulation systems the supply has a low impedance, so a breakdown between conductors quickly becomes an arc.

The progression to self-sustaining avalanches between the electrodes, by the generation of new electrons at the cathode, is the *Townsend mechanism* of breakdown. Its development can be expected to take at least the transit time of an electron across the gap [Kuf00, p.327]. It needs only the *background field* imposed by the electrodes, and is dependent on the cathode's ability to emit electrons.

7.1.7 The streamer breakdown mechanism

Later investigations, reported by Raether and Meek around 1940, proposed the *streamer mechanism* of breakdown. This explained how discharges could in some cases develop across a gap at much higher speeds than would be possible by the Townsend mechanism.

A *streamer head* is a concentration of charge sufficient to produce a local electric field of comparable strength to the background field. Further along in the direction that the head would move in the background field, the background field is enhanced by the charge in the head. Free electrons in front of the head therefore form strong avalanches, which neutralise the region that was the streamer head and charge a region further along. The head thus moves forward as a *wave* of ionisation, potentially faster than the actual charges could move. Ultra-violet emissions within avalanches produce free electrons ahead of the streamer, to form the next generations of avalanches. In contrast to the

development of a Townsend discharge, the electrodes and the coefficient γ are not very influential in the propagation of a streamer.

The critical concentration of charge in the head, necessary to produce enough local electric field for streamer propagation, is about 10^8 elementary charges, rather over 10 pC. Accumulation of this critical charge from a single electron avalanche requires satisfying the *streamer criterion*,

$$\bar{\alpha}d \gtrsim 18, \tag{7.5}$$

as can be seen from (7.3). Streamer inception has been seen to require a *pd* product of at least 5 bar·mm [Coo03, p.86]. When a streamer cannot be formed, any breakdown will be by the Townsend mechanism; this suggests that the Townsend mechanism is active for smaller gaps and lower gas-pressures. With *pd* products of about 10 bar·mm and above [Kuf00, p.327], the streamer mechanism is active instead.

A streamer is a cold discharge. It differs from all the stages of Townsend breakdown in that it is independent of cathode-emission. Like the Townsend mechanism's glow state it must change state to a highly ionised channel if it is to become a low-impedance discharge rather than dying away; this is the *streamer-spark transition*. The terms spark and arc seem to be used fairly interchangeably; in [Bar95] the distinction is only that an arc might include a continued discharge supplied from an ac source. Some minimum degree of ionisation and field in the streamer-channel is needed for the spark transition: a streamer crossing the electrode-gap is not a guarantee of complete breakdown of the gap [Coo03, p.82], but streamers with currents over some 0.1 A have been found to make reliable transitions [Lar98]. Over long gaps, such as are found in high-voltage transmission equipment, further streamers will arise in the field around a streamer's head, contributing extra current to the main streamer channel; this may be sufficient to make much of the main streamer channel become highly ionised by the time that the streamer has crossed the gap, providing a channel ready to carry high current.

Streamers can be of either polarity, with consequent differences in properties: a positive streamer causes avalanches that move towards its head, into an increasing field, making its propagation relatively easy; a negative streamer causes avalanches that move out from the head into the decreasing field. Due to the enhancement of the background field around the streamer's head, streamer propagation does not require the background field to be strong enough to sustain avalanches all the way between the electrodes. The continued propagation of a streamer requires a certain background electric field, which in atmospheric air is about 0.4 kV/mm to 0.6 kV/mm for positive streamers and 1 kV/mm to 2 kV/mm for negative streamers [Coo03, p.79], varying quite linearly with pressure, and increasing somewhat with increased humidity. The streamer mechanism is therefore particularly relevant to nonuniform gaps where streamers may start in high field and continue through fields of even just a fifth of the Townsend mechanism's critical field. At the critical background field, positive streamers in atmospheric air travel at some 2 mm/μs, which can increase by an order of magnitude in non-electronegative gases and increases also in a higher background field.

7.2 Partial Discharge origins

A *partial discharge*, *PD*, is the development of an ionised path that fails to bridge the full gap between the electrodes, and therefore can dissipate only very limited energy. The reason for a discharge being initiated but failing to bridge the electrode-gap may be a nonuniform electric field or an inhomogeneous material between the electrodes: a region of strong field allows discharges to start, but these may reach a region of so much weaker field that propagation cannot continue; a region of dielectrically weaker material allows discharges to start, but a stronger material arrests their development.

7.2.1 Classification of sources

Some classic forms of PD source are shown in figure 7.1, along with an indication of how they are classified. Variations of terminology are to be expected among the many works on PD; for example, 'corona' has sometimes been used as a synonym for any PD, and the distinction of a void as a particular form of cavity is often not made.

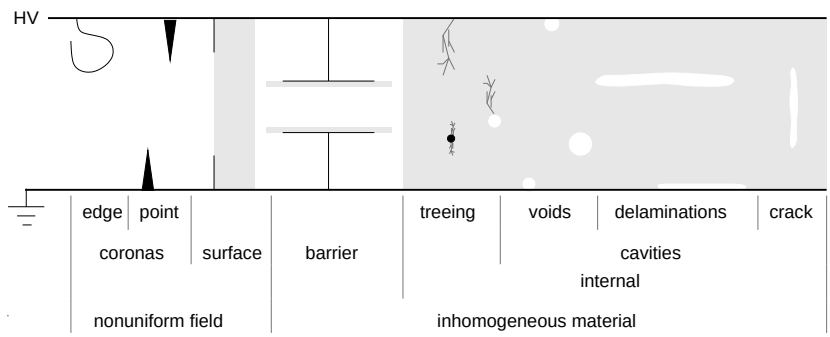

FIGURE 7.1: A crude classification of PD sources. The shaded areas represent solid insulation, and the open areas represent gas.

In the divergent field around such electrodes as a needle, rod, or the surface of a wire, discharges can start but are prevented from continuing by the reduced field further from the conductor. This is *corona*, sometimes called *external PD*. Build-up of space-charge quickly modifies the field distribution, making corona very dependent on polarity. Around bare overhead lines, acceptable corona levels are by concerns more of power loss and audible or radio-frequency noise than of damage to equipment.

A PD adjacent to an insulating surface is *surface PD*, which generally moves faster than a PD would in the gas away from the surface [Coo03, p.81]. Surface PD may occur around electrodes with divergent fields, such as the high-voltage connection to a bushing or the pin of an overhead-line insulator. The situation in a poorly graded cable termination or stator end-winding, shown in figure 19.1 [p.183], can also result in surface PD, in which case the nonuniformity of surface field and the inhomogeneity of the gas and solid insulation are both responsible for the partialness of the discharge. Mildly conducting contamination with

inhomogeneous properties can lead to breakdown along the surface of less-conducting regions, as happens on stator end-windings as well as on polluted outdoors insulators.

The *dielectric-barrier discharge* is widely used for deliberate production of PD, where plasmas are desired for their optical and chemical effects [Kog03]. It is typically done with a thin dielectric layer preventing full breakdown of a relatively large volume of gas. The gaps between different phases in an end-winding form a rather similar construction, with a large volume of gas between electrodes that are completely surrounded by solid insulation.

Electrical trees and cavities within solid insulation are the other extreme of inhomogeneous material, with a small and usually trapped volume of gas within the solid. An electrical tree may be initiated at stress-concentrations from a sharp electrode-edge, a conducting particle, or PD on a cavity surface [s.3.2.3]. Partial discharges occur within a tree in very small cavities around the point of growth [Mas81] and along existing branches [Jäv09]. Opinions differ about the detectability of PD in treeing: it has been regarded as strong only in the quick final stages [Bau91] or strong only in the slow middle stages [Lau92]; the differing ideas may stem from differences between epoxies and polyethylene, or between service and laboratory stresses.

A further form of discharge sometimes called PD occurs at poor contacts between conductors. Although the whole gap between these electrodes breaks down, the available charge is limited by further dielectric materials between these electrodes and the supply, so the discharge dies away. Contacts within some designs of HV capacitor are known for this [Har93]. In stator insulation, the vibrationally induced slot-discharge, and discharges at a poor interface between slot and end semiconductors, can be seen to be of this type, albeit with at least one nonmetallic electrode.

7.2.2 Features of coronas

Coronas are strongly polarity-dependent due to the formation of ionic space-charges and the ability of the electrode to accept or emit electrons. Corona in an asymmetrical object such as a point-plane gap is detected at lower voltage when the sharp electrode is negative rather than positive. Each polarity of corona has several distinct regimes depending on the voltage level. These are summarised in the following paragraphs; they are described in more detail in [Tri95] and [Kuf00, s.5.11].

Negative corona close to its inception voltage consists of *Trichel streamers*, each quickly stifled by the space-charge that it creates, with such consistent charge-magnitude and repetition rate that they have been used as a form of calibration for PD measurement [Hog66]; at higher voltage a *pulseless glow* ensues; at still higher voltages, negative streamers emerge from the glow.

Positive corona close to inception voltage is *burst corona*, a thin layer of glow around the electrode, consisting of many small avalanches that are stifled by their space-charge and that occupy less space and have less consistent size than the negative-corona Trichel streamers; at higher voltage *onset streamers* also occur, extending much further from the electrode; at still higher voltage the streamers are choked by the space-charge from enhanced burst corona, giving a

positive glow; at voltages some tens of percent higher, long streamers can again emerge, close to the breakdown threshold.

Corona resulting from a sinusoidal applied voltage at power frequency tends to have the discharges occurring around the peaks of the voltage waveform. This suggests that the space-charge effects happen considerably faster than the period, as the discharge is largely dependent on the instantaneous value of the voltage rather than on any earlier values.

7.2.3 Features of cavity PD

Cavities are an important PD source within many types of high-voltage equipment, arising when manufacture or operation results in inclusion of gas bubbles or of spaces within a layered material. Some examples are voids in the XLPE insulation in cables, voids in the epoxy spacers in gas-insulated switchgear (GIS), delaminations between paper layers in oil-paper insulated cables and bushings, and delaminations between layers of tape in epoxy-mica stator insulation.

Consider a gas-filled cavity, in solid insulation of relative permittivity ε_r. The PD sources towards the right in figure 7.1 are good examples, drawn in the traditional way with electrodes at top and bottom, so that the *height* of the cavity is its dimension in the field-direction, and its surfaces can be referred to as top, bottom and sides. In good insulation at power frequency the conductivity of the insulation will have negligible effect on the field distribution, which is determined by permittivity alone. Suppose that electrodes impose an electric field of strength E in the insulation remote from cavities: the electric field E_cav within the cavity will then be about $\varepsilon_\mathrm{r}E$ for a delamination lying across the direction of the field, $3\varepsilon_\mathrm{r}E/(2\varepsilon_\mathrm{r}+1)$ for a spherical void, and E for a crack; this supposes the size of the delamination or void along the field direction to be many times smaller than the electrode separation.

With excitation from a sinusoidal voltage at power frequency, the field within a cavity will vary in proportion to the applied voltage,[†] as long as the gas remains insulating. The field within solid insulation during normal operation is often beyond the breakdown strength of the gas in the cavities, as is true for high-voltage stator insulation [s.2.1.2]; in delaminations and voids the field in the gas is even higher than in the surrounding solid, as is seen from the above relations of E_cav to E, using the $\varepsilon_\mathrm{r} \simeq 4$ that is typical of stator insulation [s.5.5.2]. The gas in a cavity in high-voltage insulation is therefore likely to be exposed to an electric field beyond the critical breakdown level, but a starting-electron must also be available in order for breakdown into PD to occur.

The *statistical time-lag* τ_stat indicates the time before a starting-electron is likely to appear[‡] within the critical volume from which an avalanche can successfully form towards the anode. The rate of electron generation from natural sources [s.7.1.4] suggests that in a $1\,\mathrm{mm}^2$ cavity without free charge left by earlier PD, this time would be some minutes, rather than the milliseconds of a power-frequency period. However, even in work on cavity PD rather than PD

[†]Neglecting delays in the dielectric response of the solid insulation.

[‡]τ_stat — assuming a sufficient electric field for breakdown, and random occurrence of starting-electrons [Dev84], $\mathrm{P}(t) = 1-\exp(-t/\tau_\mathrm{stat})$, where $\mathrm{P}(t)$ is the probability of discharge happening before time t.

directly in atmospheric air, it has been claimed [Mor93, p.5] that the actual τ_{stat} can be orders of magnitude shorter, due to electrons attached to water in the gas being easily detached as starting-electrons; presumably the initial source of these electrons is earlier ionisations by natural sources. Enhanced ionisation by external sources such as X-rays allows PD in many small cavities that would not ordinarily have been noticed as PD sources [Fuj92], so the availability of starting-electrons clearly *is* a strong hindrance to PD in small cavities. Small cavities also make PD more difficult by having greater critical field, as the small *pd* product in Paschen's law [s.7.1.2] increases the critical breakdown field. When PD has already occurred in a cavity, electrons from previous discharges may be held in traps near the surface of the insulation [s.7.2.4], increasing the supply of starting-electrons.

A PD event causes electrons and positive ions to be deposited on opposite faces of the cavity, creating a dipole moment of charge in what was previously a region of neutral gas and solid. Within the cavity the field from this growing dipole opposes the external field, until the total field in the cavity becomes low enough to extinguish the discharge. In view of the usual values of field-strength and permittivity in insulation systems, the field in a neutral cavity may reach the critical breakdown level with the applied voltage on the electrodes at only a fraction of its peak service level. If starting-electrons are easily available, a succession of PD events can therefore occur as the applied voltage rises to its peak: each PD increases the dipole moment of the surface charges, reducing the field within the cavity until the external field rises enough to start a new PD. If starting-electrons are *not* easily available, the cavity can reach a substantial *overvoltage* beyond the critical breakdown level, with PD occurring late or not at all. The PD events that occur at a high overvoltage give a particularly strong breakdown and a large movement of charge. When the external field is reduced back to zero, as would happen with an ac source or with switching of a dc source, the field from the surface-charges will no longer be cancelling another field but will cause a strong reverse field in the cavity. If there were several PDs during raising of the voltage, the simple model of pure permittivity suggests there will also be several during lowering of the voltage, leaving a final dipole moment close to zero. This description of the up and down charging of the cavity then applies similarly to a half-cycle of opposite polarity.

At the other extreme from many PDs per cycle is the situation where the total change in applied voltage from zero to peak is only just enough to cause PD. With periodic applied voltage the PD inception voltage, *PDIV*, is the level at which regular PD is observed as the voltage amplitude is slowly increased. Once PD has occurred, the charges on the cavity walls enhance the field in the cavity when the external voltage is reversed, so it is possible for the critical breakdown field to be reached even if the voltage amplitude is reduced; below the PD extinction voltage, *PDEV*, PD activity is no longer regular. Typical ratios of PDIV to PDEV are given by [Kre64] as between 0.75 and 1 for cavities in practical insulation.

In studies of general gas discharges, the secondary ionisation coefficient γ is a property of metallic electrodes. In a PD cavity that is within the solid insulation,

any secondary ionisation from surfaces is from a polymer surface, which has a far lower value of γ [s.7.2.4]. A cavity that has its top or bottom formed by a metallic electrode, as in some of the examples in figure 7.1, has significantly different properties for its top and bottom surfaces, and may therefore show a polarity dependence [Hol95][For08b]; in general, PD in an electrode-bounded cavity happens more easily when the electrode is negative [Kre64].

The distinctive feature of cavity PD, in contrast to corona, is that the polarity of discharges is more related to the applied voltage's time-derivative than to its actual value: cavity-PD events can be expected to be more around the zero-crossings than the peak values of a sinusoidal applied voltage. If the applied voltage has to change by a considerable proportion of its peak value in order to build up enough field in the cavity to cause a single PD, the PD events will have a considerable delay in phase. Cavity PD is also capacitor-like in that the total charge per cycle is limited; corona is more resistor-like, continuing to move charge and dissipate energy as long as the voltage is maintained.

7.2.4 Forms of discharge in PD

Investigations of cavity PD have revealed distinct differences in the waveform and times of the current measured from outside, and in the appearance of the discharge within the gas or at its contact with the insulation surface. Two influential factors are the state of the surfaces and gas in the cavity, and the extent of the overvoltage at which the PD occurs. The surfaces and gas are affected by earlier PD, meaning that a single cavity may radically change its behaviour during long exposure to PD. The overvoltage is partly determined *by* the surfaces and gas, in how well they facilitate breakdown, as well as by the rate of voltage-rise and the presence of external ionisation.

Pulsive cavity PD can be crudely divided into two forms. The *spark-like* or *streamer-like* discharge has a fast rise and decay of current, in the order of nanoseconds; it appears as a narrow channel contacting with a small area on the insulation surface. The *Townsend-like* discharge has generally a longer rise followed by a long plateau of low current and a slow fall; it can appear as a diffuse discharge over the full volume of a cavity. In an extreme case this diffuse form of discharge may stop being detectably pulsive, when the gas is significantly ionised to a *glow*; it will then not be detectable by commonly used PD pulse measurement methods. A hybrid state where a glow contains many small pulses is sometimes termed *pseudo-glow*. The different forms of discharge are of relevance to PD measurement and aging in stator insulation [s.7.4], since sharp pulses are most strongly detectable by conventional PD measurements.

It is no surprise that a hopeless confusion of terminology exists in this area. The classification is sometimes based on the waveform of the current at the electrodes, and sometimes on the appearance of the discharging volume. Different aspects of the streamer and Townsend breakdown mechanisms are chosen as the defining properties. Investigations described in [Dev84] studied PD at varied overvoltage, describing the sharp current-waveform typical of high overvoltage as being streamer-*like*. In [Bar93] it is claimed that this simile was misunderstood in subsequent publications, which considered the streamer mechanism of breakdown to be active, while in fact "all discharges in small gaps

... are necessarily governed by the Townsend mechanism", as is indicated by the conditions in [s.7.1.7]; it is further noted that the alternative description 'spark-like' would in most cases be inappropriate under the usual definition of a spark by its high electron-density. A table comparing terminology, for more than just the above two extreme forms of PD, is presented in [Mor93, p.6], where further references are given. Different forms of PD are discussed in [Bar93], with attention to the components of the total measured current due to electrons and ions. Suggestions are given in [Bar95] for standard terminology, conforming as much as possible to practice in gas-discharge physics. Terms for use in PD measurements on stator insulation are defined in [E1434].

The work described in [Mor93] is based on cylindrical cavities in low-density polyethylene, *LDPE*, with varied dimensions in the order of a millimetre. It is a good introduction to changes in PD form with aging, and provides some further details about cavity PD; the results are summarised in the following paragraphs. Works with more connection to stator insulation are reviewed later [s.7.4].

A *virgin* cavity in LDPE has low surface-conductivity and low availability of electrons. In this state, spark-like PD is seen: the rise-times are subnanosecond, faster than the electron transit time; peak currents up to 100 mA are seen at the electrodes; the end-contacts of the channel on the insulation surfaces are small, for example less than 0.1 mm diameter for a 0.2 mm cavity-height, and increase with increased height.

After some hours of exposure to PD, the discharge changes greatly, becoming Townsend-like: rise-times are tens of nanoseconds, indicating several generations of avalanches, and a plateau is maintained for longer before gradual decline; currents may be up to hundreds of microamps; before the plateau there may be a peak of several times the plateau current, or hardly any peak; the discharge is diffuse, covering the whole area even of a cavity with 10 mm diameter.

Investigation of cavity surfaces after reaching the Townsend-like stage revealed a layer of acidic substances in the form of gel and crystals. This change to the surfaces was apparently the main influence on the discharge form: replacement of the gas in the cavity with fresh air after reaching the Townsend-like discharges made little difference, but scraping away an area of the deposited layer caused that part of the cavity to revert to spark-like discharges. The development of the layer, and consequent transition to Townsend-like discharges, required the presence of oxygen, and was made much slower by the absence of water vapour.

The surface conductivity with the deposited layer was more than five orders of magnitude higher than for the pristine polymer. To get an idea of γ [s.7.1.5], photoemission of electrons from the polymer surface was measured; it was found to be several orders of magnitude lower than for metals, and to be very little affected by the aging. Earlier works are cited as having given different results for γ for polymers, sometimes very similar to, and sometimes hundreds of times lower than, the values for metals. It is known that *traps* such as broken chains and oxidation products within the first few nanometres of the surface, can retain electrons deposited on surfaces during discharges; from shallow traps the electrons are relatively easily available as starting-electrons [Nie95] [Flo95].

It was assumed that the deposited layer made starting-electrons more easily available, by thermal activation from shallow traps with energy as low as 0.6 eV, which would permit a reduction of τ_{stat} by many orders of magnitude compared to the pristine polymer surface.

A third stage of PD was also defined, where acidic crystals intensified the field, forming starting points for later discharges and resulting in intense PD in particular small regions, which showed signs of pitting of the surface.

7.3 Frequency-dependence of PD

The *frequency-dependence* of PD refers, in this work, to how some property of the PD in a source excited by a sinusoidal voltage is affected by the frequency of that voltage. (Another possible meaning of frequency-dependence in PD measurements is the very different matter of the frequency band over which the *measurements* of signals from PD events are made.)

7.3.1 Frequencies already of practical interest

Most studies of PD phenomena in high-voltage insulation have focused on sinusoidal excitation at the power-frequency. This is to be expected: power-frequency excitation is a common service-condition for high-voltage apparatus, so the resulting PD needs to be studied in order to assess the effects of PD on insulation condition; power-frequency excitation is also commonly used for diagnostic measurements, so the resulting PD needs to be studied for good interpretation of these measurements. Other frequencies, relevant to special applications, have also received some attention; these are summarised in the following paragraphs, from high to low frequency.

In the last two or so decades *inverter-fed drives*, *IFD*, have become popular, in which a motor is supplied from an inverter that switches between two or more dc voltages to synthesise an ac voltage source of controlled amplitude and frequency. The switching is typically at some kilohertz, with sharp edges; thorough filtering implies a higher cost of the inverter, so the motors are usually expected to tolerate a considerable degree of high-frequency noise. These high frequencies drop much of their voltage across the inductance of the first turns in the stator winding, which may result in PD, particularly in random-wound stators; they also cause a greater electric and thermal stress in the end-winding stress-grading of large form-wound stators [Sto04, p.158]. The effects of IFD operation on deterioration and failure mechanisms of stator insulation have therefore become of great practical interest, and have stimulated some work on the PD caused by this type of excitation [Lin09].

Accelerated aging may apply a sinusoidal voltage whose frequency is several times higher than in service [s.3.2]. This generally assumes similarity of PD in each cycle between the high frequency and power-frequency, so study of this assumption is needed to demonstrate the validity of the acceleration [s.3.3].

Excitation of large, capacitive apparatus at power-frequency and high voltage demands a considerable current, which cannot be taken straight from the mains if the voltage is to be controllable. The required voltage-source can be made much cheaper and more portable by using low frequencies, well below the power-frequency, or by using a resonant circuit whose frequency may vary above

and below power-frequency depending on the load. In most such cases, the real aim is power-frequency PD results: the different frequency is a nuisance that is accepted for its convenient effect on the testing equipment. The similarity of PD between the different frequencies is then of interest if diagnostic results are to be compared. A widely accepted 'very low frequency' for these measurements is 0.1 Hz ±25% [E433]. The field-distribution in the epoxy-mica of a modern stator insulation system is very similar between this frequency and power-frequency, but it has been shown in [Cav06] and [For08c], experimentally and by simulation, that PD in cavities can change considerably over this range.

High-voltage dc (HVDC) applications [Mor97] include industrial equipment such as X-ray tubes and electrostatic precipitators, besides components for HVDC power-transmission. The dielectrics in HVDC cables, transformers and other equipment are exposed to largely constant voltage for long periods, but also to switching and possible polarity-reversal. The field distribution will range from being controlled by permittivities at the high frequencies of switching, to conductivities at the low frequencies of long periods of dc operation, and the build-up of space-charge during long dc operation can result in high internal fields when the voltage is changed. PD may occur in cavities when the voltage is changed, for similar permittivity-based reasons as at power-frequency; it may also even occur during long dc excitation if the conductivity of the bulk material is sufficiently high, and the surface conductivity around the cavity sufficiently low, that high voltages can keep building up across the cavity until PD occurs.

7.3.2 Varied frequency for greater information

In the above [s.7.3.1], the reasons given for studying PD with frequencies other than power frequency are either that equipment is normally operated at these other frequencies, or that a compromise is being made during testing, to permit shorter measurement times or cheaper testing-equipment. There is an implication that PD measurements would ideally be made at the normal service frequency of the apparatus.

This is true if the aim is to see what the PD is likely to be like in service; but if the aim is to make a diagnostic or prognostic inference, it is not obvious that the service frequency *is* the best choice. The reasoning behind this point is similar to that of whether online measurements give more useful results than online ones, due to the 'more realistic' operating conditions [s.4.5].

A frequency other than power frequency might therefore be a good choice for diagnostic measurements, with regard to the available information as well as cost and size of test-equipment. It has also been suggested that the frequency-*dependence* of PD may be useful in providing more detail about the nature of PD sources [For08a, p.2][Edi01], by seeing how some parameter changes with frequency, giving the PD measurement more connection to DS.

Examples of features of a PD source that may become more obvious from measurements at varied frequency are a cavity's approximate shape or size, surface-conductivity, and position within insulation or adjacent to a conductor. It is not certain that such distinctions can be reliably seen: the results might only provide some reduction in the range of plausible sources, but the increased information could be a useful further step.

7.3.3 Causes of frequency-dependence

Some of the background for discussing frequency-dependence is provided by the earlier descriptions of coronas [s.7.2.2], cavity PD [s.7.2.3], surface conductivity and secondary ionisation [s.7.2.4] and dielectric response of materials [s.5.3].

Over the rather low frequencies considered in this work, and particularly in the subhertz region, the PD behaviour of corona sources such as a point-hemisphere laboratory object has not been seen to be strongly dependent on anything other than the instantaneous value of the voltage. The conditions for this frequency-independence of a corona source are stated in [Edi01, p.13] to be a low frequency, a short gap, and a voltage not much more than the inception level; in other words, dynamic effects such as space-charge formation must happen much more quickly than the period.

Cavity PD has a far greater potential for frequency-dependence, even down in the millihertz range. The importance of cavity PD-sources in diagnostics of high-voltage equipment has resulted in studies that aid the understanding of frequency-dependence, even if this is not their aim: examples are *pulse-sequence analysis* of how PD events are affected by earlier ones [VB93][Hoo95], and models of the physics of cavity PD [Nie95][For08a].

Some of the properties of material and geometry that affect frequency-dependence of cavity PD are shown in figure 7.2. The bulk of the solid insulation

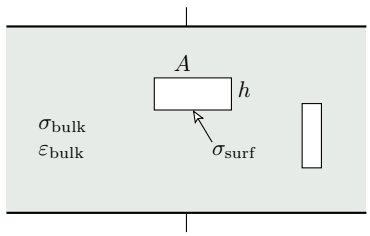

FIGURE 7.2: Some parameters determining frequency-dependence of cavity PD.

has permittivity $\varepsilon_{\text{bulk}}$ and conductivity σ_{bulk}, in the field-direction; within a cavity the relative permittivity can be assumed to be 1. The height of a cavity along the field-direction is h, and the area normal to this is A. The surface-conductivity σ_{surf} of cavity walls provides an alternative to PD for moving charges between top and bottom. Other important features can be defined, such as statistical time-lag and time-constants for decay of surface charge by trapping [For08a] or by conduction.

The following list considers one cause of frequency-dependence at a time; some will clearly have united or opposing effects. The statistical time-lag is influential if it is significant compared to the period; lower frequency makes a given time-lag a less significant part of a period, so statistical variation in phase, overvoltage and amplitude will be reduced. The availability of free charges in the gas and on surfaces can diminish over time by recombination and trapping; lower frequency permits more change to happen within a given part of a period, so electron availability is reduced and statistical time-lag increased.

Surface-conductivity on the sides of a cavity provides an alternative to PD for charging and discharging the dipole of the surface-charges; at lower frequency there is more time for movement of charge by conduction, so less charge need be transferred by PD events, which may be fewer or smaller; in the extreme of high surface-conductivity or low frequency, this could prevent all PD by screening the cavity. The insulation is likely to exhibit dispersion over the studied range of frequencies, so the field distribution between cavity and solid will be frequency-dependent; at lower frequencies the increased permittivity will require a larger charge to moved between the cavity surfaces if the cavity voltage is to be kept below its breakdown level, so more or larger PDs must occur. Conductivity in the bulk material destroys the assumption that the total charge per cycle is limited by peak voltage and permittivity; the total PD charge then can increase with the long periods of lower frequencies.

The cavity dimensions, simplified in figure 7.2 as A and h, also affect the frequency-dependence. For example, as the area is increased for a given height and surface-conductivity, the conductance between top and bottom surfaces increases as the circumference, proportional to $\sqrt{A}$, but the total (displacement and conduction) current that must pass through the cavity from the solid insulation increases as the area A; a delamination with large area cannot so easily as a small void be screened by conduction on its side surfaces, so not so low a frequency would be needed before PD in the void would be stopped by the surface conductivity.

7.4 Discharge forms of PD in epoxy and stator insulation

The development of cavity PD activity through different 'forms' of discharge was mentioned earlier [s.7.2.4], with reference to studies of cavities in LDPE. The subject is of interest in this work because the less pulse-like forms of PD are harder or impossible to detect with normal PD instruments, but are included in DS measurements. Some similar changes of discharge form occur in epoxy-based insulation: some studies of PD in cavities in plain epoxies are summarised here, followed by descriptions of discharge forms in stator insulation.

In [Hud90], [Hud93] and [Hud94], studies were made using trapped air in a 0.5 mm gap between 0.5 mm layers of epoxy on plane electrodes. Excitation of 4 kV at 60 Hz was applied for over a thousand hours; this voltage was about twice the inception level. Measurements were made of PD apparent charge, and of luminous emissions using a photomultiplier tube. Note that the details of voltage and construction were slightly different between these three publications.

The discharges were initially spark-like, with apparent charges of some hundreds of picocoulombs.[†] At a time between tens and hundreds of hours of aging, a gradual but clear transition occurred, to discharges of lower apparent charge, of the order of tens or units of picocoulombs, and with a longer rise-time and a low plateau of continued current after the peak. Within the timescale of a thousand hours, some specimens stopped having detectable pulses, but emission

[†]The rise-times for spark-like discharges are quoted in [Hud93] as about 50 ns. This is ignored here, as it it inordinately long compared to values from other studies. The usual nanosecond-scale rise-times would not have been properly resolved with the 200 MHz oscilloscope used, whatever the values of the unspecified RC detection impedance.

of light continued even when no pulses were detected, and the applied voltage was high enough that some sort of discharge must have occurred in order to prevent the cavity voltage rising enough to make noticeable pulsed discharges. The bound oxygen found in degradation products increased even long after all but the weakest PD pulses had stopped, suggesting that the glow discharge had a considerable aging effect in spite of being undetectable as pulses. The surface conductivity of the epoxy was seen to increase by some six orders of magnitude during the first hundred hours or so of the aging, due to the deposition of simple acids. The crystal form of some of the acids on the epoxy surface was hypothesised as helping to initiate discharges from the sharp edges.

In [Hol91], voids of dry air, with diameter of the order of 1 mm, were included in epoxy blocks. Fast photography was made of the spatial and temporal development of discharges, and oscilloscope measurement of the current was made using a 50 Ω series resistance and a 1 GHz oscilloscope. The two forms of pulse were seen: the spark-like discharge had a narrow channel, and rise-time less than 1 ns; the slower discharge was diffuse and less luminous, with several times longer rise-time and tail, and orders of magnitude lower peak current. Later work [Hol94] used another form of high-bandwidth measurement of PD currents, in cavities in epoxy-mica insulation in a model of a stator bar in its slot; the fast and slow discharges were again seen.

A standard for measurement of PD in stator insulation [E1434] uses similar terminology to [Bar95], dividing the forms of PD into pulsive or glow, with an overlap. All pulsive discharges are considered as spark-like, occurring by the Townsend mechanism but under varying degrees of overvoltage that result in varied sharpness. A *pulseless glow* is common when an aged cavity has such high surface-conductivity that the intense local fields needed for channel-constriction do not get a chance to form; the cavity voltage is held close to the critical level, with any increase in voltage easily counteracted by increased glow. A *pseudoglow* has properties of a glow but also some weak, slow pulses, typical of the stage of aging when a cavity transitions between the conditions for pulsive and glow discharges.

7.5 PD sources in stator insulation systems

Several features of the different PD sources found within stator insulation are important for consideration of the usefulness of different diagnostic methods. Variations in the sharpness and consequent detectability of PD pulses have already been mentioned [s.7.4]. The purpose in this section is to give an idea of the typical measured charges of PD in stator insulation, and the distributions of magnitude and phase of PD pulses from different common sources under sinusoidal excitation. These details necessarily come from industrial sources, so they relate only to power-frequency excitation. The earlier descriptions of frequency-dependence [s.7.3.3] allow some estimates of how the PD from the different sources might change with frequency.

The following will be best understood by familiarity with the PD measurement concepts described in chapter 8, such as apparent charge, limited time-resolution and effects of signal propagation in large apparatus.

Measurements of apparent charge on the terminals of a stator winding usually give magnitudes of hundreds of picocoulombs or more: according to [Sto96], virtually all stator windings operating above 6 kV, whether in air or hydrogen, have PD above 100 pC and not uncommonly up to 100 nC; according to [Far04], PD of several nanocoulombs is normal even in new stator insulation.

Figure 7.3 shows illustratively the main sources of PD in stator insulation. Most have been described in [s.2.2.2], with regard to the cause of the imperfection that gives rise to the PD and the likely importance for insulation lifetime. A standard for stator PD measurements [C3427, E.1.2] divides the

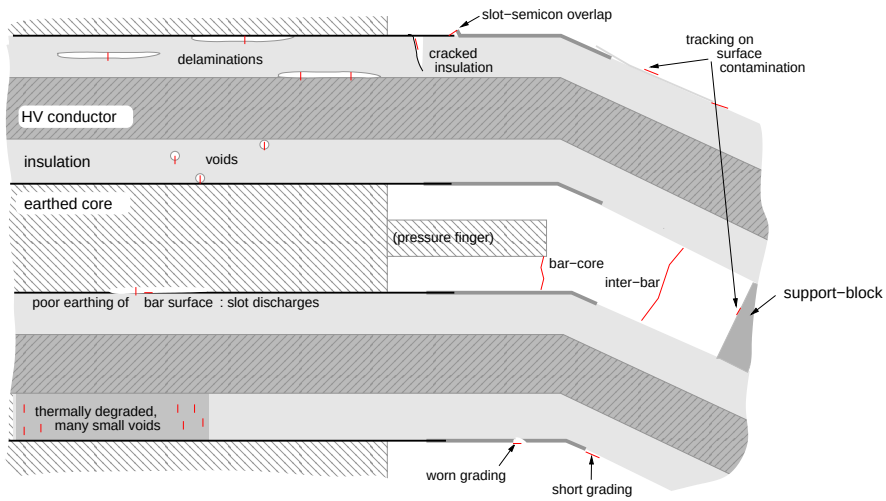

FIGURE 7.3: Sources of PD in stator insulation. This is a complement to figure 5.2 [p.50]. Since all PD sources are some sort of defect there is no 'good' bar shown here.

main PD sources into three risk-levels, in a way that is compatible with the approximate times-to-failure quoted in [s.2.2.2]. The risk assessment is based partly on what the symptoms suggest about the insulation rather than just on how much damage the different types of PD are expected to cause.

> Voids† are of low risk, not normally leading to considerable aging.
>
> End-winding and surface discharges, for example due to contamination and conducting particles, are of intermediate risk.
>
> Slot discharges, and discharges in delaminations either at the conductor or internal to insulation, are all of high risk.

Identifying the type of a PD source is an important diagnostic step. Little can be said about risk and wear by knowing just the magnitudes of PD pulses: for example, surface PD may have 10 or 100 times the magnitude of void PD without indicating aging that is likely to cause premature failure [C3427, E.1.2].

†Called 'internal voids' in [C3427]: in contrast to the general PD classification of figure 7.1 [p.79], some machine-specific references use *internal* to refer to sources between layers of insulation, thus excluding sources adjacent to the conductor.

The magnitude might not be very important even when one *does* know the type of source:

> ... the presence of delamination processes, independent of the measured PD amplitudes, indicates rapid ageing that needs to be repaired promptly. [C3427, E.1.3].

There are many publications showing examples of the PD patterns [s.8.2.4] supposedly typical of particular types of source. Some companies collect large databases of such measurement data for comparisons and for work with automated diagnoses. A rather special case is [Hud05], where efforts were taken to obtain patterns due just to one type of source at a time, using multiple objects to confirm the patterns to be representative. The main PD patterns of that work, from wide-band apparent-charge measurements in the band 40 kHz to 800 kHz, are reproduced in colour in [C3427, s.E.1.1]. They are shown here in figure 7.4, as sketches† of the main features. The magnitudes are given in relative units,

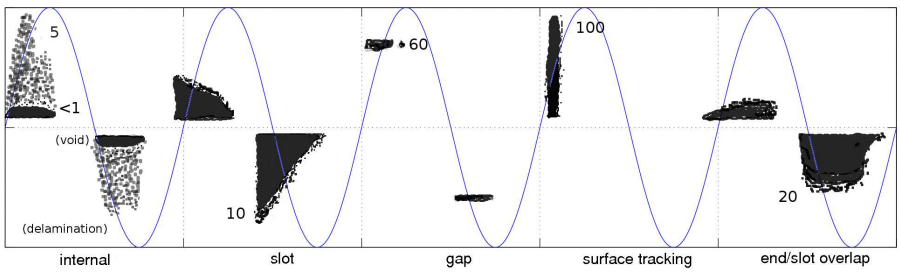

FIGURE 7.4: Some classic PD-pattern shapes for stator PD sources: this is a *sketch* based on patterns shown in [Hud05]. The horizontal axis is phase; the sinusoid shows applied voltage, with one cycle for each type of source. The vertical axis is magnitude: it is scaled differently for each type, with a number showing the magnitude of the largest pulse in the 'relative amplitude units' used in [Hud05]. Pulse polarities are reversed to show the current *into* the stator HV terminal.

which appear to use the same base in each case: bearing in mind their range, and the range of expected apparent-charge magnitudes quoted for stator PD earlier in this section, it seems likely that these units are not vastly different from nanocoulombs. It must be noted that, particularly in the case of whole machines, the calibration is dependent on the location of the source; however, in this wide and low-frequency band a good order-of-magnitude similarity is reasonable to expect.

It is apparently conventional to show stator PD patterns with the pulse polarity defined by the current in the coupling capacitor [s.8.2.3], the negation of the current into the machine terminal. The opposite convention is followed in this thesis, to be consistent with earlier laboratory work where usually the current in the test-object was measured and any results from measurements on the coupling capacitor were reversed in polarity for consistency. Data from other

†Sketches are used to permit this work to be unrestricted by external copyright: the originals are recommended for the subtle details.

sources have therefore been converted to follow the convention of the current in the test object rather than in the coupling capacitor: this avoids the need for talking of "positive polarity PD pulses, which occur mainly during the negative semicycle" [E1434, c.11.1]; these are simply negative pulses.

If the negative pulses are of larger magnitude than the positive ones, the source is probably near the slot stress-grading or end stress-grading: loose coils or bars can be expected to give negative pulses of "at least twice the magnitude and ten times the repetition rate" [E1434, c.11.1]. If the positive pulses are larger, the source is probably at the bond of the insulation to the conductor copper, or possibly between the turn and main insulation of a multiturn coil.

The patterns of figure 7.4, and other details from [Hud05] about these types of PD source are summarised in the following.

The 'inherent' void PD was always present; its inception voltage was 3.5 kV to 6.0 kV on these 13.8 kV-rated bars. During off-line tests this PD is normally the source that appears at the lowest voltage, except in cases of severe damage to slot or end stress-grading. The void PD had their magnitude and number symmetrical in polarity. The clusters in the PD pattern were quite symmetric about their phase-midpoint, which came a little later than halfway from the zero to the peak of the voltage. In laboratory and field measurements the inherent PD level was in the range 0.1 to 5 of the relative units.

An artificial delamination was made by removing turn insulation to give a significant gap from the HV conductor to the main insulation; other delaminations existed within the main insulation. Up to some 6 kV the patterns were symmetrical in polarity, but beyond this there was stronger positive PD. Magnitudes reached nearly 10 relative units.

Slot PD sources were made by removing sections of slot semiconductor. This showed large PD magnitudes, of 5 to 20 relative units. In some cases there was an initial close symmetry in polarity, but after an hour of conditioning [s.16.2] a marked asymmetry was seen in all cases; after 24 hours the ratios of negative to positive PD were about 4 for magnitude and 40 for number. The pattern was largely triangular-shaped, with a near-vertical edge at the starting phase; this phase advanced to earlier than the voltage zero-crossing with increased voltage. The magnitudes were more consistently asymmetic with polarity than the numbers, under variation of the applied voltage amplitude.

PD between bars in the end-winding can only be between phases in offline measurements, but in operation it may even be between bars near the opposite ends of one phase. The PD pattern is typical of longer, larger gap discharges than cavities: the pulse magnitudes are quite constant, and the phase-range is mainly between a zero-crossing and the next peak; there is close symmetry in polarity. Similar patterns with consistent magnitude were seen for PD between insulating surfaces and PD between an insulating surface and a conductor such as a pressure-finger: the air-gap and field appear to determine this pattern more than the material of the surface. The example shown, using a laboratory model of a discharge between the bar surface and a metal pressure-finger, gave a magnitude of 60 relative units; other examples are shown with bar to bar discharges even under 5 relative units.

Surface tracking along the end-winding gave positive discharges close to 30 ° from the voltage-zero, with magnitudes varying widely from low values up to 100 relative units, therefore producing almost a vertical bar in the PD pattern. Similar patterns have been seen for whole machines. The activity was sporadic, strongly dependent on ambient conditions, and it produced a sharp audible noise. The ratios of positive to negative pulses varied widely, including the range into which surface tracking. The phase of the PD pattern is quite similar to plain void PD, perhaps a little skewed to later phase; it has a sharper front than tail; the PR-PDP shape therefore is the best way to distinguish the polarity-dependent stress-grading junction PD from surface tracking.

Other work, studying treeing in epoxy-mica insulation with accelerated voltage-levels has shown magnitudes up to 60 nC [Kim92] [Vog03c], and generally in the region of 10 nC. The tree growth leads to delaminations [Vog03c] and gives a PD pattern that spreads up to higher magnitudes as the channel increases, with peak magnitudes around the time of the peak voltage.

Chapter 8

Partial Discharge measurement

This chapter considers first the connection between a PD event and the test-object's electrodes, then common external circuits and instruments for measuring some feature of the PD. The specific features of a stator winding as the test-object are considered after more idealised test-objects: it is seen that there are several reasons why measurements of PD pulses in stator-insulation will fail to register all of the charge of the PD sources.

8.1 PD detection and measurement in general

A practical distinction is often made between *detection* and *measurement* of PD [Kre64]. Measurement gives directly quantitative results related to the feature of PD being measured. This may for example be a level of electrical charge, or an electric field-strength or acoustic pressure at a certain distance. Detection can be seen as a subset of measurement, giving a simpler result of yes or no; this may be the case if interested in whether a measurement would or would not exceed a certain threshold. A common situation of detection is when checking whether an apparatus has any PD above a tested level of instrument-sensitivity or an acceptance level for a type of apparatus, or when measuring the PDIV and PDEV. The distinction between detection and measurement is not rigidly preserved in this thesis: terms such as 'detection impedance' are used even when the PD instrument gives a quantitative measure of PD pulses.

There are many phenomena that result from PD. The rapid movement of charges causes a charge-redistribution on the electrodes that is detected by direct electrical methods, and also results in emission of radio-frequency electromagnetic radiation which can be detected by antennas and near-field probes. Heating of the discharge channel causes expansion, leading to mechanical pulses of audible and ultrasound frequencies, which can be detected as they travel through the surrounding media. Energy from the electric field and heating stimulates emission of optical and ultra-violet photons. Heating and the creation of reactive radicals result in chemical changes such as formation of ozone (O_3) from molecular oxygen (O_2), as well as other oxides and reaction products from surrounding materials such as organic insulation.

PD measurement methods can be divided according to their possession of the following potentially useful features.

Calibration allows similar results to be obtained for a given PD event in a given construction of PD source and electrodes, regardless of other parts of the test object or measurement circuit, such as different shunt capacitance or different instruments or lengths of connecting cables. This permits more direct comparisons of PD between different test-objects or between different sources within an object.

Resolution of pulses from separate PD events allows the distinctions between many small or a few large PD events to be seen; other methods measure just aggregated effects of many pulses. Bearing in mind that only one weak spot need develop into a bridge between the electrodes to cause insulation breakdown, the behaviour of the largest PD events is arguably more important than the mean, as an indication both of a large existing defect and of a large energy being dissipated with each PD event there.† When repetition rates become high, due to multiple PD sources, the ability to resolve pulses is limited by instrument bandwidth and by reflections in the test-object.

Location of the source of detected PD can be useful in assessing the significance of the PD source and carrying out a further inspection or maintenance. This feature varies greatly between methods: a picture of corona on an external insulator can be produced from ultra-violet emissions; a directional detector can be used for ultrasound and radio emissions; triangulation can be used between multiple detectors in three-dimensions; location along a winding or cable may be done by two or more sensors or by comparing direct and reflected waves; a PD measurement that has no inherent ability to locate sources may be used together with swept exposure of regions of the insulation to ionising radiation such as X-rays, to reveal where the sources lie.

8.2 Apparent-charge measurement

A PD event moves charges at the PD site, quickly and locally. Changes in the dipole moment of these charges cause currents in an external circuit. Measurement of these currents in a frequency-band that is low enough to smooth out differently-shaped pulses and oscillations reveals the 'apparent charge', induced on the electrodes by the PD. In simple objects these apparent-charge measurements can be calibrated; in stator windings the calibration in charge is not valid [s.8.4], but the calibration procedure is widely used as a way of reducing the variation due to different instruments and connections.

8.2.1 From site to electrodes

A high-voltage insulation system can be abstractly seen as an insulating medium, separating two or more electrodes whose potential is imposed from external connections. Given the necessary conditions, such as local electric field, gas pressure and starting electron, a PD may occur in some part of an insulation system. A PD event can be over in a matter of nanoseconds, so it is reasonable to suppose that negligible charge flows in the external circuit; in a large object, such as a cable, there will not even be time for an electromagnetic wave, taking several nanoseconds to move a metre, to redistribute charges across the electrodes. During the short time of the PD the situation can therefore be treated as just the PD source and the local region of electrodes and insulation surrounding it, such as a short length of stator bar.

† The correspondence of measured PD signal to local energy at the discharge site is not direct, even when using calibrated apparent-charge measurement and considering the phase of the applied voltage; what is meant here is that pulses of several times the measured size of others will generally imply more energy at the site, except when other factors are vastly different between the different sources.

The PD event moves charges, illustrated in the left of figure 8.1 as the equal positive and negative charges $\pm\delta q$ moving apart by distance δd. Two different events are shown: in one of them the considered δq is a small final part of the charge in a PD event, moving through a local field that is modified by a charge Δq that already has moved. In either case, the $\pm\delta q$ dipole induces the

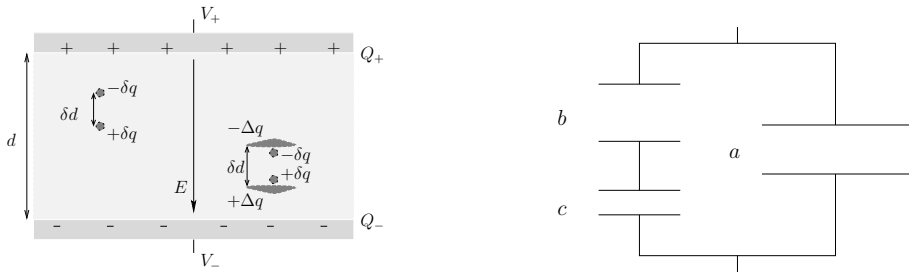

FIGURE 8.1: Left: Dipole creation by PD in a medium between electrodes. Right: the simple *abc* model.

same charge and change in potential on the electrodes. A general method for calculating the induced charge on arbitrarily placed electrodes by movement of charges is developed in [Ped91] [Ped95], for application to relating PD events to the measurable quantities at the terminals; this was stimulated by work on sensitive measurement of void PD [Cri89] in divergent fields, but it has wider applicability than cavities.

If the original voltage from before the PD event is to be restored, the charge induced at the electrodes has to be compensated by charge moving in from outside the small region of electrodes and insulation considered in this subsection. This charge is conventionally called the *apparent charge*,[†] and is related to the charges δq in the PD by a function of the geometry and materials of the object and the distance moved by the charges. It is usually reasonable to assume that the voltage will be restored to practically its original value, as a PD is usually in only a small part of the whole capacitive test-object.

A common circuit-approximation for the effect of cavity PD at the electrodes is the *abc* model [Kre64] [Bog90b], where the object of electrodes, dielectric and cavity is seen as a capacitor formed from other capicitors, as shown in the right of figure 8.1. The cavity is a capacitor c, in series with a capacitor b formed from the insulation lying between the cavity and electrodes; a capacitor a represents the parallel capacitance of the dielectric in the rest of the object. Limitations of this are described in, for example, [Ped95]; for practical measurements on a stator winding the simple model should be a sufficient guide, as there are other greater doubts about the accuracy of the measurement of apparent charge [s.8.4].

[†]Apparent charge is regarded as a bad description in [Ped91] and other work by the same group. It is used here as it is the conventional term, and it actually seems rather appropriate for practical PD measurements, even if inideal for detailed discussion of the induced charges on the electrodes.

8.2.2 From electrodes to terminals

Electrical measurements of PD are made at some point on the electrode system that may be remote from the PD site, probably the terminals used for the excitation voltage.

The change in potential on the electrodes adjacent to a PD event spreads along the electrodes: ignoring for the moment the external circuit, the charge on the electrodes ends up being redistributed so that the electrodes' potentials become uniform again, but at a slightly different level than before because of the new dipole of PD charge. In a small laboratory PD object this may happen about as quickly as the PD event. In a GIS busbar, consisting of concentric metallic tubes with gaseous dielectric and occasional polymeric spacers, the situation is close to a pure transmission line, so the PD pulse spreads out as a wave, with little distortion of its shape. Eventually, by reflections, the potential on electrodes across the whole construction will become equalised. Power-cables differ in that there are semiconducting screens that cause strong attenuation of high frequencies, so the PD pulse shape is quickly altered.

In the complicated inductive constructions of transformers and stator windings, the propagation of a PD pulse happens through many routes, such as capacitive and inductive coupling between adjacent insulated conductors, or propagation along the winding. This makes for many attenuations, couplings, reflections and resonances, which are of relevance to PD measurements [s.8.4].

8.2.3 The external circuit and detection

In objects such as GIS, that behave as transmission lines, sensitive measurements of the pulse-shape of the PD and of the apparent charge involved can be made by high-frequency measurements [Bog90a], in the range of hundreds of megahertz and even gigahertz, by knowledge of the transmission line properties. The measurement may be made by for example by capacitive sensors that detect the change in voltage as the pulse passes. Ideally, a given PD event occurring anywhere along the line would be measured similarly at any point, although with a different time-delay. The apparent-charge measurement can be calibrated by injecting a known charge with similar rise-time to the expected PD, and scaling measurements by the relative magnitudes of the waves caused by them and by the calibration pulse.

In most other equipment, particularly inductive apparatus with complex transmission of PD pulses, a measurement including very high frequencies has the problem that the location of the PD event strongly determines the voltages seen at a measurement point. Unless a calibration pulse was injected at the same point as the PD event, the calibration would not be very meaningful; in any case, the signal measured would be likely to be a confusion of signals from multiple paths and with different delays, distortions and attenuations.

The apparent-charge measurement common in power-system equipment can reduce this problem by using a band of low frequencies, usually below 1 MHz. The widely used standard for such measurements is [C270]. The classic circuit arrangement is shown in figure 8.2, where a loop is formed from the test-object

C_x and a *coupling capacitor* C_k, with a *detection impedance*† Z_{det} placed somewhere in series in this loop.

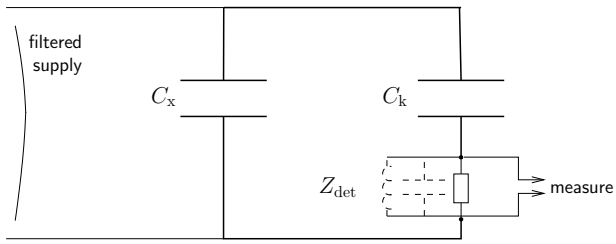

FIGURE 8.2: PD apparent-charge measurement. The detection impedance Z_{det} could be in any other location around the main loop.

The choice of position for Z_{det} is often influenced by earthing. The instrument measuring the voltage across Z_{det} is likely to have one terminal earthed, and one conductor of the supply or the test-object is likely to be earthed (assume the lower one in the figure). Unless an optical link is used, the detection impedance must therefore be in the lower connection of one of the capacitances. A test-object such as a stator or transformer will usually be solidly earthed, which leaves only the coupling capacitor's earth connection as a location for the detection impedance. In the laboratory, the detection impedance may be on the test-object connection instead. When the capacitance in the supply, or the parasitic capacitance from the connections in the test circuit, is significant compared to C_k, the currents in C_k and C_x will not be the same; a detection impedance in C_k will measure less charge. This is a problem to sensitivity rather than to calibration. A filter on the supply source can be used to forcing more of the current due to a PD to flow in the loop of C_k and C_x.

A PD event in the test object causes a local depression of voltage between the electrodes, which propagates through the object and even in the external circuit with the coupling capacitor. There may very well be high-frequency oscillations within the test object and in the whole circuit, but the relatively low bandwidth of the instrument that measures the voltage on the detection impedance results in a measurement proportional to the total charge-transfer in the circuit.

The frequency-domain view of why this happens is a common explanation [C270]: if the calibration and PD pulses are fast enough to have largely constant amplitude spectra all over the measurement band of the instrument that measures across Z_{det}, then the signal within the instrument's bandwidth will be proportional to the charge of the pulse.

A time-domain view, with a resistor as the detection impedance, is that the equilibrium state after a pulse is when C_x and C_k have reached equal voltage, which requires a charge transfer in proportion to the apparent charge: the time

† This simple component has a wide variety of names: besides detection impedance or Z_{det} as is used here, it is also called the *coupling-device (CD)* [C270], *quadrupole* [Gut95], or *power-separation filter (PSF)* [Ste91].

integral of the voltage on the resistor over the whole time taken for the circuit to reach a equilibrium is proportional to this charge, so measurement of this voltage with the low-pass filter of the instrument's input gives a response that is proportional to the apparent charge.

The inductor in Z_{det} is necessary, at least with ac applied voltage, to let the normal load-current pass through without much voltage drop. An inductor can also be used to make the detection have a tuned, *narrowband* response, rather than the *wideband* response that has a significant bandwidth compared to the centre-frequency. A capacitor in Z_{det} can be used to control the peak voltage reached on the detection impedance for a given PD size, and the time-constant with which the voltage on the detection impedance falls afterwards.

An example of the voltage across a detection impedance and the signal out of the first stage of a PD pulse measurement instrument is shown in figure 8.3. The circuit (see figure 8.2) is a small 2 nF high-voltage ceramic capacitor for

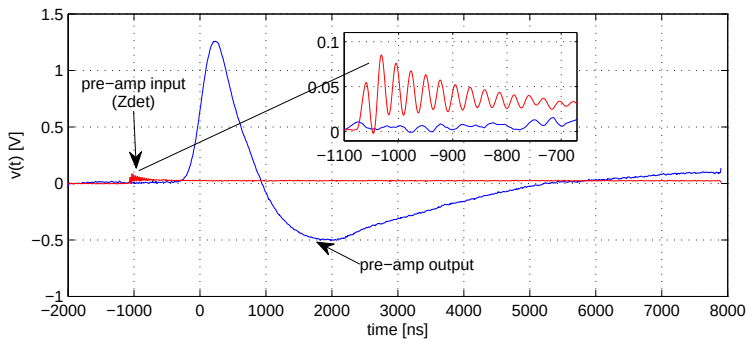

FIGURE 8.3: Signals at the input and output of the ICM PD instrument's preamplifier.

each of C_{x} and C_{k}, connected by leads on a table. The detection impedance is a 270 Ω resistor; the voltage across it is applied to the ICM instrument's preamplifier input [s.10.1.1], and also measured by an oscilloscope probe. The stimulus is a 100 pC pulse from the ICM's calibrator [s.10.1.7], applied across C_{x}, and the preamplifier gain is 10. The specification of the preamplifier is a filter-band of 20 kHz to 1.0 MHz. The result is that although the current in the circuit has an oscillatory component, the output from the preamplifier is slow and smooth, with a peak supposedly proportional to the time-integral of the input. Note how the output too has a damped oscillation: this is its natural response even to a non-oscillatory input, and is significant in PD measurements if the second peak of the response is measured as a subsequent PD.

8.2.4 Display of results

The *phase-resolved PD pattern*, *PR-PDP* or just *PDP*, is a natural and widely-used way to show results of PD pulse measurements under periodic excitation. Examples can be seen in [s.17.2]. Each detected pulse results in a count being incremented for the combination of the pulse's magnitude and the phase of

the voltage at which it occurred. The counts form a third dimension on the display, often shown as colour. Using phase rather than time does lose some information about variation in the activity, but for many cases it provides a useful simplification. The combination of results from many cycles gives more repeatable results in spite of the usual variation of PD results between cycles.

Some of the detail in a PDP is potentially interesting to study, but not easily seen: an example is the total number of PD pulses at a particular phase or of a particular magnitude. For comparison of multiple PDPs, for example from measurements at different voltage amplitudes or on different occasions, it may be useful to reduce the PDP's dimension, in order to plot some feature of all of the PDPs together, as will clearly be useful for measurements with variable frequency [s.15.3.1]. Many forms of reduction are used: the statistical moments such as skew and kurtosis are described in [Edi01, p.37], and more physical values such as maximum regularly occurring magnitude, or mean pulse size or counts per cycle are used.

8.3 Non-pulse measurement of apparent-charge

The C-tan δ measurement [s.6.4.1] sees the fundamental-frequency component of the current due to the apparent charges of all the PD. Such 'bridge methods' of measuring PD lose all the detail of individual pulses, and have a lower sensitivity bearing in mind the but they have the advantage of coping with high repetition rates [Bar90] since they do not try to distinguish separate pulses. Methods for showing the total dissipated energy have been available for decades, such as a 'loop-trace' method showing dissipated energy as the area within an oscilloscope trace. It is considered by [Bar90] to be "somewhat astounding that [these methods do] not command a higher degree of attention and popularity". Some reasons may be the perceived importance of the strongest individual sources of PD, even if too localised to affect the total current much, and the effect of disturbances such as the nonlinear end-winding stress grading.

The DS measurements considered in this work can include some detail of the PD waveform based on the harmonic currents, as shown with artificial pulses in chapter 14 and with real PD in chapter 17.

8.4 Difficulties of PD measurement in stator windings

There are several reasons why the apparent charges cannot be accurately measured as pulses for all the separate PD events in a stator winding. The result is that, in general, only a small proportion of the total PD charge will be measured. This is not necessarily a bad thing, as measuring just a small sample of the total pulses may give plenty of information about PD sources, but it does make the non-pulse methods [s.8.3] interesting as a complement to pulse methods.

8.4.1 Repetition rate

The rate at which PD pulses occur is the *repetition rate*: when this is high, an instrument working in the low frequency-range of typical apparent-charge measurements will not be able to distinguish all the pulses.

Each PD pulse in the system of a winding and external test circuit takes some time for its oscillations to fade. The conventional apparent-charge measurement

has a low bandwidth, to allow the total charge to be measured, but this has the disadvantage of giving a slow response. The output after filtering is generally oscillatory: to prevent the pulse measurement system measuring a second peak of a decaying oscillation as being a second PD of opposite sign, it may be necessary to have a *dead-time* during which no further measurement is taken. Deadtimes of tens of microseconds are common in apparent-charge measurements on stator windings. Insufficient deadtime will result in oscillations of the measurement system's response being recorded as PD pulses. Excessive deadtime will result in subsequent PD events being missed.

Stator insulation can have such high repetition rates of PD pulses, from the many sources throughout a long winding, that many According to [Gro02], *thermally aged* epoxy-mica insulation can have a repetition rate of 20 000 to 100 000 per second. The rather vague range given by [E1434, c.5.1] is that in a typical coil or bar or winding there may be many hundreds of PDs per second; as a winding might consist of a hundred bars, hundreds per bar per second could also be taken to indicate a high rate for the complete winding.

8.4.2 Noise and dynamic range

The *noise-floor*, is the level of background electromagnetic noise that affects the measurement. In a practical situation this is probably determined by external disturbances: in field-measurments of whole machines there are often many sources from other apparatus operating nearby. The measurement instrument therefore has to have a *discrimination threshold*, setting a magnitude below which pulses are ignored. This prevents detection of small pulses that might be present.

Additionally, a limited dynamic range of the instrument will result either in small pulses being missing or in large pulses causing saturation, depending on the gain: either of these situations prevents full measurement of the charge. The instrument used in this work has just 128 evenly spaced channels [s.10.1.3] on the linear bipolar range [s.13.5] that is normally used; this is low compared to the range of pulse-magnitudes that can occur between different PD sources in stator insulation [s.7.5].

8.4.3 PD-pulse propagation

Stator windings are certainly in the class of complicated inductive contructions, with consequent troubles of calibration [s.8.2.2]. The relevant standards for PD measurement, such as [E1434] and [C3427], warn against use of 'apparent charge' terminology, pointing out that the results cannot be compared to those from other objects or measurement systems.

On the other hand, laboratory work with stator insulation usually involves just a single bar or coil, with all the high-voltage conductors joined. This is true for the laboratory measurements in this work, and for industrial tests of new insulation systems. In this case, valid calibration of apparent-charge measurements can be made [C3427, c.10.2.1]. The problem of large numbers of sources is reduced when dealing with only one or a few bars, but there may still be too high a repetition rate for an apparent-charge PD instrument to be able to capture each pulse.

There was a period starting around 1990 when several groups researched PD signal transmission in stator windings, mainly with the aim of achieving an acceptable standard level for PD testing. The method was typically injection of controlled charges at different points in a winding, and measurement of the result at the terminals. Some of these pulse-propagation studies are cited in a summary in [E1434].

There is a strong distinction found between a 'fast' component of the signal, consisting of high-frequencies that travel to the terminals by shorter routes than propagation along the path of the winding, and a 'slow' component of lower frequencies whose transit time is proportional to the length of winding between the PD site and the measurement. The boundary between the frequencies of these fast and slow components is in the region of 1 MHz, but is defined or seen differently by different groups, and in some cases only the slow component is observed.

The fast coupling is of little interest for apparent-charge measurement because the resonances and attenuations in this range make the result very dependent on where the PD occurred. The fast mode is highly attenuated within the windings, by reflections at the transitions of the $\sim 20\,\Omega$ to $30\,\Omega$ slot parts and the $\sim 300\,\Omega$ end-windings [E1434], and transmission-line attenuation due to the the semiconducting layers at high frequency [Gro02]. The nature of the fast coupling that permits a shorter route than following the winding is not unanimously agreed: it is shown experimentally in [Pem06] that the absence of end-windings prevents the fast coupling, but in [Tav88] inductive coupling between slots is expected for frequencies even up to 20 MHz, for large machines; in [Gea90] the fast coupling is thought to be capacitive, but in [Zhu92] it is wondered whether it is in fact more inductive.

The slow, low-frequency, 'travelling wave' mode propagates along the conductors of the winding, possibly with inductive coupling to other bars. The attenuation of this slow mode is very low, and its propagation speed is given from about $10\,\mathrm{m/\mu s}$ [Pem06] to over $100\,\mathrm{m/\mu s}$ [Zhu92] by different references.

The frequency range of a few tens to a few hundreds of kilohertz gives the lowest variation in measured apparent charge. According to [Sto98] this range may still not be very flat, but others show quite a flat response, such as [Woo93] with spectrum-analyser (not apparent-charge) results, and [Pem06] with very little location-dependence in charge but a few times variation in voltage peaks.

The recommendation of [C3427, c.5.2] is to use wideband measurements in accordance with IEC-60270, with lower cutoff of tens of kilohertz. This is chosen in order to have 'sufficient visibility' of sources that are deep in the winding, but it is warned that there may be resonances even in this range. The recommendation of [E1434] is that offline tests on complete windings should measure at frequencies below 500 kHz, but that this has the disadvantage of pulse superposition of pulses when the repetition rate is near the instrument bandwidth.

8.5 Current practice in stator-PD measurement

There are many types of PD measurement made on rotating machines. A good summary of electrical methods is [E1434]. Rotating machines are unusual among high-voltage apparatus in not having specifications of acceptable PD levels. This is due to the trouble of calibration [s.8.4], the large magnitudes that can be tolerated by the mica-based insulation, and the great difference in acceptable magnitude between different types of PD source [s.7.5].

Online PD measurements are common on large or important machines, giving good trending and warning of rapid changes in activity. Some of these systems are very different from apparent-charge measurements, using a high frequency range of the order of tens of megahertz, with multiple detection locations and comparison of time of arrival.

Offline measurements are common as part of asset management of rotating machines. It is usual to measure at several amplitudes of an applied sinusoidal voltage at power frequency. The offline measurements can take advantage of exciting different combinations of windings, to distinguish different PD sites such as ones from phase to earth or from phase to phase [C3427]. The attenuation of PD pulses in the winding makes it sometimes worthwhile to measure at the phase and neutral ends of a winding separately, as a primitive step towards location of sources. The lower frequency apparent-charge style measurement is common, often using PDPs to analyse the results. Derived quantities are popular too, such as distributions of pulses by phase or magnitude, largest repeatedly occurring PD magnitude, quadratic rate (using the square of the magnitude), and simple calculations of energy based on the supply voltage at which a pulse occurred.

Chapter 9

The Dielectric Spectroscopy instrument

This chapter describes the operation and specification of the DS instrument used in this work, and the new programs that were written to control it. Much of the information here is not documented with the instrument, so is hoped to be a useful summary for future users in our laboratory and possibly for users elsewhere. The details are relevant to the combined use of the DS and PD instruments and to discussion in chapter 14 of measurement of PD pulses. Some tests of the instrument are described in chapter 12.

9.1 Description of the IDAX300 and HVU

A commercially available DS measurement instrument was chosen for applying and measuring the test voltage and for measuring the current through the insulation system. This is the IDAX 300 from Pax (now Megger) of Täby, Sweden, shown in figure 9.1. Earlier instruments from this model-family are well known in our group: the IDA 200 was used in the work of [Tay06], and the earlier instruments were developed in the course of the work described in [Wer01a].

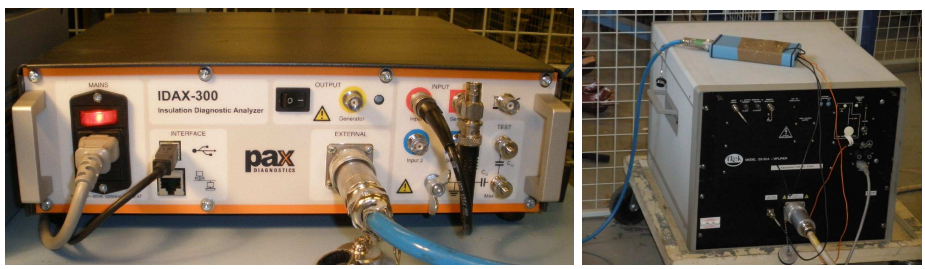

FIGURE 9.1: The IDAX 300 DS-instrument (left) and its HVU (right).

The choice was motivated by the convenience of having a compact and tested construction of the sensitive measurement components along with their protection and shielding, with the calibration already done. Discussion with the manufacturer suggested that the sufficient information could be provided for the writing of control-programs other than the supplied one.

The IDAX's main unit contains all the components needed to supply sinusoidal voltages at amplitudes up to 200 V and frequencies from 100 µHz to 10 kHz, and to measure this voltage and the current through the test object, performing DFTs to present the measured data in frequency-domain form.

A high-voltage output can be provided by an external amplifier supplied as an accessory to the IDAX, referred to as the high-voltage unit, *HVU*. Use of the HVU limits the maximum frequency to about 100 Hz. The HVU used in this

work has maximum rating of 20 mA and 20 kV. It is controlled by a 10 V signal from the IDAX.

Figure 9.2 shows the basic external view of connections used for a high-voltage measurement on a simple two-terminal test-object. The same 'measure' connection for the measured current is used regardless of the voltage source. This is usually done with a coaxial cable running to the test object, so that the sheath guards the core conductor from stray currents. The multicore cable to the HVU provides the reference signal at 1/2000 of the desired output voltage, and returns a current that is used as a measurement of the actual output voltage; the chassis of the HVU is also connected to an internal signal-earth in the IDAX 300 through this cable, to take the current from the measurement and guard back into the voltage source.

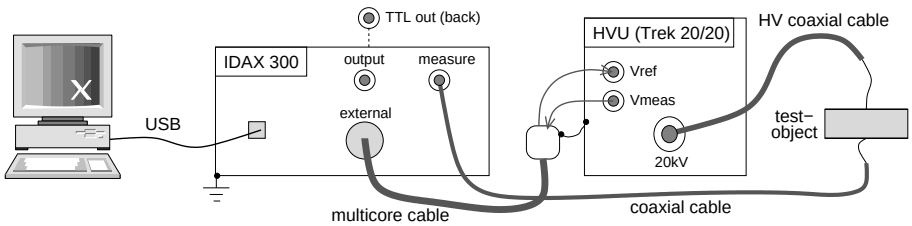

FIGURE 9.2: The IDAX 300 DS-instrument and external amplifier (HVU): typical connections.

A better idea of the internal working of the instrument is needed for understanding the purpose of some of the tests and the descriptions of limitations and pulse-measurements. A block-view of the instrument and HVU being used for a guarded UST (measurement-electrode not earthed) measurement is shown in figure 9.3. The main components are treated in approximately the order of signal flow, in the following subsections.

The development of earlier instruments is described in [Wer01a], with further detail about the modelling of feedback and reference capacitors, measuring on earthed specimens, and calibrating the system. The IDAX is similar in these respects, but it differs in many others: for example, instead of using the balancing arm and correlation filters described in [Wer01a] it measures the whole current and does frequency-separation digitally.

9.1.1 Voltage synthesis

Relevant aspects of the computer communication are covered in section 9.2. The voltage to be applied to the test-object is set as just the amplitude and frequency of a sinusoid; the signal is started from a negative-going zero point. The microprocessor generates voltage levels at a rate of 100 kHz; each one is a 16-bit signed number, so there are 2^{15} ($\simeq 32\,000$) possible levels at each polarity.

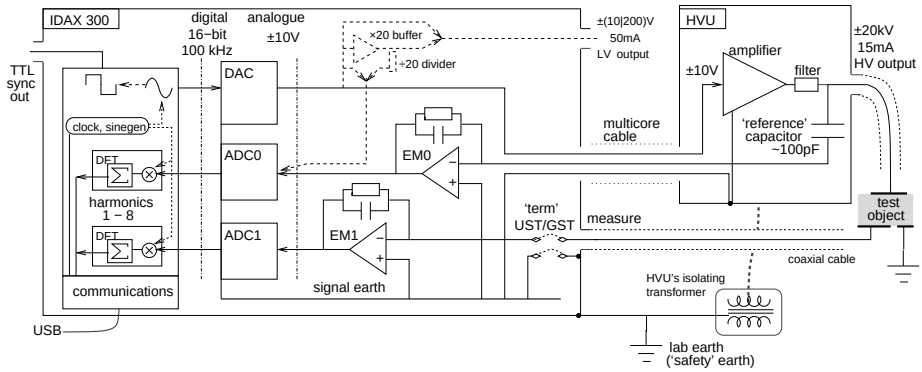

FIGURE 9.3: The IDAX 300 DS-instrument's basic circuit and signals.

An extra output was added by the manufacturer to provide a TTL† digital output showing the polarity of the output voltage. This is used for synchronising other instruments such as the PD measurement system. The TTL voltage is in the high state when the output voltage is non-negative. Many TTL devices work as active-low, so they consider this TTL signal to be 'true' when the IDAX's analogue output voltage is negative.

The digital signal is converted in the digital-analogue converter, *DAC*, to an analogue signal in the range $\pm 10\,\mathrm{V}$. Section 12.7 describes measurements of the phase-shift that is imposed between the digital signal and the analogue output by the DAC and other components. Section 12.3 shows that the analogue output is in fact filtered to be much smoother than it would if it just followed the limited number of levels of the digital signal. Depending on the choice of voltage-source, the analogue output may be supplied directly to the IDAX's low-voltage (LV) output connector, supplied to the LV output through a buffer with a $\times 20$ gain, or used to control the HVU to provide a high-voltage output. The high-voltage output is assumed for discussions of this work, since it is necessary for any work with PD.

9.1.2 The HVU

The HVU used here is based on the model 20/20A high-voltage amplifier from Trek Inc. The amplifier takes a $\pm 10\,\mathrm{V}$ input signal, and gives a regulated output voltage with a gain of 2000. A switch-mode supply is used to drive the output voltage to the desired level; the switching frequency is $\simeq 50\,\mathrm{kHz}$. The noise from this switching is very disturbing to PD pulse-measurement, but is far from the tightly filtered frequencies of the DS measurements.

† TTL: transistor-transistor logic, a widely used standard for the voltage-levels and current-demands of digital inputs and outputs, based on levels appropriate to logic circuits using bipolar-junction transistors (BJT) that were from the 1960s onwards. The low and high state are 0 V and 5 V respectively, with wide tolerances between these values. *Active low* operation is common, in which the low state is the one representing a controlled device being 'on', as the traditional TTL circuit can sink much higher currents ($\simeq 16\,\mathrm{mA}$, through a transistor) than it can source ($\simeq 0.4\,\mathrm{mA}$, through a resistor).

The amplifier's maximum output current is limited by the amplifier's internal regulation, with an absolute maximum of 20 mA and lower limits for parts of the current/voltage operating curve where the voltage is low or the power flow is into the amplifier. A distorted output voltage waveform will result if the combination of requested amplitude and frequency would cause more than the amplifier's current-limit in the connected load. The current drawn from the voltage source consists of the current through the test-object, measured in the current-electrometer EM1, the current through the reference capacitor, measured in voltage-electrometer EM0, and all currents that are guarded away from the electrometers, the shielded high-voltage cable giving a substantial contribution to this.

The reference capacitor in this HVU is a short length of cable with XLPE (cross-linked polyethylene) dielectric; its properties are included in the calibration data by specifying the complex capacitance over a range of frequencies.

9.1.3 Voltage measurement

DS requires very high accuracy for the measurement of relative phase between voltage and current. The applied voltage is therefore measured at the output terminal rather than being inferred from the signal just before or after the DAC. The analogue-digital converter ADC0 accepts a ± 10 V signal: the low-voltage 10 V output can thus be measured directly. The low-voltage 200 V output is measured through a 1/20 resistive divider, and the high-voltage output in new IDAX units is also measured as a voltage signal from a divider.

In the system used here, however, for compatibility with the old HVU and the earlier IDA 200 instrument, an older method is used, measuring the current through a known HV 'reference' capacitor. Converting this current to a voltage signal into ADC0 requires a further electrometer 'EM0' besides the one used for measuring the current through the test-object. The two electrometers are similar in specification; the description in section 9.1.5 provides the details.

9.1.4 Specimen earthing

In figure 9.3 the test-object electrode whose current is to be measured is floating with respect to earth; it can be connected directly to the input of the electrometer EM1. The *signal earth* of the circuit of the electrometer and voltage-source can therefore be connected to the instrument's chassis and thereby to the *safety earth* that connects to the chassis of all the instruments and the building structure and the earth itself; any electrodes whose current is to be guarded can also be connected to earth. The relays marked 'term UST/GST' in figure 9.3 are shown in this configuration, which is referred to as 'unearthed specimen test', *UST*. Stray currents between the supply voltage and any conductor other than the measurement electrode are guarded away from the measurement; this desirable situation is usually able to be achieved in a laboratory measurement.

In a measurement on installed apparatus such as stator windings or cables, there is often a measurement electrode that cannot feasibly be disconnected from safety earth: the stator iron is typically in electrical contact with the building construction, and a cable's sheath is often bonded to switchgear or in significant contact with soil. If the signal earth in the instrument were also connected to

safety earth as in the UST configuration, the current to be measured could bypass the electrometer by returning to the voltage source by passing through the test-object and instrument earth connections. The 'grounded' (earthed) specimen test, *GST*, swaps the connections so that the electrometer input is connected to safety earth and the 'measure' input provides a bypass straight to signal earth for any guarded electrodes. For this to work, the voltage source must draw its current from the signal earth, and not connect signal earth to safety earth. The HVU draws its current from its chassis: in order to permit GST measurements with high voltage, the HVU has to be supplied through an isolating transformer with shielding to minimise capacitively coupled hum currents [Wer01a, p.68]. A disadvantage is that any stray currents to earthed electrodes will be measured by the electrometer.

The matter of earthed or floating measurement electrodes becomes important when considering how to combine the IDAX with the ICM PD pulse-measurement instrument for simultaneous measurements in the laboratory and in the field. Practically any field-measurement on a stator winding must accept the stator as being solidly and unavoidably earthed.

9.1.5 Electrometers and feedback

A description of the purpose and practical details of feedback electrometers for DS measurement is given in section 6.2. The details known about the IDAX electrometers are the parameters from the instrument's calibration data. The open-loop gain is modelled as low-frequency value of $6.3{\times}10^5$ with frequency-response of single-pole filter with pole-frequency about 30 Hz. Its input capacitance is 12 pF. The output voltage is restricted to ± 9 V, with feedback components chosen to yield a considerably lower value, such as 7 V or less, with the expected test-object. The output voltage is measured in an analogue-digital converter and is used to calculate the input current according to (6.8).

One resistive and one capacitive feedback component can be selected by relays, to connect in parallel between the output and input of the electrometer. The available resistances are $10^{(1+n_\mathrm{r})}\,\Omega$ where the integer n_r is in the range $1 \le n_\mathrm{r} \le 9$ giving a range of 100 Ω to 10 GΩ; the special value $n_\mathrm{r} = 0$ gives an open circuit, specified as a finite value of $10^{18}\,\Omega$. The available capacitances are $10^{-(4+n_\mathrm{c})}$ F, with $1 \le n_\mathrm{r} \le 6$, a range of 10 µF down to 100 pF. These intended values are listed in table 9.1, along with examples of the reactances of the capacitors at different frequencies. For adequate calculation of the current into the electrometer the feedback values must be known very precisely, including any significant frequency-dependence. Actual measured values of the feedback components are stored in the calibration data [s.9.1.7] and are used for this calculation. For choosing which feedback components to use, the nominal values listed in table 9.1 are sufficient.

The complex capacitance C is calculated as the ratio of the measured complex current I and voltage V. For a measurement using the HVU, these quantities are in turn calculated from measured voltages at the outputs of electrometers EM1 and EM0, $V_{\mathrm{o}1}$ and$V_{\mathrm{o}0}$, based on electrometer and feedback properties (6.8). Ignoring the effect of the term multipled by $H(\omega)$ in (6.8), as though the electrometer calibration and extra shunt impedance are correctly known,

TABLE 9.1: Approximate values of the parallel feedback components for the electrometers, for resistive and capacitive feedback component numbers n_R and n_C.

n_R	R	n_C	C	$X_C(50\,\text{Hz})$	$X_C(1\,\text{mHz})$
1	100 Ω	1	10 µF	320 Ω	16 MΩ
2	1 kΩ	2	1 µF	3.2 kΩ	160 MΩ
3	10 kΩ	3	100 nF	32 kΩ	1.6 GΩ
4	100 kΩ	4	10 nF	320 kΩ	16 GΩ
5	1 MΩ	5	1 nF	3.2 MΩ	160 GΩ
6	10 MΩ	6	100 pF	32 MΩ	1.6 TΩ
7	100 MΩ	—	—	—	—
8	1 GΩ	—	—	—	—
9	10 GΩ	—	—	—	—
0	open circuit	—	—	—	—

just the complex admittances of the electrometers' feedback component pairs $Y_{1\text{fb}}$ and$Y_{0\text{fb}}$ are needed for this. The applied high-voltage is calculated as the measured current into the voltage electrometer EM0, across the calibrated impedance of the reference-capacitor, Z_{Cref}. The final result for complex capacitance therefore has magnitude and phase errors depending equally on these errors in each of the other impedances,

$$C = \frac{V_{\text{o}1} Y_{\text{fb}1}}{\text{i}\,\omega\, V_{\text{o}0} Y_{\text{fb}0} Z_{\text{Cref}}}. \tag{9.1}$$

As explained in section 6.2.5, the correct measurement of loss in a low-loss test-object is very sensitive to phase errors in any of these complex voltages, admittances or impedances.

9.1.6 ADCs and digital processing

The signal into each ADC should be in the range ± 10 V. The ADC converts this range linearly to 16-bit signed numbers at a rate of 100 kHz, after suitable anti-aliasing filtering for the sampling rate. To transfer data at this rate to the control computer would require more than the available capacity of the serial-emulated connection.

By taking a DFT [s.6.2.2] to give just a few low harmonics from the time-domain samples as they arrive, the data being sampled in the IDAX can be accumulated as a small number of variables in memory, and transferred to the computer very easily. The low harmonics provide a good deal of information about the measured waveforms, as long as very sharp changes do not have to be reproduced faithfully and variations between cycles can be averaged. The digital processing produces a complex number to describe each of the first eight harmonics, for each of the two ADC outputs, using the same timebase as is used to generate the digital output voltage. The principle is a familiar one [s.6.2.2] used in all manner of DSP (digital signal processing) applications.

The IDAX deviates from DSP convention in that the complex values describing the harmonic components have angles appropriate to sine rather than cosine functions. A time-signal transformed by (6.5) results in complex numbers from

which the time-signal, or a filtered version using just limited harmonics, can be recovered by summing cosines as in (6.7). The complex values S_n from the IDAX should be used in sine functions to approximate the measured waveform,

$$\bar{s}(t) = \sum_{n=0}^{N} |S_n| \sin\left(n\omega t + \angle S_n\right). \tag{9.2}$$

For any single harmonic order this distinction between sine and cosine is merely a time-shift, which is irrelevant when zero time has no special meaning. For non-sinusoidal waveforms, where multiple harmonic orders are added, it is essential to use the right function in order to preserve the shape of the waveform: the equal phase-shifts of the harmonics between the sine and cosine forms correspond to different time-shifts. Conversion of S_n between the sine or cosine form requires a phase-shift of $n\angle S_n$.

The absolute phase of the complex numbers returned by the IDAX's DFT appears to be based on the internally generated digital signal, while for the older IDA200 instrument it appeared quite arbitrary. The important matter is the relative value of phase between the measured voltage and current signals from the ADCs, each phase measured relative to the common reference. A dc term, $h = 0$, is also available from the DFT, this being the mean value of the samples. When capacitive feedback is used, the dc term is not directly convertible to voltage or current at the test-object. In the normal use of the IDAX the dc term is only used for checking on dc input currents when selecting suitable feedback. If using resistive feedback the information in this dc term would be good to have when measuring on asymmetric test-objects that have a non-zero mean.

In the IDAX's processing, the samples and their coefficients are signed 16-bit integers. To limit the rate at which new results must be checked for and transferred, the IDAX accumulates DFT results over whichever is the greater time of 1 s or the smallest integer number of cycles that takes more than 1 s. After this, the result is available for transfer as a list of integers in text form, and a fresh accumulation is made. For very low frequencies with periods of thousands of seconds, the accumulation of 100 kHz sampling of 16-bit integers multiplied by 16-bit integer coefficients leads to very large numbers, such that one must be careful to use suitable storage and manipulation on the control computer; double-precision floating point numbers were used throughout the control program, to ensure sufficient representation.

9.1.7 Calibration

The DFT components calculated from the two ADC outputs have to be converted into the applied voltage and the resulting current at the test-object. This calculation requires knowledge of transfer functions of many of the instrument's components. Stored in the instrument is a calibration file that can be copied to the control computer when the instrument is connected. This file includes details of components' limits and transfer-functions. Some components, for example feedback resistors, are modelled as constants; others, for example the reference capacitor and feedback capacitors, are modelled as 'universal

capacitors' following multiparameter equations as described in [Wer01a]; others, for example the buffer and divider used for the 200 V output, or the relative amplitude and phase between the two ADCs, are modelled as measurements at several frequencies, with linear interpolation. The values already in the calibration file when the instrument was delivered from the manufacturer have been used in all this work.

The instrument's specification gives an operating temperature range of 0 °C to 55 °C, and timebase relative accuracy of 10^{-4}. The accuracy of capacitance measurements is expressed as the maximum error for the case of the internal 200 V voltage source with 'optimal' choice of feedback components and a stipulated maximum hum-current. For capacitance C' the claimed error is $0.5\% + 1\,\mathrm{pF}$. For $\tan\delta$ across the range of frequency and measured capacitance. $1\% + 3\times10^{-4}$ and $2\% + 2\times10^{-3}$

Accuracy of absolute values is certainly desirable for permitting comparisons of measurements made with different instruments; the consistency of relative values, however, is much more important in this work where one instrument will be used and where there is interest in the very small changes in the measured capacitance and loss due to PD activity.

9.2 Computer control

The IDAX 300 is connected to the control computer by USB, using serial-emulation to appear as a serial-port device. Purely text-based communication is used to send commands, retrieve the measurement data, and transfer calibration data back and forth. The program that is provided with the IDAX for running on the control computer was unsuitable for this work: it runs only on a type of operating system that we have learnt to avoid, it has no means of being combined with other programs to coordinate DS and PD measurements in a loop, and it automates more of the settings such as feedback than seems desirable for this work. A control program was written using the Instrument Control Toolbox of the proprietary numerical-computing program 'Matlab' to provide the functions for serial communication. This could easily have been achieved in for example GNU Octave, but it was considered important that future users would be working in an environment already familiar to them.

There are of the order of a hundred commands that can be sent to the instrument for setting the voltage amplitude and frequency, setting feedback components and the 'termination' settings for UST or GST measurements, transferring calibration data, checking on a running measurement, and retrieving results. These commands, like all the details of the IDAX instrument other than the use of its supplied GUI control program, were undocumented. Some 'reverse engineering' was needed in order to deduce suitable commands to set up the output voltage, relay settings and feedback, and the request the results and convert them into physical values at the test-object. This was done by studying logs of the communications between the IDAX and its supplied GUI program, and by obtaining and reading some of the program-code used in those components, followed by a good deal of testing. Many sets of commands, such as those sent during initialisation or for setting the voltage sources, have simply

been accepted as blocks of 'recipe-book' programming, with no convenient way of determining what the individual commands do.

Functions have been written to do all the main tasks of connecting, calculating suitable feedback, setting up, starting a measurement, getting the results and converting them to physical parameters. To make a measurement, a script is run that calls the appropriate functions; for simple measurements only a very few lines of code are needed in this script. Many variations have been used for running tests and measurements with the IDAX on different types of test-object and in combination with other instruments such as the PD-pulse measurement instrument or function-generators and oscilloscopes. All raw results as well as derived results and time information are stored in a variable that is saved at the end of a sweep. The text displayed on screen during the sweep is logged continuously, and a copy of the script is saved before each sweep. This level of detail has several times been useful when investigating apparent problems with data.

9.3 Automatic selection of feedback-component values

The choice of suitable feedback components for an electrometer has been partially covered in section 6.2.6. Many factors must be considered. The feedback current should be always mainly in the resistor or mainly in the capacitor. A very low-capacitance object at low frequency may have such high impedance that even the highest-value available feedback resistance (apart from the open circuit option) would give unacceptably low electrometer output voltage; capacitive feedback is needed in this case. A very high-capacitance object may have such low impedance that even the largest feedback capacitor would require electrometer output voltages higher than the electrometer's range; resistive feedback is needed in this case. An object with considerable conductance may require resistive feedback in the low-frequency range where the long times allow large charges to flow. To make sure that the electrometer output voltage will not hit its limits, the feedback components must be chosen based on several matters other than the test-object and the applied signal. Electric or magnetic fields, and extraneous currents sharing part of the measurement circuit, may introduce hum currents in the measurement circuit, typically at the electricity-supply frequency. There may be a dc component in the input current or from the electrometer output, which would cause a ramping voltage with capacitive feedback or a constant extra voltage with resistive feedback. Any slow-decaying offset in the electrometer output, due to the use of nearly pure capacitive feedback together with a significantly conductive test-object, would shift the electrometer voltage closer to one of its limits.

The GUI program supplied with the IDAX does a lot of work measuring interference from hum and dc, assessing the test-object, using rules to determine feedback components, and revising the choice if any overload is detected; this makes the instrument suitable for automatic measurements on a range of HV components.

In this work and for later users of the IDAX in the lab it was thought better to involve the user more in the decision. Each measurement is made

from a program script [s.A.3.3], which makes it possible for the user to specify arbitrary rules for feedback based on knowledge of the test object and its possible nonlinear or pulsed behaviour. It might for example be that changes between capacitive and resistive feedback should be avoided, or that any big changes in CFBR should happen at the same frequency within each of several sweeps at different voltage amplitudes.

For awkward test-objects such as samples of highly nonlinear resistive material, the feedback was set in the script, using a material model to predict the current, then using the feedback resistor of resistance one decade lower than was calculated, to give a wide safety margin. For simpler objects, a function was written to automate choice of feedback components based on frequency, the expected complex-capacitance of the test-object, a preferred CFBR, and the maximum desired electrometer output voltage. The dominant type of feedback component was chosen to ensure the maximum electrometer voltage would not be exceeed. The other component was then set to whatever came closest to the requested CFBR. Practically all the measurements have actually been made with strongly resistive CFBR, around 1% or less.

Some simplifying features in most of this work are that: the problems of hum and dc currents are less in laboratory than in industrial environments; the resolution of the IDAX's ADCs makes it usually quite acceptable to fall even to 1/100 of the maximum possible electrometer output voltage, so a large margin of safety can be left to avoid electrometer overloads in difficult cases involving interference, pulses, or nonlinear test-objects.

9.4 Alternative types of instrument

Data-acquisition (DAQ) hardware can provide multiple digital and analogue interfaces between a computer and other equipment. The sample-rates and precisions now available would easily match those of the IDAX's DAC and ADCs at a much lower price than a specialised instrument, and would allow full time-domain waveforms to be recorded and arbitrary voltage signals to be generated. This, however, is only a part of the instrument's function. At least one electrometer is essential for measuring the tiny currents of subpicoamp levels, even if the output voltage can be measured directly from a divider. Electrometers of this specification are not cheap, and they require a set of well-defined feedback components with computer-controlled switching. The sensitive components must be protected against the high currents and overvoltages that can result from for example a short-circuit in the test-object, but the protective devices must avoid disturbing the tiny current of normal measurements; some of the earlier work on protection is described in [Wer01a, p.41]. Calibration is needed for the amplitude and phase responses of several of the components in the signal path, as well as of feedback-component values. Having all these features already combined and tested in a compact instrument is thus worth a lot more than just the analogue/digital interface properties. It would nevertheless be worthwhile to consider the alternatives carefully in any future measurement system, particularly if wanting more versatile control of the output signal or of the detail of recorded results.

Chapter 10

The PD pulse-measurement instrument

This chapter describes the operation and specification of the PD instrument used in this work, and the programs that were written to control it. As with the DS instrument in chapter 9, these details are of relevance when considering how to combine the DS and PD instruments and when analysing results. More of the detail of the PD instrument is already documented, so this chapter is mainly a summary. Some tests of the instrument are described in chapter 13, to determine undocumented details and assess the reliability of results.

10.1 Description of the ICM components

A commercially available instrument designed for use according to IEC-60270 has been used for the PD pulse-measurements reported in this work. This is the ICM-system, from Power Diagnostix Systems GmbH of Aachen, Germany, shown in figure 10.1 together with its preamplifier. A diagram of the basic connections is shown in figure 10.2, using the same physical layout. The choice

FIGURE 10.1: The ICM PD-pulse measurement instrument: the main unit is in the background, with its input connected to a preamplifier in the foreground.

was partly due to this type of instrument having been shown in the earlier work of [Edi01] to work for PD measurements at very low frequencies. An ICM of model version 7.60 was bought in 2007, supplementing the existing one of model version 2.00. The newer version had some differences from the old one, and some differences from its manual; various problems had to be worked around.

The ICM's main unit is a chassis containing modules that provide amplification, registration of PD pattern, and communication with a controlling computer. Some preamplification and buffering functions are done in external

boxes to allow these functions to be nearer to the signal source. The ICM is connected to the control computer by GPIB (general-purpose interface bus, IEEE-488). The control computer sends text-based commands to control all the settings, start acquisitions and request results.

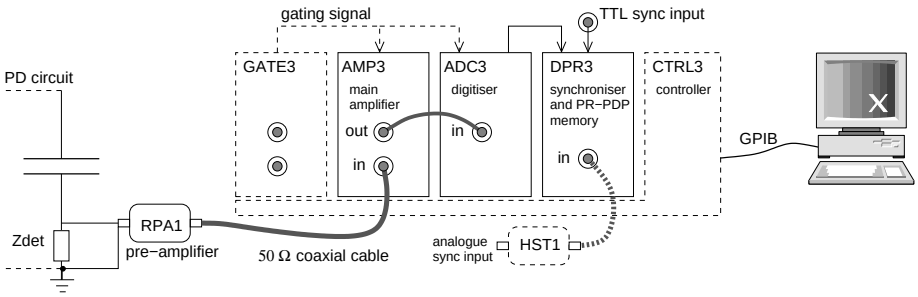

FIGURE 10.2: The ICM PD-instrument's main components. Gating has not been used in this work. The controller module communicates with all the others.

10.1.1 Preamplifier

The signal from a PD source reaches the ICM through a preamplifier. Several interchangeable preamplifiers are available to provide extra features such as optical isolation, ultrasonic transduction, or translation of higher frequency-bands down to the 40 kHz to 800 kHz band treated by the ICM.

The RPA1 preamplifier has been used in all the work here. It has the simple function of providing the first band-pass filtering and amplification of the PD signal, buffering the possibly long signal cable from the PD source so that the cable does not affect the effective detection impedance. Its BNC input-connector has a loading of 10 kΩ and 50 pF. Its BNC output-connector connects to the main-amplifier through a 50 Ω coaxial cable whose length can exceed even 40 m if low-loss cable is used. The main amplifier provides a dc voltage to power the preamplifier and to set its gain to the available multipliers of 1, 10 or 100. The PD signal from the preamplifier is superimposed on the same cable, and is ac-coupled into the main amplifier. The 6 dB (impedance) bandwidth is fixed at 20 kHz to 1.0 MHz, a little wider than the system's widest bandwidth, with a roll-off of 40 dB/decade.

10.1.2 Main amplifier

The main-amplifier is the AMP3 module in the ICM. The input BNC connector has input impedance of 50 Ω to ac signals, and provides a superimposed dc voltage to power the preamplifier unit and control its gain. Its nominal gains are all the products of a multiplier (1,2,4,8) and scaling (1,10,100). Its lower −3 dB cut-off frequency f_1 can be selected as $40, 80, 100$ kHz, and its upper cut-off frequency f_2 as $250, 600, 800$ kHz.

The AMP3 module also contains a peak-meter (sometimes called a 'charge' or 'picocoulomb' meter as the voltage peaks are supposed to relate to apparent charge). This measures the magnitude, ignoring polarity, of the output signal, quantising the 0 V to 5 V range linearly into 12 bit resolution. The peak-meter

charging time is quoted as 0.5 µs, suggesting that the recorded value reflects an average over this time. The value returned when the peak-meter is read seems to update only every half second or so, suggesting that it is the highest value in the last such period. Constant display of the peak reading is interesting when watching an ongoing measurement or when trying to reduce noise sources, but the only PD results shown for real test-objects in this work have come from the later ADC3 quantiser module that forms the PD pattern.

The normal output voltage range of the AMP3 should be ± 5 V, to be within the limits of the ADC3 conversion module and of the AMP3's own peak-meter. The actual output voltage can be considerably more: over +10 V has been observed on an oscilloscope during tests of extreme inputs and settings.

10.1.3 Digitiser

The ADC3 module contains the *ADC* (analogue-digital converter) that is used in producing the phase-resolved PD pattern [s.8.2.4]. The signal-flow diagram of figure 10.3 shows the main functions of this module in three stages.

The first part, 'acquisition logic', decides when the input signal should be sent for quantisation in the following ADC. This is actually rather complex: it is simplified in the diagram partly because the abstraction provides sufficient information and partly because we do not have much more detail than this about the inner workings. The *LLD* (low-level discriminator, or *threshold*) sets a lower limit to the voltage magnitude that must be present to cause any measurement at all; this is used to avoid measuring background noise. The choice of *first-peak* or *time-window*, along with a *deadtime*, determines how multiple peaks should be treated. With first-peak, a peak exceeding the LLD level will be sent for conversion in the ADC, then no further peak will be recorded for the deadtime, which can be set from 5 µs to 3 ms; the purpose of the deadtime is to avoid acquisition of subsequent peaks of the oscillatory voltage that a pulse input to the amplifier causes on the amplifier's output. With time-window, the deadtime defines a period over which the greatest positive and greatest negative peak are held, and the greater of these values is then converted. In this work the first-peak setting was used, with a deadtime as small as possible while not seeing signs of acquiring reverse-polarity peaks.

The ADC quantises voltages in a ±5 V range into 2^{12} (4096) digital levels, with a 0.5 µs conversion time. Only 2^8 (256) levels are used in the phase-resolved PD pattern, so the 2048 levels have to be mapped onto 256 charge-levels; several mappings, referred to as the ADC *characteristics*, are available for making the best use of the 256 charge-levels for different applications. The linear bipolar characteristic is the most obvious, mapping each group of 16 values of ADC output into a single one of the PD pattern charge-channels. For cases where the input's polarity is not important, the linear unipolar characteristic doubles the magnitude-resolution by neglecting the pulse polarity. Other options involve nonlinear mappings with a logarithmic or sine relation to enhance the resolution towards one end of the magnitude scale. In this work linear bipolar has been used, as we are always dealing with bipolar signals and no great advantage was seen in the nonlinear mappings.

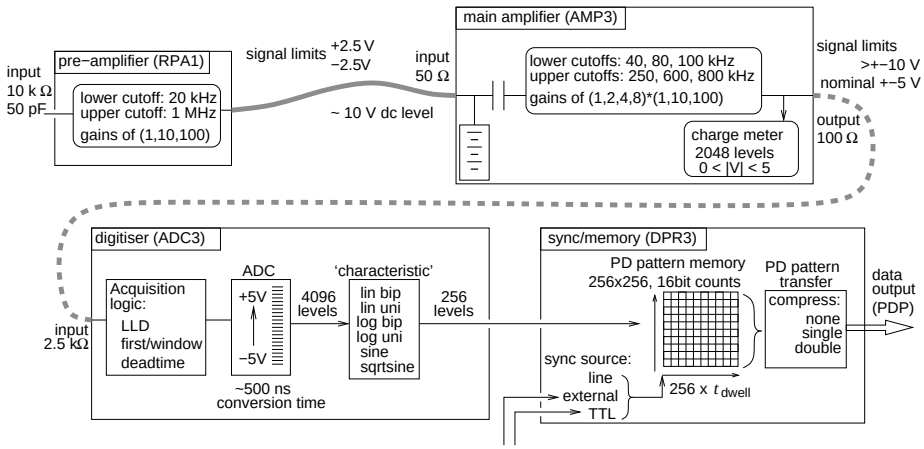

FIGURE 10.3: Signal flow and limits in the ICM, based on measurements and the manual.

10.1.4 Synchroniser and PD memory

The DPR3 'dual-port RAM' and synchronisation module increments a count in the respective magnitude/phase point in the PR-PDP for each pulse measured by the ADC3 module. The correct one of the 256 magnitude channels is already determined by the ADC3, but the DPR3 has to determine which of the 256 phase channels should be used.

Before an acquisition is started, two relevant parameters must be set. One is the *acquisition mode*, which specifies either the *single* mode in which one pass is made across all the phase channels dwelling on each for a constant time, or the *repetition* mode in which multiple passes are made across the phase channels, returning to the first phase channel each time a synchronising event occurs. The other is the *dwelltime*, which is the time to spend on each phase-channel before moving to the next: it can be set directly by specifying a time, or else the ICM can be asked to calculate the dwelltime. In single mode the calculation is just the total acquisition time divided by the number of phase-channels, but in repetition mode the ICM must be able to detect the frequency of the synchronising event before performing the dwelltime calculation. The ICM only reliably measures frequencies in the range 30 to 400 Hz; it apparently uses a PLL (phase-locked loop) that cannot reliably lock to other frequencies, but has been seen to track up to higher frequencies rather over 1 kHz as long as the frequency changes from a permitted value in quite small increments so as not to lose lock. Therefore, for the lower frequencies of main interest in this work, the frequency-detection and automatic calculation of dwelltime cannot be used, and the direct setting of dwelltime is needed. The command to calculate dwelltime automatically has to be used anyway as it has other effects of 'resetting' the acquisition hardware, but the desired dwelltime is then set from the control computer.

The source of the synchronising events can be set to the *line* (mains supply to the instrument), or to an *external* signal. (This is just like an oscilloscope's time-base, but the term 'trigger' is deliberately avoided in this description of the ICM

so as not to confuse these 'synchronising events' with the trigger command that starts an acquisition.) The front-panel input of the DPR3 can be connected to a HST1 'voltage measurement' box, which provides a high-impedance input for measuring an analogue signal of peak ±2 V (100 kΩ 200 pF) or ±200 V (10 MΩ 200 pF). The HST1 converts the input voltage to a current-signal going back to the DPR3 input; this BNC input terminal has its sheath isolated from the ICM's chassis, to prevent earth-loops in the voltage and PD-pulse measurement cables, and it provides a voltage source to power the HST1. When the synchronising source is set external, this analogue input is used if an HST1 is connected to the DPR3; if no HST1 is connected, the TTL input on the ICM's back-panel is used instead.

10.1.5 Gate

The gate module, GATE3, was not used in this work: there was no obvious occasional interference to protect against, and there was a desire to miss as little signal as possible. Its input stage is just like the AMP3 in specification and in how it is controlled; it likewise uses a preamplifier such as RPA1. Its output is deceptively different from the AMP3, being the TTL [s.†] logic signal that the GATE3 also sends internally to the AMP3 and ADC3 modules. The gating signal can be used for either or both functions of turning off the AMP3 output or blocking the ADC3 from sending digitised data to the DPR3.

10.1.6 Controller

The controller has a switch to allow the GPIB device-number to be set, and has a serial (RS232) port as a slow alternative to GPIB. It permits commands from the control computer to change and query the settings in all the other modules. The settings when the ICM is powered on are not set to any guaranteed values, so the control computer must make all the relevant settings. There are several ways of transferring the PR-PDP from the DRP3 module to the control computer, discussed further in section 13.2.

10.1.7 Calibrator

A calibrator is an important part of a PD measurement system, being the only part that makes different measurements directly comparable. The calibrator used in this work was the CAL1D model from the ICM family. It can produce charges of 10, 20, 50, 100, 200, 500 or 1000 pC, by stepping a controlled voltage behind a fixed internal series capacitor specified as < 10 pF. It synchronises either to a flickering ambient light-source or, if this cannot be found, to an internal crystal-based oscillator scaled to a 50 Hz output. One pulse is given per cycle. Other calibrators in the CAL1 model range include units with series capacitors a factor of 10 smaller or larger, with correspondingly changed charges, and a unit with very fast pulses, $t_r < 300$ ps, for UHF applications. The CAL1D specification does not explicitly mention rise-time, but claims conformance to IEC-60270 [C270]. That standard requires that the rise-time t_r be $t_r < 60$ ns in any case, and also $t_r < 0.03/f_2$ for wide-band instruments where the upper frequency limit f_2 is over 500 kHz. The ICM system has a maximum setting of $f_2 = 800$ kHz, corresponding to $t_r < 37$ ns. The rise-time of the CAL1D is in

fact considerably quicker than this, unless limited by the external circuit, as has been seen in tests of the calibrator's output current reported in section 13.8.

10.2 Computer control

The ICM's settings cannot be adjusted on the instrument itself, so all control must be done through the GPIB connection from the computer. A GUI (graphical user interface) program is provided with the ICM. This was good for running single measurements and getting used to the instrument, although with the problem that it worked only on one family of operating system. However, as is common with proprietary GUI programs, it was not suitable for the required behaviour of making multiple measurements automatically and cooperating with other instruments.

A control program was written as a set of Matlab functions, to set all relevant parameters before a measurement then to trigger an acquisition and retrieve the phase-resolved PD pattern. Tests were made to check that the control programs gave the expected results, and to determine undocumented details necessary for low-frequency measurements and synchronised operation with the IDAX. The results are described in chapter 13.

The supplied manual (rev. 3.03E) documents all the commands and their responses, as well as the format of the data files written by the GUI program. There are several significant errors in the manual, and some lacks of clarity: several of the numeric codes for setting ADC 'characteristics' are mixed up; the output files actually contain an undocumented version-number string before the other data; the response to the 'get status' (running or not) query *is* actually followed by a newline character; the words 'integer' and 'floating point' are used to describe responses that are in fact such numbers as ASCII strings; 'precision' is used in the sense of decimal places rather than significant figures.

10.3 Alternative types of instrument

The ICM has quite limited dynamic range, so that even for a single large cavity, and particularly for a range of cavities in machine insulation, there is a compromise between losing small pulses and saturating on large ones. The ICM's PD pattern and limited transfer speed also make full 'pulse sequence analysis' impossible except at very low frequency; the pulses from multiple cycles are combined in one phase-channel, or else must be captured with lower phase-resolution if using 'single' (against time) rather than 'repetitive' (against phase) mode. The shape of a PD is in any case lost, due to the low bandwidth of this type of measurement. The measurement of something as simple as positive or negative peaks can have errors of some 10% even after removal of a dc offset.

The use of an oscilloscope with programmable logic to store and transfer just the time-points around the occurrence of pulses on a detection impedance would have been one way to avoid an expensive application-specific instrument by using a general-purpose, well-documented instrument with the potential to capture more detailed information about each pulse and the sequence of pulses. Numerical integration of the waveform would allow charge-measurement. Some preamplification may still have been needed. The key point in this case would

be to program such an oscilloscope to store just the points around identified pulses, so as to reduce the required data transfers to the control computer to a manageable amount. If the shape of PD pulses can be accepted as unimportant, then filtering to the type of bandwidth used for IEC-60270 measurements could provide a slow enough signal for capture at the typical megahertz or tens of megahertz sample rate of data acquisition cards.

In view of the rapidly increasing ability and decreasing cost of general-purpose ADCs, such as *DAQs* (data-acquisition) from hundreds of kilohertz to tens of megahertz and *digitisers* from hundreds of megahertz up to some gigahertz, there seems an ever decreasing advantage to specialised measurement hardware with its high cost and limited, little-documented abilities. In industrial situations the single compact unit and the guarantee of conformance to the relevant standards gives a lot of extra value, but in a research environment there is more value in the ability to make changes and to measure finer details.

Chapter 11

Conjectured advantages of the new methods

In this chapter some threads of the earlier 'background' chapters are pulled together to make an argument for what improvements in diagnostic methods for stator insulation may be possible from the types of measurement that this project set out to investigate. The later chapters then investigate how the measurements can be made, limitations of the methods, and how to present and analyse the results.

11.1 Differences from conventional measurements

This project started with the quite open task of investigating what improvements of diagnostic information about stator insulation could be gained by combinations of two measurement methods that had been investigated for other purposes in previous projects in the department:

Frequency-domain DS at varied high voltage (HV-FDDS).

Variable-frequency phase-resolved PD analysis (VF-PRPDA).

HV-FDDS had been shown to be of use in diagnosing the condition of water-treed XLPE cables. Even just at low voltage, FDDS had been applied to transformers and paper-insulated cables with good results. It was natural to turn to the other major type of large HV insulation system and consider what might be done there.

VF-PRPDA had been investigated [Edi01] mainly with a pure interest in frequency dependence of PD, which continued in a further project [For08a]. The method was also applied to some stator bars in [Edi01]. Stator insulation is in a way an obvious choice for studies of PD-based diagnostic methods, since PD is always to be found there; in another way, it is a difficult area for developing useful diagnostic methods, since so many PD sources can be present at once, and so many sources can be tolerated without need of maintenance.

Both HV-FDDS and VF-PRPDA would extend the common C-$\tan\delta$ and PD measurements to a range of frequencies. It was hoped that the variation of frequency would provide useful additional information about the insulation. If frequency could be kept in ranges well below power frequency, further advantages could be gained by being able to use a low-power supply, giving small size, easy transportation, and less damage in the event of a breakdown in the test-object.

Since both methods involve the same sweep over multiple amplitudes and frequencies, there is an advantage in time if the two measurements are made simultaneously. Comparisons of the measurements are also facilitated by knowing that they are different views of the same events.

Some other features of DS measurement, started on in [Edi01], were also to be considered for application to stator insulation:

Use of harmonic as well as fundamental currents.

Intentional measurement of PD current in the DS measurement.

The harmonics from 1 to 8 were recorded even by the earlier DS instrument that was in use at the time that this project started. They enable a good approximation of the mean time-domain waveform to be made. This in itself is not very special, since much the same should be possible by time-domain averaging of waveforms. The frequency-domain view is, however, a way to distinguish very sensitively certain features of the current. The results of small nonlinearities that would be indistinguishable from sinusoidal when viewed as time-waveforms can be seen separately from the fundamental-frequency sinusoid. Currents from polarity-asymmetric sources will be the only even-harmonic components. Distinctions of sine and cosine parts in the Fourier series permit further separation of different types of sources. Analysis of the harmonics may therefore permit different sources of current to be distinguished.

DS measurements, on canonical laboratory objects, had been shown to have good correspondence to PD pulse measurements. By including the harmonics from DS, an approximation of the phase-distribution of PD charge could be obtained. Like the measurement of PD by the C-$\tan\delta$ method, the details of individual pulses are lost, so a few large pulses or many small pulses are not distinguished. Unlike that method, the shape of the phase-distribution is available. It was thought that there may be a case for letting the PD measurement be done by the DS instrument.

11.2 Evolution of the aim

From the aims in the initial project plans, plenty of changes happened as new information came to light when getting familiar with the subject, making investigations in the laboratory, going through the literature, and doing field-measurements.

The first thoughts about the grading on the end-windings were that this would be a source of PD at low frequencies where the earth potential of the core would extend over the whole grading length. Perhaps this 'PD inception frequency' would allow assessment of the stress-grading condition. It was soon seen that this does not happen easily, and even at millihertz frequencies PD was not readily detected around a highly stressed grading. The many other likely PD sources in a full stator winding would probably hide any such effect. The surface PD from worn stress-grading is not a very dangerous situation anyway, and visual inspections would have a good chance of revealing a problem before a time of danger.

Field-measurements [Tay06] made it very clear how expensive it is to waste time by tying up a machine on having measurements performed: it is either avoiding useful service, or delaying having maintenance personnel work on it. The use of very low frequencies, below about 10 mHz and certainly below 1 mHz, is therefore quite impractical, particularly if several voltage amplitudes are to be

used and measurements are to be made on all phases separately and together. On the other hand, the time-constraints increase the benefit of simultaneous measurement, even for for the conventional power-frequency measurement of C-tan δ and PRPD.

Some features of PD pulse-measurement, such as the widespread interest in maximum charge rather than just a mean charge, suggest that PD pulse measurement is not easily discarded: the distinction between large and small pulses is often considered important. Combined use of DS and PD, rather than replacement of PD pulse measurement, appears the better option.

One line of thought about what to look for with the proposed methods was that one should try to measure the properties of the solid insulation. This idea arises easily from the laboratory uses of DS, and from the success of HV-FDDS in assessing changes within the bulk material of cable insulation. A low-voltage measurement would avoid PD and reduce the effects of stress-grading, but would not enable study of the sort of voltage-dependence that had been shown to be useful with cable diagnostics. High voltage would result in additional currents due to PD and to the stress-grading, much more significant than these effects in cables. If simultaneous PD and DS measurements of PD charge did indeed measure the same thing, the results of PD measurement could be used to remove the PD current from the DS results. If the currents due to the end-winding stress-grading could be calculated, they could also be removed, to leave the DS results for the insulation material alone.

It was again soon clear that this would get nowhere. Variation of the bulk insulation material's capacitance with amplitude and frequency is small compared to the contributions from these disturbing sources. The PD and DS measurements can differ a lot in the charge they measure for a whole stator, due to high repetition rates, dead-times in measurement, limited dynamic range, and the impossibility of good calibration of PD in a stator winding. The stress-grading of an arbitrary machine cannot be modelled so well as to remove its effect from sensitive measurements. These points are clearly shown by results in later chapters.

The observed differences in PD charge measured by PD pulse and DS methods suggested that instead of subtracting one from the other, both could be considered as complementary measurements. Measurement of PD by DS provides the magnitude and phase-distribution of the whole PD charge, without the problems of calibrating pulse-measurement and distinguishing separate pulses; this nevertheless requires that the other currents in DS can be estimated and removed, since the PD current is much smaller than the current in the bulk insulation and may be smaller too than the contribution of end-winding stress-grading. Measurement of PD by a PD pulse method provides both the phase and amplitude distribution of individual pulses The amplitude distribution is however a vague concept in a stator winding, since similar PD events give different measured results depending on their location; the distinction between many small and few large pulses is the main virtue of the amplitude distribution in the PDP.

Correct removal of the DS current due to the bulk insulation is critical to

measurement of the much smaller PD charge. If it is reasonable to regard the insulation material as strongly linear, and the effects of stress-grading and PD as the main nonlinearities, it could be useful to ignore the fundamental-frequency component, working with just the harmonics so as to give the highly nonlinear PD a signal-to-noise advantage. It was wondered whether a good estimate of the fundamental frequency could be obtained from the harmonics, by 'physical' consideration of the range of plausible waveforms: for example, multiple zero-crossings or highly oscillatory waveforms are unlikely to result from the type of nonlinearity expected from PD and stress-grading.

The pure frequency-dependence of different PD sources is of distinct interest, as a more direct continuation of [Edi01]. One reason that it has not been studied in detail in this project is that it was already close to the subject of parallel projects. Another reason is the need for some test-objects to allow tests of the behaviour of different types of defect in real stator insulation. This would be similar to the work reported in [Hud05], but with variable frequency measurements. There would have been little chance to cover any other aspects of this project.

11.3 Matters for investigation

From the developmental process summarised in the previous sections, several points emerge for further study, which is conducted in the later chapters.

> How well do the instruments make the measurements: does the DS measurement allow the PD charge to be measured, and give consistent enough results even with different feedback components to allow subtraction of the current due to the object's linear capacitance?
>
> How can the extra data be presented?
>
> What are the relations of PD measurement by DS and PD pulse methods, on varied objects from simple laboratory objects to stator bars and windings?
>
> What effect does the end-winding stress-grading have in real bars rather than on the simple PTFE constructions studied before? The variations in materials and construction are important here, but are difficult to obtain as there are so many different types.

Chapter 12

Tests of the DS instrument

The IDAX DS instrument described in chapter 9 was tested in several ways. One purpose was to check that it worked correctly with the new control-programs. The other main purpose was to document aspects of the instrument's behaviour that are important for the combined DS and PD-pulse measurement system, and for measurement of the charge from PD pulses with the DS instrument. These uses have different demands from the usual industrial DS measurements. Some of the results are summarised in this chapter. The tests of measurement of pulsed current are presented in chapter 14.

12.1 Correctness of calculation of voltage and current

Working back from DFT results to the voltage and current at the actual test-object requires many steps: the calibration data and frequency are used to calculate the feedback component values and the scaling and phase-shift of signals through converters, amplifiers and dividers; inidealities in the electrometers and in the measurement circuit are also allowed for. It was assumed that at least the values of C' and C'' given by the GUI program supplied with the IDAX could be taken as the correct value of a measurement. The results from the GUI program were compared with the results from the new programs: the GUI program was set to do a measurement for just one second, so that just one set of DFT results would be transferred; the output data-file written by the program was then read to find the calculated voltage and current at the test object; a serial-log that had been made of all the communication with the instrument was parsed to extract the raw DFT data, which was then passed through the newly written programs to obtain their calculation based on exactly the same data.

This was done for varied termination settings (UST and both forms of GST) and sources (external HVU, internal 10 V and 200 V). The test-object was a PD coupling capacitor with capacitance a little over 1 nF and loss tangent about 10^{-3}. Measurements were made at 60 Hz, high enough to give significant phase-shifts needing compensation from the calibration data. The values of C' and C'' agreed in all cases to at least 3 significant figures, even with C'' down in the picofarad region. The agreement in C' was several significant-figures more when using the internal sources, although comparison of the voltage and current suggested the difference to be mainly in the current, not in the voltage as had been expected from the consideration that voltage-measurement of the external source relies on calculations based on a reference capacitor and a further electrometer. Harmonics in the current agreed to at least four significant figures. Comparison of harmonics in the voltage was not done: the GUI program itself had an obvious error in its recording of harmonic voltages, apparently applying the calculation for the nth harmonic to the data from the $(n-1)$th harmonic.

Comparison of the harmonics in the current and voltage recorded by the new program showed the expected correspondence for a linear test-object.

All the observed differences were considered to be practically unimportant. It would, however, have been good to have done tests at some other frequencies.

12.2 Output voltage starting and stopping phase

The consistency of what the output voltage does at turn-on, turn-off and changes of amplitude or frequency, is important when considering the choice of feedback components or the combined use of the DS and PD-pulse measurement instruments. The output voltage is only able to be sinusoidal, with specified amplitude and frequency. When turned on it starts always at a negative zero-crossing. The point in a cycle at which the output voltage stops after being turned off is less consistent. If a different frequency is set while the output voltage is on, the change happens at a peak. In this work the voltage has been turned off and on again for each new frequency or amplitude. This takes rather longer for a sweep over multiple points, but it simplifies the program and the simultaneous use of the PD pulse-measurement instrument.

12.3 Steps in output voltage

With resistive feedback chosen to keep the electrometer output voltage in the range 0.5 V to 5 V for the ideal sinusoidal applied voltage, measurements on capacitive objects using the HVU at 100 V and down to 0.1 mHz were found not to have the electrometer overloads that would be expected if the output voltage were changing sharply between the 160 quantisation levels expected at each polarity, this suggests that extra filtering, varied to match the requested frequency, is in use, as was described for an earlier 12-bit DAC in [Wer01a].

To check the smoothness of the output voltage, the HVU was used with output amplitude set to just 15 V, giving about 24 DAC levels at each polarity. This voltage was fed directly into a digital oscilloscope from which a waveform of 10 000 samples taken over 400 ms was transferred approximately once per second during a single 1 mHz cycle. In figure 12.1 the measured points are plotted along with points at the same time-points following a sinusoid of the same magnitude but with rounding to just 24 levels of each polarity, as would be expected if synthesising such a low-amplitude voltage directly from a 16-bit DAC. Occasional delays with communication have resulted in some of the delays between time-points being longer than others.

The output voltage is clearly very smooth compared to the pure digital levels, confirming the presence of extra filtering. The potential problem of steps in the output voltage can therefore safely be ignored when calculating feedback.

12.4 Interference frequency

Currents at the mains frequency of about 50 Hz get induced in any measurement circuit; these are *hum* currents. An indication of the size of these currents was seen for a simple circuit on a lab bench. Frequencies around 50 Hz were measured on the IDAX, using the LV source but without any connection from source output to measurement input. The full range of feedback resistors was

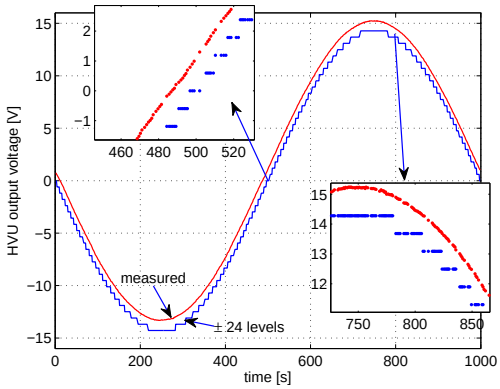

FIGURE 12.1: Measured HVU output voltages (smoother curve) throughout a 1 mHz cycle at 15 V peak; at this voltage a plain 16-bit DAC would be expected to give only about 48 different levels, which would give results like the stepped curve. The slight offset in the measurement has the advantage of making the curves clearer to compare!

used, changing by two at a time. The most extreme resistors gave a lot of noise: the highest resistance caused electrometer overload, and the lowest resistance gave too little signal for a good result. The other resistors gave quite similar results, suggesting about 2 nA of hum current; two cases are shown in figure 12.2.

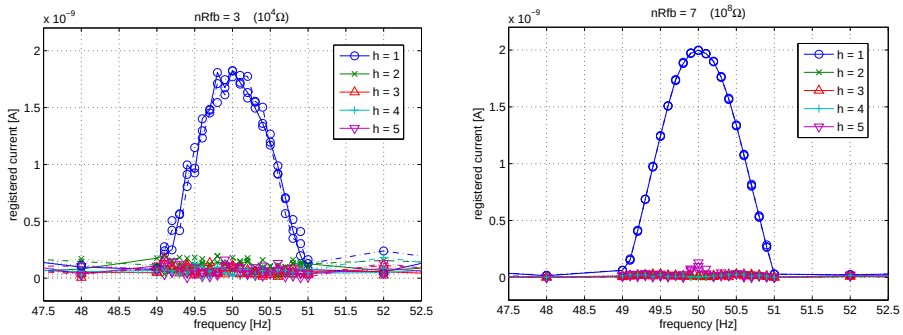

FIGURE 12.2: Mains interference (hum) when measuring without a test object. Results are shown for two values of feedback resistor: 10 kΩ on the left and 100 MΩ on the right. The harmonic order h is shown by the marker. The same sweep was made three times; these are distinguished by the solid, dashed and dotted lines joining the markers.

The hum current can be expected to vary with the measurement circuit and its environment. With large hum and small measured current such as for a capacitive object at very low frequency, the hum may be the determining factor for the choice of feedback. It is good in any case to avoid including 50 Hz in sweeps; this point usually has some visible noise, as can be seen in figure 12.6. The frequent choice of 60 Hz for single-point 'mains-like' measurements such as in the tests of pulse-measurement was motivated by mains interference.

A greater importance of the hum is when studying the harmonics. A measurement at 16.66 Hz will measure third harmonics at 50 Hz; the harmonics are typically only a small proportion of the fundamental, so are much more easily affected. It is therefore desirable to choose fundamental frequencies that keep the significant low harmonics away from the interference frequency.

12.5 Variation of results with feedback-component

In results obtained from the older model of DS instrument, which was used in earlier work, there were sometimes clear jumps in C' and C'' at certain frequencies. These were assumed to be due to changes in feedback components. Slight errors in the calibrated value of the feedback component could explain this, as could slight errors in other aspects of the calculation of test-object voltage and current if these errors vary with the voltage at the electrometer output or input or on whether the feedback is capacitive or resistive. In this work the accuracy of measurements in relation to standard physical measures is of little importance. The consistency of measurements is much more important: for measuring PD currents an initial measurement is needed below the PD inception level, and the small difference between a higher-voltage measurement and the proportionally scaled current from the PD-free measurement is taken as the PD current.

Some tests were made to compare results obtained with several different choices of feedback component, on both electrometers, during measurements with the HVU as the voltage source. The CFBR was much less than 1% away from either 0 or 1 in each case. Capacitive feedback was found not even to work on the voltage electrometer; it became overloaded very soon without strong resistive feedback, indicating a source of dc current. Since the input is from a gas capacitor it seems likely that the source of the dc current must be an extraneous one or the offset current of the electrometer itself. It should be noted that only the newly written control programs were used here: it is not certain that the GUI program supplied with the IDAX would give quite the same results.

The test-object was a PD coupling-capacitor of about 1 nF with a loss tangent of about 10^{-3}. For each of several fixed settings of feedback components on the two electrometers, the voltage was applied and five consecutive measurements were taken without interruption of the voltage. The results for complex capacitance are shown in figure 12.3, plotted against the time-order of the repeated measurements to make clear how consistent the differences due to feedback settings are. At the lowest frequency there is only a single cycle per measurement, so results are noisier and take a few cycles to settle.

These results suggest that changes between capacitive and resistive feedback are likely to cause significant jumps in measured values. Resistive feedback gave the apparently better result, in that the loss was never negative. The variations due to feedback components being changed to adjacent ones, of ten times higher or lower value, were small in all cases, in spite of the large changes in electrometer voltage with the different components. With the amplitudes, frequencies, and sizes of test-object considered in most of this work, it should be possible to keep

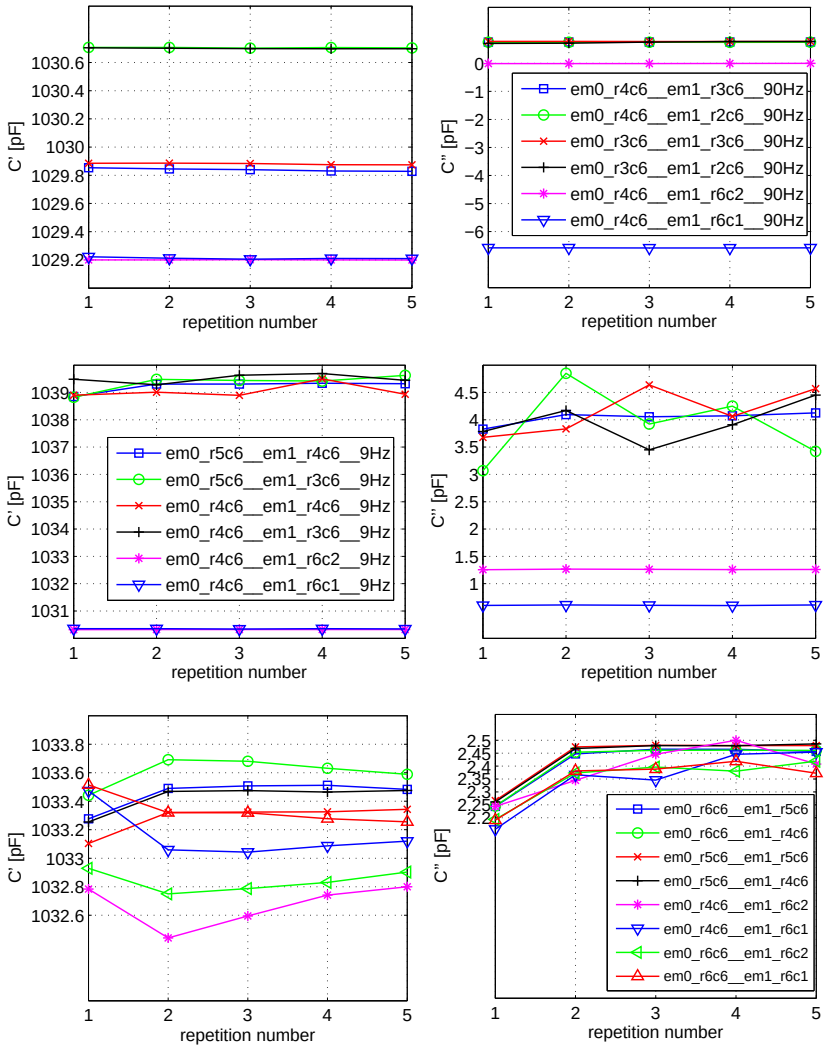

FIGURE 12.3: Variation of results with IDAX feedback components: C' (left) and C'' (right) on a $\simeq 1\,\mathrm{nF}$ capacitor, at amplitude of 1 kV and frequencies of 90 Hz (top), 9 Hz (middle) and 0.9 Hz (bottom). The keys to the curves show the selected 'r' and 'c' feedback component numbers (see table 9.1) for the voltage and current electrometers 'em0' and 'em1'.

to dominantly resistive feedback. The results became noticeably noisy with electrometer output voltage below a value somewhere from 50 mV to 70 mV.

12.6 Consistency between measurements

The consistency of results between repeated measurements is particularly important for work with measurement of PD currents against a much larger current from the test-object capacitance. A measurement below PD inception is used to calculate the current to remove from the measurement that is expected to

have PD. If there are differences in the measurements due to features of the measurement rather than of the test-object, the effect on the calculated PD current could be large. Variation of results is also of interest if any other comparison of results with small changes is to be made.

At high frequencies, $\gg 1$ Hz, many cycles will be included in the DFT, so the effect of noise is reduced. At the very low frequencies that will be used in this work there will be only one cycle per result, although several results can be averaged if the extra time can be permitted.

A pressurised SF_6 gas-capacitor rated 100 pF and 25 kV was connected for a UST measurement. This can be expected to have very little nonlinearity, dispersion or effect from previously applied voltages, so the measured capacitance and loss should be very similar for each point. The gas-capacitors of this model-family are known to exhibit a slightly increasing loss at the highest voltages and lowest frequencies, due presumably to effects other than the gas; but in the range used here this effect only appeared weakly.

The capacitance and loss are shown in figure 12.4, from a sequence of measurements with just one result (1 s or 1 cycle) per point, going up in amplitude and down in frequency at each amplitude. The feedback was resistive, with automatic selection according to a target CFBR of 0.3% and a target electrometer output voltage of 7 V. The voltage electrometer had the same feedback settings. Apart from the loss at the highest voltage and lowest frequency, the results are

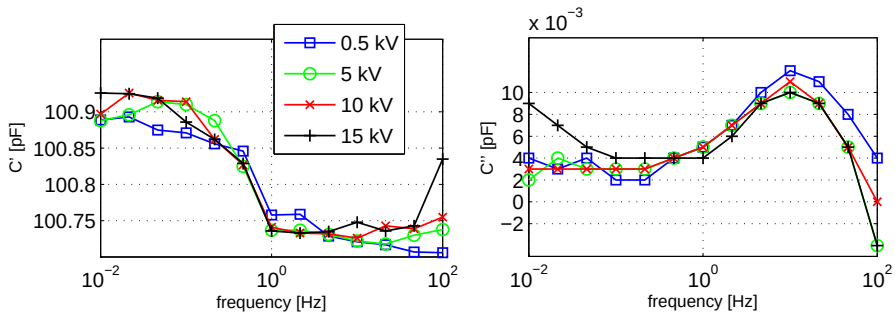

FIGURE 12.4: Capacitance measured on a 100 pF SF_6 capacitor, at several voltage-amplitudes. Note the scale of C'', in 10^{-3} pF!

remarkably consistent, in spite of the many changes in feedback resistor that are necessary for such a range of currents.

The absolute variation between measurements at different voltage levels, even with the single-cycle measurements at 1 Hz and below, is down in tens of femtofarads for C' and just a few femtofarads for C''. These are relative variations of about 10^{-3} in C', and of a large amount in C'' that is irrelevant on account of the absolute value being practically zero.

The frequency-dependence seen in all the curves is small, but cannot reasonably be attributed to a pure gas-capacitor; the frequency-dependent calibration of many components in the instrument, as well as the external circuit, will have an effect on the curve. The feedback components chosen according to the

requested CFBR and electrometer output voltage are shown in figure 12.5. All but the two most extreme feedback resistors have been used in this sweep. Their calibration must be very good for so little jumping to be seen in the capacitance measurement.

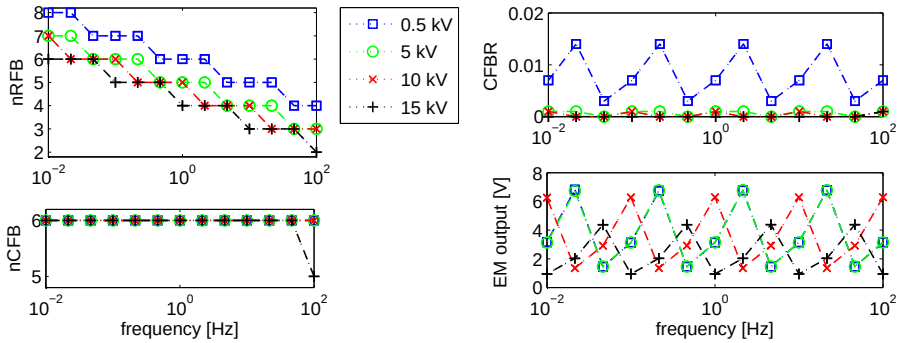

FIGURE 12.5: The feedback settings of resistor and capacitor component numbers (see table 9.1) and consequent CFBR and electrometer output voltage, during the measurements on a 100 pF gas capacitor.

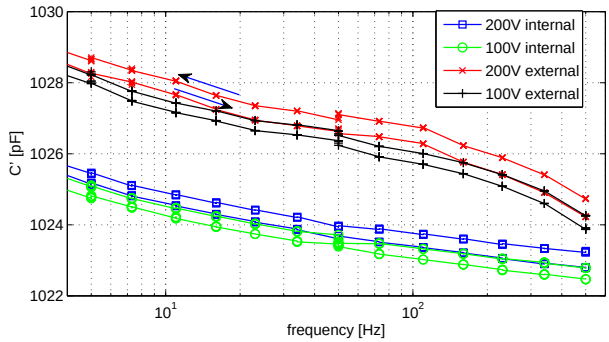

FIGURE 12.6: Capacitance C' measured on a 1.2 nF solid-dielectric capacitor with voltage-amplitudes of 100 V and 200 V using the internal and external sources. Feedback on the current electrometer was fixed at 10 kΩ and 100 pF. The points were measured from high down to low frequency then back up to high frequency. At each point 5 consecutive measurements were made, each of which is shown as a point. The upper part of each curve is the earlier part, at decreasing frequency.

No effect of ambient temperature or of warming up after turn-on were tested for the IDAX. In the lab, the temperature varies little, generally not more than 1 °C in the timescale of an hour, and the instruments are left on for long periods. For field measurements the many variables of temperature, humidity and connections mean that any groups of measurements in whose results small differences will be of interest should be made with minimal delay between them.

12.7 Output voltage phase-shift and offset

In the unmodified IDAX instrument any phase-shift between the digital signal and the analogue output voltage is irrelevant: only the relative phases of the measured voltage and current are needed. The extra TTL output on this IDAX shows the sign of the digital signal going into the DAC to set the IDAX 300's output voltage. Any phase-shift imposed by the DAC, the HVU or the small filter built in to the HVU output will cause a phase-difference between the TTL signal's edges and the zero-crossings of the high voltage that is actually applied to the test-object and measured in the voltage electrometer. The main expected use of the TTL output is in synchronising the ICM PD pulse measurement system to the applied voltage. If the phase-shift between the TTL signal and the actual output voltage is significant compared to the 1.4 ° occupied by each of the 256 'phase-channels' of that instrument, then it is desirable to model and compensate the phase-shift.

There are two main causes of a phase-shift between the TTL signal and the voltage applied to the test-object, even for the simple case of the IDAX and HVU without any additional filtering. The DAC in the IDAX introduces a constant time-delay of 38 sample-periods, giving a phase-shift directly proportional to frequency and reaching nearly 14 ° at 100 Hz; this is independent of voltage amplitude or load. The HVU has a series resistance and inductance in its output, which together with the test-object capacitance and any delay in the response of the amplifier itself causes a further phase-shift in the HVU; this is dependent on the load as well as the frequency. Figure 12.7 shows the phase-shifts between edges of the TTL output and corresponding zero-crossings of the analogue output voltage, with different markers for the phase-shifts of positive and negative crossings. An extra 4 nF load on the HVU, approximating a side of a stator coil, increased the shift by about 7 ° (5 phase-channels) at the very high frequency of 500 Hz, and only about 1 ° at 100 Hz.

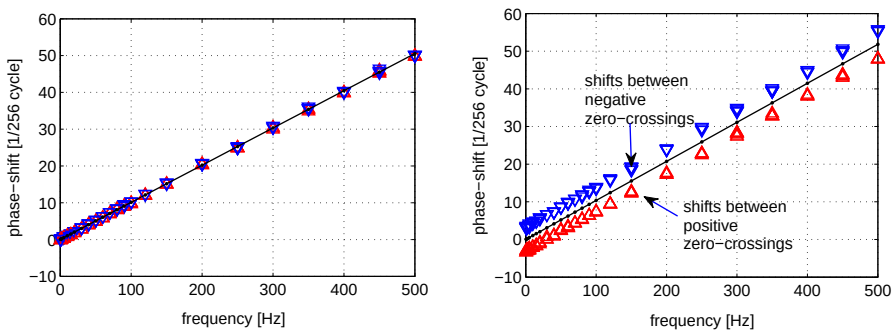

FIGURE 12.7: Phase-shifts of the IDAX analogue output voltage relative to the TTL synchronising output, expressed as the number of 1.4 ° (1/256 of a cycle) phase-channels of the ICM PD instrument. Left: the internal source, with voltage offset much less than voltage magnitude. Right: the HVU, with no test-object, peak voltage 200 V and offset in the TTL signal corresponding to about −12 V.

A further problem with the TTL output is that it includes any offset value

(dc level) that may have been specified in order to cancel offsets in the DAC, analogue circuitry and HVU. In this IDAX an offset of about −20 of the approximately ±32 000 DAC quantisation levels is needed in order to make the analogue output be zero-centred. If the output voltage is a large part of the full range, then this small amount is insignificant. Within the HVU's 20 kV range even a 200 V output is a quite small proportion, and the offset would become noticeable if not cancelled. In linear DS measurements a dc term would not affect the capacitance results, but the offset cancellation is usually applied anyway. When the offset is applied to a low-amplitude digital signal, the digital signal is significantly shifted away from being zero-centred: the TTL output, which shows the sign of the digital signal, then has an uneven duty-cycle. The effect of the offset is therefore to phase-shift the positive and negative edges of the TTL signal in opposite directions, by a phase of $\sin^{-1}(V_{\text{offset}}/V_{\text{peak}})$. If the digital offset were not applied, the same shift would still exist between the digital signal's edges and the HV signal's zero-crossings, since the HV signal would then have a proportionally similar offset. With a 200 V output from the HVU the phase-shift of TTL edges that changes the TTL to the −12 V offset can be seen to be in the order of one ICM phase-channel.

Chapter 13

Tests of the PD instrument

The ICM instrument described in chapter 10 was tested in several ways, using the newly written control-programs. The purpose was to check that documented features were working as expected, to determine some undocumented values such as maximum input and output levels, to find out what levels of noise and linearity could be expected, and to find and test the best way to synchronise to very low frequencies. Later users of the system can find more details in the lab-reports and in the written functions.

13.1 Phase-shift

In the work of [Edi01] it was found that an older ICM version, synchronising to a square-wave applied to its analogue HST1 input, showed a large increase in time-delay of recorded pulses at low frequencies. The delay varied from close to zero above 50 mHz, to nearly half a cycle ($T/2$) at 10 mHz, approximating the linear equation $t_{\text{shift}} = 0.523\,T - 9.98$, where T is the period. The PDP results in that work were therefore shifted around by a number of phase-channels corresponding to the unwanted shift.

The newer ICM was tested to see if it had any strong frequency-dependence of measured phase when using the digital TTL input for synchronisation. A TTL signal of controlled frequency was generated from the IDAX and applied to the TTL synchronising input on the back-panel of the ICM. The ICM was set to trigger on 'negative' edges of TTL logic, equivalent to rising edges of the TTL voltage. A signal generator was set up to provide a single cycle of a high-frequency ($\simeq 900$ kHz) square-wave, on either a rising or falling edge of the TTL signal. This pulse was applied to a 500 pF series capacitor leading into the ICM's preamplifier. Resistors of 50 Ω and 10 kΩ were used to shunt respectively the signal-generator and preamplifier sides of this capacitor.

Acquisitions were made with the TTL signal at frequencies from 1 kHz down to 1 mHz, with the pulses coming at the positive edge ($\phi = 0$) or negative edge ($\phi = \pi$) of the TTL voltage. The phase-channels in which the pulses were recorded are shown in figure 13.1.

Ignoring the frequencies above the 400 Hz rated maximum of the instrument, the phase is clearly measured to within one phase channel, over this whole frequency range: no adjustment is needed.

13.2 PDP compression

The raw PR-PDP can be seen as a matrix indexed by 256 phase-channels (columns) and 256 charge-channels (rows), with each element being a 16-bit unsigned integer counting the number of acquired PDs in this element's combination of phase and charge. Reading the PDP memory therefore results in

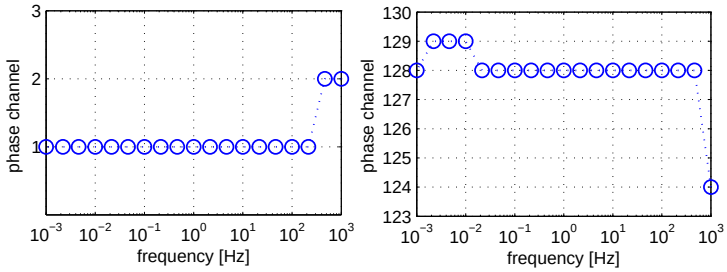

FIGURE 13.1: The ICM phase-channels into which pulses at $\phi = 0$ (left) and $\phi = \pi$ (right) fell at frequencies in and above the normal range of interest.

128 KiB† of data being transferred. The information content is generally much less than this, as PD patterns tend to be sparse or at least to have clusters of pulses of quite similar magnitude. Compression allows great reduction in the data: for example, a set of about seventy example PD patterns from whole stators can be compressed to sizes from 1.5 KiB to 25 KiB by the general-purpose compression utility *gnuzip*.

All ICM models allow the PDP memory to be read in *uncompressed* form, transferring the full 128 KiB as a stream of bytes column by column, starting at the earliest phase channel and transferring each 16-bit count as its less then its more significant byte (little-endian byte order). The recent models of the ICM, starting with version 4.00, support two compressed formats also: *single compression* replaces long runs of zero counts with a single number giving the number of zeros, and *double compression* does this along with an ability to switch to 8-bit counts for parts of the pattern with low counts. Functions were written to decompress the compressed formats to the uncompressed PDP, based on the description of these compressed formats given as example C-code in the ICM's manual. By transferring an acquired PDP in all three ways and checking that they all gave identical decompressed results, it was verified that the transfer and decompression were working as expected.

13.3 PDP transfer times

If the only use of the ICM were to run a few acquisitions in a day and retrieve the data, the speed of transfer would hardly matter; this sort of use is typical of industrial field-measurements on machines, where transporting and setting up test equipment takes far longer than a few PD measurements at power-frequency. In the use of interest here, however, there are several reasons why the transfer time matters. The ICM is to be run at many tens of voltage amplitudes and frequencies, so transfer times accumulate. At the very low frequencies each cycle will take a matter of minutes: it would be good to be able to see the intermediate

† The 'binary multiple' prefixes kibi- (Ki), mebi- (Mi), gibi- (Gi), ..., denote the powers of 2 close to the well-established SI prefixes of kilo (k), mega (M), ... The correspondence is 2^{10} (Ki) $\simeq 10^3$ (k), 2^{20} (Mi) $\simeq 10^6$ (M), etc. This quite recent notation appears in the IEEE 1541 and IEC 60027-2 standards as a way to avoid the ambiguity of using SI prefixes for binary powers 2^{10n} ($n = 1, 2, 3, \ldots$) as well as for the 'correct' decimal powers 10^{3n}.

PDP results, and to save them as a simple indication of the change in PD over time. The DS measurement that is to be run simultaneously needs reading every 1 s, and it simplifies the control program if the PD data transfer can be completed within this interval.

The transfer time depends on the type of compression, the density of the PD pattern, and on whether an acquisition is still running [s.13.4]. Transfer times recorded for the tests described in section 13.4 are shown in table 13.1. They are based on several transfers, measuring time from just before sending the command to transfer the PDP, up to the completion of the PDP read.

TABLE 13.1: Approximate times [s] for PDP transfers. The number of significant figures reflects a closely repeatable value for the conditions of these measurements, but different patterns or computer hardware/software might make far larger differences.

acquisition:	stopped	running
uncompressed, sparse	1.68	1.68
uncompressed, dense	1.68	1.75
double-compressed, sparse	0.63	0.63
double-compressed, dense	1.46	2.2

It is probable that the times would vary with type and settings of the hardware and software used in the control computer. These measurements were made on a Pentium 4 computer running linux-2.6.16 and glibc-2.9, with an internal (PCI) National Instruments (NI) GPIB card using the NI drivers of ni4882-2.5.1 and VISA-4.2, and accessing the card through the VISA interface of the Matlab-7.5 Instrument Control Toolbox (ICT).

13.4 PDP transfers while running

The PDP can be read during an acquisition. There is no documented information about how the reading and the continued writing of the PDP interact, so some simple tests were made in order to confirm assumptions. This feature of reading during acquisition may be desirable during long acquisitions in order to check that PDs are being recorded and to get an idea of the time-development of the PD activity.

Two types of signal were used for the tests. A single pulse per cycle, occurring at phase $\phi = \pi$, was taken from a signal generator with the same configuration as is described in section 13.1; this produced a very sparse pattern, with almost all counts in a single element. A 60 Hz synchronising signal was used, with acquisition time of 5 s. The PD pattern was transferred as often as possible, starting another read as soon as the previous one ended; the sparseness of the pattern made the double-compressed read require only 22 bytes, and the transfer took 0.63 s each time. In the left of figure 13.2 the total counts are shown for each transferred PDP. The counts increase linearly with time, and the final value is the 300 that is expected for 5 s of 60 Hz. Therefore, the transfer doesn't prevent acquisition or reset the pattern, and the transferred pattern is the accumulated pattern up to the time of transfer.

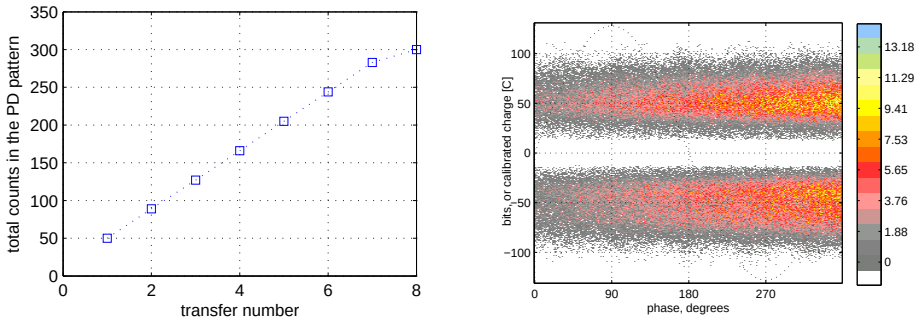

FIGURE 13.2: Reading the ICM's PDP during running acquisition: (left) total counts in a sparse pattern at 60 Hz with one pulse per cycle, with PDP transferred as often as possible; (right) a phase-resolved pattern synchronised at 120 Hz, much faster than the transfer time.

It is still not clear whether the transferred pattern is a 'snapshot' of how the pattern was at one instant, or whether the counts at different elements may be read at different times. A dense PD pattern of many counts at all phases and many amplitudes was obtained simply by turning up the gains on the background noise. The synchronising frequency, 120 Hz, gives many sweeps across the phase channels for writing the PDP in the time that it takes to read the PDP just once. The PDP was transferred several times during a 5 s acquisition. The final pattern had very similar values at all phases, but the patterns transferred during acquisition, one of which is shown in the right of figure 13.2, had a clear growth to higher phases. Plotting the total counts per phase-channel showed a linear relation. It therefore seems that the pattern is read columnwise, with the memory being written by the running acquisition in parallel with this reading.

13.5 ADC characteristics

The different 'characteristics' mentioned in [s.10.1.3] are potentially useful if a PD pattern is expected to have a wide dynamic range of charges but to need better resolution than the usual 'linear bipolar' characteristic in a particular region of the charge-scale. For all the analyses anticipated for PD pulse measurements, a conversion to points on a calibrated linear scale of charge would be needed.

The following relations have been derived and tested as the required conversion from PD-pattern charge-channels on the different 'ADC characteristic' settings, back to a normalised (per-unit) linear measure of charge that can then be calibrated in the usual way. The recorded charge-channel is an integer n, where $1 \le n \le 256$. The linear per-unit measure of charge is denoted q: $0 \le q \le 1$ unipolar or $-1 \le q \le 1$ bipolar. The compact 'ternary operator' $a\,?\,b : c$ is used, meaning 'if a, then b, else c'.

$$\textbf{linbip}\quad q = (n{>}128\ ?\ n{-}128\ :\ n{-}129)\ /\ 128$$

$$\textbf{linuni}\quad q = n/256$$

$$\textbf{logbip}\quad q = \left(n{>}128\ ?\ 100^{\frac{n-129}{127}}\ :\ -100^{\frac{128-n}{127}}\right)\ /\ 100$$

$$\textbf{loguni}\quad q = 100^{\frac{n-1}{255}}/100$$

$$\textbf{sine}\quad q = n{>}128\ ?\ \frac{2}{\pi}\sin^{-1}\left(\frac{n{-}128}{128}\right)\ :\ \frac{2}{\pi}\sin^{-1}\left(\frac{n{-}129}{128}\right)$$

$$\textbf{sqrtsine}\quad q = n{>}128\ ?\ \frac{2}{\pi}\sin^{-1}\left(\frac{n{-}128}{128}\right)^2\ :\ -\frac{2}{\pi}\sin^{-1}\left(\frac{n{-}129}{128}\right)^2$$

The manual's description is mixed up about the commands to send to the ICM to make it use each of the characteristics. In table 13.2 the documented and actual results are shown, for varied arguments to the `SAC` (set ADC characteristic) command.

TABLE 13.2: The ICM commands for setting ADC characteristics.

command	*documented effect*	*actual effect*
`SAC 0;`	(linbip)	linbip
`SAC 1;`	(linuni)	logbip
`SAC 2;`	(logbip)	sine
`SAC 3;`	(sine)	sqrtsine
`SAC 4;`	(sqrtsine)	linuni
`SAC 5;`	(loguni)	loguni

The appearance of these functions, and the range of quantisation levels that they yield, is shown in figure 13.3. The logarithmic characteristics do tend to better resolution towards the smaller charges, but the choice of just a 1% to 100% range means that the lowest available level is in fact greater than for either of the linear cases, and the resolution just above this level is quite excessively fine. Only the sqrtsine characteristic helps in going low, but this has very poor resolution in the large charges.

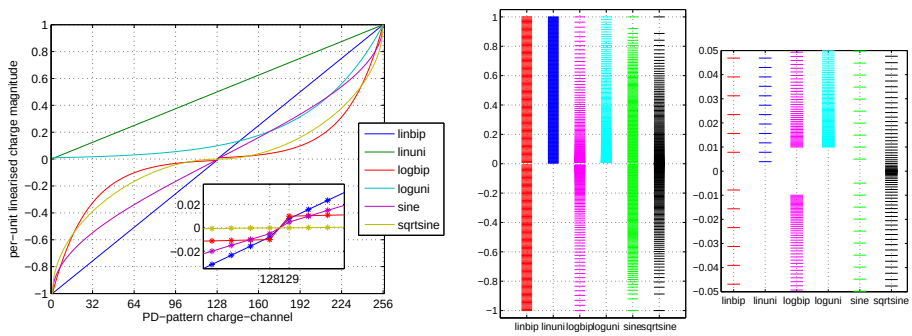

FIGURE 13.3: The functions used for the different 'ADC characteristics', and the distribution of quantisation levels.

Tests were made to ensure that each ADC characteristic was able to be requested and its results linearised; this was how the error shown in table 13.2 was noticed. A constant input signal from a 100 pC calibration pulse across a 47 Ω resistor was applied to the input of the preamplifier, which was set to a gain of 10. The main-amplifier bandwidth was set to 100 kHz to 800 kHz to make its output signal just within the range of the PD pattern for a main-amplifier gain of 100. The main-amplifier gain was then varied through all its steps from 1 to 100, and the resulting peak-meter reading and channel within the PDP were recorded. This was done for both polarities of calibrator charge. The PDP channels n in which the greatest counts were registered are shown in the left of figure 13.4, with one curve for each characteristic and polarity. The normalised linearised charges q are shown on the right, giving the expected substantial correspondence between all the results.

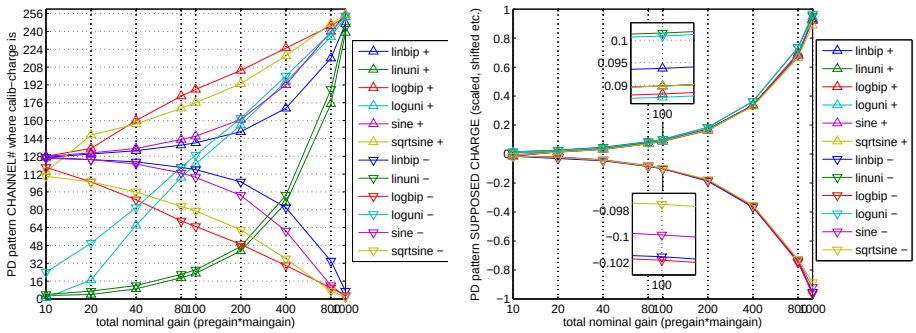

FIGURE 13.4: For all the ADC characteristics, the raw charge-channel numbers (left) and normalised charges derived from these (right), with the input to the ADC varied by changing the main-amplifier gain with a constant input pulse.

13.6 Synchronisation

In the common industrial use of the ICM instrument the frequency will be above 30 Hz, so the ICM can lock to it. It will generally be acceptable to start the applied voltage, then to trigger an acquisition of many cycles of PD data, without caring about exactly which cycle the acquisition starts in. For the intended use in this work, with very low frequencies and simultaneous measurement by the DS and PD instruments, the exact behaviour of the ICM's triggering and synchronisation becomes important. Time-constraints typically limit the measurements to just one or a very few cycles at the low frequencies. One wants to be confident that the acquisition will start at the beginning of the first applied cycle, and that the return to the first phase-channel will happen correctly each time the synchronising event occurs.

In earlier work using the older ICM version adequate synchronisation was achieved by sending the command for a 'single mode' acquisition of time equal to one period of the intended frequency, then calculating the dwell-time based on this and switching back to 'repetition mode' [Edi01, p.69]; the analogue

synchronising input was used, but with a square-wave signal to provide clear synchronising events at low frequency.

The newer ICM has a digital synchronising-input and an extra command for specifying the dwelltime directly. Several methods of setting up dwelltime were tested, over a frequency range from hundreds of hertz down to millihertz. A TTL signal from the IDAX instrument was applied to the ICM's digital synchronising input and to the gate of a pulse-generator set to produce a dense train of very similarly sized pulses that were applied to the PD preamplifier. The gating resulted in there being no pulses during the half-cycle in which the TTL voltage was low. By running for just one or a few cycles it could be seen whether the artificial PD signals during any part of the active half-cycle had been missed, and by running for many cycles it could be seen whether any PDs had been recorded at phases in the PD pattern where there shouldn't have been any. Each set of parameters was tested at least ten times in succession, to see the variation.

Only one combination of commands was seen to give good performance. This required setting the expected dwelltime directly, after running the command for automatic dwelltime calculation. It was also necessary to synchronise to the positive-going voltage on the TTL input, which is called the negative edge because the TTL input is 'active low'. Use of the other polarity gave inconsistent results; puzzlingly, this was true regardless of what phase-shift from zero to one period was put between sending the command to start the IDAX output voltage and sending the command to trigger the ICM acquisition.

Figures 13.5 and 13.6 show a few results from the tests. All of these use the TTL input, synchronising to the positive-going voltage. The presentation

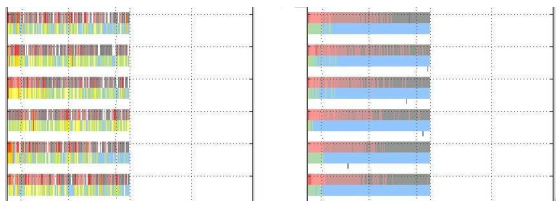

FIGURE 13.5: ICM synchronisation for different commands. Each of the six strips in each plot is a zoom of the ICM PDP, taking just the few charge-channels where the test-pulses came, but all phase-channels; the horizontal axis of each plot runs from 0 to 360 °. A signal of 100 cycles at 40 Hz was provided by the IDAX, and pulses are generated just during positive half-cycles. There should therefore be a thick and even distribution of pulses recorded up to 180 °. Left: using the same commands as with the old ICM, resulting in only one cycle being recorded (ragged pattern: counts were checked). Right: using the direct setting of dwell-time, giving an even pattern whose counts suggested the capture of 100 cycles rather than 1.

is rather peculiar, being for each case a set of six images of the small vertical range of a displayed PD pattern where the signal-generator pulses fell. The vertical direction of each plot is thus repetitions of the test, and the horizonal direction goes through the phase-channels from 0 to 360 °; coloured marks indicate nonzero counts. The commands that worked with the old system resulted, at the left of figure 13.5, in only one of the hundred cycles being measured; at the right the counts are of the order of a hundred times higher. Comparison

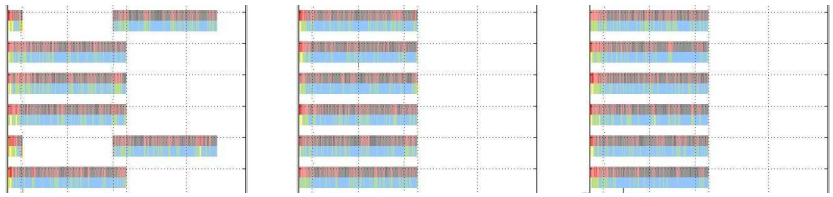

FIGURE 13.6: ICM synchronisation for varied phase of triggering. The case in the centre is similar to the right of figure 13.5, but with just 1 cycle at 5 Hz. To the right there is a half-period delay between starting the IDAX and triggering the ICM. To the left the IDAX is simply left on and the ICM starts at arbitrary phase.

of delays between IDAX start and ICM trigger showed that even a half-cycle delay gave no problem, but there can be problems of wrong synchronisation when triggering the ICM at certain phases.

13.7 Linearity

A common definition of linearity of a function $f(\cdot)$ includes the condition that $f(ka) = kf(a)$; if negative k is permitted, so that $k = -1$ can be chosen, then a PD measurement system should record positive or negative calibration pulses of similar magnitude as *having* the same magnitude, to within the system's permitted degree of non-linearity.

The ICM does not make a direct claim of its linearity or polarity dependence, but is supposed to conform to IEC-60270. In that standard the most relevant parameter that must be tested for a PD measurement system is the *scale factor*, k. This is the ratio of the measured response to the size of the applied calibration charge; it should be taken at three or more calibration charge values ranging from 10% to 100% of the instrument's full scale, and "the variation of k shall be less than $\pm 5\%$ in order to prove the linearity of the system". A calibrator is tested by measuring its charge by a method with uncertainty no more than the greater of 5% or 1 pC. Putting these two criteria together implies a possible 10% variation in linearity between 10% and 100% of scale of an approved PD measurement system.

A PD measurement system conforming to this standard may therefore have substantial differences, of some 10%, in its scale factor at different magnitudes, and it is not obvious what requirement there is on polarity-dependence. A reversal of calibrator leads is a simple way to compare the scale factor at opposite polarities, with the advantage that the calibrator charge should in this case be very consistent, thus avoiding bringing the calibrator's permitted uncertainty into the measurement of scale factor.

In view of the usual noisiness and stochastic variation of PD measurements, a 10% variation in scale factor may be acceptable for conventional industrial diagnostics. When some of the results are expected to come from small laboratory-samples, to be compared with DS measurements of PD charge, and to be analysed quite carefully, it becomes much more troublesome to have even a few percent of systematic error of magnitude with polarity. Assessment and compensation of such errors should be tried.

The users of our older ICM system noticed some years ago that similar input magnitudes of positive and negative PD signals to the preamplifier can give different measured magnitudes. From [For08a, p.25], "it was observed that for low gains and steep input pulses the amplification factor was slightly different for positive and negative pulses". In that work the problem was reduced by adapting the detection impedance to give smaller and slower input pulses, and by using quite high gains. It was immediately apparent with the newer ICM that the background noise appeared sooner in the negative part of the PDP when the gain was increased or the LLD level (threshold) was decreased into the noise. Large variations, easily 10%, were seen between measurements of positive and negative calibration pulses that should have had the same magnitude; the variation always made the negative measurement larger. Several tests were done to define the problem better.

Results from the tests of ADC characteristics reported in section 13.5 provide a good example of the polarity-dependence of the recorded charge-channels in the PDP. The ratios between measured charge magnitude for positive and negative input pulses are shown in figure 13.7 for varied main-amplifier gain. Curves are shown for several of the ADC characteristics, to provide some confirmation of the shape of the curve. The lowest point at a total gain of 10 (main-amplifier

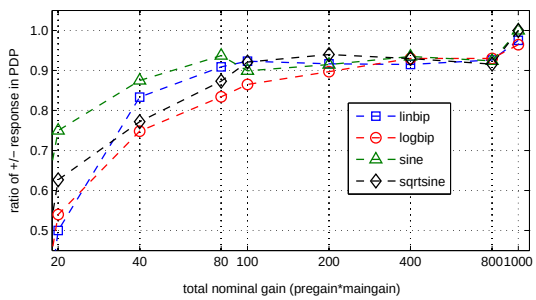

FIGURE 13.7: Ratios of peaks of the ICM main-amplifier output to + and − calibration pulses, measured from the PDP using several 'ADC characteristics' to give different spreads of quantisation levels.

gain of 1) is not shown, due to the difficulty of measuring the signal reliably at such low levels. The point at the highest gain shows artificially good results as the charge measurement is saturated. Other points show a general trend that was seen from many other measurements using the PDP's charge channels or the peak-meter output: at higher output values, such as with total gains above about 80 with this input signal, the ratio of +/− magnitudes is about 5% to 10% below the true ratio, and at lower gains this worsens to some 25%.

A fairly similar behaviour was seen when measuring the main-amplifier's output with an oscilloscope. A 50 pC calibration charge was used in this case, with the oscilloscope set to high-impedance (1 MΩ) dc-coupled. In figure 13.8 the ratios of the peak of the response to positive and negative pulses are shown for peak-measurement taken relative to the earth conductor or relative to the mean signal just before the pulse. In each case the total gain is obtained

in two ways by scaling the preamplifier and main-amplifier gains in opposite directions by a factor of 10. It seems that a dc level on the main-amplifier

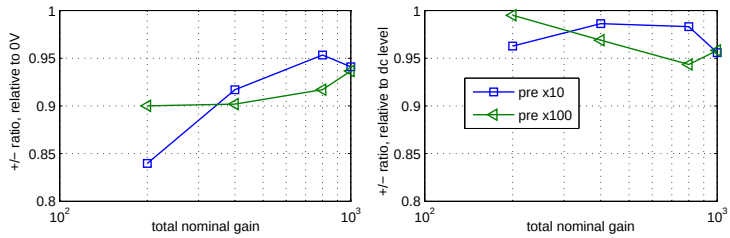

FIGURE 13.8: Ratios of peaks of the ICM main-amplifier output to + and − calibration pulses, *measured on an oscilloscope*. The peaks are taken relative to zero voltage (left) or to the 'dc' voltage that was present just before the pulse (right).

output is responsible for a lot of the polarity dependence seen in the oscilloscope measurement.

Another measurement using 100 pC calibration charges and comparing the PDP charge-channels into which positive and negative pulses fell is shown in figure 13.9. The results are displayed as ratios and differences of the charge-channels $\pm(1, 2, \ldots 128)$. A constant dc level could be responsible for much of

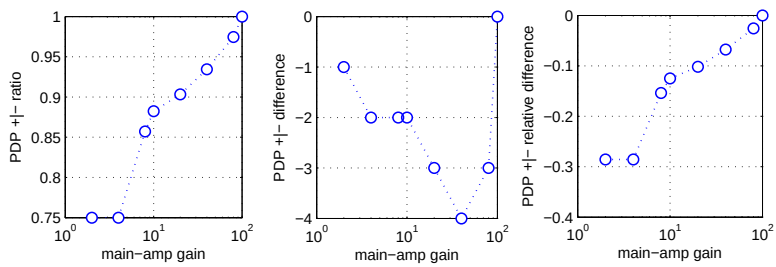

FIGURE 13.9: Differences in measured + and − magnitude in the PDP, shown as ratios and differences of charge-channels.

the difference at low signals, but something else is happening to cause multiple-channel differences in the higher signals.

To remove the dc level from the measurement of charges in the PDP, a 4.7 µF capacitor was used to connect the main-amplifier output into the digitiser input, instead of the usual short coaxial cable. Figure 13.10 shows the results for a normal measurement of 100 pC across 47 Ω without the capacitor ('direct') then for three measurements with the capacitor instead: these differ only in that one had the high-impedance oscilloscope in parallel with the digitiser, and another reversed the sequence in which the different gains were used; no difference was seen for these changes.

The removal of the dc level made the situation at the low gains have no visible polarity-dependence, rather than the difference of some 30% seen without the capacitor. The use of a much smaller capacitor, 15 nF, gave no noticeable

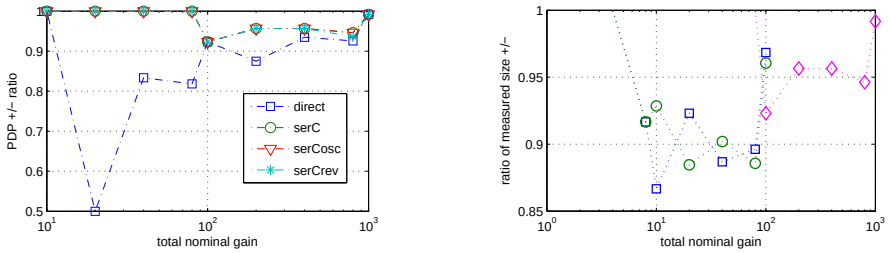

FIGURE 13.10: Series capacitor (ac-coupling) used to improve the ICM's +/− magnitude ratio. Measurements with direct 'dc' coupling versus series capacitor 'ac' coupling (left). Measurements with series capacitor coupling for pre-amplifier gains of 10 and 1, with increased calibration charge to compensate the lower gain.

difference, but it may do if pulses came very frequently. The pulses from the main-amplifier have however a time-integral of approximately zero, so there shouldn't be much signal-dependent dc-level.

The polarity-dependence at high gains was improved slightly, too. On the right a curve for a larger signal of 1000 pC is shown, with the preamplifier gain reduced from 10 to 1 to keep the output signal approximately similar. Two measurements of this larger signal are shown: the difference between the polarities is about 10%, rather than about 5% with the smaller input signal and higher gain.

It was concluded that the removal of a dc-level on the main-amplifier output is very helpful to good measurements at low points in the PDP, but that there is a bias towards measuring greater magnitudes of negative pulses, varying at least from 5% to 10%. Simply scaling all measured negative charges down by some 5% would therefore make the result closer to the truth than it currently is. Further investigation of the polarity-dependence was avoided due to lack of time.

13.8 Calibrator pulses

When investigating the ICM's linearity, section 13.7, an early question was whether the calibrator indeed did provide similar magnitudes of charge when on its positive and negative polarity settings. This was checked by comparing polarity-reversal by using the polarity switch or by reversing the calibrator leads: no significant difference was seen. The charge was also measured by integration of the voltage across a shunt resistor on the calibrator. The opportunity was then also taken of seeing what sort of time-response the calibrator output current actually has: in section 10.1.7 it was seen that only an upper limit on the rise-time is assured by the calibrator's specification.

Figure 13.11 shows the results from one test, measuring the voltage across the calibrator terminals when connected to a 50 Ω oscilloscope input, then scaling by 50 Ω to give the current. The rise-times are from about 10 ns to 20 ns, giving corner frequencies beyond 10 MHz; even with a 470 Ω shunt resistance the spectra were flat well beyond 1 MHz. The lowest charges have a two-part peak leading to a rise towards the lower frequencies of tens of kilohertz. The

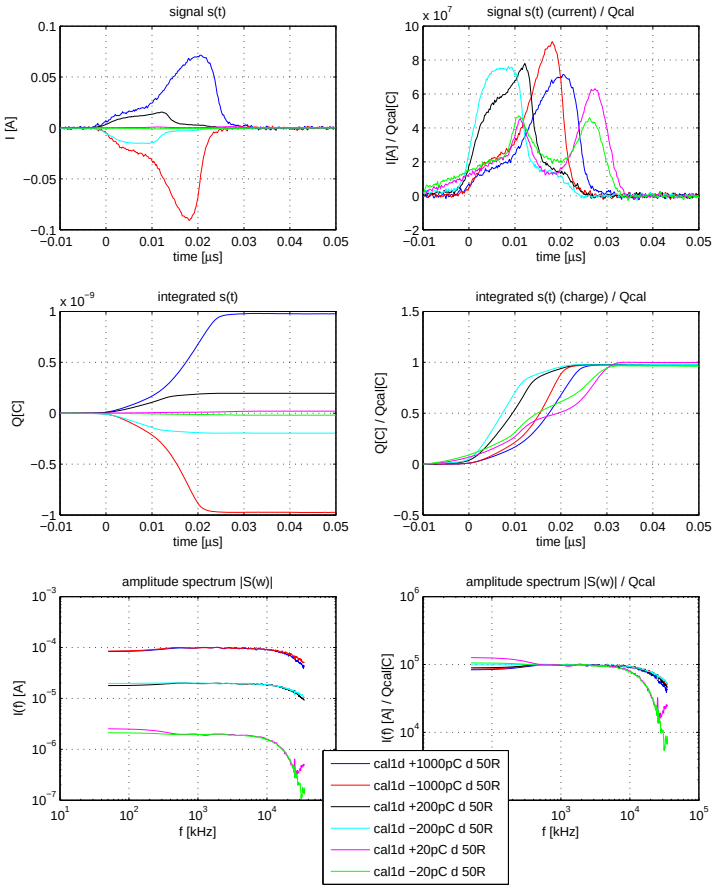

FIGURE 13.11: Pulse currents of $\pm(20, 200, 1000)$ pC from the CAL1D calibrator into 50 Ω, (top left). The currents are integrated to charge (middle left), and transformed by FFT to amplitude spectra (bottom left). On the right the same plots are normalised by the calibration charge: the two at 20 pC are the ones that are have a slow double-pulse in time, and fall off faster at high frequency; the two at 200 pC rise the fastest.

mid-range charges, 200 pC in this case, have the most ideal waveforms and spectra, but there is a general trend of sharper rises for negative pulses, seen with other shunt resistances and charge settings. The total charge within the pulse nonetheless integrates to very similar values for all the polarities and magnitudes, as seen in the plot of normalised integrated charge.

13.9 Signal limits

The combination of the gains of both amplifiers and the short-term integral of the input signal determines the signal at the main-amplifier output. Excessive values here are very obvious from saturation of the PDP charge-channels and the peak-meter: it is not obvious whether a pulse registered at the highest charge

level is in fact within that level or is higher, but one should treat anything at the highest level as suspicious. Saturation of the preamplifier will not be seen from the PDP. The limits of the preamplifier output were tested by applying positive or negative 1000 pC calibration charges across a 47 Ω resistor shunting the preamplifier's input; the preamplifier gain was 100 and the main-amplifier's gain was 8. An oscilloscope set to high-impedance (1 MΩ) was used to measure the voltage at the preamplifier output, using ac-coupling, and at the main-amplifier output, using dc-coupling. The response to an input pulse at $t = 0$ is shown in figure 13.12.

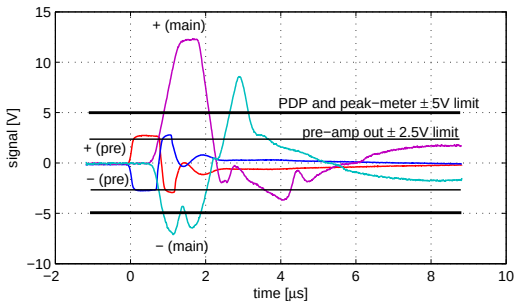

FIGURE 13.12: ICM amplifier output signal limits, tested with excessive input signal and gain.

Chapter 14

Contribution of PD to the total DS current

The DS and PD methods of measuring PD apparent charge will give results with some differences and some similarities. This chapter considers the relations of the two types of measurement to the ideal apparent charge value, and how these relations are affected by features of the instruments and of practical test-objects. This is done by some theoretical considerations and measurements of pulse-sources of controlled magnitude and phase.

14.1 Comparison of DS and PD results

A pulsive PD event in a test-object causes a rapid change in potential on the object's terminals, and a rapid pulse of current flowing in from shunt capacitances in the external circuit.

A PD-pulse measurement ideally records the overall charge-injection into a terminal of the test object or a coupling capacitor, for each PD pulse separately [s.8.2]. It can have a high sensitivity to PD pulses, as it avoids the frequency-band close to the applied voltage, in which the currents from the capacitance and conductance lie. It can register pulses separately, preserving the distinction between a few large PDs or many small PDs.

A DS measurement ideally records all charge into a terminal of the test-object [s.6.2], including the current from smooth capacitance and conductance as well as from pulsive or glow PD. The measured PD current is only an aggregated value, combining all PD events that occurred within a particular range of the phase of the applied voltage.

To estimate the current due to the PD alone, the other currents must be estimated and subtracted. In an object with large capacitance and a small proportion of volume contributing to PD events, the errors in this subtraction will easily swamp meaningful results.

14.2 Measurement of pulsed currents

The DS system needs to be able to measure PD currents, which arise as sharp pulses at the test-object. The trouble with pulsed currents and resistive feedback has already been mentioned: a resistance low enough to avoid electrometer overload during pulses is likely to be too low to provide an acceptable signal during the rest of the time, if the pulses make up much of the total measured current. Capacitive feedback would integrate the pulses, simply stepping the feedback voltage a little for each pulse that comes in, but it has undesirable features particularly where there is a significant dc term in the current.

An important property of the DS instrument if it is to be used to measure PD charge is that the recorded DFT components should include all the charge into the measurement terminal. It is not certain that this will be true: there could

be filters that let some charge from HF signals pass around the electrometer, or it could be that rapid pulses and low-resistance feedback result in a quick peak that is not fully recorded at any sampling instant of the ADC.

Pulse-measurement with resistive feedback is helped by the presence of capacitances that can buffer the pulse charge, letting it pass away through the feedback resistance without ever causing excessive voltage on the electrometer input. Even if the feedback capacitance is small enough to give an acceptably low CFBR at the frequency of the applied voltage, it may still pass significant displacement current during a quick pulse. Shunt capacitances too, such as the coaxial measurement-cable, help to reduce the voltage peak at the electrometer input during a pulse arrival. Over times much longer than a PD event but still much shorter than a cycle of the applied frequency, all charges stored on the shunt and feedback capacitances will be discharged through the feedback resistor at a speed that should make them measurable over several sample points. These capacitances therefore make it possible to set feedback resistance closer to the optimum for the expected magnitude of sinusoidal current, avoiding overloading the electrometer when large currents arrive for short times. In most practical insulation systems, rather than some canonical laboratory objects such as a point-hemisphere PD-gap, there is the further helpful feature that the displacement current in the capacitance of the test-object results in much more measured charge per cycle than all the PD sources do: the correct setting of resistive feedback will therefore be able to deal with quite high currents, and the extra shunt capacitance of the test-object will help to hold the PD charge without large change in electrometer input voltage, until the feedback resistance can take the extra charge away.

Some tests were made to investigate how easily electrometer overload could occur when measuring pulses, and how faithfully the charge of a pulse is recorded by the IDAX. An output voltage amplitude of 1 V was set for the IDAX's LV output so that the TTL output would provide a synchronising signal. An HP33120A function generator was set to trigger from positive edges of this signal, each time emitting a voltage following an 'arbitrary waveform' of 8192 points copied from the computer, spread over a single period of the IDAX voltage. This voltage, behind the function generator's 50 Ω output impedance, was applied through either a series resistor or capacitor to inject current pulses into the IDAX measurement terminal, which was set to UST termination. For longer pulses a square-wave voltage was applied to a 470 kΩ series resistor, giving the possibility of testing with significant dc terms in the current; when working with balanced bipolar pulses a 0.68 μF capacitor was added in series with the resistor to remove the effect of any slight dc term in the function-generator output voltage. For shorter pulses and better-determined charges a ramp, or step in the extreme case of only two sample points, was applied to a series HV ceramic capacitor of about 1.46 nF, without any resistance beyond the function generator's 50 Ω output impedance. The waveform was automatically generated each time to give a specified charge in a specified time.

Pulses were applied with varied charge, varied phase all the way through the cycle, varied pulse-time down to 1/4096 of a cycle, varied applied frequency, and

varied feedback components. Symmetric pairs of pulses were injected, giving a charge of $+Q$, and a charge of $-Q$ half a period later.

In figure 14.1 the fundamental components of current measured by the IDAX are shown, scaled as complex capacitance; the delay between a positive zero-crossing of the voltage and the centre of the positive pulse is varied from 0 to T, but as the phase-shift between the IDAX's digital and analogue outputs was ignored here the pulse phase is really less by some 8 °. The pulses were produced with a rectangular voltage behind a 470 kΩ series resistor. The pulse-width was $T/128$.

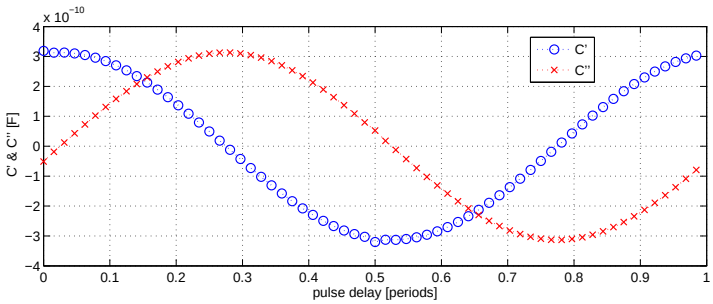

FIGURE 14.1: IDAX measurements of a constant charge injected as a symmetric pair of rectangular pulses with constant width of $T/128$ and delay from 0 to T.

With the phase of the pulse-centre held at about $\pi/4$, the width of the pulse, for constant pulse charge, was varied; the results are shown in figure 14.2. When the pulse width approaches the period of the harmonic component of interest, the $\mathrm{sinc}^2(\cdot)$ behaviour becomes apparent.

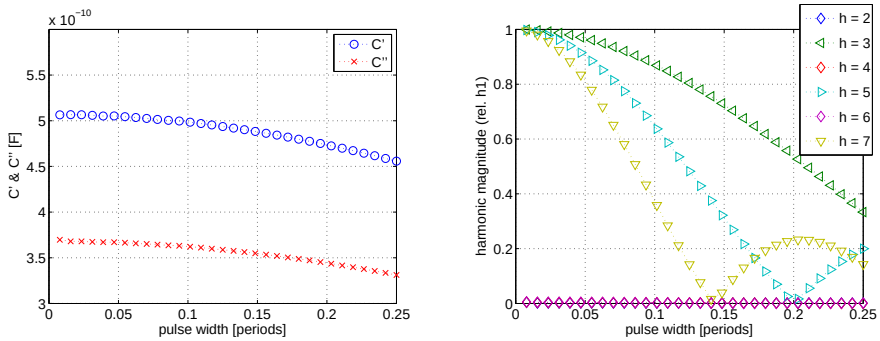

FIGURE 14.2: IDAX measurements of a constant charge of $Q = 1\,\mathrm{nC}$ injected as a symmetric pair of pulses each of this magnitude. On the left, the complex capacitance from the fundamental components of current. On the right, the magnitudes of harmonic currents relative to the magnitude of the fundamental current.

Some much sharper pulses were made using a series 1.46 nF capacitor and a stepped voltage. Measurements were made using many combinations of feedback components, charge and pulse-width. With such rapid pulses the charge was more important than the speed: an electrometer overload that went away if

halving the charge would not go away if doubling the pulse-width to halve its mean current, as would have happened with much wider pulses. Even quite large charges from a PD perspective, such as 12 nC, could be tolerated with the use of a larger feedback capacitance, while still having a very low CFBR. Even over four orders of magnitude of feedback resistance, with all other parameters fixed, the measured charge was very similar. The expected relation that the fundamental component of current would be $4/\pi$ times as large for a pulse of charge Q per half-cycle than for a sinusoid of charge Q per half-cycle, was close to the results, which gave about 1.31 rather than 1.27.

Figure 14.3 shows the effect of variation of three of these factors upon the fundamental components of current. The internal phase-shift in the IDAX has been compensated in these results, so the phase of 0 leads correctly to $C'' \simeq 0$.

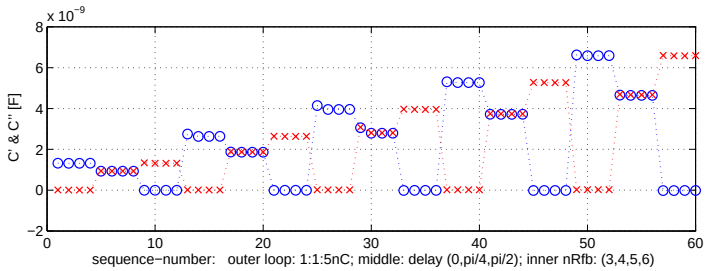

FIGURE 14.3: Fundamental components of IDAX current measurements at 60 Hz, with injected charges from sharp pulses of duration $T/4096$ with symmetry as described for figure 14.2. The results are plotted in the sequence of measurement, with nested loops giving an injected charge of $[1, 2, 3, 4, 5]$ nC, a shift of $[0, 1/8, 1/4]T$, and feedback resistance of $[10^4, 10^5, 10^6, 10^7]\,\Omega$. Feedback capacitance is 1 nF in all cases. Apparent anomalies such as for sequence-number 29 are repeatable.

The harmonic components were very close to the expected ones, of zero for even harmonics and the same magnitude as the fundamental for odd harmonics. Relative harmonic magnitudes are shown in figure 14.4 for the same data as in figure 14.3.

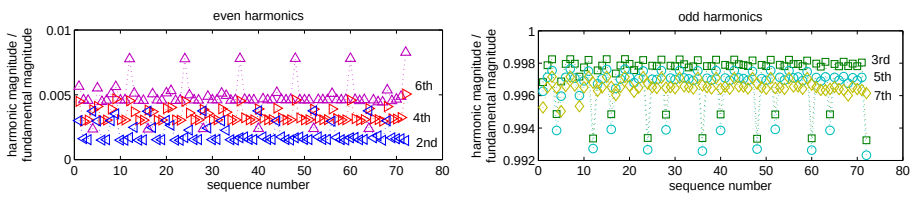

FIGURE 14.4: For the same measurements as in figure 14.3, the harmonic current magnitudes relative to the fundamental current magnitude. (Sequence numbers above 60 have an even higher feedback resistance, not shown in the other figure, which resulted in some overloads of the electrometer.)

The time-domain currents that can be calculated from the IDAX DFT components are very limited in sharpness, and have higher-frequency oscillations.

An example using all eight harmonic components is shown in figure 14.5, along with the pulse-current based on the capacitance of the series capacitor and the numerically differentiated oscilloscope-measurement of the applied voltage. The much sharper pulse measurement from the oscilloscope can be filtered until it becomes wider and with a lower peak, ending up looking similar to the IDA measurement but without the oscillations that result from the cutoff of frequencies above the eighth harmonic in the IDAX's data.

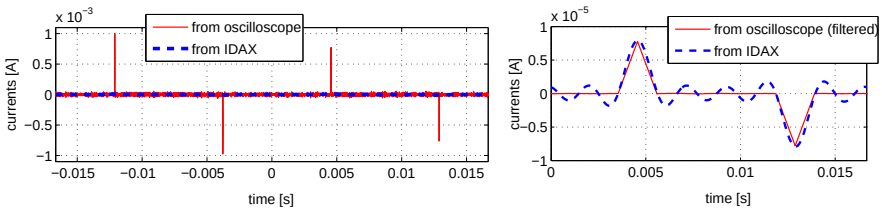

FIGURE 14.5: Time-domain currents of the pulses from sequence-number 46 of figure 14.3. The current from the IDAX is transformed into time from the eight recorded harmonics. The oscilloscope measured voltage, which has been numerically differentiated to calculate the current in the capacitor. On the left, the sharpness of pulses makes the IDAX current look negligible, due to the limitation to eight harmonics. On the right, numerical filtering smoothens the oscilloscope measurement for comparison in similar scale. The phases are clearly very well aligned.

14.3 Summary

The DFT components have been seen to be measured without losing significant charge and with the expected relations of fundamental and harmonic components to the pulse properties. The resistive feedback has been seen to work well even with considerable pulsed currents, when in combination with a moderate capacitance giving acceptably low CFBR. There is low sensitivity to the choice of feedback value.

Chapter 15

Processing and display of DS and PD results

The types of measurements being studied here produce many times as much data as the conventional diagnostic measurements made on stator insulation. The storing, processing and presenting of results thus becomes especially important if patterns and frequency dependence are to be noticed. This chapter considers what extra data the proposed methods produce, and suggests ways of presenting it.

15.1 Conventional measurements and presentation

Even the conventional offline electrical diagnostic measurements for stator insulation can generate enough data to need some attention to good forms of display, particularly for comparison and trending.

The time-domain measurements of IR and PI [s.6.4.2] can be recorded as a time-series or as a single number at a specified time. The single-frequency measurements of C-tan δ [s.6.4.1] are usually made at several voltages, recording just the pair of fundamental-frequency results at each.

Most modern PD measurements are based on a PRPDA method [s.8.2.4] where counts are recorded in a matrix of thousands of combinations of pulse magnitude and phase of occurrence; the measurement is generally made over same range of voltage levels as for C-tan δ [s.8.5]. The total information can thus be a great deal more than for the other measurements, and many ways are used of reducing the PDP to a function of one variable [s.8.2.4]. The PD measurements are clearly much the most data-intensive of the conventional methods.

Provided that the neutral point can be split, all of these measurements can be performed separately on each phase and then on all phases together [s.4.5], which increases the data by a factor of four. Separate measurements of PD at the phase end and neutral end [s.8.5] can further double the resulting data.

15.2 Further data from the proposed measurements

The methods studied in this work increase the amount of data from each measurement in several ways: harmonics are included in DS measurements, PD pulse measurements are interpreted in the form of currents as well as the usual patterns and indices, and multiple frequencies are used.

The DS results include the harmonics of voltage and current; the harmonics up to the eighth are included by the present instrument. The scope of this work is limited to applied voltages that are intended to be sinusoidal: harmonics in the voltage are only measured in order to correct the measured current. The DS data that must be presented is therefore only based on current harmonics.

The data from a DS measurement is increased by several times by including harmonics, but it is still much less than the raw PD data.

The PD results are a conventional PR-PDP for each point; from the present instrument the size is 256×256 elements. This can be studied by the conventional features such as pattern and maximum charge, and also as the waveform of mean current due to the measured charges, for comparison on similar terms with the DS results. For a winding rather than a single bar in the lab, the calibration of the pulses to true apparent charge is not possible [s.8.4], but a comparison of the waveform's shape might still be desired.

The DS and PD measurements are made over many frequencies as well as over the several voltages that are conventional. At least two decades of frequency are likely to be included in a seriously 'variable frequency' measurement, even when measuring on industrial equipment in the field. Several points per decade should be taken if trends are to be clearly seen. For a test-object with a capacitance of the hundreds of nanofarads typical for a stator phase, an upper limit of about 1 Hz is likely at high voltage, due to limitations of the voltage amplifier. To keep the measurement-time reasonable when working at several voltages and on separate and combined phases, a lower limit of about 10 mHz is likely to be needed. In the laboratory with smaller objects and longer available time, five decades from 100 Hz to 1 mHz may be studied even at high voltage. Varying the frequency therefore results in at least a five times increase in data compared to single-frequency measurements, and possibly twenty or more times in a laboratory situation.

15.3 Suggested presentation

If a single number can be used to represent the results at each combination of amplitude and frequency (each *point*), a good way of plotting the whole measurement is to plot a curve against frequency for each amplitude. This is usually preferable to plotting against amplitude: there are usually more frequency points than amplitude points, and the shape of the curve against frequency is generally of more interest than curves against amplitude, particularly for DS measurements on largely linear objects. Variable-frequency methods that have been applied in other types of insulation such as cables [s.6.3] have done this with two numbers, representing the complex capacitance at each point as C' and C'' or as C-tan δ . It would be good to be able to represent the harmonics in DS, and important features of PR-PDPs, as also just a few numbers that can be plotted in this way.

15.3.1 PD patterns

A single PR-PDP is already a complicated three-dimensional data-set, potentially holding a large amount of information. There is no direct substitute for looking at every pattern and seeing the variation with the controlled variables; no small set of indices would make clear the changes in pattern seen between different frequencies in for example [Cav06].

There may easily be tens of acquired PD patterns for a measurement with varied amplitude and frequency, even when only on one object such as a particular phase. It may be worth sacrificing or supplementing the high level of detail

of a PR-PDP in order to get the benefit of seeing a comparison of frequency and amplitude dependence all in one plot.

Reduction to one of the many conventional indices such as mean or maximum charge can be used to enable a single plot to display of some feature of all the measured points. Such indices, although derived from a PDP, are in a way a source of *extra* information as well as a way of reducing the data, since they can show trends that the eye would not notice so clearly. As an example, admittedly not with real PD, the strong linearity in figure 13.2 [p.140] was much more obvious when each pattern was reduced to total counts and plotted than when merely looking at a sequence of patterns.

Conversion of a PR-PDP to the mean PD current reduces the charge magnitude and count dimensions into one, reducing the amount of detail but still leaving a number at each of the phase-channels, 256 for the present instrument, rather than the desired single or few indices. One unconventional way of further reducing this current, which makes a lot of sense for the combined DS and PD measurements considered here, is to treat it in the same way as the DS current, converting it to its fundamental and low harmonics. The same methods of display can be used as for DS.

Some examples of reduction of PD data for plotting of frequency-dependence are use of counts per cycle and mean charge in [For08b, fig.5], and a complex-capacitance description of the fundamental component of mean PD current in [Tay07]. For comparison of PD currents measured by DS and by the mean current from pulse measurements, [Edi01, ch.4] presents harmonic components in rectangular form; this is at a single frequency, but is nevertheless a DS-like view of PD mean current rather than one of the conventional indices.

It is expected that a few conventional indices, possibly along with DS representations of mean current, will be a suitable compromise of sufficient information and not too many plots. It is important to be able to choose different indices easily, and to see the full PD patterns if wanted.

15.3.2 DS including harmonics

For conventional frequency-domain dielectric spectroscopy, studying only the fundamental-frequency components, the measured current is usually presented as a complex capacitance (6.1). This has some useful properties for measurements on insulation systems.

Division of the current's amplitude by the voltage amplitude and frequency gives a constant value if the test-object is a pure, linear, dispersion-free capacitor. The effects of dispersion and nonlinearity are then much more clearly noticed and interpreted than they would be in the current, which due to the dominantly capacitive nature of good insulation would change approximately in proportion to frequency. This is the usual principle of scaling data towards a constant, to see the variations clearly A.1.5.

The current's phase is taken relative to the applied voltage, making clear the relation of energy storage and dissipation components of the current at the fundamental-frequency.

The further ratio of these components of the current, to give $\tan\delta$ (5.8), can be used to remove the effect of geometric capacitance, permitting more

direct comparison of different test-objects. (This work has instead focused on the separate components C' and C'', partly because the division of rectangular parts of the current is a natural way to consider the stress-grading current and the effects of PD, as well as to see the features of the power-law response of the epoxy-mica material.)

Having accepted this conventional presentation of fundamental current as the indices C' and C'', one wonders if the harmonic currents can be treated in a similar way. The magnitude of fundamental current in a largely capacitive test-object can vary by many orders of magnitude over a sweep of voltage amplitude and frequency, and the harmonic currents may easily vary to the same degree. Indeed, it is likely they will vary more, as the expected nonlinearities in stator insulation have typically a higher admittance at higher voltage; it is also likely that the frequency-dependence will be strong, as with the fundamental current, since the current in most nonlinear parts of the construction, apart from cracks or leakage from the terminals, has a capacitance in series.

Some sort of scaling of harmonic currents by voltage amplitude and frequency is therefore desirable. In the measurements considered in this work, only the fundamental component of applied voltage V_1 is intended to be nonzero. Approximate currents due to voltage harmonics $V_n \neq 0$ will have been subtracted from the measured current. The only voltage by which a harmonic current can meaningfully be divided is thus the fundamental. A suitable frequency used for scaling the nth current-harmonic I_n could be argued to be either the fundamental frequency f or the harmonic frequency nf.

The harmonic current magnitude scaled in this way is

$$|C_n| = \left| \frac{I_n}{\omega V_1} \right| = \left| \frac{I_n}{I_1} C_1 \right| \tag{15.1}$$

which will be denoted C_n, the 'harmonic capacitance'. This $|C_n|$ is suitable for plotting along with C_1, typically being one or a few decades less for low harmonics in a quite nonlinear object.

A still simpler form is to use just the relative magnitude of the harmonic current to the fundamental current, which makes it easy to consider how dramatically the harmonic would affect the current-waveform, without having to see the fundamental capacitance as well,

$$|I_{n\mathrm{rel}}| = \left| \frac{I_n}{I_1} \right| \tag{15.2}$$

The phase, however, is critical to how a harmonic modifies the current waveform. Due to the mixture of capacitive and conductive currents harmonics will not always cause an increase of the peak of the fundamental; their phase cannot be assumed. There are many possible choices of how best to present current-harmonics' phase. It could be taken relative to the fundamental voltage, as is done for calculation of capacitance from fundamental current: but no clear relevance such as the distinction of energy storage and loss in C' and C'' would come from this. The relation to fundamental current is more relevant: similarly to use of relative magnitude, it helps one to visualise the effect on the current

waveform. Remaining questions are then whether shifts between zero-crossings or peaks of the fundamental and harmonic should be used, and whether the these shifts should be expressed in terms of fundamental phase ϕ or harmonic phase $n\phi$. Based on some experience with plotting these quantities for stress-grading samples, stress-gradings and PD, the harmonic phase-difference between peaks has been preferred.

The choice of plotting relative magnitudes was initially quite obvious. Having decided on the less obvious choice of phase, the question arises of whether a rectangular form would be preferable. This is the preferred way for the fundamental components, but there the distinction of energy storage and dissipation is significant. No harmonic will dissipate energy together with the fundamental voltage.

To plot all seven available harmonics would cause troublesome proliferation of data, at least when plotting with several voltage levels together. For symmetrical objects the use of just odd harmonics, sometimes omitting the seventh as being small and noisy, is a natural way to reduce the data. A check can be made that the even orders are much smaller than the third.

Other methods combine several harmonics into a single value, such as the total harmonic distortion (THD) [Pau92] widely used to describe limits of waveform distortion for electrical equipment, or harmonic loss quality (HLQ) [Gof98] proposed as a measure of stator insulation condition. These have not been examined here, as the main desire is to visualise how a waveform or degree of nonlinearity varies with frequency and voltage; the harmonic order and phase must be preserved for this.

The third harmonic magnitude alone gives a good indication of the presence of nonlinearity, and it is unlikely that higher-order harmonics would be considerably larger than the third harmonic in the sorts of waveform expected from stator insulation.

Chapter 16

Effects of previous excitation on results

Interpretation of measurements usually involves comparisons. It is necessary to have an estimate of how much variation can be expected in the results due to causes other than fixed differences between test-objects or different measurement occasions. Here, attention is given mainly to how a particular test-object during one measurement may give varied results depending on its recent treatment, such as for example the order in which measurements are made. When using multiple amplitudes and frequencies this becomes particularly important.

16.1 Physical-system properties of stator insulation

The classic easy system for analysis in signals and control engineering is one that is static, linear, time-invariant and deterministic. Of the phenomena of interest in this work, none possesses all of these simplifying features, and some possess none of them! The dynamic nature of DR and PD phenomena, compounded by some of the other deviations from the easy system, make the results of measurements be dependent not only on the state of the insulation due to long-term irreversible aging that diagnostic measurements seek to determine, but also on the state due to other parameters and recent treatment such as the ambient temperature, the time since being in operation, and even the most recently applied stimuli used in the diagnostic measurement itself.

Being *static* implies that no knowledge of the past is needed to determine the present. When this is not true, a system is *dynamic*, having some sort of *statefulness* that preserves information; the initial condition of the dynamic state is needed in order to determine the response to an input. A simple example is the series RC circuit excited by a voltage source, where knowledge of the voltage on the capacitor is needed in order to determine the current into the circuit; the dynamic state is here linked to the energy stored in the capacitor, which depends on the history of the applied voltage to the circuit. A dielectric response function describes how the state imposed by electric fields throughout the history of the dielectric affects the polarisation at later times; the single number that sufficed to describe the initial conditions of the RC circuit is not sufficient to describe this polarisation state for the general case of a response function more complex than the Debye model. For PD the situation is far more complex, with many states that may significantly affect and be affected by PD: the temperature in a cavity's gas and surroundings, the presence in the gas of chemicals from surrounding surfaces, the density of electrons and ions in the gas or electrons trapped at surfaces. . . .

Being *linear* implies the validity of scaling and superposition: if an input signal can be represented as a sum of signals then the output is the sum of

the outputs for all of these signals. This makes possible the use of frequency-based rather than time-based analyses, studying any applied signal as a sum of sinusoids analysed independently. Only dielectric response of certain types of material at moderate fields can be said to be linear. Linearity is a reasonable assumption for the solid material of stator insulation at voltages below PD inception; it is certainly not true for PD phenomena, nor is it for stress-grading around the end-windings.

Being *time-invariant* implies constant parameters. A time-*variant* parameter might be seen as making up for a lack of detail in one's model of the system: time-invariance can only be claimed if the model includes enough external disturbing parameters such as temperature changes, and enough internal state variables such as self-induced temperature changes due to loss.

Being *deterministic* implies that in the presence of the same stimuli, the same initial conditions of dynamic state, and the same values of any time-dependent parameters, the same outputs will result. This is a very desirable property for permitting the effect of a controlled variable to be seen; one would like to be confident that two measurements with variation of just that variable, will produce results whose difference is due purely to the controlled variable and not to a lack of determinism. Physical systems will have noise in the knowledge of the 'input' conditions and the measurement of output, but in some cases the variation is of very little practical importance. At the macroscopic level of our models of DR, deterministic behaviour is a reasonable approximation, but behind a sometimes strong background of measurement noise and dependence on other factors such as statefulness. At the microscopic level of a single PD event, the crucial occurrence of an initiating electron by external natural causes can only be seen as non-deterministic (*stochastic*). The aggregation of many such events, in for example a specimen with thousands of cavities and with measurements made over thousands of cycles, serves to reduce the extremity of variation due to stochastic processes. Even within a PD object that is excited for long periods with a constantly repeating signal, changes in the PD behaviour can be seen [VB93][VB95][Lin09, p.65] on a timescale much more than a single cycle of the excitation.

16.2 Standard measurement practice

The dependence of DR and PD measurements on previous treatment and disturbing parameters such as temperature is recognised in standard measurement practice.

Time-domain dielectric response measurement by PDC [p.56] requires a long period of polarisation before depolarisation, or vice versa; the material's initial state must have come close to its equilibrium for all the timescale of the dielectric response function that is to be measured. For the 'IR' tests often made on stator insulation a discharging time at least four times the charging time is recommended between subsequent measurements [E43, p.12].

Frequency-domain dielectric spectroscopy sometimes delays measuring the current until the voltage has been applied for some cycles, in order that the material and measurement circuit should give currents close to the expected

equilibrium values as if the excitation had been applied for a long time before. The sequence of applied voltages normally used by the product family of the DS instrument used in this work goes up in amplitude, and down in frequency at each amplitude, which reduces the disturbance of the excitation on the next measurement.

The widely used power-frequency 'tip-up' tests are recommended [E286] to have test voltages of increasing amplitude, to be preceded by a *conditioning* period where an excitation close to the maximum voltage of the test is applied for some 20 s to 240 s, and *not* to be preceded by a 'hi-pot' test. For newly manufactured stator insulation that has not experienced PD, the conditioning (sometimes called a 'soak') not only warms up the insulation closer to the temperature it will achieve during the measurement, but also changes pristine cavities by generating PD that increases the surface conductivity and the ionisation in the gas [Eme05].

PD pulse measurements are often preceded by conditioning of the test object by exciting it with a voltage possibly even higher than that intended for the measurement. This can be done to make internal PD sources in a pristine test-object reach a relatively steady behaviour as in [For08a, p.29] or in the soak mentioned above for tip-up tests. It can be done for a shorter time to get the PD in an aged test-object to be a better approximation of the PD during sustained voltage application, for which [C3427, p.55] recommends five minutes at the highest test voltage. Steps in voltage amplitude should be held for some 10 s to get a reliable PD pattern [C3427, p.57].

> "Mechanical, thermal and electrical stressing just before the test can affect the result of partial discharge tests. To ensure good reproducibility, a rest interval after previous stressing may be necessary before making partial discharge tests."
> [C270, clause 8.2]

16.3 Varied amplitude and frequency

The relevance of these complicating features of DR and PD to the types of measurement considered in this work, where the excitation is a voltage with varied amplitude and frequency, is how best to condition the specimens and select the order, timing and repetition of the amplitude-frequency (V-f) points in order to get a suitable trade-off of measurement speed against usefulness of the result.

Measurements motivated by scientific interest in the physical phenomena, such as the modelling of PD in [For08a], will probably be aimed at results that best approximate the values one would obtain after either having had an applied voltage of the same amplitude and frequency for a long time, or having had no applied voltage for a long time. The notion of steady state is qualified here by 'relatively' because PD can vary so much even during long periods of constant excitation. There will always be some degree of noise in a measurement, but PD sources are particularly extreme in their noisy variation *and* in that they can show short and longer term changes and cycles.

Measurements for condition assessment do not so obviously require results that reflect 'equilibria'. The important link is the one between measurement

results and the diagnostic or prognostic conclusion. If this conclusion uses some sort of pattern recognition based on past results, then it is not obvious that a choice of measurement sequence and timing that gives results closer to the quasi-equilibrium values is any better than another choice, as long as the choice is applied consistently to all the apparatuses that are measured. For this sort of practical use, minimisation of the required measurement time will be an important aspect of the optimal choice.

This work, however, does not deal with pattern recognition of defects or failures, but more with physical sources of measured values; the quasi-equilibrium values will be assumed to be the most desirable result.

16.3.1 Example of effects of recent excitation on PD

A single, complete stator coil was used as a PD source for some measurements of the effect of recent excitation on a measurement. A series of PD measurements was made, each with an applied voltage of 9 kV and 10 Hz and run for 200 s. The time waited between measurements, with no excitation, was progressively reduced. The PRPD results are shown in figure 16.1, and the associated mean

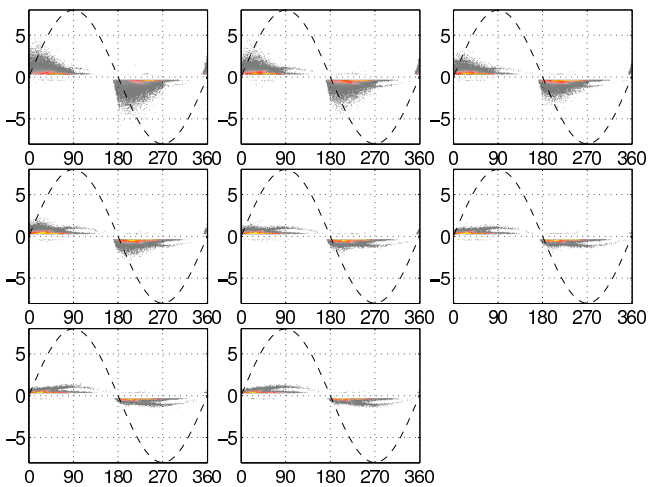

FIGURE 16.1: Phase-resolved PD patterns, to the same scale, for eight decreasing lengths of time between the last excitation and the measurement. All measurements are 9 kV, 10 Hz, 200 s. y-axis labels show PD apparent charge in nanocoulombs, x-axis labels show phase in degrees. The chronological order of the plots is left to right, top to bottom, and the corresponding off-times prior to measurement are 10000, 3600, 1800, 900, 300, 180, 60, 30 seconds.

PD currents are displayed with their fundamental components in the form of capacitance and loss in figure 16.2. It is notable that the high-charge PDs in the pattern increase greatly when the test-object has not had excitation for a long time, and that the extra capacitance value due to PD more than doubles between 30 s and 3600 s. Increases of some tens of percent have been seen when the previous excitation has been low frequency (1 mHz) rather than high frequency (20 Hz). The general trend and magnitude of the results are repeatable on

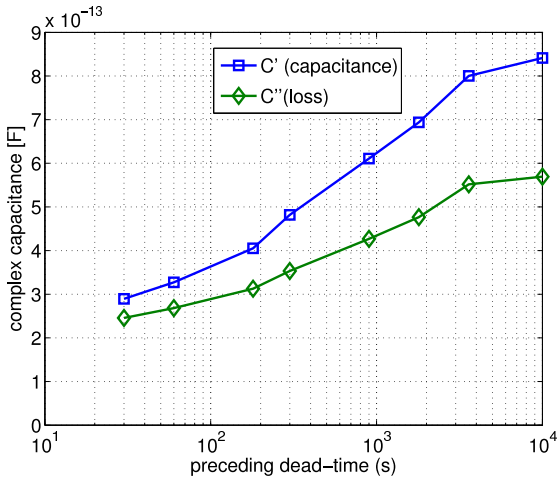

FIGURE 16.2: PD charges of the patterns shown in figure 16.1, shown as C' and C''. The order of measurement was with longest off-time first.

the same object, implying that the mechanisms of the statefulness is not just irreversible aging.

16.4 Recommendation for swept measurements

The choice of sequence for sweeping across multiple voltage amplitudes and frequencies is already established for the IDAX instrument and earlier versions as going up in amplitude, and on each amplitude going down in frequency. Among the possibilities for the simple cases where each desired point is measured without any waiting or other excitation in between, this choice does seem to be the best. For the relatively simple case of DS, the increasing amplitude makes residual polarisation be smaller relative to the measured point than it would be with decreasing amplitude. For PD measurement the effect of long polarisation may have stronger influence on a subsequent measurement at a high frequency: the linearity that simplifies treatment of DS measurements on solid insulators cannot then be assumed. Depending on the test object, the measurement of results that correspond well to long-time application of a particular voltage amplitude and frequency may require a considerable period of that type of excitation before measurement.

Chapter 17

Comparison of DS and PD measurements

The DS and PD methods of measuring PD apparent charge will give results with some differences and some similarities, depending on the form of PD [s.7.4] and on the test object and instrument [s.8.4]. Differences are of interest for the complementarity of the information about the PD sources. Similarities could be of interest if one wishes to remove the components of a DS measurement that are due to PD, or to measure PD charge distributions with just a DS instrument.

It has been shown in chapter 14 that the DS instrument can adequately record the current due even to quite large and fast pulses. This chapter compares results of PD and DS measurements of PD, on small canonical objects and a single stator coil in the laboratory. The PD currents from industrial measurements on whole stator-windings are then shown as an example of what a small contribution the measured PD pulse charges are to the total current in the insulation.

17.1 Comparison of DS and PD measurements on laboratory objects

Measurements on real PD sources were made using the objects shown in figure 17.1.

FIGURE 17.1: PD test-objects. Left to right: point-hemisphere, cavity (shown with the electrodes and insulating disks separated), stator coil

The first is a point-hemisphere corona gap, a type of object mentioned in [s.7.2.2] as an early form of calibration reference for PD measurement. The hemisphere has a 95 mm diameter at its open end, and 35 mm from the point to its apex; the point can only just be inserted in a 0.5 mm gap.

The second is a cylindrical cavity between a stack of three polycarbonate plates, like the ones described in [For08a, p.28]. Each plate is 1 mm thick, sandwiched between brass electrodes of 80 mm diameter; the middle one of these three plates has a hole of 10 mm diameter through its middle.

The third is a complete coil from a stator winding designed for operation in a 7.2 kV machine, further described in [Tay06, p.82]. Having been obtained in new condition it was subjected to some weeks of accelerated thermal aging at 180 °C, resulting in a large number of PD sources. Aluminium foil was taped tightly around the slot parts to provide electrodes suitable for the high frequencies of PD, which would have been heavily attenuated by the slot semiconductor layer alone; both ends of the multiturn coil were connected together to the HV input.

17.1.1 Point-hemisphere

This object is expected to be highly asymmetrical [s.7.2.2], with most PD pulses when the voltage on the point is negative. Measurements at 60 Hz for 5 s on the point-hemisphere gap show a negative corona with a very compact pattern, figure 17.2, due to the consistency of PD magnitude; only the negative parts are shown, as the few positive discharges seen started only at 8 kV and were too large to fit on a scale that showed the negative ones well.

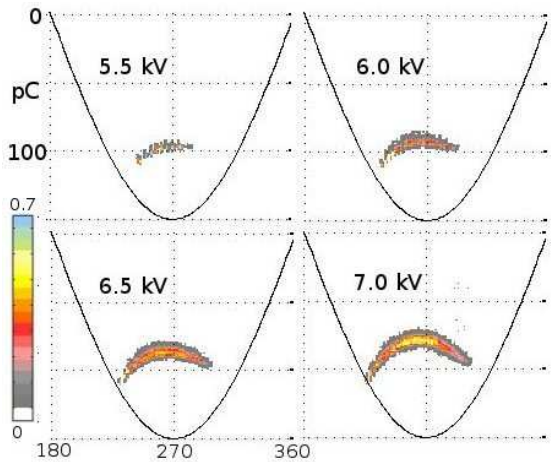

FIGURE 17.2: PDP for the point-hemisphere object with 5.5 kV to 7.0 kV, at 60 Hz, for 5 s. The 100 pC level is marked, and is the same for each pattern. The scale from 0 to 0.7 is for mean counts per cycle in each point of the PDP.

The total current was measured simultaneously by the DS instrument. To remove the components of the DS current that were not due to PD, a measurement was first made at a voltage well below the PDIV; in this case 2 kV was used. The values of capacitance and loss determined at the lower voltage were then used to calculate, by simple scaling, the current expected at the desired measurement voltage in the absence of the non-linearity of PD; this current was subtracted from the measured current.

This DS current is plotted in figure 17.3, along with the mean PD current calculated from the PDP. Two very similar curves are shown for the DS current: one, slightly higher near the origin, subtracted a fundamental component of current based on the fundamental-frequency voltage; the other used the fundamental-frequency capacitance at 2 kV together with each measured harmonic voltage, to subtract estimated harmonic currents. The harmonic

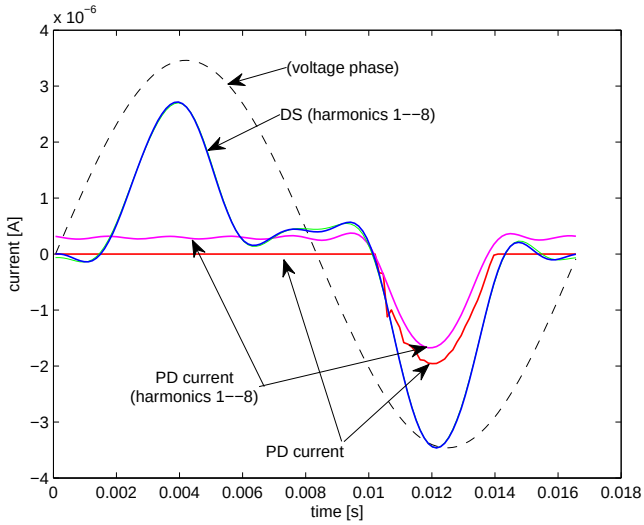

FIGURE 17.3: Measurements of PD currents for the point-hemisphere object, using the DS and PD instruments.

voltages are clearly so low in this case that the difference is negligible: at higher loading of the supply, with a larger test-object, this might not be true [s.6.2.3].

The PD current measured by the PD system is also shown after filtering in the frequency domain to remove components beyond the 8th harmonic; this was done for easier comparison of shape, as the DS system's output is limited to the first 8 harmonics.

The magnitude measured by DS is almost twice as great for the negative corona as the measurement from the PD system. How much this is due to deadtime and how much to errors in subtraction of the other currents in DS is not known. The filtered version of the PD current from the PD system makes clear that a strong asymmetry can be described in just eight harmonics, although with the artificial zero offset that is inevitable when omitting the dc term as the DS instrument does. This suggests that the considerable positive current, seen only in the DS measurement, is a genuine result that is missed in the pulse measurement; this is not surprising if non-pulsed drift can return some charges to the point when the polarity changes.

The point-hemisphere object is therefore a case with complementarity of DS and PD measurements, although the order of magnitude of currents is similar.

17.1.2 Cavity object

Measurements at 8 kV 60 Hz for 120 s on the cavity object gave strongly symmetric positive and negative parts, so only the positive part is shown, in figure 17.4. The spread of charge magnitudes is large. In the first case (a), the ICM's LLD threshold is at 4%, just above background noise, and the deadtime is at its minimum 5 μs: the pattern shows a strong cluster of pulses at the lowest charges, which are presumably subsequent oscillations, 'ringing', of the instrument's

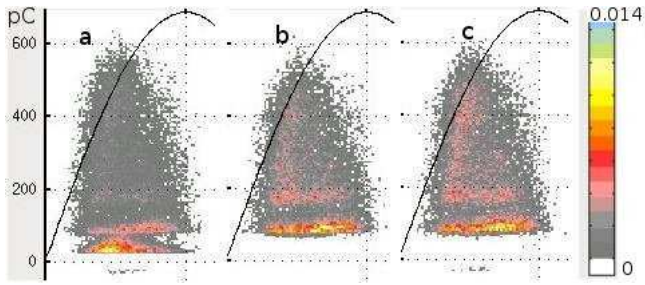

FIGURE 17.4: PDPs for the cavity object. See text for details. The coloured scale is mean counts per cycle in each point of the PDP.

response, not decayed enough in the deadtime. In (b) the threshold is 10%, still with 5 µs deadtime, removing the small pulses. In (c) the threshold is again 4%, but with 10 µs deadtime: the fact that the lower group of pulses disappears by either the deadtime or the threshold setting indicates that the small pulses were indeed artifacts of the instrument response.

The corresponding currents, and the measurement by DS, are shown in figure 17.5. The same methods have been used as with the point-hemisphere

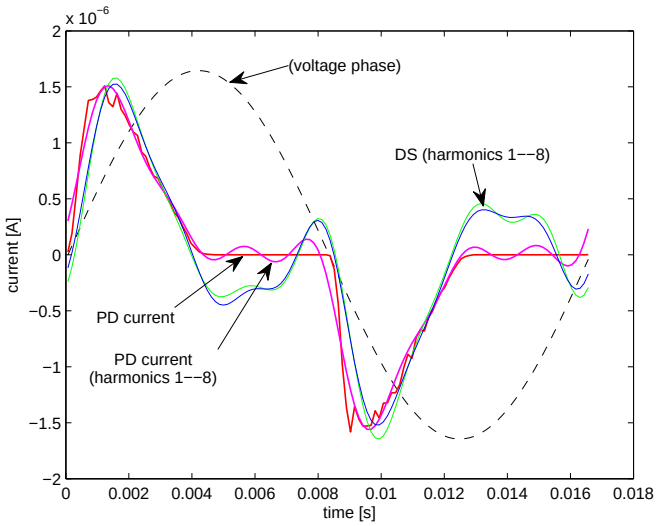

FIGURE 17.5: Measurements of PD currents for the cavity object

object, to subtract the non-PD components in the DS results and to plot a harmonic-limited (filtered) PD current for comparison. This gives remarkably close correspondence between the two measurements during the time of PD, although the filtered PD current makes it clear that poor fit around the zeros is not just an artifact of the limited harmonics in the DS results.

For this object, the DS and PD measurements therefore give similar rather than complementary results.

17.1.3 A single stator-coil

When making measurements on the stator coil of figure 17.1, the currents in the nonlinear stress-grading coatings in the end-windings were guarded away from the DS measurement, so as to include only the currents in the slot-parts of the coil. The usual method of estimating and subtracting the currents due to the object's capacitance was thereby made possible without resort to the vagueness of stress-grading models.

It should be noted that these results were made earlier [Tay06], with older instruments, and not simultaneously. It was however checked that PD behaviour was quite consistent between measurements, so that differences even of a factor of two would be very surprising.

Figure 17.6 compares the currents measured by the PD pulse and DS methods. In contrast to the two simple objects, the current from the PD pulse

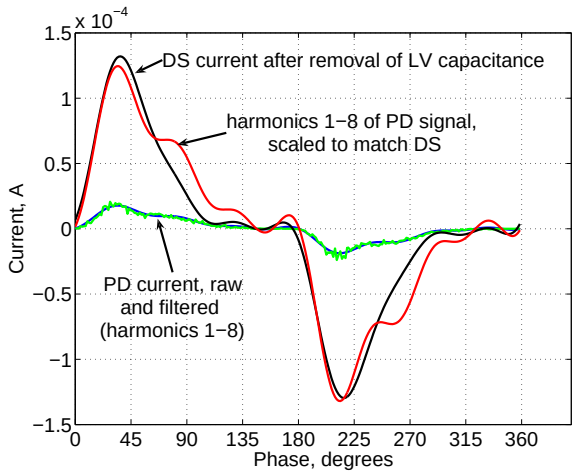

FIGURE 17.6: Stator-coil PD current from DS and PD systems

measurement has had to be scaled up by several times, to match the DS measurement.

Measurements at other frequencies are shown in figure 17.7. Large and *different* factors, marked on the graphs, were needed to make the amplitudes match. The waveforms all match well, but the amplitudes vary by up to 50 times, with the DS system measuring the larger currents. Note that if the estimated non-PD current subtracted from the DS system were severely wrong, so that this could be the main cause of the difference between the two measurements, then the resulting PD current would have a much more sinusoidal shape, since the subtracted component is practically sinusoidal.

These results strongly indicate that the PD pulse-measurement instrument is missing a lot of charge with this object, but the DS system is measuring it. This is no surprise, as even the single coil had a severe degree of aging and many, easily audible, PD sources. The necessary dead-time was 50 µs in this case, to avoid ringing from the relatively large object, so frequent PD from many sources

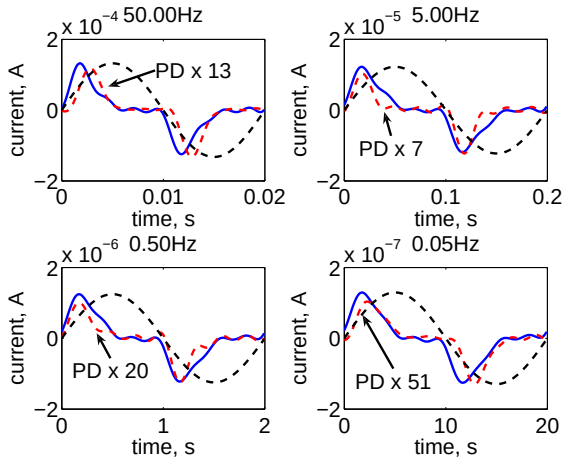

FIGURE 17.7: Stator-coil PD currents at varied frequency

would result in many missed pulses. It may be that some PD activity is also from sources that do not have a strongly pulsive form of PD.

The DS and PD results for this object are complementary.

17.2 Full stator-windings

PD measurement results were obtained from industrial offline measurements on whole stator windings of hydro-generators. The details of the generators are not well known for these example PDPs, but they are rated at about 10 kV and 10 MVA or more. The reported measurement voltages will be rms values, not the peaks used in the laboratory measurements. The data for C-tan δ tip-up measurements on a larger group of generators from the same source is shown in figure 6.4 [p.71].

The PDPs all appear to have strong ringing, where many pulses have been captured in the opposite polarity from where such PD would be expected. This is seen in figure 17.8. A deadtime of 10 µs was used, which would be low even for a small laboratory situation; using a longer deadtime would give the undesirable result of more missed pulses.

Removal of the apparent 'ringing' gives a PDP as in figure 17.9 which is suitable for estimating a PD current. The same has been done with a PDP that shows a more normal, healthy pattern, shown in figure 17.10.

The time-domain currents due to the above three PDPs are shown in figure 17.11. With the ringing included there is the expected cancellation of much of the current. Without it, the shapes of the PDPs show clearly in the time-domain current, so that in these cases at least the two PD sources could easily be distinguished by shape. The highest current is seen as about 10^{-4} A. Bearing in mind the typical capacitances of generator windings, of the order of 1 µF, the current being supplied to the insulation in this 10.5 kV and 50 Hz measurement is likely to be 1 A or more. Typical changes in C' and tan δ are some one or

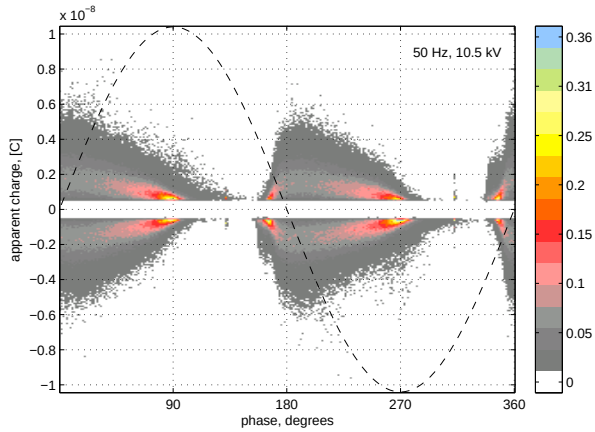

FIGURE 17.8: The raw data measured on a machine showing classic signs of slot-discharge. Counts (scale given on the right) are per-cycle.

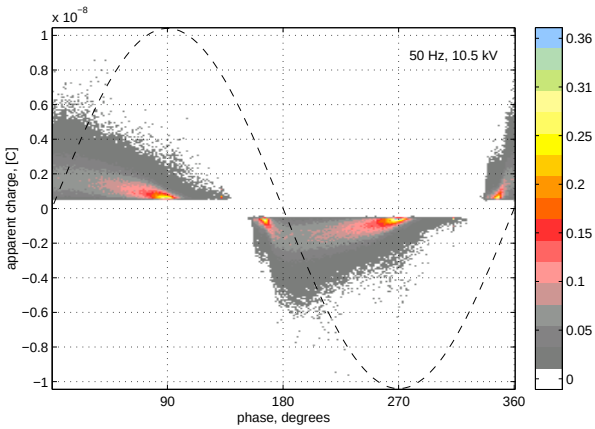

FIGURE 17.9: PDP for slot PD, as in figure 17.8, but with all pulses considered as 'ringing' removed.

few percent, based on figure 6.4. The increase of current due to the 'tip-up', generally considered to be a mixture of PD and stress-grading, is thus some hundred times larger than the current due to the measured PD pulses.

On these objects of whole stator-windings, the extremely approximate calculations based on generic capacitances and tip-ups, suggest that probably the PD current from DS and PD-pulse measurement differs by tens of times or more, which is the expected situation of complementarity of the measurements. There is no detail about waveform in the C-$\tan\delta$ results, and they are neither for the exact same machine nor measured at the same time: a study of whether the waveforms seen from PD-pulse methods and DS methods can have substantial differences will require some field measurements using the DS and PD

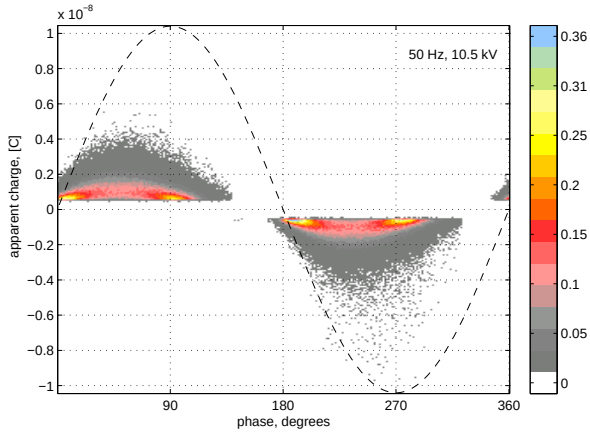

FIGURE 17.10: PDP for a 'normal' stator winding. As with figure 17.9, this has had quite similar clusters of pulses with opposite signs removed.

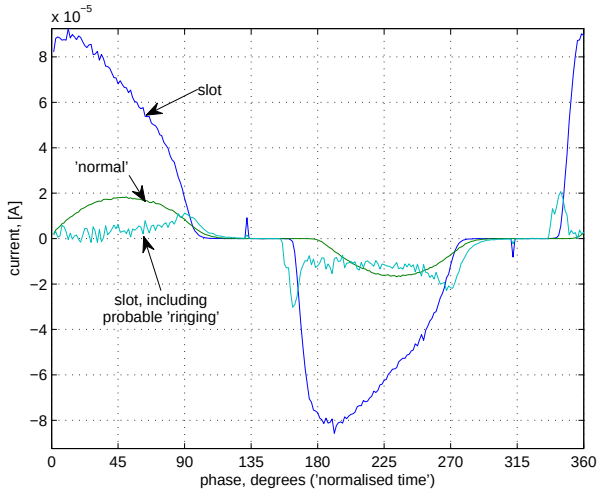

FIGURE 17.11: Mean currents due to the PDPs in figures 17.10 (normal), 17.9 (slot-PD), and 17.8 (slot-PD, including 'ringing').

instruments together.

Chapter 18

Stator coils used as test-objects

Several newly manufactured multiturn coils were obtained for measurements of material properties, end-grading currents and thermal aging. Three of them were used for measurements reported in this work. This chapter describes the coils and the oven made for heating them, and presents results from dielectric measurements made on the main insulation. Material properties of the end-winding stress-grading are presented in chapter 20, and the contribution of the end-windings to the total dielectric response is presented in chapter 19. Measurements of DS and PD on an earlier batch of coils after strong thermal aging have been described already in [Tay06].

18.1 Construction

Three coils were manufactured to the same specification, in the same batch. After VPI and curing, each of the three coils was sawn through at its extreme ends, to make two coil-halves (hereafter called bars) for easier handling and separate testing. The six bars are shown in figure 18.1.

FIGURE 18.1: Left: all six stator-bars, showing half the slot-section and part of the end; in the background are the two bars without metal plates, for material measurements. Right: end-view showing strands before (top) and after (bottom) connecting with conductive paint.

The conductors in the coils were 6 turns of 4 parallel copper conductors (strands), in two stacks; the bars therefore have two stacks of 12 separate strands. For measurements the strands were all connected together at both ends. A copper wire was stretched across between the stacks, and a silver-based conductive paint was used to connect all the surfaces to each other and to the wire; soldering even with a blowlamp was infeasible because of the high thermal conductivity of the copper.

Two of the coils were kept with the normal construction, but had two metal L-section plates applied along each slot section and bound hard with heat-shrink tape before VPI, as an approximation of a stator core. The plates and pressure reduce swelling of the mica paper with the impregnant when put through VPI without being in a tightly-fitting stator slot; they also make the construction more realistic than using just a metal tape or wire as the earth electrode when doing DS or PD measurements or accelerated aging. The four bars from these coils have been named `C1l`, `C1r`, `C2l` and `C2r`. They have been used for measurements of the dielectric response of complete bars [s.19.5.2], and are intended for later experiments with aging. Figure 18.2 shows the dimensions of the bars, based on a half-length. The region covered with slot semiconductor

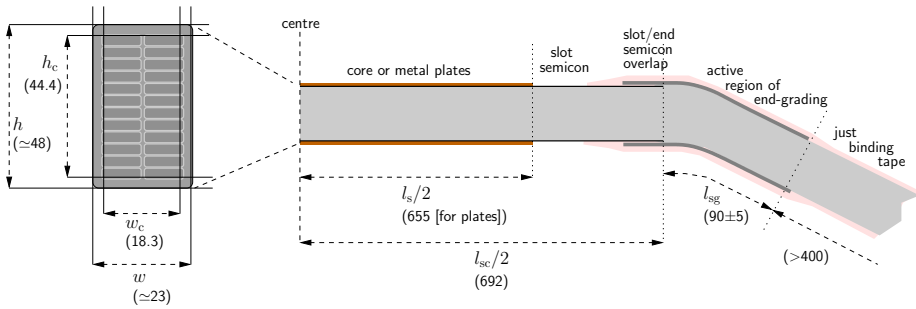

FIGURE 18.2: Constructional details of the new coil-halves. All dimensions are in millimetres.

is 1384 mm long. The metal plates are 1310 mm long, very close to the design slot-length. The *active length* by which the end-grading extends beyond the slot semiconductor is 90 mm (± 5 mm), which extends around the bar's curve. The end-winding region beyond the end-grading goes on for nearly 500 mm. An insulating outer binding-tape covers the whole end-winding region apart from a short distance of slot semicondutor at the end of the plates. Design-distances h_c and w_c between the external copper faces of the conductor bundle are 44.4 mm × 18.3 mm. The outer dimensions of the cross-section after curing were judged by measuring between opposite surfaces of the metal plates at several points and subtracting a 1 mm thickness for each plate: this gave estimates as $h = 48$ mm and $w = 22.4$ mm.

On the remaining coil, one bar was used for multiple samples of stress-grading material, described further in [s.20.3], and the other bar was used for guarded measurements. This guarded bar did not have metal plates applied, since measurements of slot semiconductor properties were also of interest. Guard-gaps of about 1 mm width were cut into the slot semiconductor before VPI, close to the stress-graded ends. Between centres of the guard-gaps the length of slot semiconductor was 1340 mm. The cross-section on the outside of the slot-part of the bar was about $h = 48.5$ mm and $w = 23.5$ mm, but was not very consistent along the length, partly due to excess epoxy on the outside. The circumference was about 134 mm, which is of interest for calculations of conductivities measured along the bar.

18.2 Heating

Earlier work in this project used severe thermal aging to change pristine stator coils into intensely PD-infested test-objects, as reported in [Tay06]. This involved time-consuming transportation to and from a borrowed oven of large enough size in another town. It was hard to make progressive measurements during aging, and was clearly not a reasonable long-term approach. A large oven was instead built in the laboratory, to permit versatile work with aging.

An aluminium box of 2.5 m × 1.25 m × 0.75 m was built, and was insulated on all faces with rockwool of 45 mm thickness, surrounded by an outer layer of aluminium foil to reduce air movement and radiative loss. The outside and inside are shown in figure 18.3. Four hot-plates from the top of a domestic

FIGURE 18.3: The large laboratory-oven for thermal aging. On the left, with and without the lid and its insulation. On the right, four normal bars and two material-sample bars are in place, and heater elements are visible at the right.

cooker were used as heaters; they were placed along the base of the box at one side, connected with wires insulated with silicone-rubber. Wire-mesh baskets were placed along the other side as shelves for the test-objects, which thus rested at about half the height of the box, at the other side from the heaters.

The heaters each had three available resistances; connections were chosen to give two groups, of powers 1.6 kW and 2.1 kW, with the four heaters contributing quite similarly to each. The 1.6 kW group alone gave an equilibrium temperature of about 160 °C. Warm-up from room temperature to 180 °C took just under an hour with both groups together. A domestic oven-thermostat was used for temperature-control. Depending on the required temperature, either

or both of the groups could be connected to the thermostat or directly to the supply, to minimise the rate of temperature change due to thermostat hysteresis.

An electronic thermometer was used to measure temperatures at a probe placed on the test-objects. The temperature varation measured at this point, due to the thermostat's hysteresis, covered a band of about 5 °C. With regard to requirements for accelerated aging in [E434], this variation would be within the required ± 3 °C , but the oven currently lacks the required forced air-movement and is not 'ventilated'. Before doing highly accelerated thermal aging it would be good to have an internal fan for more even temperature-distribution, and to have a shield to prevent direct radiative heating of the bars.

The main intended use of the oven was in experiments with progressive aging on multiple bars, making regular DS and PD measurements and endurance tests; these experiments have not yet been performed. The oven has however been useful for gentle post-curing of newly manufactured insulation and stress-grading materials.

18.3 DS measurements on the guarded slot-part

DS measurements were made on the slot-part of the guarded bar, with the end parts guarded out of the measurement. The raw results are shown in figure 18.4. As well as a clear order-of-magnitude change in loss over the six-

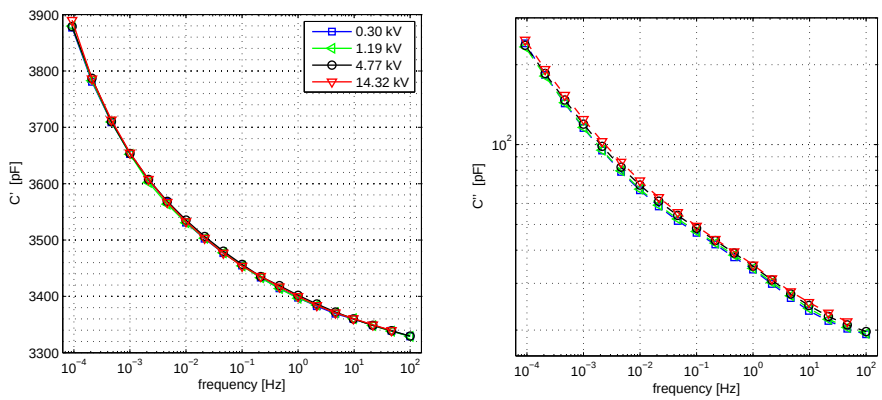

FIGURE 18.4: The direct, measured fundamental-frequency results for the guarded slot-part.

decade frequency-range, there is a distinct nonlinearity apparent in the loss, with curves rising slightly towards higher voltage. As the bars are fresh from production, it may be that they will become more linear after further curing.

In figure 18.5, the same results are shown after calculation of $\Delta C'$ based on a C_∞ found simply by adjusting a number until the result was as straight as possible between the extremes of bending downwards at high frequency (subtracting too much) and bending up away from the straight line to a constant value (subtracting too little). The value found was 3250 pF, and changes of 50 pF either way gave a noticeably worse result. The $\Delta C'$ is seen to be very straight except for a tip up towards low frequencies in the lowest decade. The

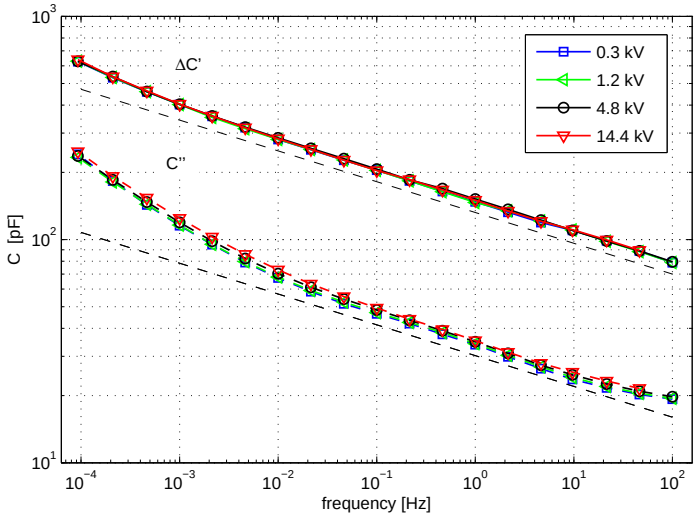

FIGURE 18.5: The results from figure 18.4, with an estimated $C_\infty = 3250\,\mathrm{pF}$ subtracted from C' to give $\Delta C'$, and with straight power-law relations of slope -0.138 shown as dashed lines just below the curves.

loss shows a large tip in the lowest two decades, and a flattening towards high frequencies in the highest decade. The high-frequency effect may be explained by series resistance in the outer electrode of semiconductor, since the metal tape used as the earth electrode only ran along one side-surface of the bar rather than enclosing it; the effect was reduced by further conductive tapes. The low-frequency effect apparently involves the capacitance as well as loss.

The gradients of the straightest parts of the $\Delta C'$ and C'' curves were found to be respectively -0.138 and -0.140 as the visual best fits. These gradients are shown by the black dashed lines just below the two sets of curves

Taking the *ratios* of $C''/\Delta C'$, equal to χ''/χ' if neglecting conductivity, at two frequency points (1 Hz, 10 Hz), gave respectively 4.31 and 4.46. Using 4.35 as a compromise value, the exponent n in the fractional power-law $(\mathrm{i}\omega)^{n-1}$ is $n \simeq 2\ \mathrm{acot}(1/4.35)/\pi = 0.86$, from (5.13). Judging n from the gradients, which both round to -0.14 to two significant figures, $n = 1 - 0.14 = 0.86$.

Figure 18.6 considers the apparent nonlinearity more carefully. There is, as was thought by looking at earlier plots, much more voltage-dependence in the loss, C''. When using C' instead of $\Delta C'$, the voltage-dependence of C' is of course much less still, as a constant capacitance of at least ten times the size of $\Delta C'$ has thus been added. The voltage-dependence in C'' is the only one with a consistent, practically (except at the very lowest frequencies) monotonic effect of voltage.

It was wondered if the nonlinearity might be due to the material being new and not fully cured. The bars were exposed to 120 °C for four weeks in the oven, finishing with one day at 150 °C. The results of re-measuring are shown in figure 18.7, along with the old results. The variations after this heating are

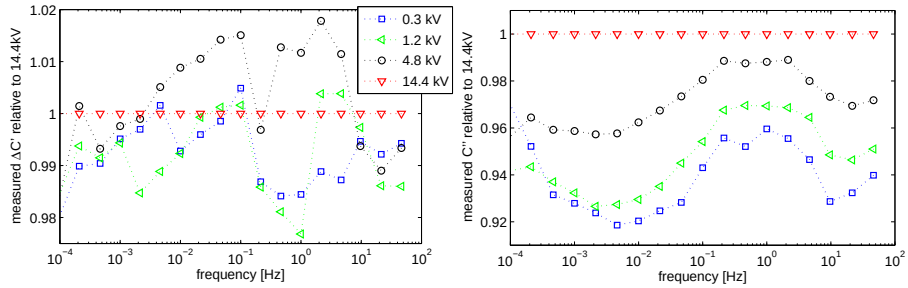

FIGURE 18.6: For $\Delta C'$ and C'', the ratios of the curves at all four voltages to the values obtained at the highest voltage.

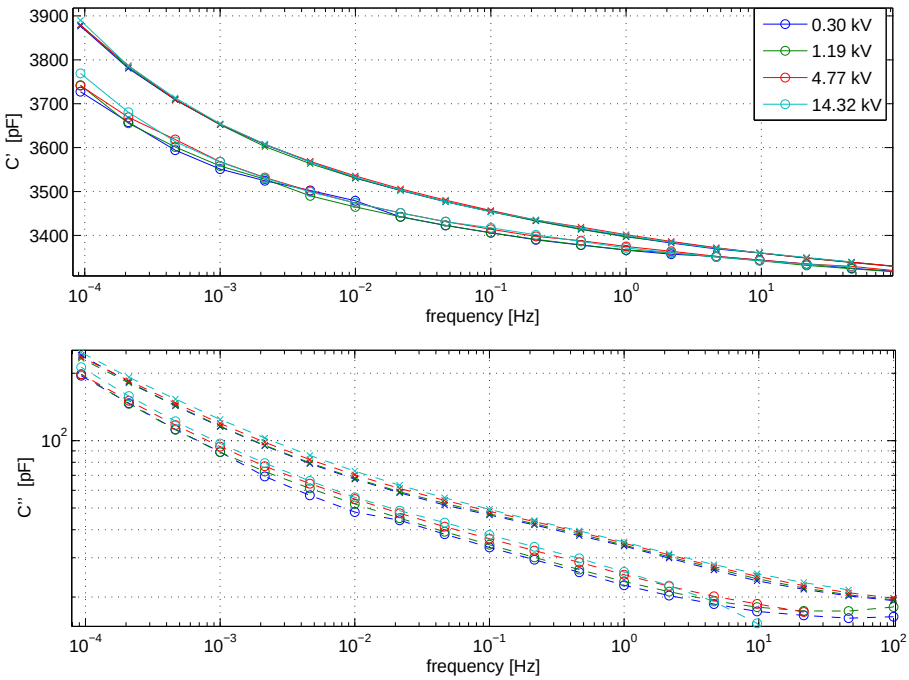

FIGURE 18.7: Capacitance and loss for the guarded slot part, before (x) and after (o) 'postcuring' at about 120 °C for four weeks.

even somewhat larger, although not so consistent. A measurement on a 100 pF gas capacitor using the same connections showed no clear trend with voltage, so it does seem likely that the bar is the main source of nonlinearity. Compared to the effect of the stress-graded end-windings, this is very small variation with voltage, but it is interesting to know that the linearity might be a problem if wanting to make sensitive measurements of PD current by DS methods.

Chapter 19

End-grading currents

It has been seen in section 2.1.3 that in high-voltage stators a material of high and nonlinear resistivity continues on the outside of the end-windings for some centimetres beyond the end of the slot semiconductor. The currents that flow in this material during some electrical diagnostic measurements impose a considerable disturbance on the results. This chapter considers measurements and models of how the capacitance, loss and harmonic currents seen in DS measurements due to the end-windings depend on the amplitude and frequency of the applied voltage. Models for the nonlinear material are studied separately, in chapter 20.

19.1 Stress-grading methods

In figure 19.1 a generic *truncated electrode-dielectric*† construction is shown, with permittivities appropriate to stator insulation with surrounding gas. Around the truncated edge of the upper electrode the electric field at the surface will be much higher than at points further away from the earth-potential. With the 'fluid' material being probably dielectrically weaker than the solid, there may arise PD at this edge.

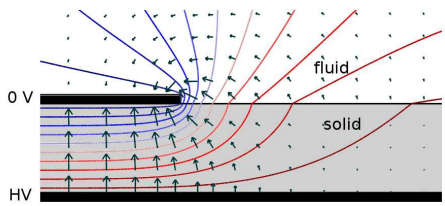

FIGURE 19.1: Electrostatic field around a truncated electrode-dielectric system *without* stress-grading. Equipotential lines are at 10% intervals. The arrows show the electric field E at the point where their tails start; their length is proportional to the field-strength. The 'solid' insulation has ε_r=4.5 (epoxy-mica) and the 'fluid' insulation has ε_r=1 (air).

An instance of this type of construction is terminations of high-voltage cables, where the earthed screen is cut back to end some centimetres from the exposed conductor; this avoids a strong field at the end of the cable where the insulation stops, but it causes a strong field across the insulation surface around the edge of the screen. This field has to be graded, to spread the change in potential more gradually along the insulation surface: methods include dielectrics with specially chosen geometry, and layers of nonlinear resistive material [Mår00].

† This conveniently expressive and short description is found in [Dav07] and in the conference paper from 2005 on which it builds.

In stator windings the insulation of the end-winding region is particularly sensitive; there are hand-made joints made between the ends of coils or bars and possibly their cooling pipes too, and there is a consequent difficulty of avoiding substantial voids where tapes have not fully come together and impregnant has not totally filled the space. From [Sto04, p.26], "Decades of experience shows that even a fully insulated connection between adjacent coils will be a weak spot that may prompt a future insulation failure if a ground potential is nearby". The earthed slot-semiconductor therefore ends a short distance beyond the core, to allow the outer surfaces of the end-windings to be at floating potential.

For machines rated above some 5 kV the surface electric-field could cause PD, particularly in machines operating only at atmospheric pressure. Space is particularly scarce in stator insulation, so external geometric grading of the field is not practicable. Some early machines used floating conductive layers *within* the insulation [Sto04, p.26], as is common in bushings; there is renewed interest [Sha08] in such methods to cope with high-frequencies in motors used in IFDs [s.7.3.1]. However, most machines currently in operation beyond about 5 kV use a thin layer of nonlinearly resistive material around the bar's surface for some centimetres beyond the end of the slot-semiconductor; some 5 cm to 10 cm is common [Sto04, p.26].

19.2 Cylindrical laboratory-models on PTFE

Simple gradings were made in the laboratory to study as purely as possible the effects of the grading material and geometry. A PTFE (polytetrafluoroethylene) tube was fitted tightly around a longer metal pipe, and an outer electrode of copper tape was applied for a short distance along the middle of the tube's length. The surface of the tube beyond the outer electrode was coated with one of two types of commercial stress-grading material for stator end-windings, a paint or a tape. A cross-section is shown in figure 19.2.

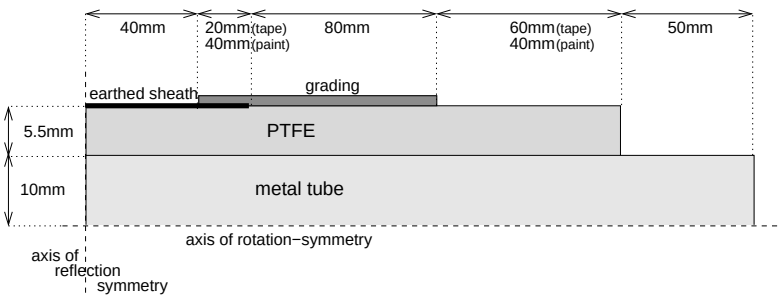

FIGURE 19.2: A quarter cross-section of the simple physical models.

The cylindrical shape was chosen for convenience of assembly and for easy analysis. The PTFE insulation was chosen for ease of handling, tolerance of the required two hours at 160°C for curing resin-based grading tapes, and for its low dispersion in our frequency range such that it can reasonably be regarded as having a fixed permittivity. The two-ended construction was used to prevent PD or leakage that could occur if one end were left open. The middle section

with the copper tape electrode was needed for the measurement connection, for providing the manufacturer-prescribed overlap distance of the stress-grading material along the electrode, and to give a realistic field-distibution around the start of the grading; this section adds a near-constant capacitance to the measured value.

Two bars were made for of each of the two materials, as a simple check of variance. There was not a strong difference seen between the behavior of the duplicates: the taped ones were very similar, and the painted ones had variation that would easily be explained by the variation of the paint's thickness. One bar with each type of material is shown in figure 19.3. Only results from the bar

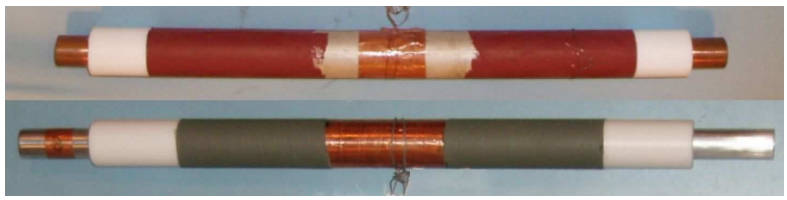

FIGURE 19.3: PTFE tubes with gradings using paint (top) and tape (bottom).

using the tape are shown in this paper, as they had better-defined properties and the higher conductance caused more of the details of the response to occur in the frequency-range of interest; the painted bars' responses were shifted some two decades to lower frequencies.

19.3 Spectroscopy Results

Frequency-domain dielectric measurements were made on the laboratory models using the IDAX instrument and its external 20 kV amplifier. A bar was suspended in the air, and one end of the inner tube was connected to the high-voltage supply. The measurement cable leading to the instrument's electrometer was connected to the middle of the outer conductor.

The capacitance and loss measured for a simple taped object are shown in figure 19.5. The IDAX instrument was used: at each amplitude and frequency point it maintained the voltage for long enough to take three consecutive measurements of the greater time of 1 s or 1 cycle; it was checked that the second and third were very similar, and the results from the third were used; the first was expectedly quite different, on account of the turn-on and previous excitation.

19.3.1 Fundamental-frequency components of current

In order to obtain the currents in just the graded parts, the capacitance measured between the outer electrode and the inner tube, before application of the stress-grading material, was used together with the applied amplitude and frequency of the voltage to calculate the current to subtract from the measurements. This subtraction is important not just to make the changes more visible but also to emphasise some fundamental relations of C' and C'' in the 'dielectric response' of the grading's current.

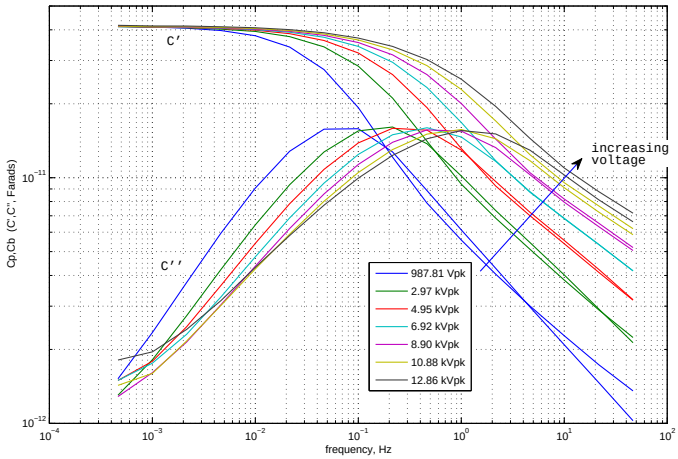

FIGURE 19.4: Fundamental-frequency components measured for bar5 (taped).

Several distinctive features can be seen. Towards low frequencies the capacitance tends to a constant irrespective of the amplitude of the voltage. This constant value is the capacitance of the PTFE insulation along the full length of the gradings: at low enough frequency the zero-potential from the electrode at the start of the grading has spread all along the grading, because the impedance of the capacitive insulation is so high at the low frequency.

The loss curves have peaks that are shifted up in frequency and very slightly down in value, with increased voltage. A primitive description of the grading as a series RC circuit with a resistance that decreases with increased voltage, suggests that this shift to higher frequencies, i.e. to lower time-constants RC, with increased voltage is reasonable. At frequencies above the loss peak the capacitance and loss tend to straight lines: for the lower voltages these lines are not only parallel but are indeed superposed. More attention is given to this later, when discussing models.

19.3.2 Harmonic currents

When the measured object is significantly nonlinear, as is the case here, the fundamental-frequency components of current in response to the sinusoidal applied voltage are only a part of the object's description. The harmonics in the current give an idea of the nonlinearity. Even-order harmonics are not expected, as the object has symmetric properties with respect to polarity: the magnitudes of the all even harmonics in current were well below the 7th harmonic shown here. The third harmonic reaches 15 % of the fundamental, and its relative value has much more dependence on the frequency than on the amplitude of the applied voltage over the reasonable dynamic range of these two parameters.

19.4 Numerical Models

Some previous users of a (1D) 'transmission-line' model are listed for applications to cable terminations, in references 5 – 10 of [Lup96] and to stator end-windings in references 38 – 41 of [Dav07].

Other forms of model include an assumption of $i(t) \propto t^{-1/2}$ for the end-grading current in time-domain spectroscopy [Gof00], and a model based on a 'perfect' sharp nonlinearity such that the material is insulating below a certain field, then prevents any further rise of the field [Kel67], developed further into expressions for FDDS results in [Pin98].

The numerical model that is used at the end of this section is based on a one-dimensional distribution of parallel fixed capacitance and nonlinear series resistance using the material properties described in chapter 20. This type of model has been used in other work cited in the previous section, in studies of stress-distribution and heating at high frequencies. On the way to this model, several steps of detail are used, explaining the causes of the features noted about the experimental results for C' and C'' as functions of voltage amplitude and frequency. The models consider a single grading, one end of the tubular laboratory-model.

The basic features of the results from the four levels of model are shown in figure 19.5. The models are explained, and their results studied, in the following subsections.

19.4.1 Linear, discrete

A very simple model of the grading is a single discrete resistance and capacitance in series. The current into this arrangement, seen in the usual form of capacitance and loss, gives the classic Debye response. As the model is linear there is no voltage-dependence of the curves. As a simple first step to modeling the nonlinearity, the resistance is varied instead, depending on the applied voltage amplitude. Only the 'tape' grading material is used, as it had so much more consistent properties than the paint.

As an example a capacitance of 21.3 pF was used, which is the total capacitance of the PTFE tube under the 80 mm length of the grading, excluding fringing. A resistance of 145 GΩ was chosen, which is the zero-field resistance of the 80 mm grading length.

Towards high frequencies the slopes are much too steep, compared to the experimental results, being Debye slopes where C' and C'' fall off at slopes -2 and -1 'decades per decade'. The experimental results had both slopes around -0.5 at low voltages, and at higher voltage they were even shallower. Towards low frequencies the electric field in the grading is so low that the conductivity is near its zero-field value and is not much dependent on the applied voltage. The experimental results show this in that the loss curves at different voltages converging towards low frequency; the fixed resistance used here for each applied voltage cannot show this effect.

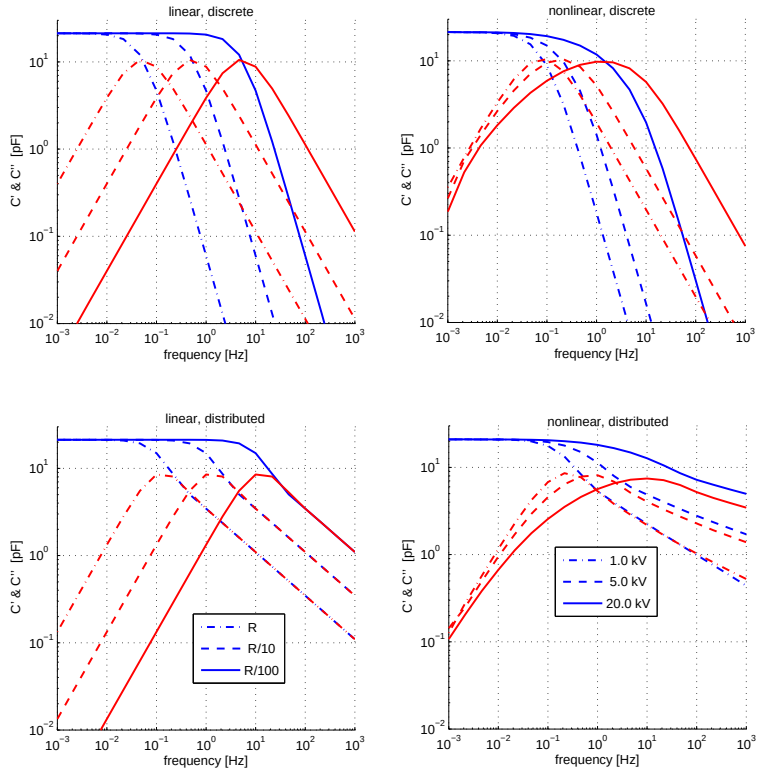

FIGURE 19.5: Capacitance and loss corresponding to the fundamental components of grading currents, for a one-dimensional numerical model with all four combinations of discrete or distributed components, linear or nonlinear.

19.4.2 Linear, distributed

The linear discrete model, above, can have more and more RC sections joined to each other, to make a network of sections having series resistors and parallel capacitors.

The result then tends to the distributed case, looking more like the experimental results at the higher frequencies. When the frequency is high enough that a single discrete section has a significant part of the voltage dropped across it, the results tend to the discrete model.

For the linear case it is easy to solve the distributed model, using the generalised transmission-line equations in the frequency-domain, which permit arbitrary complex values of series impedance and parallel admittance in each elemental length of the line [Che89]. Several previous users of this method are listed in [Dav07]. It is described there and in [Tay06].

The grading is a short length of transmission line, with a sinusoidal voltage applied at its near end and an open circuit or lumped capacitance at its far end. The parallel admittance is $Y_\mathrm{p} = j\omega C_\mathrm{p}$, where C_p is constant and real

to a good approximation for PTFE. The series impedance $Z_\mathrm{s} = R$, to which one may wish to add a parallel capacitive component for the higher frequencies where the conductivity of the grading material is not dominant over the effective permittivity in the grading material and the parallel air and solid insulation. The situation thus described is diffusion rather than the wave-propagation that occurs when there is significant series inductance. with typical grading parameters the speed at which the applied voltage travels along the grading is very slow, as is seen from the experimental results that show the low frequencies, and therefore the long periods, which the applied voltage must have before the end of the grading becomes significant and causes C' to stop rising.

The desired output value from the model is the current into the distributed network. The closest standard transmission line value [Che89] to the input current or the complex capacitance is the input impedance Z_in,

$$Z_\mathrm{in} = Z_0 \frac{Z_\mathrm{end} + Z_0 \tanh(\gamma l)}{Z_0 + Z_\mathrm{end} \tanh(\gamma l)} \tag{19.1}$$

where l is the length of the line (grading), Z_end is the impedance terminating the far end, and the characteristic-impedance Z_0 and propagation constant γ are given by

$$Z_0 = \sqrt{\frac{Z_\mathrm{s}}{Y_\mathrm{p}}} = \sqrt{\frac{R}{\mathrm{i}\omega C}}$$
$$\gamma = \sqrt{Z_\mathrm{s} Y_\mathrm{p}} = \sqrt{\mathrm{i}\omega C R}$$

in which R and C, and therefore Z_s, Y_p and γ, are all values per unit length. In a simple open-ended model (19.1) needs to be cancelled to

$$Z_\mathrm{in} = \frac{Z_0}{\tanh(\gamma l)} \quad (\text{when } Z_\mathrm{end} = \infty) \tag{19.2}$$

Any function of frequency can be used in Z_s and Y_p. For example, C may be a complex capacitance, or a capacitance may be included in parallel with R. The simple RC case is treated here, since it extends the linear discrete model in just one way. The complex capacitance is found as

$$C' - \mathrm{i}C'' = \frac{1}{\mathrm{i}\omega Z_\mathrm{in}}, \tag{19.3}$$

which for the open-ended case is

$$C' - \mathrm{i}C'' = \sqrt{\frac{C}{\mathrm{i}\omega R}} \tanh\left(l\sqrt{\mathrm{i}\omega C R}\right). \tag{19.4}$$

The results from this model are shown using the same R and C values as for the linear discrete case, distributed over the 80 mm length of the grading.

There is much better fit to the experimental results around the high-frequency parts. The reason for the slope of -0.5 is clear from (19.4), where the tanh

term tends to a real value of 1 as its argument grows, and the other term includes $1/\sqrt{\omega}$ to give the slope, and $1/\sqrt{\mathrm{i}}$ to split this equally between real and imaginary parts. This special case of the 'universal law', with $n = 0.5$, is true for any infinite network of constant series resistance and parallel capacitance, regardless of the values R and C [Jon83, p.80].

For the finite length of our practical case, the infinite network is a good approximation as long as the potential from the input end doesn't significantly change the potential at the far end. In the low-voltage experimental results this is true down to about 1 Hz, but then the end of the grading starts to be reached by the diffusion within each period of the applied voltage, and the results become similar to the linear discrete case, deviating considerably from those in the measurements. The linear discrete and distributed cases differ from each other too at the low frequencies, as the effective resistance is higher in the discrete case where the total capacitance was lumped at the end of the total resistance. This could be improved by scaling the resistance, but these simplest models were only intended to give qualitative comparions.

At high voltages the material behaves sufficiently nonlinearly that it does not so strongly show the power-law $n = 0.5$ response: the values of C' are shifted higher than C'', and the gradient is less steep, both of these features corresponding to $n > 0.5$. The grading no longer can be modelled as having its parameter R constant along its length.

19.4.3 Nonlinear, discrete

The effect of nonlinearity, but without the distributed RC nature, can be seen by replacing the discrete resistor with a conductance with voltage-dependence following the material conductivity equation such as (20.3). The total capacitance and total zero-field series resistance of the 80 mm grading were used, as in the linear discrete model.

With a sinusoidal applied voltage v_{in} across the series-connected capacitance C and nonlinear resistance of zero-voltage resistance R, the voltage v_{c} across the capacitor is the state-variable in an ODE,

$$C\frac{\mathrm{d}v_{\mathrm{c}}}{\mathrm{d}t} = (v_{\mathrm{in}} - v_{\mathrm{c}})\,\frac{1}{R}\exp\left(n\,|v_{\mathrm{in}} - v_{\mathrm{c}}|^{2/3}\right). \tag{19.5}$$

This was solved numerically, using the `ode45` ODE solver in Matlab 7.5. The current into the grading is provided by the same solution, as it is the right-hand side of (19.5). The initial condition was $v_{\mathrm{c}} = 0$; the calculation was run for four cycles to reach an equilibrium, then 32 values of current at evenly spaced times were taken from each of the next two cycles. An FFT was performed to obtain the capacitance and loss as well as the low harmonics. The whole calculation was repeated over a range of amplitudes and frequencies of v_{in}.

Towards higher frequencies the excessively steep gradients are seen, as in the linear discrete model. The heights of the loss-peaks do show a slight increase at lower voltages, as in the experimental results. The main improvement that has happened here, compared to the linear discrete model, is the convergence of the values of C'' towards low frequency; the nonlinear model has less voltage across the nonlinear resistance when at lower frequencies.

19.4.4 Nonlinear, distributed

The final level of one-dimensional model combines the properties of nonlinearity and distributed parameters.

As well as R_s and C_p, which have been used in the previous models, there are optional components that represent permittivity of the grading and its surrounding in C_s, loss in the insulation in G_p, and discrete components at the end to allow for fringing of the field or conductivity there. The possible components are shown in figure 19.6, in a general form for discrete or continuous models.

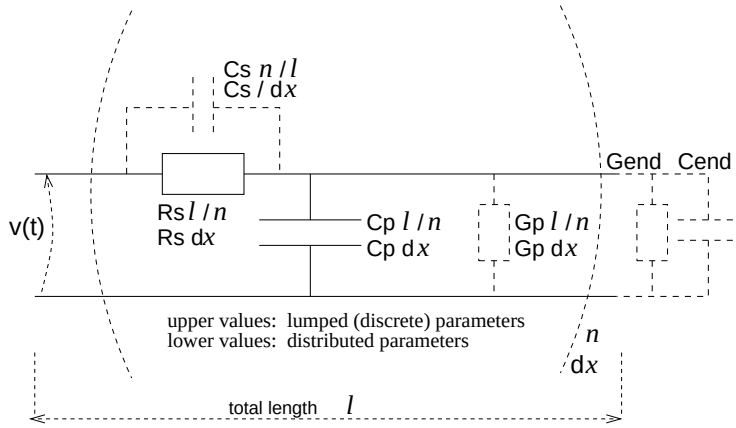

FIGURE 19.6: Components of 1D grading model

Variations on all of these components, including nonlinearities in the lumped conductance at the end, have been tried, along with variations in the material model's parameters. No single change had a large benefit to the fit to the measured results without also worsening the fit in other parts of the range of frequencies. The simple model using just directly measured dimensions, and material properties measured on samples on PTFE tubes [s.20.2] has therefore been taken here, rather than arbitrarily adjusting the many possible parameters for a better fit of the measured results.

An analytical solution for the desired frequency-domain currents is not feasible with the nonlinearity and the possible extra components such as C_s and those at the end. Numerical solution is easily done. The ODE solution from the nonlinear discrete model was tried, introducing an extra dynamic state for each of 32 sections. It was however quicker to solve the system as a PDE, as the ODE solution needed a lot of sections to reach acceptable behaviour even at high amplitude and frequency of the appplied voltage.

A solution is needed for the potential v, which is a function of the the time t and the position x along the grading from the zero-potential end to the open end. For simplicity of expression, the high-voltage conductor is regarded as zero potential and the end of the conductive outer electrode at the start of the grading is regarded as the negation of the actual applied voltage, so that the lower conductor in figure 19.6 is at 0 V. The boundary conditions are then the

applied voltage as a Dirichlet condition at the start of the grading $x = 0$, and at the far end a Neumann condition of zero current for an open grading, or a mixed condition if including the lumped 'end' components shown in figure 19.6.

When just R_s and C_p are used, and R_s is nonlinear according to (20.3) with zero-field value R_{s_0}, the PDE describing this system is

$$C_\mathrm{p}\frac{\partial v}{\partial t} = \frac{\partial}{\partial x}\left(\frac{\partial v}{\partial x}\,\frac{1}{R_{\mathrm{s}_0}}\exp\left(n\left|\frac{\partial v}{\partial x}\right|^{2/3}\right)\right) \tag{19.6}$$

The solution was implemented in the `pdepe` PDE-solver in Matlab, with a spatial mesh of 32 points. A FEM-based solver in Comsol Multiphysics was necessary when implementing some more complex details such as C_s, but it required tight tolerance settings for convergence and took longer, so was used only when necessary. Initial conditions of zero potential everywhere were chosen. Time could have been saved by using the final state of a previous solution at slightly different amplitude or frequency, but this was not critical in our case.

As in the nonlinear discrete model, calculation was run for four cycles to reach an equilibrium, then the results from the next two cycles were used. The currents flowing into the grading were calculated from the 'flow'-term of (19.6), i.e. the term inside the outer parentheses of the right-hand side. An FFT was performed to obtain the capacitance and loss as well as some higher harmonics. The whole calculation was repeated for each amplitude and frequency. The values of C_p and zero-field R_s from the previous models were used, both given as values per unit length. The length of grading was 80 mm. The results are shown in figure 19.7.

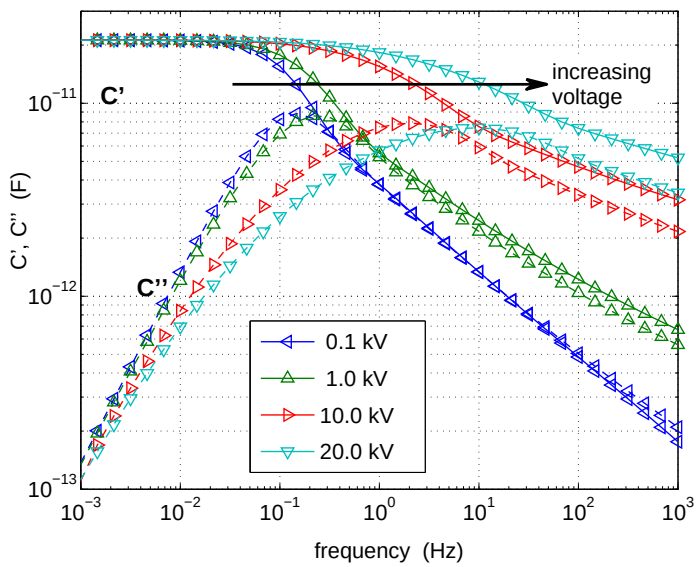

FIGURE 19.7: Results from nonlinear distributed 1D model

All but one of the main features of the measurement results of figure 19.4 are qualitatively reproduced here. The one missing feature is the upwards tendency of the higher voltages when moving to the lowest frequencies. This probably has an origin outside the basic properties of the material and geometry of a grading, such as PD or surface conductance on the insulator, at the far end of the grading: when the earth-potential spreads to the far end, there are strong electric fields around the grading's edge. The rise in both C' and C'' with voltage at 10 mHz was seen in the experimental results to be about 2 pF over the full voltage-range.

For direct comparison of the measurement results and the nonlinear distributed model, curves for measured and calculated values at just three voltage points are plotted in figure 19.8, with the calculated values doubled to match the double-ended bars. The quantitative differences between the measured and

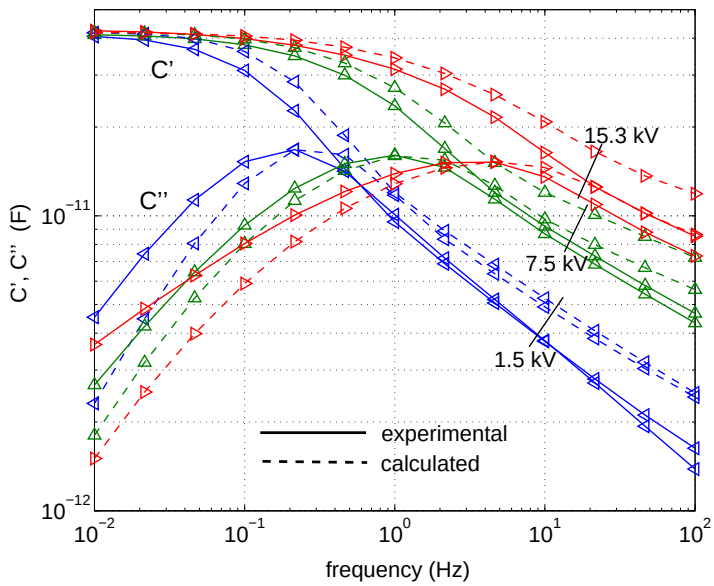

FIGURE 19.8: Comparison measurement with 1D nonlinear distributed model

calculated results are, above the loss-peak, all with the measured values lower than the calculated values: it can be seen that this could be a consequence of an excessively high material conductivity used in the calculation. The considerable difference nevertheless makes clear the difficulty of good modelling of end-grading currents, when materials have poorly defined properties as supplied and then are wrapped by hand onto many bars, as well as having variations due to aging.

19.4.5 Discussion of model results

There are several differences between the laboratory models and real stator end-windings. Most important is the capacitance per unit square between the inner conductor and grading surface. For real stator insulation around

the 10 kV level, with a thickness of a few millimetres and relative permittivity around 4.5, this capacitance is several times higher than for the PTFE tubes of thickness 5 mm and relative permittivity 2.1. Having a larger capacitance per unit length, without a correspondingly large increase in series conductivity, would shift the qualitative features to lower frequencies. We are not aware of the availability of more conductive stress-grading tapes than the one used here, but some other ones have lower surface-conductivity. The paint, even when quite thickly applied, had lower surface-conductivity.

The most important part of the curves for practical dielectric measurements seems therefore to be at frequencies above the loss peak. In this range the far end of the grading is scarcely influenced by the potential at the stator end, and approximations of an infinite length are reasonable. Time-domain spectroscopy on stator insulation has sometimes been used with an assumption of a t^{-k} behavior of current in the end-winding, which fits with the power-law response in the frequency-domain [Jon83]. This clearly assumes that the end is not reached within the times used. Dielectric measurements on unguarded new stator coils rated at 7.2 kV and using the same type of stress-grading tape have only begun to show the loss-peak at the lowest frequency used, 1 mHz. This was at around the rated voltage.

Having a distributed but linear model gave a better approximation at frequencies above the loss-peak than a discrete nonlinear model. The linear model, even if conductivity is uniformly scaled as some function of applied voltage, does not however capture how at increasing voltages C' gets larger than C'' and their gradients get shallower, due to the higher conductivity in the higher-field section at the start of the grading. This behavior of C' and C'' corresponds to a increased slope in the time-domain if using linear power-law models of dielectric response.

The noncircular cross-section of stator bars, the proximity of bars from the same or other phases close to the graded section in an end-winding, and the possibility of significant dispersion or conductivity in the insulation material, are further differences between the laboratory models and real end-windings. On simple analyses these are not expected to be at all as important to the relevance of the presented results as the difference in capacitance discussed above.

Painted stress-grading material can clearly vary a lot in thickness depending on how it is painted. Even the taped material has been suggested, in the literature, to vary with age or treatment, and various types are offered by several manufacturers. Accurate models of stress-grading currents are not plausible if needing to have measured material properties and geometries. It might be that a sufficient model for the substantial removal of the end-winding current in order to see the current due to PD can be acheived through estimation of the grading parameters using measurements at sub-inception voltages.

Laboratory models have shown the features of the dielectric response due to just the geometry and material of stator end-winding stress grading. The response at frequencies above the loss-peak is the most relevant to real end-windings, due to their higher capacitance than the models. At these frequencies C' and C'' at low voltage are similar to the case of a linear distributed-RC

line, giving slopes of −0.5 decades per decade against frequency, but at higher voltages the slopes decrease and C' exceeds C'' as the nonlinearity changes the conductivity along the grading.

Towards lower frequencies the displacement current in the insulation under the grading is so low that the grading's conductivity starts to influence the potential at the grading's far end. This happens more easily if using lower frequencies, higher voltages, more conductive grading, less capacitive insulation, or if the grading is shorter. When the grading's end does become significant the dielectric response changes a lot, with the power-law curves seen for C' and C'' at the higher frequencies turning to more Debye-like curves that indicate a limit to the total charge. that can move. The curves for C' tends to the capacitance that the whole length of the grading would have if the grading were conductive. As the electric field in the grading material is very low at low frequency, the nonlinearity becomes insignificant and the C'' curves also converge with each other as they diminish towards low frequency.

19.5 Measurements on real stator insulation

Measurements on real stator bars were made to see how different the end-winding currents are when the SiC-tape material has been wound on epoxy-mica insulation and treated with VPI, as well as having a different cross-sectional shape and a different insulation thickness and permittivity. The difference between the DS results of the nearly linear slot part alone, then the whole bar with both ends, is also shown, to make clear how great the effect from the end-grading can be.

19.5.1 Dielectric response of end-windings alone

The fundamental-frequency capacitance and loss, including the contribution of the short ($\simeq$ 30 mm) length of insulation under the electrode, is shown in figure 19.9 for all three of these gradings over a wide range of frequencies. The shorter grading shows the expected tendency to a lower value of low-frequency capacitance, with this and the associated loss-peak happening at higher frequencies than for the normal-length gradings.

The current expected from the electrode was then subtracted from the results, based on the earlier measurements of the dielectric response of the guarded slot-part that is shown in figure 18.4. Each measured point had a subtraction of the current that had been measured in the slot part at the same voltage amplitude and frequency, scaled by the electrode length. To measure the length would have the troubles that the insulation thickness may not be the same along the electrode as its average value in the slot, so the per-unit-length properties may not be quite right; and the electrode length is not very precisely known. Lengths were 'chosen', close to the expected values of about 30 mm, based on the best fit of the results, giving straight and parallel C' and C'' at low-voltage points towards high-frequency. The lengths thus chosen were 29.0 mm for the end of the bar named 'good' (because of not having ever had damage to its guard-band), and 28.4 mm for the end named 'bad' (a repaired guard-band, which seems to have had no effect on the results). The resulting 'pure' dielectric responses seen for the region of the grading material over the stator insulation

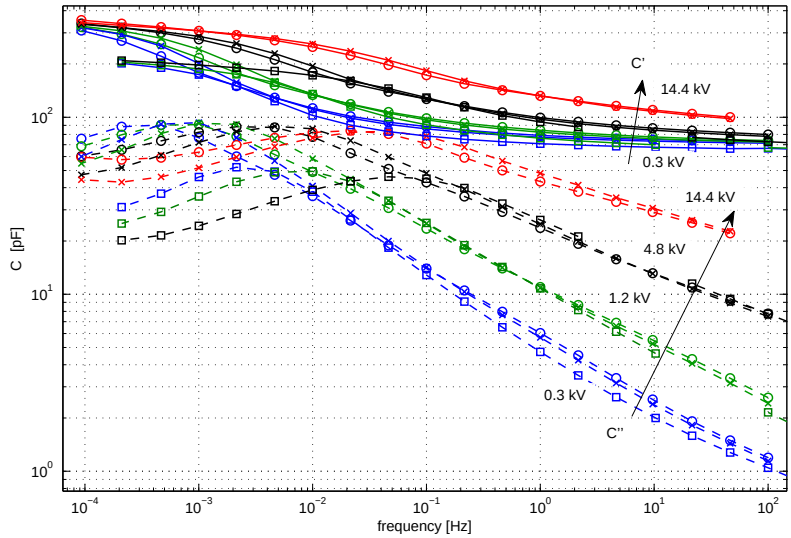

FIGURE 19.9: The raw (no removal of the capacitance from the electrode) measurements on two similar gradings on the guarded bar and the shorter grading (□) on the samples bar.

material are shown in figure 19.10. The results are very similar in form to those

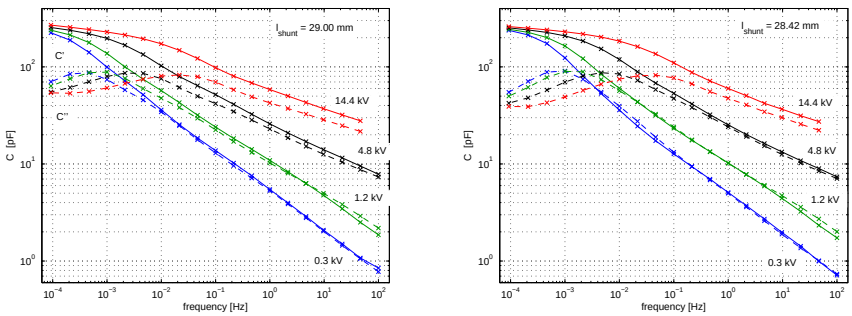

FIGURE 19.10: Both ends of the guarded bar ('good' end left, 'bad' right): C' and C'' of the grading part *with* subtraction of the addition capacitance from the electrode, based on the measured properties of the slot part.

from the simpler test objects made from PTFE tubes, although the insulation of the real stator bar has greater variation of its own with frequency. Even the low-frequency behaviour of the loss, starting to rise again at the lowest frequencies, is seen in both cases: this would be more understandable with the stator insulation, where the material under the grading has its own rising loss, but its presence even with the PTFE insulation suggests that, at least in that case, it owes more to leakage or discharge around the open end of the grading than to the properties of the solid material.

The importance of using a good material model is seen in figure figure 19.11, where the earlier compensated measurement of the pure response of the grading (right) is compared to the best fit that was acheived by subtracting a constant (linear, dispersion free, lossless) capacitance. The high-frequency parts in par-

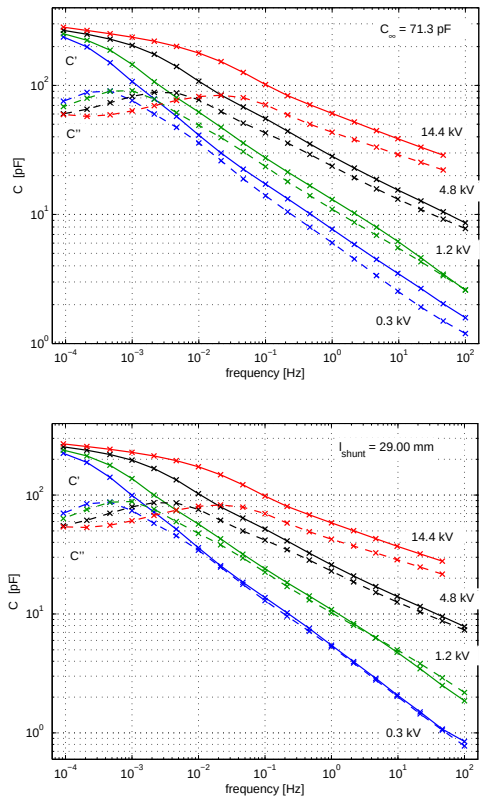

FIGURE 19.11: Comparison of subtraction of the capacitance under the electrodes by (top) the *constant* loss-free capacitance that gives best results or (bottom) the effective electrode-length that gives best results when used to scale the measurements of the slot part (identical to the left part of figure 19.10).

ticular do not show the same gradual separation of capacitance and loss towards higher voltages. This may seem rather unnecessarily fine detail when in reality the stress-grading model for a whole stator will be based on quite poorly defined materials and geometry in tens or hundreds of varied gradings. It is presented to show what are the main features of a grading construction, and that the real stator bar does give very similar results to those of the simpler cylindrical PTFE tubes used earlier in the laboratory.

The nonlinearity of the grading not only causes the dependence of C' and C'' on the amplitude of an applied sinusoidal voltage, making it more difficult to distinguish other nonlinearities such as PD, but it also necessarily contributes harmonics that disturb the other possible way of distinguishing PD and other

defects from the behaviour of good insulation. The odd harmonics from the measurements whose fundamental-frequency results are shown in figure 19.10 are plotted in figure 19.12 in the form of harmonic current magnitudes relative to the fundamental component. There is a reassuring similarity between the two

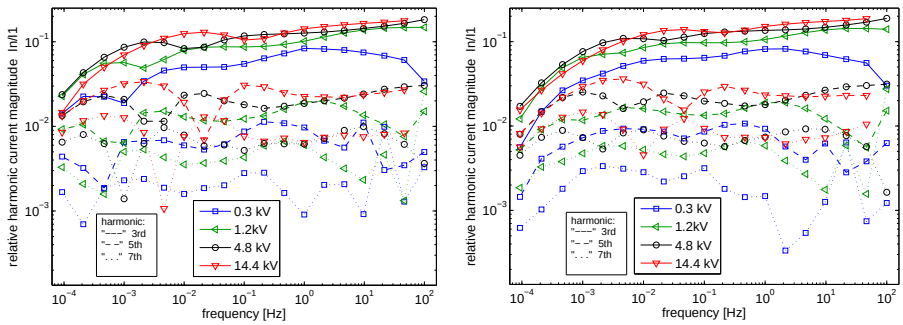

FIGURE 19.12: Odd-harmonic current magnitudes, without compensation for voltage harmonics, relative to the fundamental current for the good (left) and bad (right) ends. Line-style denotes harmonic order, marker and colour denote (independently, for those of you watching in black and white) the voltage.

ends. This does not mean that trends cannot be due to external matters such as the feedback settings: both measurements were made with the same control script and settings, so the feedback choices will be the same in both cases. The central minima, near 1×10^{-2} Hz, in the 5th and 7th harmonic at the highest voltage are not easily explained by consideration of the test-object alone. In the third harmonic, particularly, the trend is clear, and similar between all but the lowest voltage. The sharp fall-off towards the lowest frequency corresponds to the low stress in the material, exhibiting less nonlinearity. The fall-off of the 300 V results to high frequency includes too many points to be due just to poor measurement; it is also very similar in both ends. At the extreme, with high voltage and high frequency, the 3rd harmonic is seen to be nearly 20% of the fundamental.

19.5.2 Dielectric response of entire bars

The appearance of the familiar $\Delta C'$,C'' plot when the relatively linear current from the main insulation in the slot part (see figure 18.5) is combined with the contribution from end-grading (both parts of figure 19.10) is shown in figure 19.13. The effect of the end-windings is clearly enormous, on any attempt at studying the voltage-dependence (as would be necessary if doing PD measurement or looking for other nonlinearities) or on the shapes of the curves towards low frequencies.

The results for the total current and the slot-part current are compared in figure 19.14, using the directly measured values of C' rather than $\Delta C'$.

Relative magnitudes of the odd current harmonics are shown in figure 19.15, for comparison with figure 19.12. There is as expected a lower relative value, since much of the fundamental current comes from the approximately linear slot-part.

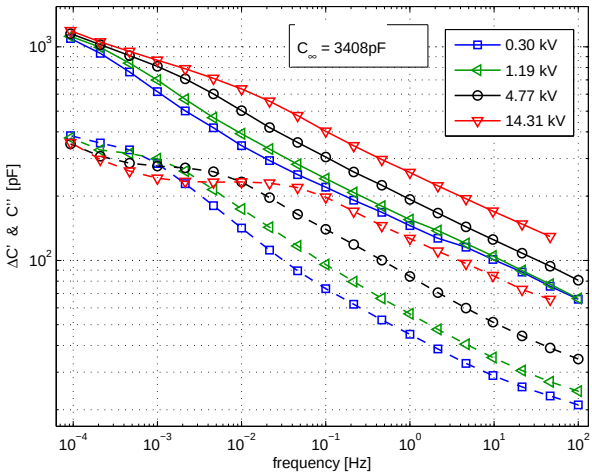

FIGURE 19.13: The complete 'guarded' bar, slot and end parts, with removal of a constant estimated C_∞.

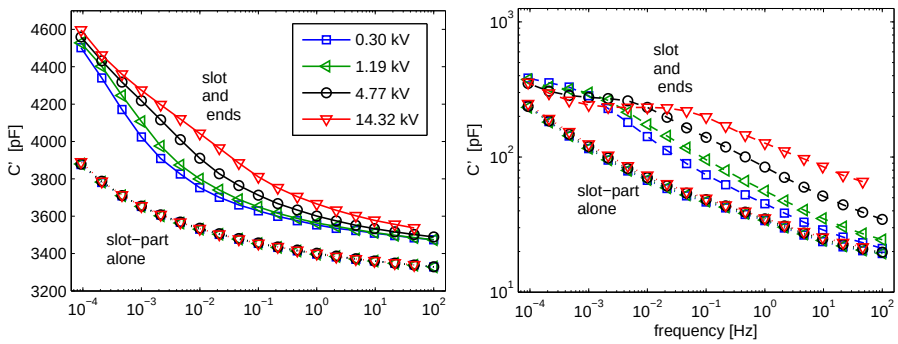

FIGURE 19.14: Comparison of raw capacitance and loss, (no removal of $\Delta C'$) of the guarded bar with and without the graded ends guarded.

As an example of the variation found between different bars that have supposedly got the same parameters, figure 19.16 shows the results for measurements on the four complete bars without guardbands, described in chapter 18, showing a spread in both C' and C'' that is about as much as the difference between measurements at different voltage levels.

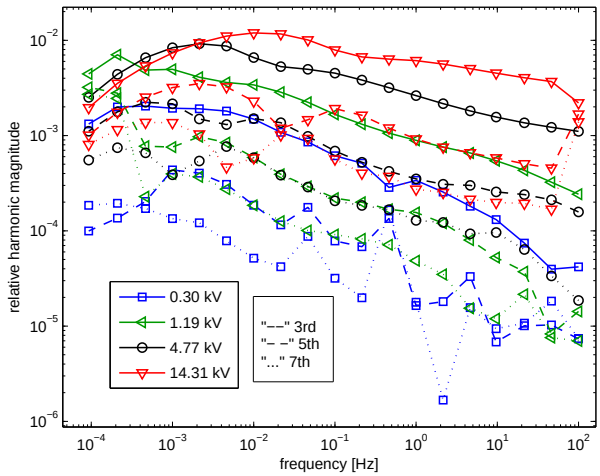

FIGURE 19.15: Relative magnitudes of odd harmonics in the measured current in the complete bar ('guarded' bar) with slot and end parts together.

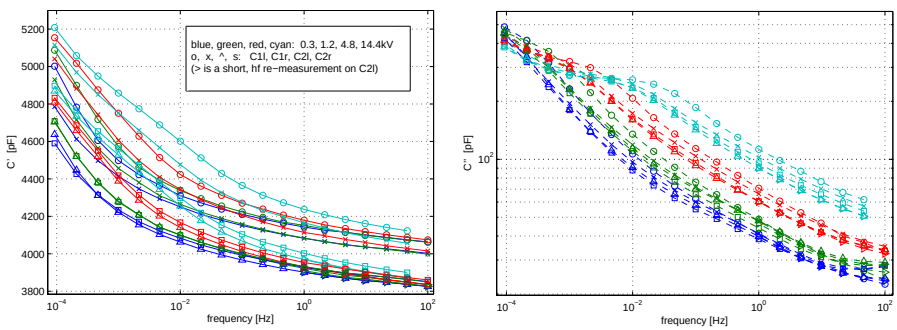

FIGURE 19.16: C' and C'' from the four complete bars with metal plates along the slot part and no guard-gaps. All had the same sequence, in room-temperature of $22 \pm 2\,^{\circ}\mathrm{C}$. Compare to figure 19.14 which gives a clearer view of the curves at different voltages, for just one object.

Chapter 20

SiC-based stress-grading material

The models in chapter 19 rely on a description of the electrical properties of the SiC-based materials that form the active part of the stress-grading system. There is insufficient information in the literature on this subject to permit confident choice of models and parameters.

This chapter describes several groups of measurements that have been made to establish suitable descriptions of conductivity and permittivity over the range of electric fields and frequencies of interest in the models. The main material studied was an SiC-based B-stage tape, whose electrical properties have been measured with dc and ac fields, at several temperatures, and on simple tubes and complete stator bars.

20.1 Literature on the material properties

The normal use of stress-grading is simply the prevention of excessive surface fields, without excessive loss. This puts no tight demand on the properties, and the materials' properties are therefore defined only very loosely by manufacturers. An example of specifications of three models of stress-grading material can be seen in [Con05, fig.8].

20.1.1 Models of electrical properties

There is very little in the literature about the desired relations of conductivity and permittivity to electric field and frequency, or about the extent of similarity between the different materials available for this application or how their properties vary with age. Previous investigations of end-winding grading have been interested in the heating-effect of the loss, or the distribution of electric field, particularly at frequencies much higher than the line-frequency such as for inverter-fed drives [EC05] [Whe07].

Investigations of slot and end-winding corona-protection materials are reported in [Eme96], but the emphasis is still on the normal function of the material, rather than on modelling of currents over a wide range of amplitudes and frequencies of the voltage. For a density of axial current of about 80 nA/mm around the circumference, an acceptable range of surface-resistivity is given as 2.5 GΩ/sq to 4.0 GΩ/sq, but the material is not characterised under the wide range of stresses that is needed for modeling of the currents at widely varied amplitude and frequency of the applied voltage.

There is a close relation to the study of grading systems with similar purpose in medium-voltage cable terminations, where again the higher-frequency fields and heating are the main interest. The cable terminations also use powders, such as carbon-black or SiC, but distributed less densely, in a polymer matrix.

Two simple empirical descriptions of conductivity σ as a function of electric field E are widely found in published models of gradings at cable terminations and end-windings. One is the power-law or 'varistor' equation of the form

$$\sigma(E) = k|E|^{n_{\mathrm{P}}}, \tag{20.1}$$

used in some works on cable-terminations and end-windings [Ref88] [Rob95] [Rhy97] and in a more numerically friendly form with a finite conductivity at zero field in [Lup96]. The other is the exponential relation of the form

$$\sigma(E) = k \exp(n_{\mathrm{e}} E), \tag{20.2}$$

widely used for end-windings [Riv99] [EK03] [EC05] [Dav07] [Min07] and having inherently good numerical properties of not vanishing at zero field; this has also sometimes been used for cable-terminations [Qi04].

It is clear that these two types of function cannot be a good fit to the same data except over a very limited range, yet both are being used in each of two applications of SiC-based stress-grading. We want to be able to model the grading over a wide range of amplitudes and frequencies of the applied voltage, so it is important to have confidence that the chosen model is suitable. In [Mår01a] [Mår01b] the electrical properties of SiC powders are studied; the dense nature of stress-grading materials for machines makes the powders more relevant than for cables; plots of the logarithm of conductivity against electric field rise more slowly than linearly, suggesting that an exponential function rises too fast to model the conductivity well. Some of those results are shown here in figure 20.3.

In [Gul00] and some later works citing it, a different form (20.3) is given, having properties that are a hybrid of the power-law and exponential forms:

$$\sigma(E) = \sigma_0 \exp\left(n\,|E|^{2/3}\right) \tag{20.3}$$

where σ_0 is the zero-field conductivity. This is claimed to fit well to a range of end-winding grading materials, and it has been found to fit well to our results, as will be seen in the later sections. It fits a lot better than either of the pure functions mentioned earlier. Making the exponent 2/3 variable is sometimes an advantage.

20.1.2 Complications: further parameters and variation

Bearing in mind the variation that is to be expected between stress-grading materials, due to different specifications, loose tolerance, variations between batches, changes during aging, and differences in processing, it is of interest to know which parameters of a model are likely to vary much between different machines. If, ideally, all SiC-based grading materials varied only in a scale-factor (such as σ_0 in (20.3), modelling would be much easier, requiring estimation only of this parameter and the length of the grading. Such a convenient situation appears, unfortunately, not to be true. Other possible complications are the effect of other variables on the results, such as effects of frequency and temperature, and anisotropy and inhomogeneity.

In [Min07] the conductivity is claimed to be dependent on the frequency as well as on the electric field, changing by a factor of two in the range from line-frequency to 1 kHz. A frequency-dependence of conductivity has not been confirmed to be of significant in the frequency range from power-frequency and down, as used in this work.

In a short comment without referencing or data, [Tuc99] claims that extruded polymer containing carbon-black has an exponential relation of conductivity to electric field in the axial direction, power-law radially and a constant tangentially. The extrusion is likely to be an important feature in that case, with the tapes and paints of stator end-grading being unlikely to be so varied. The tapes, however, do have clear inhomogeneity due to the lapped contacts between turns. A poor contact between layers of a B-stage tape-material was reported in [Gul00], sufficient that PD was observed between turns of the tape at a high voltage. If this were true for the tapes studied in this work, one would expect significant differences between measurements along short electrode-gaps where the 25 mm-wide tape spans the whole gap with its width, and longer gaps where the helical path of the tape would be easier than the direct path: this was not observed.

The final properties of a given type of tape depend on how it is used: "different insulation systems and processing can affect the final semiconductive properties" [Gul00]. The common practice of making material and aging measurements of tapes on light insulating tubes has been shown to give greater variation in results than more realistic tests of aging of the material made on real stator bars [Gul00]. With E in kV/cm and $K = 1/\sigma$ in Ω/sq, some parameters for (20.3) measured with dc applied voltage were found to be as in table 20.1. These gave good similarity between measured and FEM-calculated potentials

TABLE 20.1: Grading-material parameters for (20.3), on different substrates. From [Gul00].

substrate	K, GΩ	n
thin-walled tube	28	4.3
13.8 kV bar	88	4.4
20 kV bar	347	3.5

for 15 cm along the grading of a 13.8 kV bar, studied at (presumably) power frequency and a high overvoltage of $2V_{\text{line}}$. The similarity was not so good for the 20 kV bar, which had shown such a difference in K and n. The parameters of the material model were found to be affected by aging: the value of n changed by about 10% by electrical aging, and over 20% by thermal and electrical aging, in both cases nonmonotonically.

20.2 Material measurements on PTFE tubes

The grading materials of tape and the paint that were used in the simple grading models on PTFE tubes [s.19.2] are based on SiC particles in a binding material. The tape has a woven backing, bearing the SiC together with a 'B-stage' epoxy that needs to be cured. It is the most conductive of the few types available from

its manufacturer. In non-resin-rich insulation systems the tape would normally be applied to the stator insulation before impregnation and curing; in our case it was cured without impregnation. The tape was wound half-lapped according to its specification. The paint was more awkward to apply, and it turned out that the thickness could easily vary enough to cause large (order of magnitude) changes in conductivity. PTFE is a difficult substrate compared to real stator insulation. The properties of the tape and paint materials were measured by applying a dc voltage up to 3 kV across coatings of the materials between copper-tape electrodes on PTFE tubes of 30 mm diameter, and measuring the resulting current with a Keithley 617 electrometer. These tubes of samples are shown in figure 20.1.

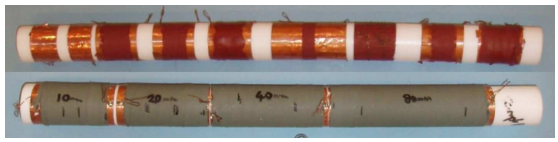

FIGURE 20.1: Samples of the SiC paint (upper) and tape (lower) materials applied between copper electrodes on PTFE tubes.

Electrode separations of 10, 20, 40 and 80 mm were used for the tape. By using different lengths it was possible to check that the current was very closely dependent on the ratio of applied voltage to length, and therefore that there was good contact between the electrode and the grading material right at the edge of the electrode. The thickness of the cured tape was about 0.5 mm, consistent between all the samples. Electrode separations of 10 mm were used for the paint, but because of the obvious variability of the paint's thickness three different samples were made with intentionally different thickness. All were too inconsistent in their thickness for a meaningful number to be reported. Even the thickest was thinner than the tape and was found to have lower surface-conductivity.

The relation in (20.3) was used to relate the current I along the axis of the tube to the zero-field end-to-end conductance G_0 and the mean applied electric field $E = V/l$ where V is the applied voltage and l the length of the material: this gives (20.4)

$$I = E\, G_0 \exp\left(n\,|E|^{2/3}\right) \tag{20.4}$$

which has been fitted to the measured data for each case, in figure 20.2, using the parameter values shown in table 20.2. Plain SI units of S, A and V/m are used, necessitating a small value of n to compensate for the large numbers describing the electric field; this is in contrast to the power-law relation where the exponent n is unit-independent and therefore describes the material's nonlinearity in an absolute way. In the log-log scaling used in (missing figure) it is clear that the measured results grow more quickly than the power-law. Either of the common models would have been a bad fit over a significant part of the range of electric fields used here. Conductivity data from [Mår01b] were also found to be fitted well by (20.3).

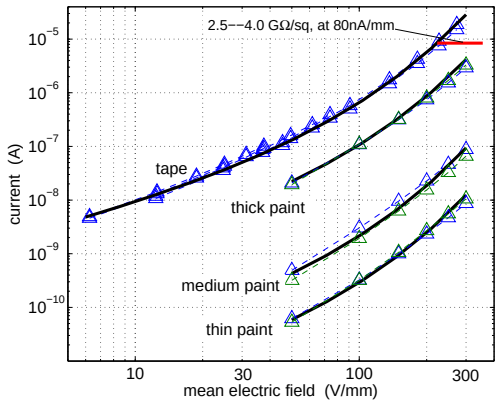

FIGURE 20.2: Measurement of dc I/V for samples on PTFE tubes, fitted to (20.4) using the parameters of table 20.2. The horizontal line of '2.5 – 4.0 GΩ/sq' is the range given in [Eme96].

TABLE 20.2: Material model parameters fitting equation (20.4) to (figure). The unit Sm is intended: it is the conductance of a 1 m length. Alternatively: A/(V/m).

Material	G_0 [Sm]	n	$\rho_{\text{surf}}(0) = 2\pi r/G_0$
Tape	5.5×10^{-13}	0.00115	1.7×10^{11}
Paint (thin)	2.5×10^{-16}	0.00114	3.9×10^{14}
Paint (medium)	1.8×10^{-15}	0.00115	5.4×10^{13}
Paint (thick)	1.0×10^{-13}	0.00110	9.7×10^{11}

The curves' parallel appearance makes it clear that the difference, in spite of the wide variation in current between the different samples, is due to differences mainly in the scaling factor G_0.

Some models have considered the permittivity of the grading material, too. The permittivity of SiC powders is shown in [Mår01b] to double from a low-field value of relative permittivity of 20, when coming up to 1.5 kV/mm. In end-winding stress grading the field is generally not above some 500 V/mm: at this level the relative permittivity from [Mår01b] is about 30. The data from [Mår01b] are plotted in figure 20.3, with the permittivity and conductivity fitted by a linear relation and (20.3) respectively. The voltage-dependence is thus much weaker than for the conductivity. The possibility of a significant and non-linear permittivity is considered in the model of [Rhy97]. That model, as with most work on stress-grading, is aimed more at high-frequency phenomena than at diagnostic measurements. The importance of the permittivity becomes less at lower frequencies.

20.2.1 Temperature-dependence of the SiC material

The temperature-dependence of the SiC material may be important: if it changes much in relative value, or changes in the shape of I/V relation, at plausible tem-

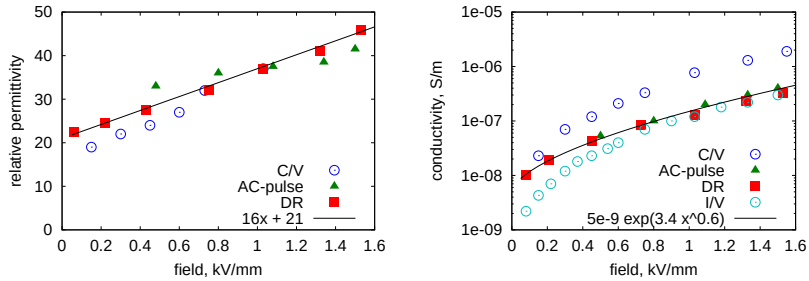

FIGURE 20.3: Data for SiC powder, from [Mår01b], fitted with linear relation for permittivity and the exponential-of-power equation (20.3) for conductivity.

peratures for machine measurements, then the likely variation in temperature between practical industrial measurements will affect the goodness of a model.

Measurements of dc I/V relation were made in the 10 mm sample on the hollow PTFE samples-tube that was used for the earlier measurements of material properties. The curves for temperatures from 20 °C to 100 °C are shown in figure 20.4. The plot against mean electric field shows just the measurements

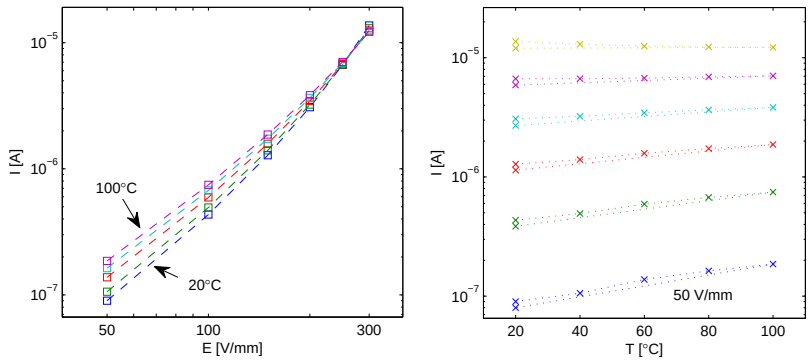

FIGURE 20.4: The dc I/V relation at temperatures of 20 °C to 100 °C in 20 °C increments. The data on the left and right are the same, plotted against the mean field and the temperature respectively. Curves between the marked extremes of parameter-values correspond to evenly spaced changes in the parameter.

taken with rising temperature. The oven† took about ten minutes to do each 20 °C and get the test-object to a sufficiently constant temperature: the electrometer reading at a moderate 500 V applied voltage was observed to reach a quite steady value before starting the proper measurement sequence at each new temperature. The plot against temperature, on the right, includes also a final measurement at room temperature of 20 ± 2 °C taken the day after, as a check that there was no long-term effect: this point on each curve is linked straight to the 100 °C point. Given the uncertainty of temperature, and the lower value of the result at the repeated 20 °C point, it seems the trend seen

† Weiss 305SB/+10IU/80DU "refrigerated/heated/humidified test cabinet".

with temperature was due to the temperature itself and not to a permanent change in the material.

20.2.2 Electrode contact with SiC material

As a somewhat related matter, resulting from an attempt at measuring the resistivity of sections of a model grading on the PTFE tubes, figure 20.5 shows measurements of I/V relation of SiC tape, made between copper tape electrodes placed around the *outside* of an already cured section of the stress-grading material. One electrode was kept fixed, and the other was moved in towards it, so that no section of grading active during measurement would have any contamination from the tape's adhesive. Note that this type of tape is intended

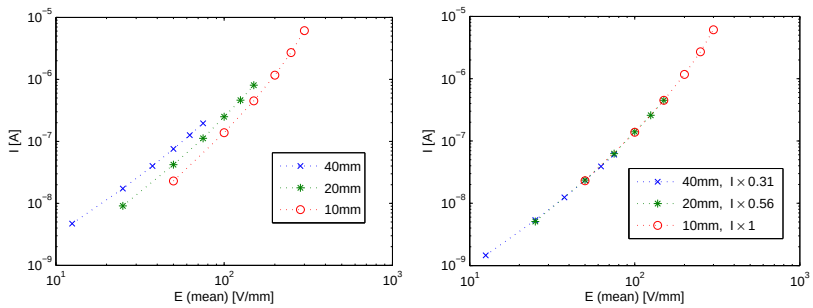

FIGURE 20.5: Measurements of current between copper-tape electrodes spaced at 10 mm, 20 mm and 40 mm on the outside of already cured SiC tape. The raw points are shown at the left, and large scaling (up to a factor of 3) of the current I is used at the right to align the curves.

for electrical use, and good conductivity has been observed between it and metallic surfaces through its adhesive.

The results suggest that in this case the relation of current to the ratio of applied voltage to gap length between facing edges of the electrodes was strongly dependent on the gap, in contrast to the earlier measurements with electrodes placed under the tightly wrapped stress-grading before curing. The shift in the curves is in the right direction to be caused by a significant contact-length of adjacent electrode/grading surface being needed: the gap over which the current travels is not well described by the distance between facing edges. Simple addition of a constant length (or any length) did not move the curves to align so well as the scalings of current that were used in the right of the figure.

The implication is that even if a grading in a real machine could be accessed, without the usual outer covering of insulating tape or varnish, measurement of material properties would not be easily made.

20.3 Material measurements on real stator insulation

The SiC-tape samples on PTFE tubes were suitable for material measurements for modelling of the simple gradings around similar tubes. For measurements of material properties of the stress-grading on the whole stator bars [s.18.1] it

should be considered that the stress-grading has been through the VPI process, is in contact with a different insulation and with a binding tape around it, and is not in a cylindrical geometry.

One of the bars described in [s.18.1] had all its outer tapes stripped off except the binding tape far in the end-winding region, leaving the plain mica-based main-insulation tapes exposed. It is shown in four pictures, from end to end, in figure 20.6. These new samples differ from the PTFE in being on a real

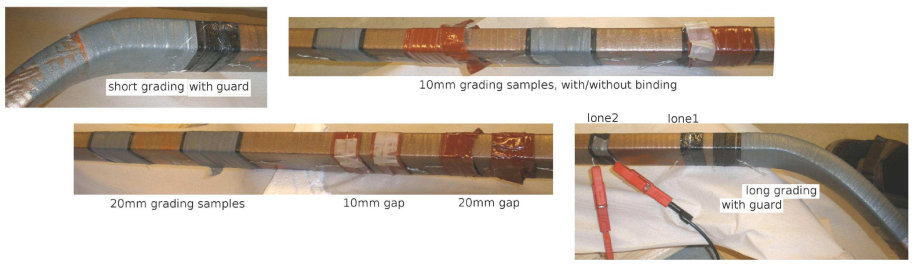

FIGURE 20.6: Samples of the SiC tape applied between short electrodes of wire and slot-semiconductor tape along a real stator bar, with the treated with VPI and curing.

bar, with non-circular cross-section and with considerable capacitance to the (floating) central conductor-bundle, and they have been through the VPI and curing process for the whole insulation system. Some of the samples are also covered in the slightly shrinkable insulating binding-tape that is applied to the end-windings of the manufacturer's machines.

Pairs of electrodes made from the 25 mm-thick slot semiconductor tape with a twist of tinned copper (probably) wire beneath, were put along the slot-part, most of them having a sample of the SiC-based tape for end-winding grading wrapped between them.

Empty electrode-pairs, having just electrodes on the insulation surface, without any intentionally conducting material between, were made with 10 mm and 20 mm gaps, were used to give an idea of the capacitance measured in the absence of stress-grading material.

Electrode-pairs with stress-grading material wrapped in the prescribed half-lapped way around and between them were used to get an estimate of material properties of the material: 10 mm and 20 mm lengths were used to allow judgement of how important the contact of tape to electrode was.

Multiple samples of stress-grading material were made, some with and some and without a further tightly wrapped outer tape, to see if it the binding makes much difference (the real end-windings are wrapped in this tape, but earlier models and samples that we have used did nothing to take this into account). Two supposedly identical constructions of each type (combination of length, material, wrapped or not) were used, for assessment of variance.

Some extra test-objects such as two wires placed a little apart under a single slot-semiconductor tape were also applied, in order to measure the resistance of the electrodes from the external wires to the bulk of the slot-semiconductor tape wrapped around these wires. The electrode resistances were confirmed

to be trivial compared even to the high-field resistance of the stress-grading samples.

Towards each end of the samples bar an 'end grading' was added, starting from an electrode of a short length of slot-semiconductor, with a guard-electrode close by its non-graded end. The active length (length beyond the electrode) of the stress-grading in the construction of the normal coils 9 cm; the ends on the samples bar were made with one having twice this active length, the other half of it. The two lengths were to give a good chance of checking low-frequency behaviour with and without the earth-potential reaching to the end of the grading; it was not known in advance quite how easily this would happen, but only that 1 mHz 10 kV (?) measurements on some earlier bars (2006) had shown only a hint of loss-peak.

20.3.1 Measurements with dc

Figure 20.7 shows the results from dc measurements on all six samples, using the same supply and electrometer as for the samples on the PTFE tube, and therefore limited to 3 kV. Bearing in mind the obvious sources of variation, in

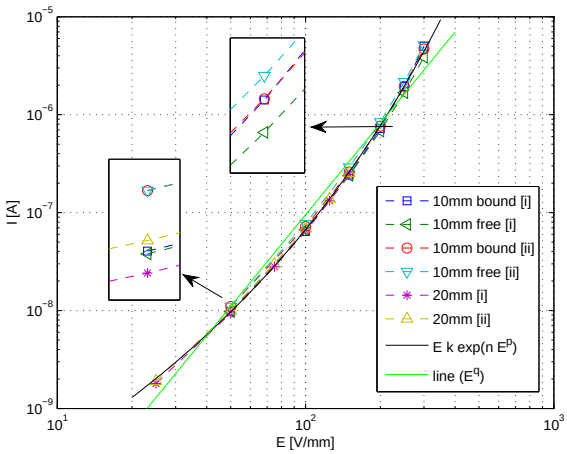

FIGURE 20.7: I/E relations with dc, for the six samples of SiC tape between electrodes on a bar surface.

particular the tightness and lapping (amount of overlap) of the tapes, besides variation in actual electrode separation and in material properties of different pieces of tape, the similarity between the samples is good. The 20 mm samples showed no obvious deviation from the 10 mm samples in their I/E relation, suggesting that the contacts are of little importance compared to the 'active' part of the SiC between the electrodes. The trend is certainly not a power-law (straight line) but is much better fitted by the familiar

$$I = Ek \exp\left(n|E|^p\right), \tag{20.5}$$

although appearing better in this case with an exponent p rather closer to 1/2 than to 2/3. It does in fact seem that this exponent is less critical to the fit

than had earlier been expected, with adjustment of n and k able to allow for some of the variation. A greater dynamic range of stimulus, going beyond 3 kV, would help in determining the best parameters. More attention to the lower values too, instead of just 0.5 kV and 1.0 kV, could be of practical interest, since, particularly at low frequency, so much of the grading is under just mild stress.

20.3.2 Measurements with ac

Measurements with ac were desired in order to see whether the permittivity of the SiC-based material carries significant current compared to the surrounding insulation, and whether it has considerable variation with electric field or frequency. Any frequency-dependence of the conductivity is also of interest.

Measurements along the same samples on the stator bar were made with the usual IDAX300 and HVU. The fundamental-frequency currents, in the familiar form of their scaled quadrature and in-phase components C' and C'' (respectively, with respect to the sinusoidal applied voltage) are shown in figure 20.8. Results are shown from all six samples, with 'compensation' for the admittance of the materials around the tape being done by substraction of results from a similar measurement-sequence on an untaped gap of the same length.

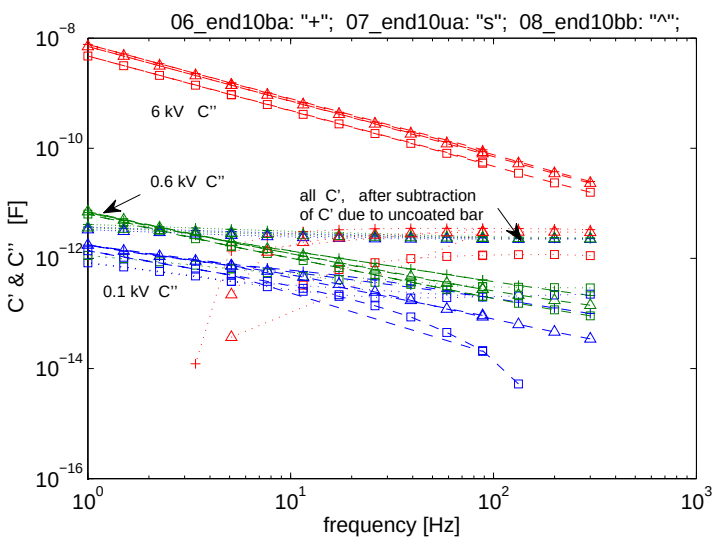

FIGURE 20.8: C'' and compensated C', from the three 10 mm-long samples. The 'compensated' points have had the C' from an empty 10 mm gap subtracted, to approximate the added C'' due to the material.

The straight lines rising strongly to low frequency are the C'' components, without any alteration from the measured values; they range from measurements at 0.25 kV as the lowest, to 5 kV peak on the highest, which can be seen to span three more orders of magnitude in current than in field.

In contrast to earlier measurements of tapes around empty PTFE tubes, there is strong dispersion in the stator insulation, and there is a strong path

between electrodes and the central conductor under the insulation. The capacitance C' is shown with compensation for this. From the compensated C' the lowest fields, of just some 100 V/mm, were seen to give quite similar magnitudes of displacement and conduction current in the grading material, but for higher fields, and even at low fields below about 1 Hz, the conduction is dominant. Results for the capacitance 'due to the grading' should be treated with caution anyway, due both to their derivation as a difference between order-of-magnitude larger values dependent on the construction of gaps, and to their measurement along with a (usually) stronger conduction current and with problems in the instrument.

The lowest-frequency measurements, at 0.1 Hz, are shown with fundamental or peak currents plotted against voltage in the following figures, as an approximation of the more familiar dc measurements. Three attempts at showing the conduction current are given in figure 20.9. The fundamental component

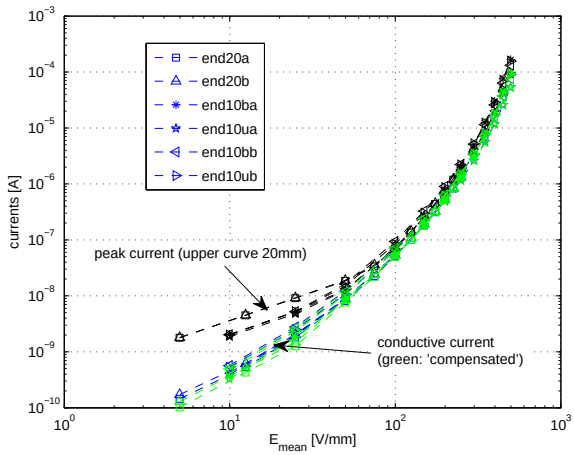

FIGURE 20.9: I/V curves at 0.1 Hz, showing mainly the conductive current: the 'peak' current curves tend to the (uncompensated) capacitive current at low voltage; the others are the fundamental components of in-phase current, shown with and without compensation, which makes little difference.

in phase with the voltage (therefore, the quantity used to calculate C'') is shown with and without the compensation by removal of the contribution of an empty gap: there is little difference. Bearing in mind that the highly nonlinear material will result in currents with higher peak values than the amplitude of their fundamental component, the peak current is also plotted. This has the disadvantage of including the capacitive current, which becomes dominant at low field. A compromise would be to remove just the fundamental quadrature component, that would arise from linear capacitance, then take the peak of the resulting waveform. Note also the separation of the results from 10 mm and 20 mm gaps at low field, due presumably to the path between electrodes via the central conductor (therefore not changed by gap length) being significant for the capacitance.

20.4 Summary

The exponential-of-power equation (20.3) using an exponent 2/3 gives a good fit to the measured dependence of conductivity on applied field, for the SiC-based stress-grading materials examined here. The 2/3 is not definitely the best choice; The variation in samples due to how the tape is applied puts a limit on how good a fit it is meaningful to pursue. It seems that many old hydro-generators have painted stress-grading, which is likely to lead to even larger variations.

The conductivity has a dominant current over the permittivity, except at the highest frequencies and lowest fields considered here. The permittivity has relatively small variation with field, which based on the measurements and references appears to be up to about a factor of two, rather than of several orders of magnitude for conductivity, up to the maximum expected fields of around 0.5 kV/mm. In the real applications, the permittivity is in parallel with other permittivities in the insulation and air, while the conductivity of the SiC material is the main conductive path, so the field-dependence matters still less.

Temperature can change the conductivity considerably at low fields, but very little at the high fields. The 20 °C variation that one might reasonably find between different industrial measurements affected the low-field conductivity in the order of ten percent.

For models of stress grading aimed at the current in low-frequency measurements, rather than the field during power-frequency and high-frequency excitation, the material measurements suggest that the modelling of the material by just a nonlinear conductivity is a good approximation. This is confirmed by the grading models and measurements.

Chapter 21
Conclusions

21.1 Main results

21.1.1 PD measurement by DS

The DS instrument measures the total charge input reliably even when this arrives as sharp pulses [s.14.2], provided that feedback components are suitably set to avoid overload. The currents due to PD events within a test-object are therefore included in the DS results. The DS instrument can give remarkable consistency of measurements in spite of changes of feedback components, electrometer voltage, and frequency, as shown on a gas capacitor [s.12.6]. Given a test-object that is linear apart from PD, the current from a DS measurement at a voltage below PD inception should be able to be scaled and subtracted from the current in a high-voltage measurement to give a good approximation of the total current due to PD [s.17.1].

21.1.2 PD charge by DS or PD-pulse

There are several reasons why the total PD charge measured by DS and by PD methods becomes very different as one moves to larger or more PD-intensive objects. The complementarity of these measurements may be useful when combined with the DS system's measurement of harmonics, as a way to see the phase-distribution of the whole PD charge as well as seeing the PD patterns that distinguish individual pulses but miss a lot of pulses in doing so.

21.1.3 Stress-grading response

Measurements on real stator bars have shown that, particularly at high voltage, the loss-peak in the dielectric response is well within the frequency range of interest, not below it as had been concluded as likely in [Tay06]. This makes it even more important to consider these models of the response instead of the simple models that have been popular in studies at relatively high frequencies.

21.1.4 Frequency-dependence of PD

An aspect that has not received much attention here is the frequency-dependence of pure PD-pulse measurements on stator insulation. This has some promise for distinguishing PD sources: it seems for example likely that delaminations might be more readily distinguished from voids with varied frequency, and that this is an important distinction to make. A problem is the need for only a low-frequency range, such as under 1 Hz, when measuring on large capacitances like a stator winding, at high voltage. Several cycles, preferably tens, would be needed at each point, and each cycle would take one or many seconds. This may be impractically time-consuming.

21.2 Suggestions for future investigation

The following are some directions that would be natural continuations of this work, without opening completely new branches.

21.2.1 Frequency-dependence

The dependence of common PD sources in stator insulation on the frequency of the applied voltage has not yet been studied in detail. Up to now these matters have been displaced by investigations of similarity and differences of DS and PD, partly because there already have been studies of PD frequency-dependence going on within the research group. It would be good to make VF-PRPD measurements on some well-defined examples of common stator-insulation defects. It would be of particular interest if defects with significantly different prognostic implications can be shown to give reliably different results with variable frequency methods but not with conventional measurements at a single frequency.

21.2.2 Simultaneous DS and PD on whole windings

Some theoretical attention has been given to measurements on whole stator windings, but so far the simultaneous, varied-frequency measurement of DS and PD has only been applied to single bars in the laboratory. It would be good to make measurements on a whole stator. The difference between PD measurement by DS and PD-pulse methods is expected to be much greater on a whole stator than in the laboratory, owing to the matters of pulse propagation and far larger total number of PD sources, besides the greater likelihood of glow-type PD in highly aged cavities than in quickly aged specimens in the laboratory. The differences such as solid earthing and long distances for connecting cables can be expected to make the PD pulse method have even greater troubles of deadtime and calibration, but might also have adverse effects on the combined measurement.

Although the references in section 8.4 give a thorough study of pulse propagation in stator windings, it would also be good to witness the results obtained with calibration pulses injected on opposite ends of the winding. One cannot properly verify subtraction of end-winding currents in the whole stator, since the very trouble about these currents is that they cannot be practically guarded away. The results from attempts at parameter-fitting from voltages below PD-inception would be interesting to see anyway.

21.2.3 Parameter estimation for end-grading models

If end-winding grading models are to be used seriously, in removing some of the disturbances in measurements of total PD charge, some more attention should be given to estimation of material and geometry parameters. It is clear that the variations between different machines, or even the individual bars studied in this work, can be enough to change a model's results by an amount that would correspond to a large error in the calculated PD current.

The possibility of estimating parameters from measurements made at voltages below PD-inception is of interest, as a way of avoiding the variation between

different machines, degrees of aging and temperature. As with any estimation or fitting problem, it is useful to restrict the fitted variables by establishing some parameters as being either constant or of a limited range.

Relevant investigations to enable this include the following: How varied are the materials between being new, impregnated, cured and aged? What variations are there between different manufacturers' materials? How much do applied thicknesses vary, and how well can differing parameters on parallel end-winding gradings within a stator be aggregated?

21.2.4 Study of service-aged bars

Measurements could be made on naturally aged bars from old machines, possibly followed by breakdown tests. Breakdown tests cannot be taken as a direct measure of the lifetime an object might have had in service, but there is no obvious better method of comparing quality within acceptably short times.

The natural aging, compared to very unnaturally accelerated aging that is the alternative if starting with new bars, would arguably make the results more meaningful as tests of the diagnostic value of the proposed methods,

21.2.5 Ignoring or estimating the fundamental current

The mixture of large currents from an approximately linear system of solid insulation, together with smaller but much more strongly nonsinusoidal currents from PD and stress-grading, suggests the possible advantage of using just the measured harmonic currents.

The fundamental component might be ignored, or might be estimated from the harmonics on criteria of physical plausibility. For very large linear currents from the bulk of the insulation, that swamp the small currents from PD or other nonlinearity, this may be more reliable than trying to compensate the disturbing current by subtraction, since small relative errors in the estimated value being subtracted could be large errors relative to the small harmonic currents.

21.2.6 Time-sequence, and non-sinusoidal excitation

This work considered only sinusoidal voltages for excitation, and gave results of DS current and PD charges only with respect to phase, aggregated over all measured cycles.

More versatile measurements can preserve details of the current and PD pulses within time. This is very sensible, as the phase-based methods of this work can be immediately derived from the time-based results, but the time-sequence includes extra information.

The applied voltage could use nonsinusoidal waveforms, whether steps, ramps, or more complicated patterns. This might be chosen to show up a particular type of PD source or to allow easier analysis.

In order to make investigation of these extra details feasible it would be necessary to simplify some other features of the measurement: there is a remarkable amount of data to consider even from the input variables of amplitude and frequency of the applied voltage and the output variables of harmonics and various PD statistics.

Another sort of excitation is a sinusoid superimposed on a quasi-dc level. This has the virtues of high stress on the insulation, low current-demand from the source, and separation of conduction and displacement currents in the measurement. Some work on non-sinusoidal excitation has already started in a related project within the department.

Appendix A
Principles

This chapter is a mixture of threads that have some connection to the process of using reference sources, performing calculations such as computer simulations, designing and conducting experiments, analysing results, drawing conclusions, and presenting results. The subjects were inspired by experiences with laboratory work and computing, and by reading around for ideas about better ways of working, particularly in experimentation and programming. In some ways this is an explanation of methods adopted in this work, or a defence of cases where a common recommendation or practice has been flouted. In others it is a suggestion that, probably, many people would benefit from learning and thinking about the different focuses and attitudes found in other subject-areas, and the wide range of available methods and tools. It is hard to bring all these ideas together coherently: the result is nowhere near the original aspirations for breadth and clarity, yet it feels disturbingly long and often rather trite. It is included as an appendix in the hope that it will be appreciated by someone for providing a new idea, an interesting reference, or just a general stimulus to consider better working-practices.

A.1 Precision of expression

If a statement can be changed to make it more easily tested or challenged, it probably *should* be changed. Although the virtue of precision is obvious in principle, its practice requires effort in gathering the necessary evidence or formulating the statement, and it is therefore all too easily avoided. It is good for the experimenter, reasoner or writer to be forced to think in detail, rather than to risk glossing over an assumed or neglected detail ... but it does take longer.

A.1.1 Numbers

Statements such as "there was a large increase in resistivity after aging" or "there was a considerable difference" are common, but are so vague that a reader might in some cases not be able to infer the actual values within an order of magnitude. Numbers and ranges make the claim far more useful, even if still as vague as "approximately doubled" or "a difference of some 5% to 10%". Making these tighter claims often requires going back to the data to check more thoroughly.

The principle of thinking-in-numbers should extend also to the case where results deviate from expectations: it is all too easy to dismiss such a deviation as being "probably due to ...", without analysing carefully the consequences of that conjecture's truth so as to check that the supposed explanation is at least quantitatively plausible. Many times in this work a peculiar result has seemed almost forgivable, but has been probed further and eventually found to have an

error of settings, equipment or analysis lying behind it. Even apparently good results are worth checking in several ways, since the belief of goodness may result from a double error, something that has happened surprisingly often.

A.1.2 Equations

If an equation can be used instead of the wordy alternative, this will often be preferable. Forcing the writer to formulate the idea more precisely can show up weaknesses in understanding or definition, and an equation is generally more accessible and memorable to a technically minded reader.

A derived equation can so easily have an error, such as a wrong sign, that simple checks should be made. There are the simple methods of checking the correct response to "x goes up, y comes down" or "what should y do as $x \to 0$", or dimensional consistency. Computers are helpful too: a derived analytical solution can be plotted against a more simply programmed numerical approximation to reveal errors, and computer-algebra programs can discover the slips that creep into pen-and-paper working.

A.1.3 Sensitivity

Sensitivity analysis considers how much a change in one variable would affect another. This is clearly strongly relevant in experimental design and analysis [s.A.2], but it should be considered in all manner of situations where differences or similarities in values prompt a conclusion that may turn out to have been strongly influenced by apparently modest disturbances, or to be true only under special conditions of other variables that were not identified as being important.

A.1.4 Examples

Even in matters that cannot be clarified by numbers or equations, more clarity might be given to statements by using concrete examples of the implication of statements. The phrases *for example* and *such as* may become a little tedious, particularly later in this chapter [s.A.2], but it is hoped that they make the points much clearer.

A.1.5 Graphical presentation

Graphical information such as pictures, drawings, diagrams and graphs, can serve enormously to clarify an explanation. More should doubtless have been used in this thesis, but unfortunately the clearer, more precise, often better form of presentation can take a long time to plan and produce.

Diagrams can help a whole set of interlinked thoughts to fasten clearly in the reader's mind, as well as showing up defects in the writer's mental model by forcing claims to be stated in so explicit a way. They can be useful for showing how concepts fit together, as well as for the obvious technical cases of representing circuits and constructions. That they are so time-consuming is in a way a consequence of their goodness: by being able to imply so many relations in a small space, there are many ways in which they can seem slightly wrong and in need of revision.

Graphs of data can greatly increase how much information can be digested. Trends and outliers can be seen that would be unnoticed from tabular numbers.

Even a function that could be written as an equation may benefit from being presented in a graph as well, to clarify its nature and allow comparison with others. An example of a work with highly graphical and effective presentation of ideas and data is [Mac03]. As with diagrams, it is often hard to decide the best, clearest way of making a graph, and it can be surprisingly time-consuming.

Some 'good practices' in graphing are included in [Kir09], with general and technical examples that extend even to a mention of Paschen's law. The following are a few points most relevant to technical use of graphs: rather than plotting data in its raw form, scaling should be used to show the deviation from an expected relation, making it clearer whether the deviation is largely noise or is a particular trend; a *key* or *legend* is commonly used to label the symbols used for each data-set, but if it is possible to include direct labelling next to the data, this can make the plot more easily accessible; extra lines such as grid-lines and a box all around a plot are probably rather over-used; 'joining the dots' with lines between data-points is by no means always a good idea, and is inappropriate for some types of data.

The scaling of data is widely used in the sorts of subjects considered in this thesis; indeed, graphs of capacitance are an example of a current being scaled by voltage and frequency in order to show the important trends more clearly. Many graphs could be improved by more work on replacing keys with labels directly by the data; the increased time, particularly if a graph is re-plotted, is the major reason against this good idea. The extra clutter of grid-lines has often been accepted, to make it easier to judge gradients, which are particularly important in graphs of capacitance and loss. The data-points in graphs have often been joined, for reasons discussed below.

It is clearly desirable to show the actual measured or calculated points on a graph, rather than just a fitted curve, unless there are so many points that there would be negligible space between them. Many experimentally based works show *only* the points, in order not to make any suggestions about what was not studied; an example is [Hel00]. But when plotting several data-sets on one graph, it can be helpful to have at least a weak line joining the points of each set, to clarify their relation. Some data can meaningfully be interpolated between the measured or calculated points; an example is the variation of capacitance or loss between closely-spaced frequencies, where joining helps the reader to make this interpolation. Other data, such as the harmonics of a periodic signal, cannot meaningfully be interpolated between points; even so, connecting the points of each data-set can make it easier to distinguish the sets. Bar-charts or unjoined points were used early in this work when trying to display harmonic values against harmonic order in the 'correct' non-interpolated way, with one data-set for each of several combinations of voltage amplitude and frequency; the results were much less clear in this way than with simple points and lines.

The display of intervals instead of points is useful for indicating a range of estimated error or variance; this is considered in [s.A.2.7], as it is connected to more general presentation of data than just graphs.

A.2 Comparison of 'research methods'

Scientific investigations are made of many various phenomena, for many reasons: it is no surprise that many different methods are used, and that researchers in different areas have little in common in their opinions about the most crucial considerations in experimentation and inference. Reading about 'experimental design and analysis' in several areas, it seems that the types of problems and methods often fit into one of a few broad categories, between which there is little similarity in the approach.

Some of the differences in methods can be explained by differences in the studied phenomena and disturbances, or differences in the intended application of the results. Other differences, however, may be due only to the backgrounds of people working in the different areas, or to historical matters such as long-established methods developed before improvements in concepts or apparatus. The methods in common use in any area are therefore not necessarily the best ones available, and it may be worth investing some time in learning about the methods used in other areas with related problems. The 'tree' of all the areas, subareas and so on must have many leaves that in spite of being far from each other are trying study and solve very similar problems; there might be useful exchanges between them if only they knew of each other's existence.

This section compares the phenomena, aims and commonly used methods in several areas, and briefly considers their potential usefulness in the general areas of DS, PD and reliability. There is no claim of covering the many areas and methods completely or fairly. An area may have subdivisions that fit into very different classifications. Areas change over time; biology, for example, has in the last century changed from a focus on classification[†] to detailed molecular knowledge and heavy computation. The terminology here may seem a little forced, from trying to be general enough to describe investigations in such areas as dielectrics, astronomy, reliability and psychology. Examples of the general term and (typical term in our area) are observation (measurement) and disturbance (noise or error). Also, 'controlled' is used in the sense of being regulated, nothing to do with a 'control group' as a base-case for comparison of results.

A.2.1 Aims

The aim of an investigation may be simply to present early results in an easily accessible way for other people to study; even in this case there are many choices to be made about how to display and compare results, and how to show the likely ranges of measurement-errors or variation between specimens. Another type of aim is to estimate a constant, or to describe the functional form of a relation between variables. Other aims may be more clearly related to the the standard description of testing a hypothesis.

The form of such hypotheses is very varied. Fundamental classical physics is typified by hypotheses in the form of equations that claim a precise law about the relation of several variables; a single demonstrable exception, anywhere, at any time, would require a revision of the law or a restriction of its scope. At

[†] *There are two forms of science: physics and stamp-collecting.* — Ernest Rutherford.

a less fundamental level, a choice may have to be made between hypotheses of competing models, from which the one best describing the data must be selected even if it is clear that none of them gives a very good description. A different form of hypothesis is "Mars has at some time supported life", which would be validated by a single discovered confirmation; this is admittedly more a matter of history than of the predictive statements normally associated with science. Studies of subjects with lots of variation, such as people, may be content with the hypothesis that a controllable variable does have *some* observable effect, or (noncausally) that a particular population does possess a particular property. In either case the result is likely to be sufficiently noisy that a modest proportion of investigations giving opposite results to the rest would more likely be treated as the result of noise than as indicating errors in the studies or a need for a revised hypothesis; such areas are sometimes called *soft* sciences.

The steps between the observations that can be made and the result at which the investigation is aimed can be complex, requiring a lot of thought and calculation. Some material properties may be measured quite directly, with the main complexity being the possible treatment of noise; but if observations are to be used to select the most suitable of several models of the underlying causes, a lot of computation may be needed.

An investigation must often be of a causal relation, since this is what is important in many practical applications where the results will be used to decide how to control a phenomenon. The variable whose effect is to be studied must then be controlled [Pea00, p.43], unless one is content with correlational studies and dependence on further assumptions.

Absolute values, or in other words values relative to an accepted reference, are necessary in some cases such as characterisation of materials, for comparison with other work. In other cases, such as studying differences between differently treated groups of people, or the peak positions of a dielectric response, only the relative values within set of measurements are important.

With such variation in aim between subject-areas, large differences can be expected in their methods of setting up experiments and analysing and presenting the results.

A.2.2 Disturbances

In the simplest sort of investigation, observations of a phenomenon could be made without significant influence of measurement errors or disturbances, and the results would need little or no processing to achieve the aim. Many factors conspire to make actual investigations more complex: the following list attempts to be general enough to be relevant to all areas, even if some of them normally group disturbances differently.

Observations of physical phenomena have a limited accuracy.[†] Errors arise

[†] Here, *accuracy* is how close a result is to the *true value*, the difference being *error*. These are obvious notions in numerical computing, but are often disliked in physical situations when the true value is not measurable, particularly when fundamental physical uncertainty is relevant. They are accepted here as useful notions for many cases, where a true value can be approached much more closely by the best available methods than by the methods actually used under the constraints of time and cost.

from external disturbances that affect the path from the object being studied, and from imperfect calibration of instruments or variability of judgements made by human observers. Examples are thermal noise, externally-coupled noise, uncompensated parasitic impedances in measurement-circuits, instruments with poor linearity or poor calibration, differences between the people making assessments of the conditions of patients, or incomplete gathering of a crop-yield. Important features of error sources are whether they are constant, follow some function or are random,[†] and whether they tend more to be additive or multiplicative in their effect.

Other variables may need to be controlled, or at least known through observations, while observing the main result. Examples are the time at which an astronomical observation is made, the temperature at which a material-measurement is made, the dimensions of a sample, or supposedly relevant features, such as age, of people on whom an experiment is performed. Errors in the measurement of these variables can arise from the same sources as for the main observed variable.

The object being investigated may also vary in ways that are not fully known to the experimenter. The problem is most obvious when the properties of a class of object are to be determined; different objects within that class give somewhat different results, necessitating measurements on more than one to make the result sufficiently representative. Examples are the establishment of a relation between a diagnostic result and later failure, estimates of material properties from samples, and tests of medical treatments on people.

If the properties of a particular object alone are important, as for a diagnostic measurement on a particular stator, there is not the need for these extra measurements to confirm that the object is representative of its kind. There may, however, be variations of the observed variable between repetitions of the measurement, not easily explained by error in the control or observation of other variables. An example is how PD can change in time due to the complicated internal states involved in the phenomenon. Several measurements may then be needed anyway, to give confidence in the result.

Some types of object can only be used once. This makes it necessary to use different objects for the measurements made at different levels of controlled variables, which introduces extra disturbance due to the variation between the objects. This is the case for samples used for destructive tests of insulation, or for samples that will be compared after being prepared with different additives; it is a very common situation in experiments on living things. An example where the object *can* be used many times is a piece of insulation having DS measurements made at many frequencies of a mild voltage.

A.2.3 Classes of subject-area

The following paragraphs give a very general classification of some different subject-areas, based on the sorts of differences in phenomena and aims outlined above. There will doubtless be plenty of omissions, over-simplifications and exceptional subareas, but there are several clear groups.

[†] Unpredictable at each moment, so best described by a statistical distribution.

At one extreme are areas that are 'noisy' due to variation between objects and to poorly controllable disturbances: examples are agronomy, medicine, psychology, economics and sociology, as well as reliability within engineering. The classic situation is that the effect of a controllable variable on an observed variable is to be determined, on objects such as plants, people or products. The noise may well cause a variance in results that is greater than the mean effect of the controlled variable under study.

In a simple case the controlled variable has just two levels, such as the presence or absence of a recommended amount of some nutrient or drug, or two constructions of a prototype. The large degree of disturbance necessitates measurements on many samples at each value of the variable in order to make a confident claim, but the cost of each sample can be high: production of prototypes for destructive testing is expensive; there may be few patients needing a particular treatment; experiments may have timescales of months or years. The small effects against strong noise also make it necessary to compare groups of objects with and without some treatment, rather than comparing results from a treated group with an accepted 'usual value'.

The potential application of the results can be large, if applied to all the subsequent production of a product or to choices concerning a whole population, so it is of great utility to detect even a small effect of the controlled variable. In these areas, therefore, 'statistical' methods are widespread, to identify small effects against the noise and to optimise experiments from the beginning to produce sufficient information using a minimum of samples.

> The science of statistics has been developed for the purpose of assisting in the separation of chance effects from true regularities.
> [BW52, p.169]

At another extreme are some parts of the physical sciences, opposite in almost every respect. An example is DS measurements on well-defined linear substances: any number of measurements can be made on the same sample, and effects from previous measurements can be largely predicted or avoided; given good shielding and some sort of averaging, the resulting signal can be very strong compared to the noise; measurements are typically made over many frequencies, with the smoothness of the results giving a good indication of the degree of noise; before seeing the results there will already be a good idea of a reasonable range; it is likely to be well known, even quantitatively, which other variables, for example temperature, are significant.

These features are clearly easier to work with than those of noisy areas, but there are often much higher demands upon the results. In some areas, great attention may be paid to dealing with relatively small levels of noise, and results may have to be accurate relative to a remote standard rather than just to other locally measured results. Physical constants are determined down to many significant figures. Effects of controlled variables are studied highly quantitatively, and models have to reproduce them well besides being appealingly simple. Getting the results in the first place may involve very clever and complex work with instruments and test-arrangements, rather than the opposite extreme of a 'yes' or 'no' answer in a questionnaire. In these areas,

methods described as 'error analysis' are common for simple treatments of the results, assessing the combined effect of the many sources of error.

The following quotation is an amusing example of how a principle held as important in one area may be irrelevant or contrary to another. The first sentence is a principle of areas with strong noise and statistical analysis: in a data-set with several variables there is a good chance that some pair of variables can be found between which the noise has caused an apparently significant effect; hence the insistence on advance declaration.

> ... experimental data can never be used as evidence for hypotheses which were not listed in advance of the experiment.
> In physics, at least, exactly the opposite viewpoint is often expressed. If a given interpretation of the data was not thought of until after the experiment, this is often put forward as evidence that the experimental results could not have been influenced by bias in favour of the theory.
> [BW52, p.294]

Although the physics-like view is appropriate for much of this work, the ability to fool oneself in reliability studies, with noisy results of several variables measured on small numbers of objects, should be kept in mind.

Moving away from the traditional extremes, there are other noisy areas that use methods more commonly described as signal-processing than as statistics. The noise is often from external disturbances and instruments: it may be much greater than the signal of interest, as in the traditional noisy subjects, but the aim typically demands extraction of much more detailed information than the presence of a 'significant difference' between groups. Examples are modern astronomy, wireless communication, detection of targets by radar, processing of NMR data [Bre88], and particle physics experiments. Most of these situations are quite recent, as automation has made it feasible to collect and process enough data to provide useful results in spite of the noise.

Such problems are attacked with methods that are suggestive of workers with wide-ranging backgrounds: for example, Fourier and related analyses, Bayesian inference, information theory, orthodox statistics, and 'learning' networks. Methods capable of such complex tasks can, at best, be general enough that the methods of other areas, such as error analysis and orthodox statistical testing, are just special cases [Jay03].

A.2.4 Classification of this work

In insulation diagnostics based on the types of method considered in this work, there are several very different subdivisions of the subject-area.

Prognoses are the ultimate aim [s.4.1] of diagnostic measurements; the area of engineering-reliability, which deals with prognoses, has been seen [s.A.2.3] to have many features of a noisy area. Results from historical operation-data of equipment, and from experiments with varied degrees of similarity to real service conditions [s.3.3], are usefully treated in a formal statistical way. Current methods are commonly based on orthodox statistics [s.A.2.5]. The Weibull distribution is in wide use for representing failure data in industrial equipment;

experience can suggest 'rules' such as that different Weibull slopes at different stresses or ages generally indicate different mechanisms.

DS investigations on materials have been cited in the previous section as an example of a 'deterministic' physical-science subject, although complexity can be introduced by inhomogeneity or effects of electrode contacts. Applied to whole stators, DS measurements include currents due to the material itself, PD, and end-windings. Depending on which of these is the desired measurand, the measurement might be said to have a quite consistent, but strong and poorly known, disturbance. The lack of dependable differences, such as phase or harmonic spectrum, between these currents makes it likely that special inference methods [s.A.2.5] would not have a strong advantage over the obvious methods of modelling and subtraction.

PD investigations are in several ways more like the noisy areas: there is substantial variation between apparently similar objects and between different measurements on the same object; several variables of external influences and internal state can affect the results, and it is not obvious which influences and interactions can be neglected; long-term changes in the material may necessitate tests to continue for long periods. Investigations of PD are therefore much more likely than investigations of DS to benefit from methods used in other areas that deal regularly with noisy phenomena.

People working in areas using DS and PD measurements, at least in the diagnostic applications, seem seldom to discuss explicitly the possible sources of noise or of false trends. There does seem to be a good appreciation of the likely simple error sources, although not so good about subtle systematic errors that might be caused by time-sequences or batches [s.A.2.6]. Perhaps the biggest failing is an underestimation of how much can be done to get meaningful results out of an apparent mess by the use of methods from signal processing, modelling, and the traditional noisy-area methods of multiple samples and specially chosen or random selections of time-sequence, samples and so on. A similar view is expressed in [Tic98] about the attitudes in some areas of computer science towards research that would involve studies of people: what researchers in psychology or medicine might see as a standard experimental situation can appear to those from a rather more pure and abstract background to be too noisy and difficult to be worth pursuing. On the other hand, it may be that instead of working very hard to study a difficult and noisy problem, one would have a good chance of finding and studying less noisy problems with similar worth.

A.2.5 Formal methods of analysis

Among the subject-areas mentioned in [s.A.2.3] it was noted that several quite different approaches are taken to the analysis and presentation of results. About the only word broad enough to include all of these methods is *inference*, which includes all the mentioned areas such as error analysis, spectrum analysis, noise reduction and significance testing, besides others such as optimisation and 'decision-theory'. Among the methods applied to problems of inference are *Bayesian* methods, or 'probability as logic'. An enticing case is made in

[Jef98], [Jay03], [Bre88] and [Mac03], for the virtues of Bayesian methods for experimental analysis, signal-processing and other purposes.

The easy direction for dealing with probabilities is from a set of events with certain probabilities, through to the consequent probabilities of outcomes that depend in some way on these events. Many useful questions work the other way, seeing a certain outcome and wondering what events are likely to lie behind it. The aims of investigations [s.A.2.1] can often be achieved by starting with the measured data and possibly some prior knowledge about the subject, and calculating the probabilities of different proposed hypotheses being true or of the true value of a constant or parameter lying within a certain range. Since the time of Bayes [Bay63], such uses of 'inverse probability' have been made, particularly in physics, where Laplace was a notable early user and proponent; some history is given by Jaynes [Jay03].

Around 1900, the use of statistical methods grew in biologically oriented areas, taking a different approach based on sampling-theory; this became the base of modern orthodox statistics. Probability was defined as strictly a relative frequency of occurrence within a (probably hypothetical) large number of repetitions; this makes it unacceptable to consider, as was done in the previous paragraph, the probability that a true value lies in a given range. The explicit use of any information other than the results of an experiment was considered unobjective. Tests were developed for judging the significance of results, in the sense of the unlikeliness that a particular result would arise by chance from the variance alone; this was a reasonable approach in the original applications. This group of principles and methods is widely applied in the noisy areas [s.A.2.3].

Parallel with the rise of orthodox statistics, but less conspicuously, there remained an interest in the Bayesian methods, particularly within some branches of physics. Jeffreys, starting around 1920, wrote papers and a book [Jef98] about probability theory in scientific research, with applications to the problems of orthodox statistics as well as to further problems in the geophysics and astronomy in which he worked.

> What Fisher was never able to see is that, from Jeffreys' viewpoint, Fisher's biological problems were trivial, both mathematically and conceptually. In his early chapters, Jeffreys disposes of them in a few lines, obtaining Fisher's inference results far more easily than Fisher did, as the simplest possible applications of Bayes's theorem, ...
> [Jay03, p.497]

Others contributed with proofs of optimality of Bayesian methods, on certain axioms. Several orthodox methods were shown to follow from Bayesian ones made with assumptions of no prior knowledge.

> Thus, in the long run, attempts to evade the use of Bayes' theorem do not lead to different final results; they only make us work an order of magnitude harder to get them. [Jay03, p.544]

When strong prior knowledge can be included in the calculations as well as the data from measurements, even better results can be obtained.

Jaynes, starting around 1950, presented applications to everyday situations, experimental analysis and signal-processsing, culminating in a book [Jay03]

about the use of Bayesian methods as a very general form of reasoning that actively benefits from its definition of probability and its attention to prior knowledge as well as experimental data. Now that computation is so easily available, and that many demanding applications exist, Bayesian methods are widespread in areas such as physical and biological research, artificial intelligence, and signal-processing.

Having come across orthodox statistics at levels from school to reliability-specific courses, I had discarded such ideas as significance-tests as a remarkable lot of recipe-following work for a result which for most of my applications would not be as meaningful as plotting a few graphs of raw data and various functions thereof. It was interesting to find that there exist other methods of analysis, highly developed, and used in areas closer to my own, that may be useful for comparing models and expressing the reliability of a result.

> Whereas orthodox statisticians offer twenty ways of solving a problem, and another twenty different criteria for deciding which of these solutions is the best, Bayesian statistics only offers one answer to a well-posed problem.
> [Mac03, p.50]

> This suboptimality of sampling theory, achieved with great effort, is why I am passionate about Bayesian methods. Bayesian methods are straightforward, and they optimally use all the information in the data.
> [Mac03, p.465]

Reliability is the only area connected to this work in which it is normal to use statistical methods, usually of the orthodox type. An application of Bayesian methods to reliability of power-system components is explained in [Lin08], where the condition of equipment, such as life-expectation, leads to a calculation of probability of failure; these estimated probabilities are updated by details of failures, and the condition assessment uses inverse probability to determine probability of failure given the results of diagnostic measurements.

Away from experimental analysis, the principle of using inverse probability to compare possible causes of observed data is useful in signal-processing. Signal-processing methods learnt in basic electronic-engineering education have rather an emphasis on traditional methods from analogue times, passing signals through cascaded stages such as filters, phase-shifts and modulators. In some cases Bayesian methods have been found to give great improvements, even by orders of magnitude, over traditional methods intuitively pieced together from the standard assortment of signal processing tools. Examples are oil prospecting, radar target-location [Jay03] and processing of NMR results [Bre88]. The presence of earlier stages of filtering and conditioning of the data, typical in conventional signal-processing, is then unnecessary, and even destructive of useful information. The usefulness of Bayesian methods is increased by tighter specification of the sought signal; for example, if the signal is known to be a sinusoid of a particular frequency or amplitude, then other properties can be found against noise to a greater accuracy.

In the DS measurements made in this work, the signal-processing is mainly a DFT focused on a fundamental frequency that is known exactly [s.6.2.2]

because the excitation comes from a local source. This situation, given some reasonable assumptions about noise, makes the DFT work well, without there being an advantage in using more detailed probability-based methods [Bre88, p.20]. In the PD measurements, the situation has been equally simple, with the instrument [s.10.1] using analogue filtering and rejection of pulses based on deadtime and threshold. In some other work with PD, where pulses are very small compared to the noise, or where different sources of PD must be distinguished, more attention is given to the measurement arrangements and to signal-processing. In such cases, it could be interesting to try Bayesian methods on the measured current, specifying details of the expected pulse-shape for different types of PD source.

A.2.6 Experimental design

The key features for 'designing' an investigation are highly dependent on the type of subject-area. In physical science in particular, suitable specification and setting up of instruments and experimental conditions may be the main complexity of the work. There exist many books devoted to methods of making sensitive and accurate measurements of various types, and a study of these along with imaginative methods described in papers is instructive as a source of ideas and as a stimulus to try to find better methods even if there are difficulties with the early attempts. Some of this type of detail, in the simple forms relevant to this work, has been considered in the chapters about measurement of DS and PD, so no more attention is given to it here.

The term 'experimental design', although sounding very broad, seems to be used mainly for methods appropriate to those areas that focus on orthodox hypothesis-testing, where the design must optimise the strength of the conclusion and the number of samples needed to achieve this. Several key points are found in [Fis26], from the times when these methods were established, and more detail is contained in the later work [Fis53]. An eloquent introduction is also given in [BW52], but with further principles and examples more relevant to the needs of physical science.

The following paragraphs are a summary of some points from orthodox experimental design that are worth considering as principles, even though such aims as significance tests are not of interest in physics-based studies of DS and PD. The division of subjects by their insistence on defined 'tests' is made in the following quotation, whose context is journals that set a significance-level as a publication requirement.

> Physicists and engineers have been largely spared from such fiascoes because they hardly ever took orthodox teachings seriously anyway; but others working in economics, artificial intelligence, biology, or medical research ... have not been so fortunate.
> [Jay03, p.525]

In the situation of ideal instruments, no variation between objects, all controlled variables exactly as intended, and no other disturbances, the relation between a controlled and an observed variable could be directly seen without need of repetitions or of special design and analysis.

Some disturbances introduce a varying error, for example 'random noise'; their effect can be reduced by having repetitions, such as further samples or repeated measurements at each value of the controlled variable, then comparing the mean values of the groups of repetitions. With large numbers of repetitions one would expect the effect of the noise to become negligible, so that the mean of a group would vary little between groups. Realistic numbers of repetitions, limited by cost and time, will have a mean that still is noisy around the ideal value, but not as badly as the individual results. The variance seen in the observations within each group allows estimation of the probability of a given result having arisen purely due to the noise and the limited number of samples, rather than due to a real difference in the means; this is the 'significance' that is popular in presentations of results.

A feature of early work such as [Fis26] was the appreciation that design should not focus purely on reducing the error of the estimate of the mean: a good estimate of the variance is crucial for judging how much significance to attach to a difference in means between groups. Even in areas where significance-tests are alien, it may be worth paying more attention to assessment of the variance of results. This is related to sensitivity analysis [s.A.1.3]: the variance indicates how likely certain degrees of error are in the results, and therefore how likely a conclusion is to be wrong.

Some other disturbances may introduce a component of constant error in all results, which is therefore not reduced by using mean values. This is clearly a problem when an absolute type of result is needed, as when measuring certain material properties. When instead groups are to be compared with each other, such as plants or polymers with different treatments, a constant error over all groups is not a problem to the final result.

Problems in comparative measurements do however arise when there is a difference in the mean results of the groups due to causes other than the intended controlled variable. One way in which this can happen is if the controlled variable is in some way correlated with the level of a disturbance. There are many ways in which this can happen: in DS measurements a sweep may cover a range of frequencies in sequence, so that disturbances that change gradually with time, such as air-temperature during a day, are correlated to the frequency; likewise for PD, but with humidity also being relevant; heating and aging of test objects also may vary with time and therefore with sequential controlled variables such as frequency or voltage; material samples may be taken for one group, then later for another with different treatment, in which case the groups may end up consisting mainly of samples from different production-batches with potentially different original properties; where people are the objects the need for 'blindness' in both directions is well known, with many examples of experimenters turning out to have introduced bias by treating people in control and treatment groups differently.

A key concept for dealing with the influence of systematic disturbances that might affect the means of groups was randomisation [Fis26]. Objects, such as seeds, people or stator bars, are assigned randomly to the groups that will be treated in different ways. Anything else that could affect the

results is also assigned randomly to objects: the following are examples of other classes of potential disturbances that can be randomly assigned. Variables that are intended to be held constant may in fact vary with some parameter: nutrients or water may depend on the position of crops within a field, the mental state of a person may depend on the room in which a treatment or interview is conducted, or on the day and time at which that happens; the exact temperature profile or mechanical stress may depend on the batch in which stator bars are subjected to thermal aging or the position of bars within the oven; the position in a time-sequence in which measurements are made can cause correlations with effects like aging or other independently time-varying disturbances. The observations may be made in ways that give different results, such as the different people gathering and weighing a crop, the person making judgements about the condition of patients, or the instruments and test-rig used for measurements.

Randomisation 'breaks the link' between the controlled variable and the disturbances with which that variable may happen to be correlated [Pea00]. It does not, of course, guarantee that the groups *will* have results with the same mean, apart from the influence of the controlled variable: it might be that a considerable difference in means occurs by chance. There are two important benefits, of which the first is the main one in the DS and PD areas. First, a disturbance that would have made differences between the means of the groups without any warning is randomised into a (usually) smaller difference together with a greater variance which gives a warning of the unreliability of the results. Second, the probability of a particular difference in the mean occurring due to the randomised disturbances can now be calculated by probability, to give rigour to a statement of significance.

When setting up an experiment some features of objects and their environment are already known to differ, such as the model or year of a machine, the particular instrument used for a measurement, the time of day at which measurements are made, or the age, sex, address or habits of a person. Some of these features can quite reasonably be expected to be correlated with the results that one would observe given similar values of controlled variables: for example the age of insulation might be strongly correlated to its results in some endurance test. Other identifiable features may have similar correlations even if a mechanism is not obvious. Random assignment randomises all the differences in results that might be correlated with differences in these features. It is certainly better at preventing systematic errors than such a foolish method as putting all the oldest machines or people into one group and the others in another, but it would be good to reduce the chance of a considerable difference in means of groups arising from the noise introduced by randomisation. If objects can be arranged in sets of those that have very similar features, and are therefore expected to give quite similar results, then objects from each set can be randomly assigned to the groups: this gives the advantages of randomisation together with a reduced random noise.

This is the widely used principle of dealing with predictable disturbances by intelligent choices then dealing with remaining unknown disturbances by

randomisation. It is clearly of use when wanting to make good inferences about small effects. Even in a subject where the studied relations are strong compared to the disturbances, randomisation may be useful for converting systematic influences to increased noise. An example is high-voltage measurements, where the aging, heating or charging caused during each measurement may affect the next; measurements with monotonically changing voltage will not distinguish the effect of the voltage itself from the effect of the changes in the object. However, simple precautions such as a final measurement at the same voltage as the first, or two interleaved sweeps, could reasonably be argued as a sufficient means of detecting this sort of problem.

The convention in early applications of orthodox statistics, such as agronomy, was to study a relation between a single factor (controlled variable) and observed variable; all other factors were kept contant, and replications (further samples treated in the same way) were used to estimate and reduce the effect of noise. To study a different factor a separate experiment would be made. A *factorial design*, instead of keeping all the other factors constant, varies them. Usually, for each value of any one factor, the other factors are varied over a fixed set of combinations; the effect of a particular factor can then be studied by comparing the mean of the results for each of its values. Fewer samples are needed, or better estimates of mean and variance are possible, compared to running a separate experiment to study each factor alone. The traditional treatment of results from factorial experiments is 'analysis of variance', studying how the results are affected by each single factor, and showing interactions where one factor influences the effect of another factor.

Even in the areas not usually concerned with variances and statistical hypothesis testing, there is some relevance in the arguments for factorial design given in [Fis53, ch.VI]. Suppose that one wishes to study the relation between a single controlled variable A and an observed one O, and needs to make several repetitions at each value of the controlled variable in order to get a good estimate. If there is a further controlled variable B that is assumed not to influence the results, it can be used at several values for each value of A, instead of being kept constant. If B indeed turns out to have negligible effect, in that there is no clear trend of results O with B, then for each value of A the multiple results with varied B can all be treated as replications. If instead B turns out to have an effect, a wrong assumption will have been corrected and A can still be studied through separate curves for each value of B or by averaging all results for each value of A. Even if B *is* expected to influence the results, it is often sensible to vary it so that the generality of the studied relation between A and O can be seen; only if the investigation is *purely* interested in this relation at a particular value of all other variables would it be pointless to vary B.

Reliability-oriented studies, such as aging tests, have much in common with the areas in which the problems and methods described above are used. Such tests have not yet been made in this work, except for some simple measurements on a very few bars before and after severe thermal aging. Before embarking on detailed studies, it would be good to consider the methods suggested by standards [s.3.3] as well as ideas from conventional experimental design.

In studies of DS it is unconventional to use any of the above methods explicitly, in the way they are used in areas that have to deal with high noise. The problems of variation and disturbance are present, but are not of the same magnitude; the effects of interest are generally well above the noise. At one stage in this work, randomisation was used for the time-sequence of voltage amplitude and frequency points in DS measurements, to avoid systematic errors from for example specimen aging. The influence of previous excitations was then generally greater than in the normal case of a sweep with increasing amplitude and decreasing frequency, and it seemed a better plan to interleave measurements or measure a few points in the opposite direction.

In studies of PD there would be more justification for repeated measurements, matching objects, and varying other factors instead of making pure repetitions, to show up what factors have an effect.

A.2.7 Presentation of results

Whether numerical results are expressed in tabular or graphical form, it is often desirable to indicate estimates of error and variation in the values.

In any measurement there may be errors from imperfect calibration or from disturbances, so that the results differ from the values that would be approached by a better measurement applied to the same object. A common way of showing the range around the measured result in which the true value is estimated to lie is the absolute $A \pm a$ or relative $A \pm a\%$ format, or corresponding error-bars on graphs. This is typical in less-noisy areas, when it is reasonable to assume that instruments and noise sources do behave within quite tight and well-defined limits, so that the estimated range will be meaningfully narrow.

Arguably somewhat different is the variance that would exist between results on supposedly similar samples even if perfect measurements were made. This is important if wanting to estimate the properties of a material rather than of one particular sample of it, and it is likely that the experimenter cannot so easily put bounds on this variation as on for example instrument calibration.

In areas with strong noise the possible variation may be so great that an attempt at hard bounds would result in a meaninglessly broad range. In this case probabilistic bounds are appropriate. The widely-used confidence interval of orthodox statistics is the bounds between which the results would fall with a stated relative frequency in repeated experiments, based on an assumed sampling distribution; mean values may be plotted together with for example a '90% confidence interval'. A Bayesian calculation of posterior probability gives the fundamentally different result, generally more desirable, of the bounds within which the *actual* value has a specified probability of lying given the measured results; this has been used long ago for such purposes as estimating planetary masses, and continues in areas that have to process complex data. A comparison of these two approaches is given in [Mac03, p.464], favouring the Bayesian one as answering the right question and being simpler and more robust; a more detailed discussion is [Jay76]. Either form of interval could be augmented by further lines or points showing intervals of other choices of probability, to give a more detailed description; the usual practice is just a single interval such as 90% or 95%.

It is uncommon for DS measurements to be presented with explicit bounds of error or variance. Even the typically more variable PD measurements, although sometimes presented with confidence intervals [For07], are often presented as single values. It is certainly advisable for the experimenter to make simple checks such as a repeated point after the main sweep [s.A.2.6]. If such a repetition confirms that there is insignificant variance, the results can reasonably be reduced to mean values, with an indication in the text of how small the variance was; if instead repetitions show significant variance, but only a few repetitions were made, one may as well plot the repeated results directly and leave the conclusions to the reader.

Intervals, means and so on are intended to hide a lot of information in order to simplify the results; this can be useful, particularly when there is little background knowledge about the mechanisms of the investigated phenomenon and disturbances. In raw results from DS and PD a lot of background knowledge can be used for interpretation: noise shows up as nonsmooth variations in curves; variations in the object result in differences between repetitions; patterns with particular combinations of voltage amplitude and frequency suggest troubles with particular feedback components; nonlinearity may show up as largely independent of frequency or having a dependence that suggests a particular cause inside or outside the test-object. Graphs make it possible to notice a lot of these subtle details: unless a lot of data must be plotted together it is hard to justify the loss of information that comes from reducing the data.

In this work no use has been made of explicit error bounds or confidence intervals. The consistency of instruments has been indicated in the chapters describing the tests performed on them. Absolute calibration is not critical, as variations with voltage amplitude and frequency are the main focus. Only a few different objects have needed to be compared at a time, so it is feasible to plot all their results together for detailed comparison.

A.2.8 Aggregation and comparison

In the area of insulation diagnostics it is rare to see detailed aggregation and comparison of results from other investigations. The usual style of theses and papers suggests that each work should involve a 'model, measure, compare' sequence, or at least should involve new results from measurement or simulation. The work of getting multiple sources together, and displaying them for detailed comparison, is time-consuming but can also very useful; in some cases it must be more so than adding to the profusion of results and models.

Aggregation is common when determining physical constants or material properties, with the independent results from different methods and researchers collected together for better confidence in the conclusion. Useful aggregation and comparison is also seen in comparing competing models with each other and with experimental data, an example of this being [Jon83, p.198].

In noisy areas, *metastudies* are often used to pool statistical data from previous work, in an attempt to make a test that is less influenced by noise. As these areas tend to have high noise and a penchant for yes/no conclusions, it likely that some individual studies will have contradictory results. Methods

and sample sizes will vary between studies, so more detailed analysis is needed than just a vote on the individual conclusions.

The most that is offered in this work is the summaries of DS and PD properties of stator insulation, both of which are very vague thanks to the range of materials, constructions and sizes of machine, and the variety of defects.

A.3 Working practices

Laboratory and simulation work, or even general calculations and searching after information, often result in time being wasted on false starts and unforeseen troubles. The optimal choice of how to go about such work often depends upon details that are not known in advance; experience may improve the estimates of such unknowns, but not (yet) to a very high degree.

A.3.1 Preparation

Before a laboratory measurement or a simulation, plans and calculations may show up problems, and some literature searching may suggest potential problems and good methods. It might even turn out that the sought results have already been published, so that there is no need for any more than a quick repetition. But these potentially useful precautions can be time-consuming, and might not give any useful result at all: getting the right balance seems to need more experience than I have yet had. When actually getting down to the work, further difficulties will probably arise; the planning and literature-searching stage may be needed several times. One should accept that things will take far longer and be far more complicated than it initially seemed they should; until this is accepted, hurried attempts just end up needing repetition.

A.3.2 Notes and data

The laboratory notebook is the focus of old-style laboratory work: filled with ideas, diagrams and results, it requires its author to think through the aims and results and make them available for later use. Compared to a computer, a notebook has the advantage that it is very suitable for quick writing of equations and diagrams, can be carried about easily, can be quickly skimmed through when looking for old notes, and does not cause EMC[†] problems.

The main advantages of writing the traditional contents of a notebook onto a computer would be that one could have multiple copies and backups, and could plot and copy results easily. Measurements now often take advantage of computers to log far more data than could be done manually, so the computer necessarily takes over this task from the notebook. It is then reasonable to store some details of what these results are along with the data. The role of the notebook is declining in importance, although it is good for intermediate calculations and as an aid to thinking.

The preferred method in this work has been to use a notebook for thinking in the laboratory, but to make automatic records of as much data as possible. Notes

[†] Electromagnetic compatibility: (not) causing interference or being interfered with. For example, when trying to write results of conductivity measurements on SiC grading-materials directly into an IBM Thinkpad T20 computer, the results were bizarrely varied until the computer was moved away from the Keithley 247 unit that was providing the applied voltage.

have been stored on the computer as photographs and text files, sometimes augmented with thorough reports including graphs. The scripts written for plotting the data provide useful documentation too [s.A.3.4].

Automated recording of data saves time and gives much better chance of avoiding mistakes and ensuring consistency in the structure of data and the naming of variables and files; this consistency is important when processing results. A program to do this may be written wrongly, but the errors thus generated are likely to be at least *consistent* and therefore more readily detected and possibly even corrected; small slips with naming, or with forgetting to change one of several factors in a loop, are almost inevitable if a human is to run many measurement points manually.

Some laboratory time may be spent on work that will turn out after some minutes or days to have been fruitless and therefore to be replaced by another method. This was often true in this work when writing and testing control programs for the instruments and testing the instruments' function and the noise in the PD circuit. The notes and saved files needed for documenting all the steps would have taken a long time to produce, and would in most cases never have been used again; only during a few short periods was the excessive note-taking attempted. Here again, getting the right balance seems to improve only slowly with experience.

A.3.3 Control-programs

It would be conventional nowadays to write a control program as a *graphical user-interface* (GUI). This has its advantages in some cases, particularly when the required functionality is very closely defined, the program is to appeal to new users with a minimum of training, or a lot of interaction is needed, such as selecting arbitrary groups of files or variables to plot.

Alternatively, a text-based script can be used, calling functions that permit all the most common tasks to be done as single lines; the script shows concisely what it will do, and enables direct modification for variations of its task; it is also easily saved to record exactly what was done. For laboratory work in a university, rather than industrial batch tests, this approach will often be superior on account of its transparency and adaptability. There is much truth in the widely-quoted statement that "GUIs normally make it simple to accomplish simple actions, and impossible to accomplish complex actions".

Scripts were used to coordinate all computer-controlled measurements in this work; during testing of the system almost every new measurement required some small change in its copy of the script, but later measurements of real test-objects needed just minor changes of parameters.

Raw data from the instruments was recorded along with the derived values, in case of later doubts about the correctness of conversion. Any other variables in use within the program were included in the recorded data, such as the time at which each measured point was started, the feedback components or gains requested at each point, and the estimated and actual electrometer voltages. This came in useful when fault-finding on several occasions, when it was possible to run back through the events and find patterns between strange results and for example particular steps in frequency or particular feedback components.

The script printed summary information to the screen during the measurement, and gave warnings about overloads or alarmingly strange values. Stopping with an error message was avoided for most problems, such as overloads or excessively low voltages. Instead, a clear warning was given, and results obtained from problematic measurements were replaced with `NaN` (undefined) to avoid their accidental use; the raw data allowed the original value to be extracted if really desired.

Output files for each measurements had names starting with an automatic serial number and a short description. As well as saving the data, all text printed to the screen during the measurement was saved as a log, and a copy of the script was made in case of later doubt about settings or desire to repeat the same measurement. Notes about the test-object and apparatus were saved manually along with the data [s.A.3.2].

A downside to all this automation is the temptation to put on a time-consuming many-point measurement and leave it, discovering only later that some other settings would have been good for avoiding a problem such as overloads or noise, or for showing more detail around where the interesting changes in the data occurred. A short preliminary measurement is a good idea, with careful thought about its results. The height of folly is making several sets of measurements before properly studying the results; during the development of a rather insidious problem with one the the instruments in this work, measurements from several weeks contained some erroneous results.

A.3.4 Processing of results

When it becomes time to analyse the data from automatic logging in the laboratory or from simulation output, a research environment poses a more difficult problem than an industrial production environment where the desired features of the data to present are likely to be well defined. It will almost certainly be necessary to experiment with plotting different quantities against each other to get an idea of the results, particularly when a new type of measurement has been made. Fault-finding in equipment is helped by the ability to plot all manner of unexpected quantities against each other, such as the feedback-component numbers that helped in identifying a problem in the DS instrument.

A good initial choice of data structures[†] is important, and the utility of more sophisticated data structures than plain arrays has been clear during this work. For example, the best choice yet for storing results is an array of a structures, one for each measured point, with multiple fields holding the arrays of data such as voltages, currents and settings. Conversion of just the desired features into simple arrays is then done for plotting, using a set of functions written specially for the purpose. The functions have been defined to permit just a few lines within a script to do all the work from loading the measured data through to producing any of a large number of possible plots. The short script is clear and can be quickly adapted, and the functions reduce code-duplication, making it

[†]In this context the data structures are the programming-language constructs such as vectors, arrays, structures of arrays and so on, providing useful abstractions for extracting particular subsets of data for plotting or other analyses.

possible to correct errors in just one place and to verify correct behaviour more thoroughly in a long script with duplicated sections of code.

After a measurement, a suitable plotting-script is copied and possibly slightly modified to plot the results. The script is saved together with the data: this allows quick later access to the results, plotting of different features, and assessment of whether there was an error in making plots from the results. A particular advantage of saving such a script along with the results is that it provides documentation of the structure of the data, in a form that has already been checked for ambiguities and errors by having been run on the computer and having produced plausible output.

Automation of derived results can easily run into trouble when the results lack the expected consistency. An example of this has been seen in attempts at automatically recording the ICM charge-channel in which a known calibration charge was measured: in a few cases the automatically selected gains and thresholds caused an echo of the calibration pulse to join with the noise-floor, resulting in the simple algorithm choosing this highest count rather than the point that was obvious to the eye; the presence of all the raw data permitted the anomalous points to be corrected without repetition of the work.

A.4 Computers and programs

In the last two or so decades, computers have taken over as the focal point of most technical activities. Vast amounts of technical literature and data can be searched and accessed in next to no time compared to old library-based methods. Laboratory data can be acquired automatically and processed with millions of calculations in a second, so measurements that would have been difficult to coordinate or to analyse have become easy. Calculations, simulations and data visualisation can be done to degrees that would have been unapproachable just two decades ago. There is so much choice, change and complexity that it can be difficult to stay on top of the subject and do things in the best way.

A.4.1 Awareness of the possibilities

Computing resources are likely to be chosen and used suboptimally if one does not keep up with developments in hardware and software, or if one chooses the first vaguely suitable program that comes to hand.

The mass market is an important driver for the development of goods that can also be used in specialised applications. Now that computers are mundane consumer goods, the brands of workstation computers that were used in technical subjects are in most cases far more expensive but no better than mass-market computers, whose processing, memory, storage and graphics have improved immensely. Nevertheless, some people who have worked with computationally intensive tasks during the earlier times do not fully appreciate how slow their old equipment is, or how needlessly expensive its descendants.

There exists likewise a large difference in cost (and, in the opposite direction, in quality of documentation) between the specialist small-market instruments used in this work and the general-purpose mass-market instruments such as function generators, oscilloscopes, data-acquisition cards and sound cards. It will often be advantageous to choose equipment with a wide market-base.

Software changes quickly too, and there can be many different programs available for a given purpose. In a research project it is likely that a few programs for calculation, display, and possibly laboratory data-acquisition, will be chosen and then will be used extensively for several years; it is important to make the right choice. It is worth spending some time to look up several options, and it may even be worth spending days or weeks attempting to use each, to show up the problems.

Had such investigations not been made in this work, it is likely that the control programs for the laboratory activities would have been attempted in a widely used graphical based programming environment, rather than in a matrix-oriented text based environment. Occasional experiences with the former only serve to confirm what a time-consuming and inferior method it would have been.

In another project the choice of a proprietary field-solver within a simulation loop was probably made in the hope of saving time by using something already available and familiar; in view of the problems encountered with speed, memory, bugs and licensing, and the reductions in model detail that were required to make it useable, it might have been better to have invested even a large part of a year on finding, testing and adapting some free code in a compiled language.

In the everyday matters also, unsuitable programs are chosen. Computer-users find an assortment of programs already installed, and try to apply them every task where they can possibly fit. Word-processors are used for dealing with plain text that would be better handled in a good text-editor; at the other extreme they are used for long documents with many equations and diagrams, for which word-processor programs are so clearly unsuited in speed, stability and quality of output. On-screen calculators pointlessly imitate pocket-calculators: a command-based numerical program like Octave has advantages such as showing the whole, editable, calculation before the answer is requested and storing hundreds of previous commands for repeating a calculation with new data or checking why a previous calculation gave a strange result. Spreadsheets may be handy for dealing with a screenful of data or for producing simple reports; but in almost any technical calculation there are constants, parameters and variables, and a high chance that control-structures such as loops and conditionals will be needed. Such calculations are better suited to a text-file in a numerical scripting language, using meaningful names to describe the variables, and permitting the operations to be listed almost as clearly as if they were typeset maths; plenty of silly mistakes need debugging even without the added difficulties of hiding the program behind cells and ‘macros’.

A.4.2 Toolchains and cooperation

There is a long but widely neglected history of computer programs that are designed to do simple, well-defined tasks and to interface easily with others. This description may sound like part of an explanation of the role of *functions* in a programming language, where a well-defined behaviour and interface specification allow the internal workings to be hidden and the function to be used in ways that the author need not even have considered. At a higher level, whole programs too can follow these principles, to make them easily combined for doing more complex tasks.

This has been a core theme throughout the history of Unix systems and their descendants. The operating-system makes it easy to keep running new instances of a program, and for these *processes* to interact through several forms of inter-process communication. Many small non-graphical programs, *commands*, are provided for common tasks such as sorting, pattern-matching and editing, filesystem manipulation and compilation. A *shell* program interprets text from a script or an interactive session, providing an easy way to start and combine processes and deal with variables, conditionals and loops. Each program can be in one of many compiled or interpreted (scripted) languages, and may itself be a shell-script that coordinates other programs; new programs are easily added to the collection.

The result is a very flexible way of creating complicated effects using simple, existing tools, and with such generality as to be suitable for administration of a server, laboratory measurements and checking of results, recoding batches of videos or managing a photo collection. Being able to bring together so many already available programs with such ease makes it possible to build a new program for a new task in a short time, sometimes literally seconds. This has been valuable in some way on almost every day in this work, yet many computer-users are unaware of the existence or value of these 'building-blocks'. Even in such cases as fast-repeating loops, where the overheads of running many small programs at each iteration become significant, the short programming time makes this a good method for one-off tasks or prototypes. A classic book [Ker84] gives detailed justification and examples of the use of this style of many small programs in many languages being used in a shell to build bigger structures for special tasks. There is also a good review of design principles given in [Ray03], including a more recent view of the principle of small cooperating programs.

Computer software, whether intended for running a calculation, interacting across a network, or controlling an instrument or digital camera, might be used for many purposes; it is most helpful to its users if it supports being used in different ways. A sensible approach [Ray03] is that such software should provide functions that can be called from other programs to give access to its features; simple non-graphical programs using these functions can then be provided as commands to run in a shell, so that many users can avoid writing and compiling programs. If a GUI is desired, then with the exception of large data-flows such as real-time plotting, a good way for it to interact with the underlying program is to use these commands and give an option for showing how it does so. This allows the user to switch easily from the supposedly intuitive interaction with the GUI to the scriptable convenience of text-based commands.

The tendency in modern computer programs, even for technical purposes such as performing simulations or controlling laboratory equipment, is quite the opposite extreme. For the two main instruments in this work, and for other instruments such as a microscope and camera and a simple multimeter, the only supplied program was a GUI-based one, suitable just for one family of operating system, and (except for the PD instrument) with no documentation about how to communicate with the instrument from other programs. Getting results on the first run might be quicker in this way than if only a command-based program

were supplied, but automation of measurements and coordination with other instruments is near to impossible. It is a farcical situation when one has to write a program to fake mouse-clicks on the GUI of another program, just to approximate the effect of having a simple command to run within a script.

A.4.3 Speeding things up

There is often a compromise between the time that a user takes to write or modify a program and the time a computer takes to run it. Improving performance in any language takes extra programming time and increases the risk of mistakes. Higher-level languages may be slower at running, but the programming is generally quicker and more reliable.

If a program only needs to be run a few times and is unlikely to need many iterations in its development, it is probably best to choose whatever language and algorithms will minimise the time to develop it. If it is to be used many times, the total running time may become significant; in particular, if the development will involve many trials and modifications, a long running time will waste a lot of person-time.

Apart from changing the language or algorithm, speed may be increased by 'throwing more computing power' at the problem. If the bottleneck is in the processing, rather than the memory or disk, the replacement of a modern but mediocre processor with one from near the top of the range is unlikely to give an improvement of more than a few tens of percent.

The current inability to push single processors much higher in speed has lead to multiple processors becoming common even in very basic computers, often as multiple processor 'cores' in a single package confusingly referred to as a 'processor'. For a program to obtain a speed increase by using multiple processors, it must use an algorithm that permits efficient execution of parallel operations, and it must be suitably written to run with parallel threads. Many programs used for simulation have poor or no support for this, and few users have the ability or time to write their own programs in a suitable way; not all types of problem *can* be made parallel. In spite of the claims made for several proprietary programs for general numerical work and field-solution, we have found it unusually lucky to get even a doubling in speed by offering 2, 4 or 8 processors rather than 1.

Fortunately, all the really time-consuming situations in this work and neighbouring projects have involved a calculation that is to be run many times with different input parameters; an example is calculation of the current into a stress-grading [s.19.4] at each of many combinations of voltage amplitude and frequency. There are thus inherently many separate processes, which can be run independently; there is no need for special adaptation of entire programs, and the speed of finishing the whole batch increases nearly directly with the number of available processors regardless of whether they are in the same computer.

Following the principle of using existing programs as building-blocks [s.A.4.2], shell-scripts were written to automate execution of a list of files on each of a list of computers, keeping a specified number of processes running on each until all file had been run. The executable files could be compiled programs, or scripts that would run another program such as a numerical-computing

environment or solver. Communication was by a shared NFS file-system, with public-key SSH logins used to start a coordinator script on each computer. There are several programs already available for running batches of jobs; the chosen method involved no changes to the installed programs, and was easily implemented. The purchase of multi-core computers with plenty of memory made execution of batches a real advantage in time, and permitted other people to leave long-running or memory-hungry programs running on stable remote computers. Sixteen fast processors were provided for the cost of about one employee-month: in some cases simple 'brute-force' methods are more efficient with resources than spending time on clever optimisations.

The optimisation of computer programs may in some cases improve speeds by many times, but the cost can be high. It takes more time to write a program with attention to optimisation, and the result is likely to be a program with less clarity of expression, making for more mistakes in the initial version and more difficulty in making any subsequent changes. It is generally hard to foresee where the bottlenecks will be, so optimisations other than corrections of egregiously poor programming can easily be made in places where they are no use. The concept of avoiding 'premature optimisation' [Knu74, p.268] and focusing on the proven worst parts has been much cited, and is dwelt on several times in [Ray03] with more detail about typical modern programs and hardware. A sensible approach is to spend little or no time on optimisations during the initial programming unless it is well-known that certain choices will make a large difference; when the program at least works, and if it shows unacceptable performance, then the time has come to investigate, with timings and profiling, to see where the inefficiencies are and try to solve the most severe ones.

A.4.4 Numerical versus Analytical

The usefulness of numerical approximations has increased greatly with the increased availability of computers. The balance of importance between traditional mathematics with analytical solutions, and numerical methods on computers, has been taken up in [Hof04], with an interest in levels from school up to big engineering problems.

A good knowledge of analytical ways of solving a problem, solving an adequate approximation of a problem, or adapting a problem for more efficient numerical solution, can be very advantageous even in this age of widely available numerical solvers for common physical situations. Many problems, however, cannot readily be solved analytically, but can be solved by numerical methods. Examples range from the apparently simple three-body problem [Fey70] through to many engineering situations [Hof04]. In high-voltage engineering there can be awkward geometries and nonlinear materials; these are easily included in a general-purpose FEM (finite-element method) program for solving fields, but would require many approximations to get an analytical solution.

An advantage of the generality of programs implementing numerical methods is that they can be applied to so many cases that severe errors are likely to be discovered sooner than in one-off programs. There is more potential for errors in the working when approximated analytical solutions are derived for each geometry or material-model. Being able to get good approximations of

solutions, often of better accuracy than one would actually need for practical uses, from simple input of physical dimensions and materials, is very useful for optimising designs and testing new ideas.

For the models of nonlinear stress-grading used in this work, the frequency-domain current into the grading was found not by analytical approximations but by a full time-domain FEM solution of a 1-dimensional or 2-dimensional model of the geometry. Several initial cycles were calculated without using their results, to allow the solution to approach an equilibrium from a simple initial condition such as zero. The solution was followed by post-processing to find the current over the end of the grading and to perform an FFT on this time-domain current. Lots of processor cycles were therefore substituted for potentially cleverer, more efficient methods such as better approximation of initial conditions, or approximations that would have made the results less accurate. Throwing more computing power at the problem was probably a better use of resources than spending more time to make a cleverer and probably more buggy and less easily modified program. It is prudent, however, not just to trust blindly even well-established solvers to give good solutions: some testing against cases with known results gives some reassurance of proper operation.

A.4.5 Numerical inidealities

The modern user of computers for numerical work may understandably treat the computer-based equations as being similar to those of symbolic maths: many familiar functions are available, and the precision usually available makes the computer's numbers appear as a continuum for many uses. A computer can calculate to arbitrary precision, given time, memory and the right programs; the behaviour of most numerical programming languages, however, is to use floating point arithmetic[†] at the precision directly available in the computer's processor, in order to achieve high speed. In modern computers this will be *double-precision* according to the IEEE 754 standard, as described in [Gol91]; intermediate results are often treated in even higher *extended* precision until written to memory. These floating point numbers are limited to the finite set that can be represented by the number of bits used. The range can be huge: IEEE 754 double precision has an exponent range giving magnitudes of $10^{\pm 308}$, but the limited number of distinct values gives a fixed relative precision of 2.22×10^{-16}, meaning that the steps between the largest representable numbers would be huge numbers in themselves.

There exist many ways for calculations on discrete and limited number-ranges to cause problems: searching the Web for something like 'disasters numerical computing' gives a good introduction to crashed rockets, failed missile

[†]Floating point is one — the dominant — way of using a fixed-size set of digits to represent a wide range of numbers, small and large. Let the $1 + n + m$ digits (bits for binary floating point) representing the number be denoted $s, p_{n-1}, \cdots, p_0, e_{m-1}, \cdots, e_0$; the floating point value is then $(-1)^s \times p_{n-1} \,.\, p_{n-2} \cdots p_0 \times \beta^{e_{m-1} \cdots e_0}$. Here, the bits p_{n-1} to p_0 form a fixed-point number (note the point between p_{n-1} and p_{n-2}); this part is the *significand*, or in older terminology the *mantissa*. β is the *radix*, the same as the base used for the numbers p, so $\beta = 2$ in normal computers. e is the *exponent*; the bits that represent it, as an integer, are interpreted in such a way as to allow e to be positive or negative, providing very large or very small values.

protection and plenty of less exotic examples, that have resulted from numerical errors, often due to neglecting that common computer arithmetic is far from symbolic maths. Some examples are given in [Gol91], and in [Ein05, ch.1] along with examples of common sources of errors.

Simple rearrangements of equations that are symbolically equivalent can result in wildly different numerical behaviour in the presence of rounding and finite range; it is wise to use well-tested functions rather than writing one's own. Even if a program works well with thousands of test-cases, it is not obvious that it is robust and well-written: particular data inputs may expose a severe numerical bug that was not seen before. Numerical results can depend on the hardware and even on the choice of compiler options: there exist settings, not always made available by a compiler or program, and often unknown to the users, that control how floating-point operations deal with rounding, comparisons and with warning about any problems that have occurred.

One cannot expect many people to take the time to become really knowledgeable about numerical methods for technical computing work; an introduction such as the above cited works serves as a quick and interesting warning. The easiest way to avoid problems is probably to use building-blocks of very well-established functions and programs as much as possible, and to read enough about common pitfalls to have some idea of the most important errors to avoid.

Another issue is the extent of error in particular solution methods, such as FEM, compared to an ideal analytical case. This generally has to do with the approximations and discretisation between the idealised problem and its representation in the numerical method, rather than differences between pure and floating-point arithmetic in the underlying calculation.

In this work the models of current in end-winding stress grading required integration of a flux term over a surface. The finite-element method is not very well suited to this (according to the authors of the solver), and the material nonlinearity only made the situation worse. Simple test-cases involving nonlinear material in a geometry with a constant field-strength, or linear materials in an analytically soluble geometry, showed some severe deviations in the result, even beyond ten percent; these were improved by changing the model, but it was instructive that such errors could be given without any warning of a poor solution.

The often-quoted intention of such field-solvers is to allow the user to experiment directly with the 'physics'. The results actually owe a lot to the oddities of the numerical methods from which they come, and the user may benefit from some understanding *and testing* of these.

Index of definitions

Bibliography

[Bar90] R. Bartnikas. Detection of partial discharges (corona) in electrical apparatus. *IEEE Transactions on Electrical Insulation*, 1990. 25(1):111–124.

[Bar93] R. Bartnikas, J. P. Novak. On the character of different forms of partial discharge and their related terminologies. *IEEE Transactions on Electrical Insulation*, 1993. 28(6):956–968.

[Bar95] R. Bartnikas, J. P. Novak. Effect of overvoltage on the risetime and amplitude of PD pulses. *IEEE Transactions on Dielectrics and Electrical Insulation*, 1995. 2(4):557–566.

[Bau91] R. Baumgartner, B. Fruth, W. Lanz, K. Pettersson. Partial discharge. IX. PD in gas-insulated substations — Fundamental considerations. *IEEE Electrical Insulation Magazine*, 1991. 7(6):5–13.

[Bay63] T. Bayes. An esay towards solving a problem in the doctrine of chances. *Philosophical Transactions of the Royal Society*, 1763. 53:370–418. `http://www.york.ac.uk/depts/maths/histstat/essay.pdf`.

[Bog90a] S. A. Boggs. Partial discharge. II. Detection sensitivity. *IEEE Electrical Insulation Magazine*, 1990. 6(5):35–42.

[Bog90b] S. A. Boggs. Partial discharge. III. Cavity-induced PD in solid dielectrics. *IEEE Electrical Insulation Magazine*, 1990. 6(6):11–16, 19–20.

[Bog90c] S. A. Boggs. Partial discharge: Overview and signal generation. *IEEE Electrical Insulation Magazine*, 1990. 6(4):33–39.

[Bou04] E. A. Boulter, G. C. Stone. Historical development of rotor and stator winding insulation materials and systems. *IEEE Electrical Insulation Magazine*, 2004. 20(31):25–39.

[Bre88] G. L. Bretthorst. *Bayesian Spectrum Analysis and Parameter Estimation*, *Lecture Notes in Statistics*, vol. 48. Springer-Verlag, Berlin/Heidelberg, 1988. `http://bayes.wustl.edu/glb/book.pdf`.

[Bru08a] R. Bruetsch. High voltage insulation failure mechanisms. *International Symposium on Electrical Insulation (ISEI)*. 2008 pp. 162–165.

[Bru08b] R. Bruetsch, M. Tari, K. Fröhlich, T. Weiers, R. Vogelsang. Insulation failure mechanisms of power generators [feature article]. *IEEE Electrical Insulation Magazine*, 2008. 24(4):17–25.

[Bur88] K. G. Burnley, J. L. T. Exon. Mechanical effects associated with the application of high voltage to generator stator bar insulation. *International Conference on Properties and Applications of Dielectric Materials (ICPADM)*. 1988 pp. 383–386.

[BW52] E. Bright Wilson, Jr. *An Introduction to Scientific Research*. McGraw-Hill Book Company, Inc., New York, 1952.

[C001] *High-voltage test techniques, part 1 — General definitions and test requirements*. International Electrotechnical Commission, second edition, 1991 edn., 1989. IEC Standard 60-001, 1989-11.

[C270] *High-voltage test techniques — Partial discharge measurements*. International Electrotechnical Commission, 3rd edn., 2000. IEC Standard 60270.

[C3427] *Off-line partial discharge measurements on the stator winding insulation of rotating electrical machines*. International Electrotechnical Commission, December 2006. IEC Standard: IEC-TS-60034-27 (has 'Committee Draft' stamped on it).

[Cav06] A. Cavallini, G. C. Montanari. Effect of supply voltage frequency on testing of insulation system. *IEEE Transactions on Dielectrics and Electrical Insulation*, February 2006. 13(1):111–121.

[Cha85a] M. A. Chaudhry, A. K. Jonscher. The dielectric properties of mica paper in variable temperature and humidity. *Journal of Materials Science*, 1985. 20(10):3581–3589.

[Cha85b] M. A. Chaudhry, A. K. Jonscher, R. M. Hill. The dielectric properties of muscovite mica along the cleavage planes. *Journal of Physics D: Applied Physics*, 1985. 18(6):1207–1212.

[Che89] D. K. Cheng. *Field and wave electromagnetics*. Addison-Wesley, 1989.

[Con05] D. J. Conley, N. Frost. Fundamentals of semi-conductive systems for high voltage stress grading. *Proceedings Electrical Insulation Conference and Electrical Manufacturing Expo, 2005*. 2005 pp. 89–92.

[Coo03] V. Cooray (editor). *The Lightning Flash*. IEE Power and Energy series, 2003.

[Cri89] G. C. Crichton, P. W. Karlsson, A. Pedersen. Partial discharges in ellipsoidal and spheroidal voids. *IEEE Transactions on Electrical Insulation*, 1989. 24(2):335–342.

[Dac89] J. Dacier, R. Goffaux. Contribution to the overall and local characterization of the condition of electric ageing of HV insulation in large rotation machines. *International Conference on Conduction and Breakdown in Solid Dielectrics (ICSD)*. 1989 pp. 602–607.

[Dav06] E. David, A. Nair, T. Godin, J. Bellemare. Modeling of a generator i-v curve from the ramped direct voltage method. *International Symposium on Electrical Insulation (ISEI)*. 2006 pp. 10–13.

[Dav07] E. David, L. Lamarre. Low-frequency dielectric response of epoxy-mica insulated generator bars during multi-stress aging. *IEEE Transactions on Dielectrics and Electrical Insulation*, 2007. 14(1):212–226.

[Dev84] J. C. Devins. The 1984 J. B. Whitehead Memorial Lecture: The physics of partial discharges in solid dielectrics. *IEEE Transactions on Electrical Insulation*, 1984. EI-19(5):475–495.

[Dye24] D. W. Dye, L. Hartshorn. The dielectric properties of mica. *Proceedings of the Physical Society of London*, 1924. 37:42–57.

[E43] *IEEE Recommended Practice for Testing Insulation Resistance of Rotating Machinery*. 2000. IEEE Standard 43-2000.

[E56] *IEEE Guide for Insulation Maintenance of Large Alternating-Current Rotating Machinery (10,000 kVA and Larger)*. 1977. ANSI/IEEE Standard 56-1977.

[E95] *IEEE Recommended Practice for Insulation Testing of AC Electric Machinery (2300 V and Above) With High Direct Voltage*. 2002. IEEE Standard 95-2002 (Revision of IEEE Standard 95-1977).

[E286] *IEEE Recommended Practice for Measurement of Power Factor Tip-Up of Electric Machinery Stator Coil Insulation*. 2001. IEEE Standard 286-2000.

[E433] *IEEE Recommended Practice for Insulation Testing of Large AC Rotating Machinery With High Voltage at Very Low Frequency*. 1974. ANSI/IEEE Standard 433-1974.

[E434] *IEEE Guide for Functional Evaluation of Insulation Systems for AC Electric Machines Rated 2300 V and Above*. 2007. IEEE Standard 434-2006 (Revision of IEEE Standard 434-1991).

[E792] *IEEE Trial Use Recommended Practice for the Evaluation of the Impulse Voltage Capability of Insulation Systems for AC Electric Machinery Employing Form-Wound Stator Coils*. 1988. IEEE Standard 792-1988.

[E943] *IEEE Guide for Aging Mechanisms and Diagnostic Procedures in Evaluating Electrical Insulation Systems*. 1986. ANSI/IEEE Standard 943-1986.

[E1043] *IEEE Recommended Practice for Voltage-Endurance Testing of Form-Wound Bars and Coils*. 1997. IEEE Standard 1043-1996.

[E1310] *IEEE Trial Use Recommended Practice for Thermal Cycle Testing of Form-Wound Stator Bars and Coils for Large Generators*. 1996. IEEE Standard 1310-1996.

[E1434] *IEEE Trial-Use Guide to the Measurement of Partial Discharges in Rotating Machinery*. 2000. IEEE Standard 1434-2000.

[EC05] F. P. Espino-Cortes, E. A. Cherney, S. Jayaram. Effectiveness of stress grading coatings on form wound stator coil groundwall insulation under fast rise time pulse voltages. *IEEE Transactions on Energy Conversion*, 2005. 20(4):844–851.

[Edi01] H. Edin. *Partial Discharges Studied with Variable Frequency of the Applied Voltage*. Ph.D. thesis, Kungl Tekniska Högskolan (KTH), Stockholm, 2001. `http://kth.diva-portal.org/smash/get/diva2:8984/FULLTEXT01`.

[Ein05] B. Einarsson (editor). *Accuracy and Reliability in Scientific Computing*. SIAM Press, Philadelphia, 2005. `http://www.nsc.liu.se/wg25/book/contents.html`.

[EK03] H. El-Kishky, M. Abdel-Salam, H. Wedaa, Y. Sayed. Time-domain analysis of nonlinear stress-grading systems for high voltage rotating machines. *Conference on Electrical Insulation and Dielectric Phenomena (CEIDP)*. 2003 pp. 482–485.

[Eme05] F. T. Emery. Partial discharge, dissipation factor, and corona aspects for high voltage electric generator stator bars and windings. *IEEE Transactions on Dielectrics and Electrical Insulation*, 2005. 12(2):347–361.

[Eme96] F. T. Emery. The application of conductive and stress grading tapes to vacuum pressure impregnated, high voltage stator coils. *IEEE Electrical Insulation Magazine*, 1996. 12(4):15–22.

[Eva81] D. L. Evans. IEEE working group report of problems with hydrogenerator thermoset stator windings. Part I — Analysis of survey. *IEEE Transactions on Power Apparatus and Systems*, 1981. PAS-100(7):3284–3291.

[Far04] M. Farahani, H. Borsi, E. Gockenbach, M. Kaufhold. Investigations on characteristic parameters to evaluate the condition of the insulation system for high voltage rotating machines. *International Symposium on Electrical Insulation (ISEI)*. 2004 pp. 4–7.

[Fey70] R. P. Feynman, R. B. Leighton, M. Sands. Conservation of momentum. *The Feynman Lectures on Physics*. Addison Wesley Longman, vol. 1, Chapter 10, 1970 p. 10.1.

[Fis26] R. A. Fisher. The arrangement of field experiments. *Journal of the Ministry of Agriculture of Great Britain*, 1926. 33:503–513. `http://digital.library.adelaide.edu.au/coll/special/fisher/48.pdf`.

[Fis53] R. A. Fisher. *The design of experiments*. Oliver and Boyd, London, 6th edn., 1953.

[Flo95] B. Florkowska. Assessment of temperature influence on partial discharges in epoxy/mica insulation. *International Conference on Conduction and Breakdown in Solid Dielectrics (ICSD)*. 1995 pp. 356–360.

[For07] C. Forssén, H. Edin. Measured partial discharge inception voltage for a cavity at different applied frequencies. *Proceedings of the 20th Nordic Insulation Symposium (NordIS)*. June 2007 pp. 59–62.

[For08a] C. Forssén. *Modelling of cavity partial discharges at variable applied frequency*. Ph.D. thesis, Kungl Tekniska Högskolan (KTH), Stockholm, May 2008. `http://kth.diva-portal.org/smash/get/diva2:13791/FULLTEXT01`. TRITA-EE 2008:018.

[For08b] C. Forssén, H. Edin. Partial discharges in a cavity at variable applied frequency Part 1: Measurements. *IEEE Transactions on Dielectrics and Electrical Insulation*, 2008. 15(6):1601–1609.

[For08c] C. Forssén, H. Edin. Partial discharges in a cavity at variable applied frequency part 2: measurements and modeling. *IEEE Transactions on Dielectrics and Electrical Insulation*, 2008. 15(6):1610–1616.

[Fuj92] N. Fujimoto, S. Rizzetto, J. M. Braun. Partial discharge. XV. Improved PD testing of solid dielectrics using X-ray induced discharge initiation. *IEEE Electrical Insulation Magazine*, 1992. 8(6):33–41.

[Gäf04] U. Gäfvert. Dielectric response analysis of real insulation systems. *International Conference on Solid Dielectrics (ICSD)*. 2004 pp. 1–10 Vol.1.

[Gea90] R. Geary, I. J. Kemp, A. Wilson, J. W. Wood. Towards improved calibration in the measurement of partial discharges in rotating machinery. *International Symposium on Electrical Insulation (ISEI)*. 1990 pp. 141–144.

[Ged95] U. W. Gedde. *Polymer Physics*. Kluwer, 1995.

[Gof00] R. Goffaux, B. Comte, M. Cottet, B. Fruth. Quality assurance of generator and motor insulation system. *International Symposium on Electrical Insulation (ISEI)*. 2000 pp. 512–515.

[Gof78] R. Goffaux. On the nature of dielectric loss in high-voltage insulation. *IEEE Transactions on Electrical Insulation*, 1978. EI-13(1):1–8.

[Gof98] R. Goffeaux*[sic]*, M. Krecke, B. Comte, M. Cottet, B. Fruth. Dielectric test methods for rotating machine stator insulation. *Conference on Electrical Insulation and Dielectric Phenomena (CEIDP)*. vol. 2, 1998 pp. 528–533.

[Gol91] D. Goldberg. What every computer scientist should know about floating-point arithmetic. *ACM Computing Surveys*, 1991. 23(1):5–48. `http://dlc.sun.com/pdf/800-7895/800-7895.pdf`. Easily found on the Web, as the original or as a reprint in an appendix to documentation from Sun microsystems.

[Gro02] D. W. Gross. Partial discharge measurement and monitoring on rotating machines. *International Symposium on Electrical Insulation (ISEI)*. 2002 pp. 570–574.

[Gub03] S. M. Gubanski, P. Boss, G. Csépes, V. D. Houhanessian, J. Filippini, P. Guuinic, U. Gäfvert, V. Karius, J. Lapworth, G. Urbani, P. Werelius, W. Zaengl. Dielectric response methods for diagnostics of power transformers. *IEEE Electrical Insulation Magazine*, 2003. 19(3):12–18. A report from Cigre TF 15.01.09.

[Gul00] A. M. Gully, J. C. G. Wheeler. The performance of aged stress grading materials for use in electrical machines. *International Conference on Properties and Applications of Dielectric Materials (ICPADM)*. 2000 pp. 392–396.

[Gup96] B. K. Gupta, W. T. Fink. A proposed type test for interturn insulation in multi-turn coils. *International Symposium on Electrical Insulation (ISEI)*. vol. 1, 1996 pp. 235–238.

[Gut95] F. Gutfleisch, L. Niemeyer. Measurement and simulation of PD in epoxy voids. *IEEE Transactions on Dielectrics and Electrical Insulation*, October 1995. 2(5):729–743.

[Har93] R. Harrold. Partial discharge. XVI. Ultrasonic sensing of PD within large capacitors. *IEEE Electrical Insulation Magazine*, 1993. 9(3):21–28.

[Hel00] A. Helgeson. *Analysis of dielectric response measurement methods and dielectric properties of resin-rich insulation during processing*. Ph.D. thesis, Kungl Tekniska Högskolan (KTH), Stockholm, 2000. `http://kth.diva-portal.org/smash/get/diva2:8714/FULLTEXT01`.

[Hof04] J. Hoffman, C. Johnson, A. Logg. *Dreams of Calculus: Perspectives on Mathematics Education*. Springer, 2004. `http://www.bodysoulmath.org/books/dreams-of-calculus.pdf`.

[Hog66] W. K. Hogg, C. A. Walley. An assessment of the point-hemisphere discharge gap as a partial discharge reference. *Journal of Scientific Instruments*, January 1966. 43(1):11–15.

[Hol91] J. T. Holbøll, J. M. Braun, N. Fujimoto, G. C. Stone. Temporal and spatial development of partial discharges in spherical voids in epoxy related to the detected electrical signal. *Conference on Electrical Insulation and Dielectric Phenomena (CEIDP)*. 1991 pp. 581–588.

[Hol94] J. T. Holbøll, M. Henriksen, A. Jensen, F. Sørensen. PD-pulse characteristics in rotating machine insulation. *International Symposium on Electrical Insulating Materials (ISEM)*. 1994 pp. 322–326. ISBN: 0-7803-1942-7.

[Hol95] J. T. Holbøll, J. M. Braun, N. Fujimoto, G. C. Stone. Partial discharges in flat, dielectric/metallic bounded cavities. *IEE Proceedings — Science, Measurement and Technology*, November 1995. 142(6):490–494.

[Hoo95] M. Hoof, R. Patsch. Pulse-sequence analysis: a new method for investigating the physics of PD-induced ageing. *IEE Proceedings — Science, Measurement and Technology*, 1995. 142(1):95–101.

[Hud05] C. Hudon, M. Belec. Partial discharge signal interpretation for generator diagnostics. *IEEE Transactions on Dielectrics and Electrical Insulation*, 2005. 12(2):297–319.

[Hud90] C. Hudon, R. Bartnikas, M. R. Wertheimer. Surface conductivity of epoxy specimens subjected to partial discharges. *International Symposium on Electrical Insulation (ISEI)*. 1990 pp. 153–155.

[Hud93] C. Hudon, R. Bartnikas, M. R. Wertheimer. Spark-to-glow discharge transition due to increased surface conductivity on epoxy resin specimens. *IEEE Transactions on Electrical Insulation*, 1993. 28(1):1–8.

[Hud94] C. Hudon, R. Bartnikas, M. R. Wertheimer. Chemical and physical degradation effects on epoxy surfaces exposed to partial discharges. *International Conference on Properties and Applications of Dielectric Materials (ICPADM)*. vol. 2, 1994 pp. 811–814.

[Jäv09] N. Jäverberg, H. Edin. Applied voltage frequency dependence of partial discharges in electrical trees. *Proceedings of the 21st Nordic Insulation Symposium (NordIS)*. Gothenburg, Sweden, June 2009 .

[Jac82] R. J. Jackson, A. Wilson. Slot-discharge activity in air-cooled motors and generators. *IEE Proceedings B: Electric Power Applications*, 1982. 129(3):159–167.

[Jay03] E. T. Jaynes. *Probability Theory: The Logic of Science*. Cambridge University Press, 2003. `http://omega.albany.edu:8008/JaynesBook.html`. The freely available online version is a 1994 draft; devotees of the computer-modern typeface may even prefer it. The book was published posthumously, lightly edited by G. Larry Bretthorst, but with largely the same content.

[Jay76] E. T. Jaynes. Confidence Intervals vs Bayesian Intervals. W. L. Harper, C. A. Hooker (editors), *Foundations of Probability Theory, Statistical Inference, and Statistical Theories of Science*, Reidel Publishing Co., Dordrecht, Holland, vol. II. 1976. `http://bayes.wustl.edu/etj/articles/confidence.pdf`.

[Jef98] H. Jeffreys. *The theory of probability*. Oxford classic texts in the physical sciences. Oxford University Press, 3rd edn., 1998. First edition 1939; third edition 1961, then 1983 with corrections. Reprint 1998.

[Jia06] Z. Jia, Y. Hao, H. Xie. The degradation assessment of epoxy/mica insulation under multi-stresses aging. *IEEE Transactions on Dielectrics and Electrical Insulation*, 2006. 13(2):415–422.

[Joh79] D. R. Johnston, J. T. Laforte, P. E. Podhorez, H. N. Galpern. Frequency acceleration of voltage endurance. *IEEE Transactions on Electrical Insulation*, June 1979. EI-14(3):121–126.

[Jon83] A. K. Jonscher. *Dielectric relaxation in solids*. Chelsea Dielectrics Press, London, 1983. Corrected impression, 1996.

[Jon90] A. K. Jonscher. The 'universal' dielectric response. Part I. *IEEE Electrical Insulation Magazine*, March 1990. 6(2):16–22.

[Jon96] A. K. Jonscher. *Universal relaxation law*. Chelsea Dielectrics Press, London, 1996.

[Kau02] M. Kaufhold, K. Schafer, K. Bauer, A. Bethge, J. Risse. Interface phenomena in stator winding insulation — challenges in design, diagnosis, and service experience. *IEEE Electrical Insulation Magazine*, 2002. 18(2):27–36.

[Kei04] *Low Level Measurements Handbook*. Keithley Electronics, 6th edn., 2004. `http://www.keithley.com/wb/201`. Printed version is supplied at no cost. Also available online.

[Kel67] A. Kelen. On the theory of non-linear resistive field grading coatings on insulating surfaces. *Elteknik*, 1967. 6:109–112.

[Ker84] B. W. Kernighan, R. Pike. *The Unix Programming Environment*. Prentice Hall, Inc., Englewood Cliffs, NJ, 1st edn., 1984.

[Kim92] Y. J. Kim, J. K. Nelson. Assessment of deterioration in epoxy/mica machine insulation. *IEEE Transactions on Electrical Insulation*, 1992. 27(5):1026–1039.

[Kir09] H. Kirkham, R. C. Dumas. *The Right Graph: A Manual for Technical and Scientific Authors*. Wiley, 2009.

[Kle04] G. Klempner, I. Kerszenbaum. *Operation and Maintenance of Large Turbo-Generators*. John Wiley & Sons, Inc., Hoboken, NJ, 2004.

[Knu74] D. E. Knuth. Structured programming with `go to` statements. *ACM Computing Surveys*, 1974. 6(4):261–301.

[Kog03] U. Kogelschatz. Dielectric barrier discharges: Their history, discharge physics and industrial application. *Plasma chemistry and plasma processing*, March 2003. 23(1):1–46.

[Kre64] F. H. Kreuger. *Discharge Detection in High Voltage Equipment*. Temple Press Books Ltd, London, 1964.

[Kuf00] E. Kuffel, W. S. Zaengl, J. Kuffel. *High Voltage Engineering: Fundamentals*. Newnes, Oxford, 2nd edn., 2000.

[LaF82] J. J. LaForest (editor). *Transmission line reference book (345 kV and above)*. Electric Power Research Institute (EPRI), Palo Alto, CA, 2nd edn., 1982. 'The (EPRI) Red Book'.

[Lai66] E. R. Laithwaite. *Induction machines for special purposes*. Newnes international monographs on electrical engineering and electronics. Newnes, London, 1966.

[Lar98] A. Larsson. The effect of a large series resistance on the streamer-to-spark transition in dry air. *Journal of Physics D: Applied Physics*, 1998. 31(9):1100.

[Lau92] C. Laurent, C. Mayoux. Partial discharge. XI. Limitations to PD as a diagnostic for deterioration and remaining life. *IEEE Electrical Insulation Magazine*, 1992. 8(2):14–17.

[Lin08] T. Lindquist. *On reliability and maintenance modelling of ageing equipment in electric power systems*. Ph.D. thesis, Kungl Tekniska Högskolan (KTH), Stockholm, 2008. `http://kth.diva-portal.org/smash/get/diva2:13436/FULLTEXT01`. Trita-EE 2008:016.

[Lin09] E. Lindell. *Partial Discharges at Repetitive Rapidly Changing Voltages*. Ph.D. thesis, Chalmers Tekniska Högskola, Göteborg, 2009.

[Lup96] G. Lupo, G. Miano, V. Tucci, M. Vitelli. Field distribution in cable terminations from a quasi-static approximation of the Maxwell equations. *IEEE Transactions on Dielectrics and Electrical Insulation*, 1996. 3(3):399–409.

[Mår00] E. Mårtensson. Electrical characteristics of SiC powders. Licentiate thesis, Kungl Tekniska Högskolan (KTH), Stockholm, 2000.

[Mår01a] E. Mårtensson, U. Gäfvert, U. Lindefelt. Direct current conduction in SiC powders. *Journal of Applied Physics*, 2001. 90(6):2862–2869.

[Mår01b] E. Mårtensson, U. Gäfvert, C. Önneby. Alternate current characteristics of SiC powders. *Journal of Applied Physics*, 2001. 90(6):2870–2878.

[Mac03] D. J. C. MacKay. *Information Theory, Inference, and Learning Algorithms*. Cambridge University Press, 2003. `http://www.inference.phy.cam.ac.uk/mackay/itila/`.

[Mas81] J. H. Mason. Assessing the resistance of polymers to electrical treeing. *IEE Proceedings — Science, Measurement and Technology*, April 1981. 128(3):193–201.

[McD00] W. McDermid. Dielectric absorption characteristics of generator stator insulation. *International Symposium on Electrical Insulation (ISEI)*. 2000 pp. 516–519.

[McD93] W. McDermid. Insulation systems and monitoring for stator windings of large rotating machines. *IEEE Electrical Insulation Magazine*, 1993. 9(4):7–15.

[Min07] L. Ming, F. Sahlén, K. Johansson, E. Mårtensson, H.-Å. Eriksson, O. Koponen, S. Pääkkönen. Effects of repetitive pulse voltages on surface potential distribution at end corona protection region of high voltage motors. *International Symposium on High Voltage Engineering (ISH)*. 2007 pp. paper T2–68.

[Mor93] P. H. F. Morshuis. *Partial discharge mechanisms*. Ph.D. thesis, Technische Universiteit Delft, 1993.

[Mor97] P. Morshuis, M. Jeroense, J. Beyer. Partial discharge. part XXIV: The analysis of PD in HVDC equipment. *IEEE Electrical Insulation Magazine*, 1997. 13(2):6–16.

[Nei04] R. Neimanis, R. Eriksson. Diagnosis of moisture in oil/paper distribution cables — Part I: Estimation of moisture content using frequency-domain spectroscopy. *IEEE Transactions on Power Delivery*, January 2004. 19(1):9–14.

[Nie95] L. Niemeyer. A generalized approach to partial discharge modeling. *IEEE Transactions on Dielectrics and Electrical Insulation*, 1995. 2(4):510–528.

[Pau92] C. R. Paul. *Introduction to electromagnetic compatibility*. Wiley Interscience, 1992.

[Pea00] J. Pearl. *Causality: models, reasoning, and inference*. Cambridge University Press, 2000.

[Ped91] A. Pedersen, G. C. Crichton, I. W. McAllister. The theory and measurement of partial discharge transients. *IEEE Transactions on Electrical Insulation*, 1991. 26(3):487–497.

[Ped95] A. Pedersen, G. C. Crichton, I. W. McAllister. The functional relation between partial discharges and induced charge. *IEEE Transactions on Dielectrics and Electrical Insulation*, 1995. 2(4):535–543.

[Pem06] A. J. M. Pemen, P. C. T. van der Laan, W. de Leeuw. Propagation of partial discharge signals in stator windings of turbine generators. *IEEE Transactions on Energy Conversion*, 2006. 21(1):155–161.

[Pin91] C. Pinto. Variations in the capacitance of delaminated HV stator insulation. *Proceedings of the 20th Electrical Electronics Insulation Conference, 1991. Boston '91 EEIC/ICWA Exposition.* 1991 pp. 65–69.

[Pin98] C. Pinto. A generalized approach for the study of the non linear behaviour of stator winding insulation. *International Conference on Conduction and Breakdown in Solid Dielectrics (ICSD).* 1998 pp. 528–532.

[Qi04] X. Qi, Z. Zheng, S. Boggs. Engineering with nonlinear dielectrics. *IEEE Electrical Insulation Magazine*, 2004. 20(6):27–34.

[Ray03] E. S. Raymond. *The Art of UNIX Programming.* Addison-Wesley Professional Computing Series. Addison-Wesley Professional, Boston, MA, 1st edn., 2003. `http://catb.org/esr/writings/taoup/html/graphics/taoup.pdf`.

[Ref88] A. Refsum. Characterisation of SiC loaded insulators. *International Conference on Properties and Applications of Dielectric Materials (ICPADM).* 1988 pp. 147–150.

[Rhy97] J. Rhyner, M. G. Bou-Diab. One-dimensional model for nonlinear stress control in cable terminations. *IEEE Transactions on Dielectrics and Electrical Insulation*, 1997. 4(6):785–791.

[Riv99] J. P. Rivenc, T. Lebey. An overview of electrical properties for stress grading optimization. *IEEE Transactions on Dielectrics and Electrical Insulation*, 1999. 6(3):309–318.

[Rob95] A. Roberts. Stress grading for high voltage motor and generator coils. *IEEE Electrical Insulation Magazine*, 1995. 11(4):26–31.

[Rux04] L. M. Rux. *The physical phenomena associated with stator winding insulation condition as detected by the ramped direct high-voltage method.* Ph.D. thesis, Mississippi State University, 2004.

[Sed91] A. S. Sedra, K. C. Smith. *Microelectronic Circuits.* Oxford University Press, 3rd edn., 1991.

[Sen86] S. Senturia, N. Sheppard. Dielectric analysis of thermoset cure. K. Dusek (editor), *Epoxy Resins and Composites IV*, Springer, Berlin/Heidelberg, *Advances in Polymer Science*, vol. 80, pp. 1–47. 1986.

[Sha08] E. Sharifi, S. Jayaram, E. A. Cherney. Capacitive grading of 13.8 kV form-wound motor coil ends for pulse width modulated drive operation. *International Symposium on Electrical Insulation (ISEI).* 2008 pp. 632–635.

[Sta99] J. Stastna, L. Zanzotto. Linear response of regular asphalts to external harmonic fields. *Journal of Rheology*, 1999. 43(3):719–734.

[Ste91] J. P. Steiner. Partial discharge. IV. Commercial PD testing. *IEEE Electrical Insulation Magazine*, 1991. 7(1):20–33.

[Sto04] G. C. Stone, E. A. Boulter, I. Culbert, H. Dhirani. *Electrical insulation for rotating machines.* IEEE Press series on Power Engineering. IEEE Press, 2004.

[Sto96] G. C. Stone. The use of partial discharge measurements to assess the condition of rotating machine insulation. *IEEE Electrical Insulation Magazine*, 1996. 12(4):23–27.

[Sto98] G. C. Stone. Partial discharge. XXV. Calibration of PD measurements for motor and generator windings — why it can't be done. *IEEE Electrical Insulation Magazine*, 1998. 14(1):9–12.

[T150] *Standard Test Methods for AC Loss Characteristics and Permittivity (Dielectric Constant) of Solid Electrical Insulation*. ASTM International, 2004. ASTM Standard D150-98.

[T351] *Standard Classification for Natural Muscovite Block Mica and Thins Based on Visual Quality*. ASTM International, 2003. ASTM Standard D351-97.

[Tav08] P. Tavner, L. Ran, J. Penman, H. Sedding. *Condition Monitoring of Rotating Electrical Machines*. Power and Energy Series (56). IET, 2008.

[Tav88] P. J. Tavner, R. J. Jackson. Coupling of discharge currents between conductors of electrical machines owing to laminated steel core. *IEE Proceedings B: Electric Power Applications*, 1988. 135(6):295–307.

[Tay04] N. Taylor, H. Edin. Utilisation of voltage and frequency dependence of stress-grading materials in dielectric diagnostics. *Conference on Electrical Insulation and Dielectric Phenomena (CEIDP)*. 2004 pp. 178–181.

[Tay05] N. Taylor, H. Edin. The dielectric response of stator end-winding stress-grading. *International Symposium on High Voltage Engineering (ISH)*. 2005 p. H56.

[Tay06] N. Taylor. Diagnostics of stator insulation by dielectric response and variable frequency partial discharge measurements, October 2006. `http://kth.diva-portal.org/smash/get/diva2:11239/FULLTEXT01`. Licentiate Thesis, Kungl Tekniska Högskolan (KTH), Stockholm.

[Tay07] N. Taylor, H. Edin. Partial discharge measurement at varied low frequency, and some results from thermally aged stator insulation. *Proceedings of the 20th Nordic Insulation Symposium (NordIS)*. 2007 pp. 185–188.

[Tay09] N. Taylor, H. Edin. Differences between PD charges measured by differences between PD charges measured by partial discharge and dielectric spectroscopy systems. *Proceedings of the 21st Nordic Insulation Symposium (NordIS)*. Gothenburg, Sweden, 2009 pp. 69–73.

[Tay10] N. Taylor. This thesis, 2010.

[Tic98] W. F. Tichy. Should computer scientists experiment more? *Computer*, 1998. 31(5):32–40.

[Tri95] N. G. Trinh. Partial discharge XIX: Discharge in air part I: Physical mechanisms. *IEEE Electrical Insulation Magazine*, 1995. 11(2):23–29.

[Tuc99] V. Tucci, J. Rhyner. Comment on "1-dimensional model for nonlinear stress control in cable terminations" [and reply]. *IEEE Transactions on Dielectrics and Electrical Insulation*, 1999. 6(2):267–270.

[VB93] R. J. Van Brunt, E. W. Cernyar, P. von Glahn. Importance of unraveling memory propagation effects in interpreting data on partial discharge statistics. *IEEE Transactions on Electrical Insulation*, December 1993. 28(6):905–916.

[VB95] R. J. Van Brunt, P. von Glahn, T. Las. Nonstationary behaviour of partial discharge during discharge induced ageing of dielectrics. *IEE Proceedings — Science, Measurement and Technology*, 1995. 142(1):37–45.

[Vog03a] R. Vogelsang, R. Brütsch, K. Fröhlich. Effect of electrical tree propagation on breakdown in mica insulations. *International Symposium on High Voltage Engineering (ISH)*. August 2003 pp. 1–4.

[Vog03b] R. Vogelsang, R. Brütsch, K. Fröhlich. How imperfections in mica tape barriers influence tree growth and breakdown time. *Conference on Electrical Insulation and Dielectric Phenomena (CEIDP)*. 2003 pp. 657–660.

[Vog03c] R. Vogelsang, B. Fruth, K. Fröhlich. Detection of electrical tree propagation in generator bar insulations by partial discharge measurements. *International Conference on Properties and Applications of Dielectric Materials (ICPADM)*. vol. 1, 2003 pp. 281–285.

[Vog05] R. Vogelsang, B. Fruth, T. Farr, K. Fröhlich. Detection of electrical tree propagation by partial discharge measurements. *European Transactions on Electrical Power*, 2005. 15(3):271–284.

[Vog06] R. Vogelsang, T. Weiers, K. Fröhlich, R. Bruetsch. Electrical breakdown in high-voltage winding insulations of different manufacturing qualities. *IEEE Electrical Insulation Magazine*, 2006. 22(3):5–12.

[Wei05] T. Weiers, D. Keller, R. Vogelsang. The impact of low amplitude 100 Hz vibrations on the winding insulation of rotating high voltage machines. *International Symposium on High Voltage Engineering (ISH)*. 2005 p. I09. `http://www.eeh.ee.ethz.ch/fileadmin/user_upload/eeh/publications/hvl/weiers_ISH2005_The_impact_of_100hz_vibrations.pdf`.

[Wer01a] P. Werelius. *Development and application of high voltage dielectric spectroscopy for diagnosis of medium voltage XLPE cables*. Ph.D. thesis, Kungl Tekniska Högskolan (KTH), Stockholm, 2001. `http://kth.diva-portal.org/smash/get/diva2:9062/FULLTEXT01`.

[Wer01b] P. Werelius, P. Thärning, R. Eriksson, B. Holmgren, U. Gäfvert. Dielectric spectroscopy for diagnosis of water tree deterioration in XLPE cables. *IEEE Transactions on Dielectrics and Electrical Insulation*, 2001. 8(1):27–42.

[Whe07] J. C. G. Wheeler, A. M. Gully, A. E. Baker, F. A. Perrot. Novel stress grading systems for converter-fed motors. *IEEE Electrical Insulation Magazine*, 2007. 23(1):29–35.

[Woo93] J. W. Wood, H. G. Sedding, W. K. Hogg, I. J. Kemp, H. Zhu. Partial discharges in HV machines; initial considerations for a PD specification. *IEE Proceedings — Science, Measurement and Technology*, 1993. 140(5):409–416.

[Zhu92] H. Zhu, I. J. Kemp. Pulse propagation in rotating machines and its relationship to partial discharge measurements. *International Symposium on Electrical Insulation (ISEI)*. 1992 pp. 411–414.